## *Preparation and thermal decomposition of zinc/copper trimellitates and pyromellitates*

Gavin Stuart Walker

# PREPARATION AND THERMAL DECOMPOSITION OF ZINC/COPPER TRIMELLITATES AND PYROMELLITATES

Gavin Stuart Walker

University of Durham
Department of Chemistry

1995

*A thesis submitted in candidature for the degree of Doctor of Philosophy*



# PREPARATION AND THERMAL DECOMPOSITION OF ZINC/COPPER TRIMELLITATES AND PYROMELLITATES

Gavin Stuart Walker

Ph.D. Thesis Abstract

University of Durham 1995

The aim of this research was to prepare and characterise zinc, copper and mixed zinc/copper trimellitates (1,2,4-benzene tricarboxylates) and pyromellitates (1,2,4,5-benzene tetracarboxylates). The characterisation included a study of the thermal decomposition for selected salts.

The literature is reviewed, discussing the synthesis, structural properties, and thermal decompostions of carboxylate salts. This review highlights the growing interest in benzene carboxylates, and a summary of the applications of such salts is given at the end of the review.

The preparative route investigated in the work reported here involved reacting zinc/copper hydroxycarbonate, $(Zn_xCu_{1-x})_n(CO_2)_p(OH)_q$, with the carboxylic acid. This preparation was chosen in an attempt to overcome problems encountered during previous projects, which are discussed in the introduction. The preparation and characterisation of zinc/copper hydroxycarbonates were studied, concentrating on the preparation of single phase products.

The hydroxycarbonate route was successful in producing single metal and mixed metal salts of trimellitic and pyromellitic acid. Limits of the solid solution series were deduced for the mixed metal carboxylates.

Three trimellitate crystal structures, $Zn_2OH(C_6H_3(COO)_3) \cdot 2H_2O$, $ZnCuOH(C_6H_3(COO)_3) \cdot 2H_2O$, $CuH(C_6H_3(COO)_3) \cdot 2.5H_2O$, and one pyromellitate structure, $ZnH_2(C_6H_2(COO)_4) \cdot 6H_2O$, were determined. The trimellitate structures were all polymeric layers, with the anion bridging between the metal sites. The pyromellitate had an ionic structure with $[Zn(H_2O)_6]^{2+}$ cations and $[H_2(C_6H_2(COO)_4)]^{2-}$ anions. The dianion had very strong, intramolecular H-bonding. Using these and other crystal structures, it was possible to deduce a correlation between IR absorptions for carboxylate groups and the type of carboxylate coordination.

The thermal decomposition of the metal salts was studied. An investigation was undertaken using DSC and temperature programmed decomposition to deduce the mechanism for the thermal decomposition of selected salts. The effect of the cation ratio (for the mixed metal salts) upon the decomposition was also studied.

The work reported here has shown the success of the hydroxycarbonate route for the formation of polycarboxylate salts. Characterisation for a number of new zinc/copper salts is reported. A study of the thermal decompositions for selected salts has deduced the mechanism and factors affecting the decomposition.

# CONTENTS

# DECLARATION

The work described in this thesis was carried out at the University of Durham between October 1991 and September 1994. This thesis is the original work of the author except where acknowledged by reference, and no part has been submitted for a degree in this or any other university.

# ACKNOWLEDGEMENTS

I would like to express my thanks to Prof. Ken Wade and Dr. Jas Pal S. Badyal for their supervision, advice and encouragement throughout this research. I am also indebted to Dr Z.V. Hauptman whose genuine enthusiasm and wealth of knowledge was a constant source of inspiration.

I also wish to thank Penny Herbertson for the help and encouragement she has given, especially while I have been writing up away from Durham. I am grateful to all the technical staff associated with the Department of Chemistry at Durham for their help and assistance.

A grant from the E.P.S.R.C. and ICI studentship are gratefully acknowledged.

Finally, I wish to acknowledge the enormous support, help and understanding provided by my wife, Lorna Jowett. Words cannot express my most sincere thanks for all the hard work she has done, and also the support and encouragement given me during these past years.

# GLOSSARY AND ABBREVIATIONS

| | |
|---|---|
| DSC | differential scanning calorimetry |
| Hemimellitic acid | 1,2,3-benzene tricarboxylic acid |
| IR | infrared |
| Isophthalic acid | 1,3-benzene dicarboxylic acid |
| Mellitic acid | benzene hexacarboxylic acid |
| $OPr^i$ | isopropoxide, $OCH(CH_3)_2$ |
| Phthalic acid | 1,2-benzene dicarboxylic acid |
| PM | pyromellitate (1,2,4,5-benzene tetracarboxylate) |
| Pyromellitic acid | 1,2,4,5-benzene tetracarboxylic acid |
| Terephthalic acid | 1,4-benzene dicarboxylic acid |
| TM | trimellitate (1,2,4-benzene tricarboxylate) |
| TPDec | temperature programmed decomposition |
| Trimesic acid | 1,3,5-benzene tricarboxylic acid |
| Trimellitic acid | 1,2,4-benzene tricarboxylic acid |
| XRD | x-ray diffraction |

*Discussion of spectra*

| | |
|---|---|
| b | broad |
| m/e | mass ion (mass/charge) |
| s | strong |
| sh | shoulder |
| v | very |
| w | weak |

# 1. INTRODUCTION

This thesis describes work undertaken to prepare and characterise novel zinc/copper salts. 'Zinc/copper' is used here to cover not only mixed metal salts, but also the single metal compounds. A study of the thermal decompositions of selected salts is also reported. This introductory chapter is split into three sections. The first section is a brief introduction to this area of chemistry and to some of the concepts behind the project. This is followed by a summary of the previous work carried out by this research group. Finally there is an overview of the thesis, providing a brief summary of the subsequent chapters.

## 1.1 Zinc/Copper Carboxylates

The project was a continuation of research undertaken at Durham, studying zinc/copper carboxylates[1-3]. This earlier work is summarised in section 1.2. The project as a whole has centred around the preparation of mixed metal, zinc/copper carboxylates. The formation of these mixed metal salts has not been as simple as might have been expected.

A mixed metal compound has the general formula $A_xB_{1-x}L_y \cdot nH_2O$, where A and B are two different metals, L is the anion and x = 0–1. A system able to have one cation substituted for the other (known as ion-ion exchange) across the whole range of x is referred to as a continuous solid solution series[4]. A limited solution series is one in which certain A/B ratios are not tolerated. Goldschmidt's rule states that a continuous solid solution cannot be obtained if the difference in ionic radii is greater than 15% of the smallest cation[5]. $Cu^{2+}$ and $Zn^{2+}$ have very similar radii (0.72Å and 0.74Å, respectively[6]), well within the limits set by Goldschmidt. However, the two cations have different electron configurations, which means that they normally have different coordination geometries. $Zn^{2+}$ has a $d^{10}$ configuration and is associated with regular, cubic coordination geometries. $Cu^{2+}$ has a $d^9$ configuration and is subject to Jahn Teller distortions if placed in an environment of cubic symmetry. $Cu^{2+}$ is normally associated with irregular coordination geometries. Because of the difference in geometries, a continuous solid solution series is unlikely to exist between $Cu^{2+}$ and $Zn^{2+}$. However, it is very probable that there will be a limited solution series and it is this that we wish to explore.

An alternative to $Cu^{2+}$ is $Cu^{+}$. The latter ion has a $d^{10}$ electron configuration and is therefore associated with regular coordination geometries like $Zn^{2+}$. However, $Cu^{+}$ has an ionic radius of[7] 0.96Å, 24% larger than $Zn^{2+}$, and therefore will not form a continuous solution series with $Zn^{2+}$. A further problem is that substituting $Zn^{2+}$ for

$Cu^{+}$ would create a charge imbalance and would require incorporation of a co-cation to balance the charge. Taking into consideration the above information, it was concluded that $Cu^{2+}$ was more likely to substitute a zinc cation than $Cu^{+}$.

Another area of interest is how the crystal structure is affected by ion-ion exchange. For example, whether the structure becomes distorted to accommodate the other cation, and if the cations preferentially occupy specific sites or are randomly distributed.

Earlier work attempting to prepare mixed metal salts of formate and oxalate proved unsuccessful[1]. It was postulated that a large multidentate ligand would be more successful in accommodating the two cations[3]. A ligand with multiple donor sites can coordinate to a different metal via each donor site. A large ligand is less rigid and may be able to compensate for structural changes of the crystal brought about by ion-ion exchange (because of the differing coordination geometries of copper and zinc). Trimellitic acid and pyromellitic acid, figure 1.1, were selected for further study as these were relatively bulky polycarboxylic acids and were readily available.

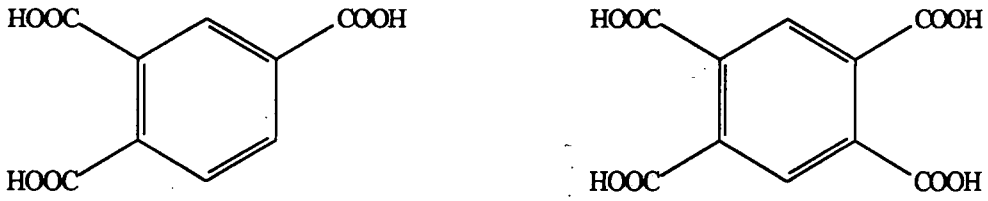


Figure 1.1 Trimellitic and pyromellitic acid.

There is a growing interest in the chemistry and applications of metal benzene polycarboxylates (>2 carboxylates) as is illustrated in chapter 2. This project was seen as an excellent opportunity to increase the science base for benzene polycarboxylates and to open up this rich area of chemistry. Current areas of interest include the magnetic properties of the copper salts[8,9], the use of zinc salts as fire retardants in polymers[10-12] and the use of the silver carboxylates as precursors for silver catalysts[13]. A possible use for zinc/copper mixed metal salts is as precursors for methanol synthesis catalysts[14]. Methanol is produced by passing synthesis gas (carbon dioxide, carbon monoxide and hydrogen) over a copper/zinc oxide catalyst. Zinc/copper compounds can be calcined, producing the metal oxides, and then reduced, yielding copper and zinc oxide. The current methanol synthesis catalyst is prepared from a zinc/copper hydroxycarbonate[14]. The thermal decomposition of zinc/copper carboxylates has been studied because of their potential use as catalyst precursors. Further aims of the current project were to deduce the mechanism of decomposition and the factors influencing the decomposition.

In summary, the aims of this project were:

- to prepare and characterise zinc, copper and mixed metal trimellitates and pyromellitates;
- to study the thermal decomposition of selected salts; and
- to prepare single crystals of the salts for X-ray structural analysis.

## 1.2 Previous Work

Prior to the current project, some research had already been undertaken, studying the preparation of zinc/copper formates, oxalates, trimellitates and pyromellitates[1-3]. The preparation of zinc/copper formates and oxalates was attempted first[1]. Zinc and copper formate are both soluble in water and a solution containing both salts was used to cocrystallise mixed metal formate. The product did contain some mixed metal formate but the majority of the solid was the single metal salts. Similar findings have also been reported in the literature[15]. Coprecipitation experiments were attempted for the less soluble oxalate salts. However, all the products obtained were physical mixtures of the single metal salts.

Having had little success with small carboxylates, we decided that larger polybasic acids might be more successful in forming mixed metal salts for the reasons outlined in section 1.1. The preparation of single metal salts was first attempted[2]. Pyromellitate salts were precipitated by the addition of a potassium pyromellitate solution to a copper sulphate solution. The potassium salt of the acid was used because the acid has a low solubility. It was found that without careful control of the pH during the reaction a mixture of phases resulted. The products obtained when the pH was carefully controlled illustrates the sensitivity of the reaction to pH[2].

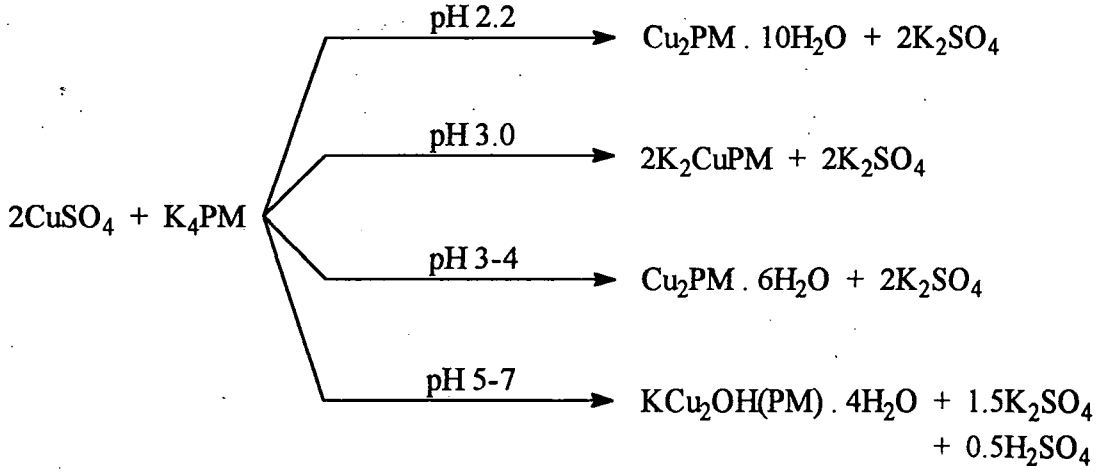


It was also found that the phases obtained differed when different reagents were used, e.g. copper nitrate and sodium pyromellitate solutions[3]. Similar problems were

encountered when trying to prepare copper trimellitates. Invariably the products were mixed metal copper/alkali metal salts:

$$Cu(NO_3)_2 + 2M_3TM \longrightarrow CuM_2H_2TM_2 \cdot 4H_2O \quad (M = Na \text{ or } K)$$

To overcome these problems, reactions between zinc/copper hydroxycarbonates and the free acid were investigated. The hydroxycarbonates are insoluble, as are the zinc/copper trimellitates and pyromellitates. The reaction therefore entails the conversion of one insoluble solid into another, which may result in incomplete conversions (e.g. starting material encapsulated by product). The advantages of the hydroxycarbonate route are:

i) exclusion of the alkali metal;
ii) buffer effect, controlling the pH of the reaction mixture;
iii) the hydroxycarbonates acting as templates for the formation of mixed metal, zinc/copper carboxylates.

No problems were encountered with incomplete conversions. Copper pyromellitate hexahydrate and a zinc/copper hydroxytrimellitate salt were prepared via this route. An objective of the present project was to further investigate the preparation of trimellitates and pyromellitates via the hydroxycarbonate route.

The crystal structures of three pyromellitates have been determined.

- $Cu_2PM \cdot 6H_2O$
- $CuK_2PM \cdot 4H_2O$
- $(Zn_{0.75}Cu_{0.25})_{2.5}OH(PM) \cdot 7H_2O$

These structures are discussed in the introductory section of chapter 5, Preparation of Zinc/Copper Pyromellitates. Because of the insolubility of the salts, crystals were produced using the gel method[16], a technique for growing crystals by controlling the rate of reaction and nucleation (discussed further in section 2.1). This work has been continued in order to develop a wider understanding of the structural chemistry of benzene polycarboxylates.

## 1.3 Thesis Overview

*Chapter 2. Preparation, properties and uses of metal carboxylates.* The following topics are covered in this review of the literature on metal carboxylates: synthesis; structural properties; thermal decomposition; and applications. The section on structural properties discusses the modes of coordination found for the carboxylate group. The crystal structures of metal(II) benzene polycarboxylates are discussed in more detail, highlighting the range of carboxylate coordination and types of crystal

structures found. The use of IR to deduce structural features of metal carboxylates is also discussed.

*Chapter 3. Preparation of zinc/copper hydroxycarbonates.* The first experimental chapter is devoted to the preparation and characterisation of zinc/copper hydroxycarbonates. As already mentioned, the hydroxycarbonates were used as reactants for the formation of zinc/copper salts. For them to act as templates for the mixed metal carboxylates, they should be single phase compounds. If more than one phase exists, each phase might have a different cation ratio which would lead to the formation of a carboxylate product with regions of different cation ratios. Six mineral phases were encountered in this investigation. Although much has been reported[17-22], it was found that the preparation of single phase zinc/copper hydroxycarbonates was more difficult than was implied in the literature. An investigation was undertaken to deduce the most favourable reaction conditions for preparing zinc/copper hydroxycarbonates over a range of cation ratios.

Some of the products reported in this chapter were used in the reactions reported in chapters 4 and 5. To avoid duplication, these compounds have been cross-referenced to their experimental details in chapter 3.

*Chapter 4. Preparation of zinc/copper trimellitates.* A polybasic acid like trimellitic acid can form basic, $M_4OH(TM)$ (where M is a monovalent metal and $H_3TM$ is trimellitic acid), neutral, $M_3TM$, and acidic salts, $M_2HTM$ and $MH_2TM$. All these salts were encountered in this investigation and are discussed separately. Two limited solid solution series were identified, $(Zn_xCu_{1-x})_{2.5}(OH)_2TM \cdot 2.5H_2O$ and $(Zn_xCu_{1-x})_{1.5}TM \cdot 2H_2O$. Three crystal structures are reported, two of which are members of the basic solid solution series. From the crystallographic data, a discussion on the factors influencing the limits of the solid solution series is presented.

*Chapter 5. Preparation of zinc/copper pyromellitates.* The introduction is a review of previous work and includes three unpublished crystal structures obtained by the Durham research group. The structures are compared with the metal(II) pyromellitate structures reported in the literature. Two limited solid solution series were identified, $(Zn_xCu_{1-x})_{2.5}OH(PM) \cdot 7H_2O$ and $(Zn_xCu_{1-x})_2PM \cdot nH_2O$ (where $H_4PM$ is pyromellitic acid). The series based on the basic salt could accommodate most cation ratios (x = 0.1-0.9), but no single metal analogues of this salt were obtained. The crystal structure of $ZnH_2PM \cdot 6H_2O$ is reported, as well as a further discussion on the use of IR to determine structural features of carboxylates, incorporating the findings from this study.

*Chapter 6. Thermal decomposition of zinc/copper mixed metal trimellitates and pyromellitates.* The thermal decompositions of selected salts were studied by DSC (differential scanning calorimetry) and TPDec (temperature programmed decomposition). The mechanisms of decomposition and the effect of ion-ion exchange on the decompositions have been deduced from these results.

*Chapter 7. Conclusions and proposals for future work.* A summary of the conclusions from each chapter is given here, along with some proposals for future work. There is also a discussion about the reasons for the success of the hydroxycarbonate route, and the factors controlling the success of ion-ion exchange for zinc/copper solid solution series.

*References.* All the references have been compiled after the conclusions. References made in the text are denoted by a superscript numeral.

*Appendix.* There are two appendices, the first details the specifications of equipment used. The other is a list of symposia and meetings attended during the Ph.D.

*Glossary.* A glossary of terms and abbreviations used in the thesis is situated at the front of the thesis, after the contents page.

# 2. PREPARATION, PROPERTIES AND USES OF METAL CARBOXYLATES

This chapter is a brief review of the literature on metal carboxylates. A discussion of the preparation of carboxylates precedes a review of the varied structural chemistry found for metal carboxylates. An introduction to the field of thermal decompositions and topochemical reactions follows, and finally a summary of the uses of metal carboxylates is given. The examples used will, where appropriate, be taken from the literature on benzene polycarboxylates as these are of more relevance to this project.

## 2.1 Preparation of Carboxylates[23]

The preparative routes to metal carboxylates can be classified as either aqueous or non-aqueous reactions. In general, aqueous reactions are used to form metal carboxylates as these are straightforward preparations. Aqueous preparations normally produce hydrated salts. However, if anhydrous products are required, the more satisfactory route is non-aqueous.

### *2.1a Aqueous reactions*

*Anion exchange reactions*

Metal carboxylates can be prepared by the reaction of a metal oxide, hydroxide or salt (e.g. chloride, nitrate, sulphate or carbonate) with a carboxylic acid (either as the free acid, or its alkali metal/ammonium salt). For some systems it is necessary to control the pH of the reaction in order to obtain a single phase (cf. section 1.2).

$$MX_n + nRCO_2Y \longrightarrow M(O_2CR)_n + nXY$$

$X = Cl, NO_3, SO_4, OH, O, CO_3$

$Y = H, Na, K, NH_4$

Because of the low solubility of most aromatic polycarboxylic acids, preparations of these carboxylates often use the more soluble alkali metal[24,25] or ammonium[26] salt.

$$2Co(NO_3)_2 + Na_4PM \longrightarrow Co_2PM \cdot 18H_2O + 4NaNO_3$$

$$3Cu(NO_3)_2 + 2(NH_4)_3TM \longrightarrow Cu_3TM_2 \cdot 3H_2O + 6NH_4NO_3$$

$H_4PM$ = pyromellitic acid; $H_3TM$ = trimellitic acid.

The use of a soluble salt of the acid to form a carboxylate can also produce mixed metal salts[27] e.g. $Na_2Zn_2(1,3,5\text{-}C_9H_3O_6)_2 \cdot 11H_2O$. With polycarboxylates partial

reaction is possible, forming acidic salts (i.e. some carboxylic acid groups remain), for example[28,29] $Cu(1,3,5\text{-}C_6H_3(CO_2)_3H) \cdot 3H_2O$ or $Cu(1,2,3\text{-}C_6H_3(CO_2)_3H_2)_2 \cdot 3H_2O$.

*Electrochemical synthesis*

Metal carboxylates can be prepared by electrolysis. Copper benzoate and copper phthalate were prepared using a solution of the carboxylic acid as the electrolyte, and a sacrificial copper anode[30]. When a potential was applied across the electrodes the acid reacted with the sacrificial electrode, producing the copper salt.

*Crystal growth of aromatic polycarboxylates[16]*

The growth of single crystals of aromatic polycarboxylates suitable for X-ray structural analysis can be very difficult because of the low solubilities found for many of these salts. In general metal phthalate compounds have sufficient solubility for recrystallisation, but the tri-, tetra- and hexa-carboxylates often have low solubilities, making it difficult to obtain single crystals by recrystallisation. The gel method has been used to obtain crystals of single metal[31,32] and mixed metal[27] aromatic polycarboxylates. This method is a technique for slow crystal growth. There are several variations of the experiment, and some of these are shown in figure 2.1. The simplest gel experiment, and often the most effective, is shown in figure 2.1a. This consists of a silica gel impregnated with one of the reagents and a dilute solution of the other on top of the gel. For example, a solution of copper nitrate on top of a gel impregnated with a sodium pyromellitate solution produced crystals of copper pyromellitate (section 1.2). Crystals are produced after days, or even weeks, depending on the conditions of the experiment.

The rate of reaction is limited by the diffusion of the reactants through the gel. The nucleation rate of the crystals is affected by the density of the gel, i.e. a denser gel will have a lower nucleation rate. These two factors control the success of the experiment. One problem encountered when trying to grow crystals of a mixed metal compound is that the stoichiometry of the crystals grown rarely reflects the cation ratio of the supernatant solution. Further, it has been found that exchanging the reagent in the gel with the supernatant solution can affect the crystals produced (size, habit and stoichiometry). Also shown in figure 2.1d is a method for enlarging crystals. Crystals are seeded above the middle of the gel and the reactants diffuse through the gel to the solution surrounding the crystals, allowing slow crystal growth.

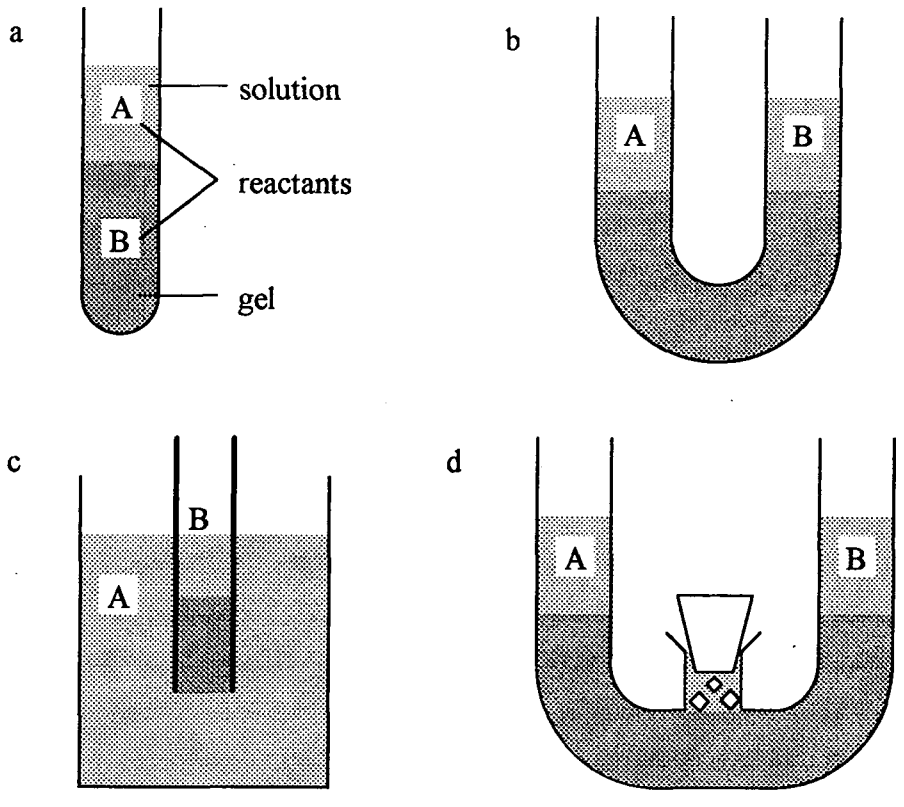


Figure 2.1 Four variations of the gel method for the growth of single crystals.

### *2.1b Non-aqueous reactions*[23]

If anhydrous salts are required it is often more practical to prepare the salt via a non-aqueous route rather than by dehydrating a hydrated salt. This is because some decomposition of the salt may occur during the dehydration. Some metal carboxylates are susceptible to hydrolysis and can only be prepared in non-aqueous media. For example, aluminium tricarboxylates cannot be prepared in an aqueous reaction because hydrolysis produces the basic dicarboxylate $Al(OH)(O_2CR)_2$.

*Reaction with metal halides*

Anhydrous copper and zinc acetate can be prepared by the reaction of the metal chloride with a mixture of glacial acetic acid and acetic anhydride[33]. The anhydride is present to remove any water in the system.

$$CuCl_2 + 2CH_3CO_2H \longrightarrow Cu(CH_3CO_2)_2 + 2HCl$$

*Reaction with metal alkoxide*

The reaction of metal alkoxide with carboxylic acid is a convenient route to aluminium tricarboxylates. The advantage over the halide route is the less reactive side product, i.e. an alcohol, as opposed to hydrogen chloride.

$$Al(OPr^i)_3 + 3RCO_2H \longrightarrow Al(O_2CR)_3 + 3HOPr^i$$

This route can also be used to prepare alkoxide carboxylates e.g.

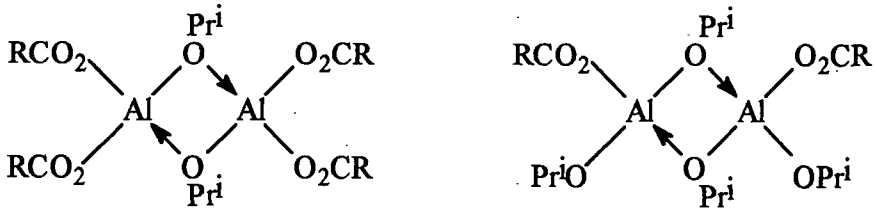

The monoisopropoxide dicarboxylates can be converted into aluminium oxide carboxylates by heating under reduced pressure.

$$Al(OPr^i)(O_2CR)_2 \xrightarrow{\Delta} AlO(O_2CR) + RCO_2Pr^i$$

These oxide soaps can also be prepared by controlled hydrolysis, followed by thermal condensation.

$$Al(OPr^i)_2(O_2CR) + H_2O \xrightarrow[\text{benzene}]{\Delta} Al(OPr^i)(OH)O_2CR + {}^iPrOH$$

$$Al(OPr^i)(OH)O_2CR \xrightarrow{\Delta,\ \sim 170^\circ C} AlO(O_2CR) + {}^iPrOH$$

The aluminium oxide soaps are oligomers (8-10 units) and may have either ring or chain structures.

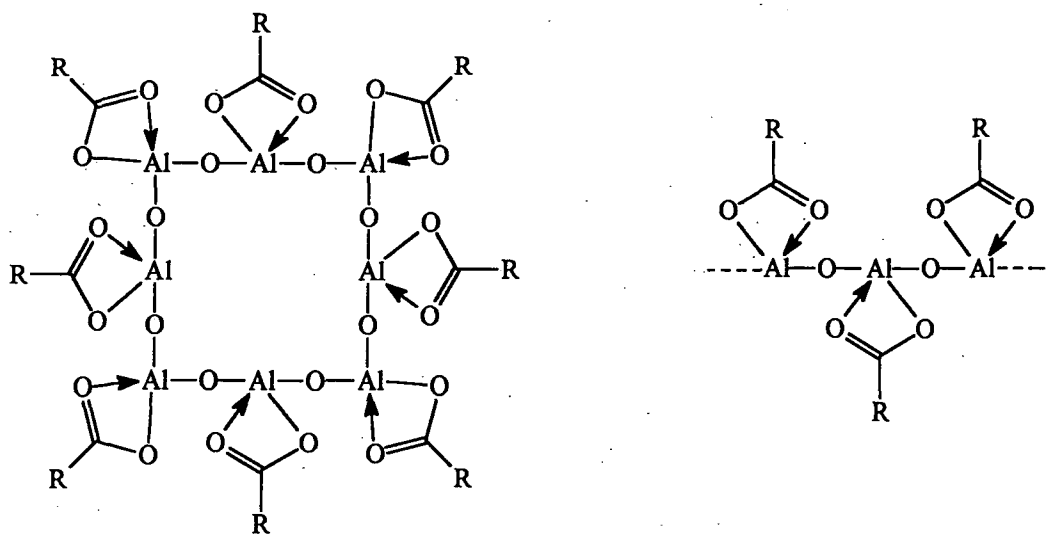

Figure 2.2 Ring and chain structures of aluminium oxide soaps.

*Exchange reaction*

It is possible to exchange the carboxylate group by reaction with another carboxylic acid. An example of this is the conversion of tin (IV) acetate to tin (IV) succinate (1,4 butandioate). The reaction is pushed to completion by the removal of acetic acid as its toluene azeotrope[34].

$$Sn(O_2CCH_3)_4 + 2(HO_2C)_2C_2H_4 \longrightarrow Sn((O_2C)_2C_2H_4)_2 + 4CH_3CO_2H$$

*Reaction with other metal derivatives*

Some metal carboxylates have been prepared by reacting carboxylic acids with metal alkyls, carbonyls and hydrides. For example, triphenyl aluminium reacts with acetic acid in a stepwise manner to produce aluminium triacetate. The mono- and di-carboxylate intermediates can be isolated[35].

$$AlPh_3 + 3CH_3CO_2H \longrightarrow Al(O_2CCH_3)_3 + 3PhH$$

## 2.2 Structural Properties of Metal Carboxylates[23]

### *2.2a Coordination*

Single crystal X-ray diffraction has been used to solve the structures of many carboxylate compounds. The coordination found between the carboxylate ion and the metal can be divided into the following four categories.

*i) Ionic*

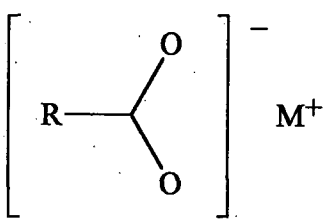

For simple ionic carboxylates there appears to be little cation-anion interaction[23]. Sodium formate is an example of a carboxylate with an ionic structure, the electrons are delocalised in the carboxylate group and both C-O bonds are 1.27Å long[36].

*ii) Monodentate*

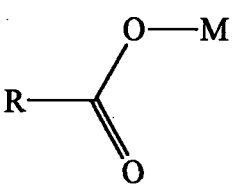

In lithium acetate dihydrate the acetate ion functions as a monodentate ligand[37]. It was found that the C-O bond length for the oxygen coordinated to lithium was longer than the other (1.33Å compared with 1.22Å).

*iii) Chelating*

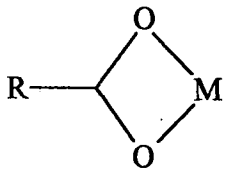

It is possible for the carboxylate ion to act as a bidentate ligand, chelating to a metal centre, forming a four membered ring. For example, the acetate ion in zinc acetate dihydrate chelates to the zinc[38]. The C-O bond lengths for the carboxylate group are often similar but not necessarily identical. The C-O bond lengths in zinc acetate dihydrate were 1.30, 1.38Å.

*iv) Bridging*

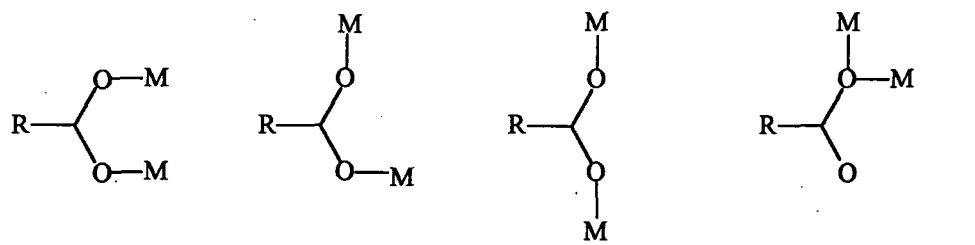

| syn-syn | anti-syn | anti-anti | monatomic |
|---|---|---|---|
| $Cu(O_2CMe)_2 . 2H_2O$ [39] | $Cu(O_2CH)_2$ [40] | $Cu(O_2CH) . 4H_2O$ [41] | $Hg(O_2CMe)_2(C_6H_{11})_3P)$ [42] |

Figure 2.3 Carboxylate bridges.

There are four basic types of bridging possible and these are shown in figure 2.3, along with examples for each mode. The geometry of the syn-syn bridge is the only one that can bring the metal atoms close enough to form a metal-metal bond. In copper carboxylates these metal-metal interactions have led to unusual magnetic properties[43,44]. In copper(II) acetate dihydrate binuclear clusters are formed by four syn-syn carboxylate bridges. The two copper atoms are bridged (syn-syn) by four carboxylate groups, figure 2.4.

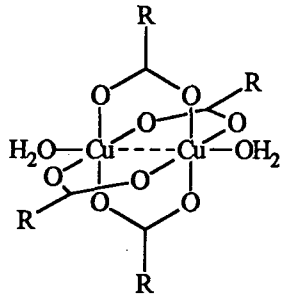

Figure 2.4 Binuclear cluster found for copper(II) acetate dihydrate.

Polymeric structures are only found for monocarboxylates that have either anti-syn or anti-anti configurations, e.g. anhydrous copper(II) formate[40] and its tetrahydrate[41] respectively.

Combinations of the above modes of coordination are also possible, producing three or four coordinate carboxylate groups. The combinations are shown in figure 2.5, with examples.

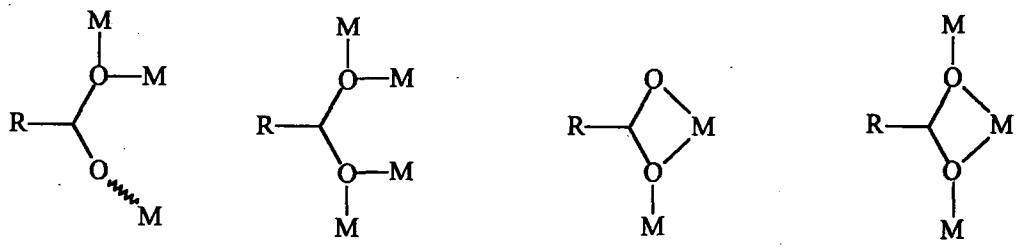

$Cu(O_2CMe)$ [45] $AgCu_2(pht)OH \cdot 5H_2O$ [46] $CaCu(O_2CMe)_4(H_2O)_6$ [47] $Ca_2(H_2Mel) \cdot 9H_2O$ [48]

Figure 2.5 Three and four coordinate carboxylate bridges.

The polymeric structure of copper(I) acetate, figure 2.6, is based on an eight-membered ring formed by two copper atoms and two carboxylate groups[45]. These rings are similar to those found for copper(II) acetate dihydrate, figure 2.4. In copper(I) acetate one oxygen from each carboxylate group also forms a monatomic bridge which links the rings together, forming a polymeric chain. The distance between the copper atoms is 2.556Å.

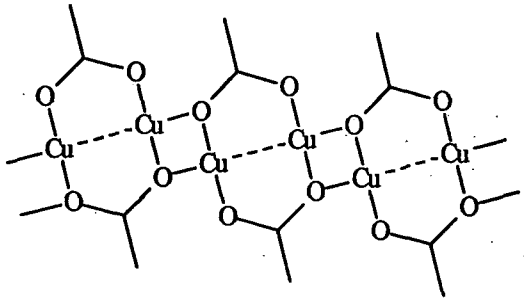

Figure 2.6 Polymeric structure of copper(I) acetate.

The modes of coordination described are also valid for polycarboxylates. However, the presence of two or more carboxylate groups per ligand increases the scope for bridging. Because of this, the crystal structures found for many benzene polycarboxylates are polymeric. A review of reported crystal structures for benzene polycarboxylates now follows.

### *2.2b Crystal structures of benzene polycarboxylates*

There are over a hundred structures solved for benzene polycarboxylates and a discussion of them all is beyond the scope of this review. For the dicarboxylates only the copper salts will be discussed (no structures were found in the literature of any zinc

salts). The review of the other anions includes other metal(II) carboxylates because there are fewer reported structures of copper and zinc salts.

*Benzene dicarboxylates*

Examples of copper benzene dicarboxylates are given in table 2.1. Included in the table are the carboxylate coordination, coordination around the copper, and the type of crystal structure. As reflected by table 2.1, structures for a range of copper phthalate salts have been reported, but only a few for terephthalate and none for copper isophthalate (the acids are shown in figure 2.7). The increased propensity of the dicarboxylates for bridging is evidenced by the number of compounds with polymeric structures, either chains or layers.

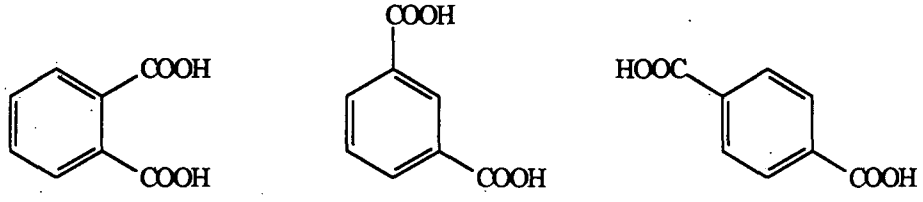


Phthalic Isophthalic Terephthalic

Figure 2.7 Benzene dicarboxylic acids.

Crystal structures of three copper phthalate salts have been determined: the monohydrate[51], dihydrate[50], and an acidic salt di(hydrogen phthalate) dihydrate[49]. The acidic salt is the only copper benzene dicarboxylate found in the literature with a monomeric crystal structure. One of the carboxylate groups is an acid site and does not coordinate to copper. The other carboxylate group chelates to the metal centre. Extensive H-bonding between the carboxylate groups and water holds the structure together.

| Compound | [a]Carboxylate Coord | Copper Coord[n] | Crystal Structure | Reference |
|---|---|---|---|---|
| $Cu(Hpht)_2 . 2H_2O$ | acidic [b]chelate (4) | octahedral | monomeric | 49 |
| $Cu(pht) . 2H_2O$ | monodentate anti-syn | square based pyramidal | layer | 50 |
| $Cu(pht) . H_2O$ | monodentate monatomic + syn | octahedral | layer | 51 |
| $M_2Cu(pht)_2 . 2H_2O$ (M = Li [c], K, Rb, Cs) | 2 x monodentate | square planar | chain | 52, 53 |
| $Na_2Cu(pht)_2 . 2H_2O$ | 2 x monodentate | square planar | layer | 53 |
| $MgCu(pht)_2 . 2H_2O$ | monodentate anti-syn | square planar | layer | 54 |
| $SrCu(pht)_2 . 3H_2O$ | monodentate anti-syn [d]{chelating (7)} | octahedral | chain | 54 |
| $BaCu(pht)_2 . 2H_2O$ | monodentate noncoordinate / 2 x monodentate [d]{chelating (7)} | square based pyramidal | ionic | 55 |
| $AgCu_2(pht)_2OH . 5H_2O$ | 2 x monatomic / monatomic + syn monodentate | octahedral and square based pyramidal | chain | 46 |
| $Cu(pht)(NH_3)_2$ | monodentate [b]chelate (4) | square based pyramidal | chain | 56 |
| $Cu(pht)pyr_2$ | monodentate [b]chelate (4) | square based pyramidal | chain | 57 |
| $Cu(pht)phen . 1.5H_2O$ | 2 x monodentate | square based pyramidal | chain | 58 |
| $Cu(pht)bipy . 2H_2O$ | monodentate monatomic [d]{chelating (7)} | square based pyramidal | dimeric | 59 |
| $Cu(Tpht)en . 2H_2O$ | 2 x monodentate | square based pyramidal | chain | 60 |
| [e] $Cu_2(Tpht)(pdt)_2(ClO_4)_2 . H_2O$ | 2 x monodentate | square based pyramidal | chain | 61 |

Table 2.1 Structural data for crystals of copper(II) phthalate (pht) and terephthalate (Tpht) salts.

[a] Dotted line separates the coordination of crystallographically different phthalate groups.

[b] Chelate (4), 4 membered chelate ring.

[c] The Li salt was tetrahydrate.

[d] Chelating (7), 7 membered chelate ring formed by two carboxylate groups.

[e] pdt, pentamethyldiethylenetriamine or pentaethyldiethylenetriamine.

The mono and dihydrates both have layer structures, but as indicated by the coordination found for the salts, the structures are very different. In the dihydrate the coordination around copper is square based pyramidal, and the phthalate ion bridges between three metal centres. As shown in figure 2.8, the coppers are bridged by the

phthalate ion forming chains. The apical site of the copper coordination is occupied by a carboxylate oxygen from an adjacent chain, bridging between the chains, forming layers.

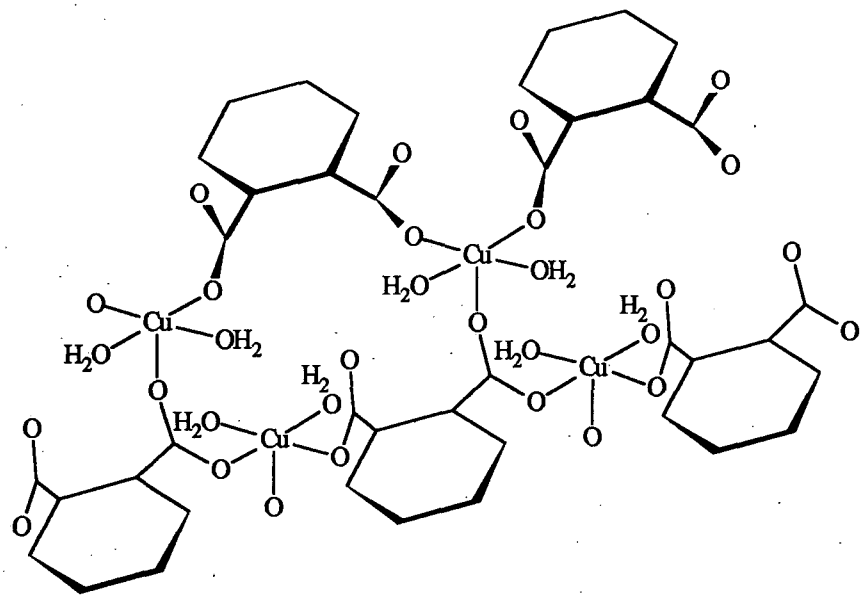

Figure 2.8 Layer structure of copper phthalate dihydrate.

Although copper phthalate monohydrate has very similar stoichiometry to the dihydrate, the crystal structure is very different. The difference in the structures is in part due to the versatility of the carboxylate coordination. For the monohydrate each phthalate ion coordinates to four metal sites. The distorted octahedral coordination around copper is composed of four carboxyl oxygens (from different phthalate groups) and two waters (axial). The octahedra share two edges, forming chains as shown in figure 2.9. These chains are bridged together by the phthalate ions, forming layers.

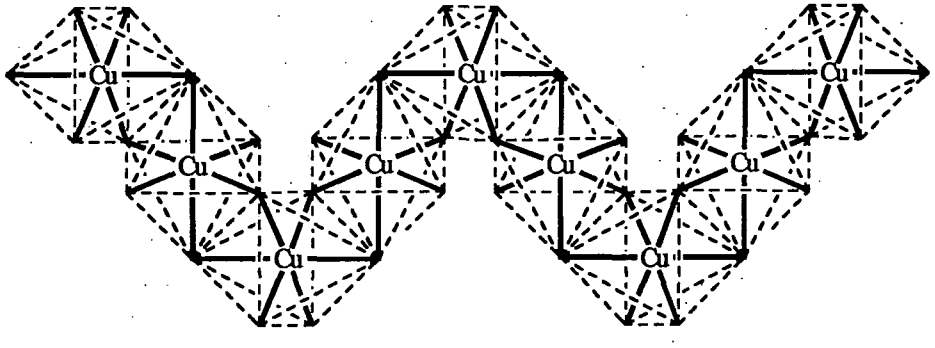

Figure 2.9 Chain of octahedral coppers in copper phthalate monohydrate.

A number of crystal structures have been reported for phthalate and terephthalate compounds which also have other ligands coordinated to the copper. Most of the structures are polymeric chains, the phthalate ion simply bridging between two metal centres. One exception is copper phthalate bipyridine dihydrate. This crystallises as a

dimer, the two copper centres are coordinated together by two monatomic bridges[59], figure 2.10.

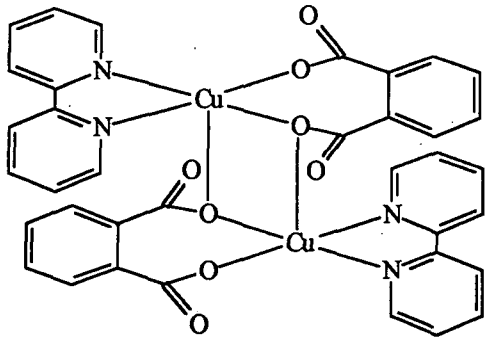

Figure 2.10 Copper phthalate bipyridine dihydrate.

A series of crystal structures was reported by Cingi *et al* as part of a study of the influence of alkaline and alkaline earth cations on the structures of polymeric copper(II) phthalate[52-55]. They found that when the co-cation was an alkali metal, the coordination around the copper was square planar[52,53] (cf. square based pyramidal or octahedral). The compounds also had similar chain structures, shown in figure 2.11; the alkali cations were situated between the chains. The copper/sodium salt was the only exception and this had a layer structure. The copper alkaline earth phthalates crystallised with various copper coordinations and different structures (e.g. $Mg^{2+}$, layer; $Ba^{2+}$, monomeric; $Sr^{2+}$, chain)[54,55].

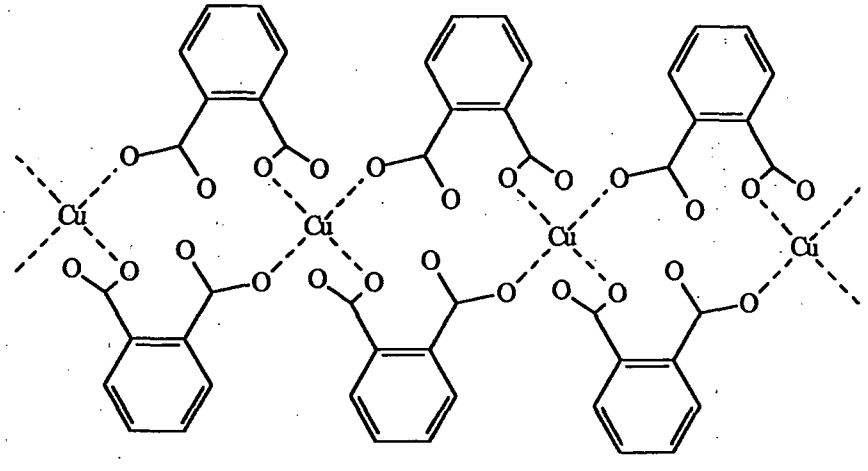

Figure 2.11 Copper phthalate chain present in the crystal structure of $M_2Cu(pht) . 2H_2O$ (M = Li, K, Rb).

Cingi *et al* also published the crystal structure for a silver/copper mixed metal phthalate[46]. This compound had a complicated, highly coordinated chain structure. The chain structures previously mentioned all had the phthalate ion bridging between two metal centres. The chain structure found for the silver/copper salt was unusual because

of the degree of bridging present. There are two crystallographically distinct phthalate ions; one bridges between four metal centres, and the other between three.

Of the compounds listed in table 2.1, the majority of structures are polymeric chains. There are also four layer structures, but only three mono/dimeric structures. The preference of the salts to form polymeric structures can be attributed to the enhanced ability of the dianions to bridge between metal centres compared with monocarboxylates.

*Benzene tricarboxylates*

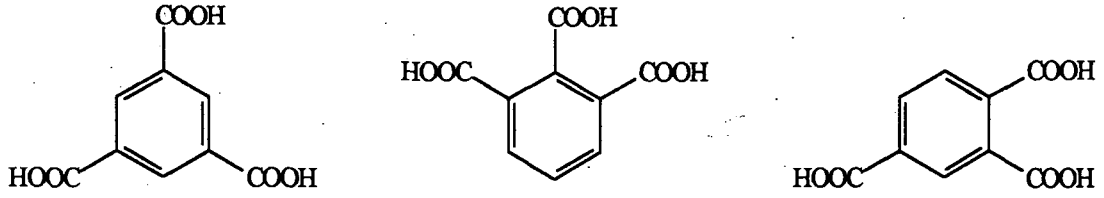


Trimesic Hemimellitic Trimellitic

Figure 2.12 Benzene tricarboxylic acids.

As can be seen from table 2.2, there are very few reported crystal structures of metal(II) benzene tricarboxylates. The two copper salts shown in the table both contain acidic groups. In the hemimellitate compound the copper has displaced only one of the acidic protons (from the 2 position)[29]. The coordination polyhedron is square based pyramidal, formed by two monodentate carboxylate groups, trans in the base, and three waters occupying the other positions, figure 2.13a. Copper hydrogen trimesate has one acidic proton remaining[28]. The trimesate dianion bridges between the coppers, forming polymeric chains, figure 2.13b.

| Compound | Carboxylate Coord$^n$ | Copper or Zinc Coord$^n$ | Crystal Structure | Reference |
|---|---|---|---|---|
| $CuH(tms) . 3H_2O$ | acidic<br>2 x monodentate | square based pyramidal | chain | 28 |
| $Na_2Zn_2(tms)_2 . 11H_2O$ | noncoordinated<br>2 x (monatomic + anti) | trigonal bipyramidal | layer | 27 |
| $CuH_2(hmel)_2 . 6H_2O$ | 2 x acidic monodentate | square based pyramidal | monomeric | 29 |

Table 2.2 Structural data for crystals of copper(II) and zinc trimesate (tms) and hemimellitate (hmel) salts.

The structure of a sodium/zinc mixed metal trimesate has also been reported[27]. Only two of the carboxylate groups coordinated to metal centres, but the high connectivity for the crystal structure produced polymeric layers (each trimesate group coordinates to six different metal sites).

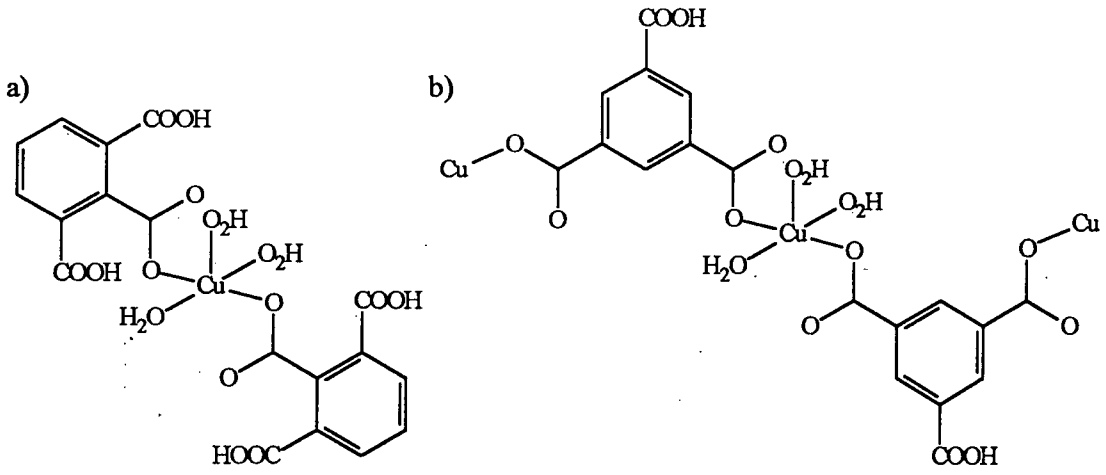


Figure 2.13 a) Copper bis(dihydrogen hemimellitate) hexahydrate and
b) Copper hydrogen trimesate trihydrate.

With so few structures reported for the tricarboxylates, it is difficult to make generalisations about the structural chemistry of these salts.

*Benzene tetracarboxylates*

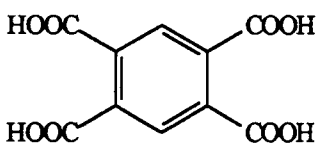


Figure 2.14 Pyromellitic acid

Apart from pyromellitic acid, figure 2.14, there are two other tetracarboxylic acids, 1,2,3,5- and 1,2,3,4-, but no crystal structures have been reported for the salts of these acids. Structural information on metal(II) pyromellitates reported in the literature is given in table 2.3. Salts with other ligands attached to the metal centre have not been included. It is evident from table 2.3 that the most common type of crystal structure for the pyromellitates is a polymeric layer. One might expect this to be a common structure because of the geometry of the tetra-anion. The ion consists of four carboxylate groups positioned symmetrically around a planar ring; ideal for bridging between metals to form layers. Both copper and zinc pyromellitates have polymeric layer structures. The copper salt has planar sheets[64] whereas the zinc salt has corrugated layers[31]. The coordination around the copper is square based pyramidal. This would appear to be a common coordination polyhedron for copper benzene polycarboxylates.

| Compound | Carboxylate Coord$^n$. | Metal Coord$^n$ | Crystal Structure | Reference |
|---|---|---|---|---|
| $Co_2PM \cdot 18H_2O$ | 2 x noncoordinated<br>2 x monodentate | octahedral | chain | 25, 62 |
| $Zn_2PM \cdot 7H_2O$ | 3 x monodentate<br>anti-syn | octahedral and tetrahedral | layer | 31 |
| $Ca_2PM \cdot 6H_2O$ | 2 x chelate (4)<br>2 x (chelate (4) + anti) | 8 coordinate | layer | 32 |
| $Na_2ZnPM \cdot 9H_2O$ | monodentate<br>anti-syn<br>monatomic<br>monatomic + anti | tetrahedral (Zn)<br>octahedral (Na) | 3D channel structure | 63 |
| $Cu_2PM \cdot 10H_2O$ | 4 x monodentate | square based pyramid | layer | 64 |
| $CoH_2PM \cdot 6H_2O$ | [a] noncoordinated | octahedral | ionic | 65 |

Table 2.3 Structural data for crystals of metal(II) pyromellitates (PM).
[a] Adjacent carboxylates are bridged via a very strong intramolecular H-bond.

Cobalt dihydrogen pyromellitate has an unusual ionic structure[65], in which $H_2PM^{2-}$ anions are balanced by $[Co(H_2O)_6]^{2+}$ ions. The acidic protons of the pyromellitate dianion are intramolecularly H-bonded between adjacent carboxylate groups, forming an unusually strong H-bond (O-H, 1.21Å), figure 2.15

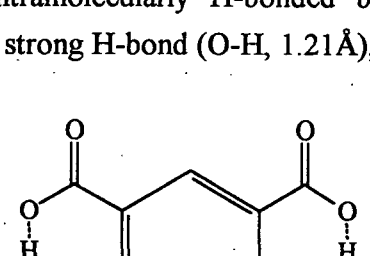

Figure 2.15 $H_2PM$ dianion from $CoH_2PM \cdot 6H_2O$.

Cobalt pyromellitate octadecahydrate has a polymeric chain structure consisting of $[Co(H_2O)_4PM]_n^{2-}$ units[25]. The pyromellitate group acts as a bismonodentate ligand, two para carboxylate groups coordinating to the cobalts. The charge is balanced by $Co(H_2O)_6^{2+}$ ions which are intercalated between the chains. Compared with the other pyromellitate structures in table 2.3, it is the only compound to have two uncoordinated carboxylate groups. These two carboxylate groups are involved in extensive H-bonding with water.

A three-dimensional channel structure was found for crystals of zinc disodium pyromellitate nonahydrate[63]. The sides of the quadrangular channels consisted of aligned pyromellitate groups. These were coordinated together by tetrahedral zincs situated at the intersections, figure 2.16. The sodium atoms were coordinated to the

pyromellitates and water. The water was located within the channels. H-bonding was an important part of the structure and attempts to remove the water led to the collapse of the structure.

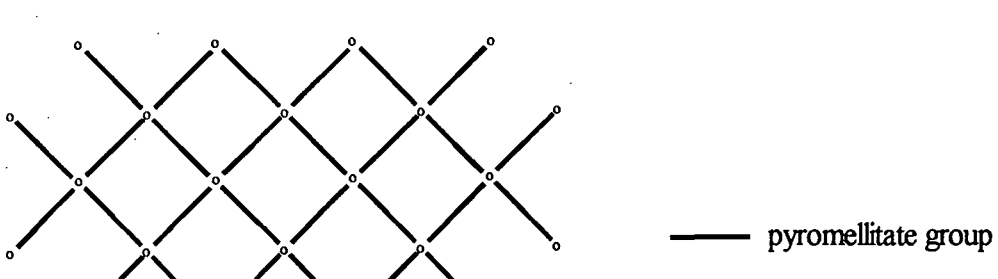


Figure 2.16 Schematic view down the channel structure of $Na_2ZnPM \cdot 9H_2O$.

*Benzene hexacarboxylates*

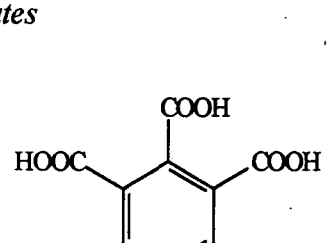


Figure 2.17 Mellitic acid.

There is no benzene pentacarboxylate section because there was little in the literature about these salts and no crystal structures. Mellitic acid has six carboxylic acid groups positioned around a phenyl ring, figure 2.17. The metal salts with known crystal structures are listed in table 2.4.

| Compound | Carboxylate Coord$^n$ | Metal Coord$^n$ | Crystal Structure | Reference |
|---|---|---|---|---|
| $Ca_2H_2Mel \cdot 9H_2O$ | 2 x acidic<br>2 x noncoordinated<br>2 x ([a]chelate (4) + anti-anti) | 7 and 8 coordinate | layer | 48 |
| $Co_3Mel \cdot 18H_2O$ | 6 x monodentate<br>{2 x [b]chelating (7)} | octahedral | chain | 67 |
| $Cu_5(HMel)_2 \cdot 22H_2O$ | 2 x noncoordinate<br>3 x monodentate<br>anti-syn | octahedral and square based pyramidal | layer | 68 |
| $Cu_7(OH)_4(HMel)_2 \cdot 26H_2O$ | acidic<br>syn-syn<br>4 x monodentate | square based pyramidal | layer | 69 |

Table 2.4 Structural data for crystals of metal(II) mellitates (Mel).
[a] Chelate (4), 4 membered chelate ring.
[b] Chelating (7), 7 membered chelate ring formed by two carboxylate groups.

Of the four examples, in only one compound had the metal displaced all six acidic protons. In one of the copper salts there were hydroxyl groups as well as a protonated mellitate ion. The difficulty in forming a mellitate hexa-anion can be related to the ease of dissociation of the protons. Table 2.5 gives the dissociation constants for the successive deprotonation of mellitic acid[66]. One can see from these results that the final proton dissociated is very weakly acidic. This explains why the mellitate was not completely deprotonated in three of the examples in table 2.4.

| $K_1$ | $K_2$ | $K_3$ | $K_4$ | $K_5$ | $K_6$ |
|---|---|---|---|---|---|
| $4.0 \times 10^{-2}$ | $6.4 \times 10^{-3}$ | $4.9 \times 10^{-4}$ | $1.7 \times 10^{-5}$ | $1.3 \times 10^{-6}$ | $1.1 \times 10^{-7}$ |

Table 2.5 Dissociation constants for mellitic acid[66].

An uncommon type of carboxylate bridging, chelating plus anti-anti, was found for calcium dihydrogen mellitate nonahydrate[48]. Only two carboxylate groups (para) coordinate to the metals. The structure consists of calcium carboxylate chains, as shown in figure 2.18, bridged together via the phenyl ring, forming layers.

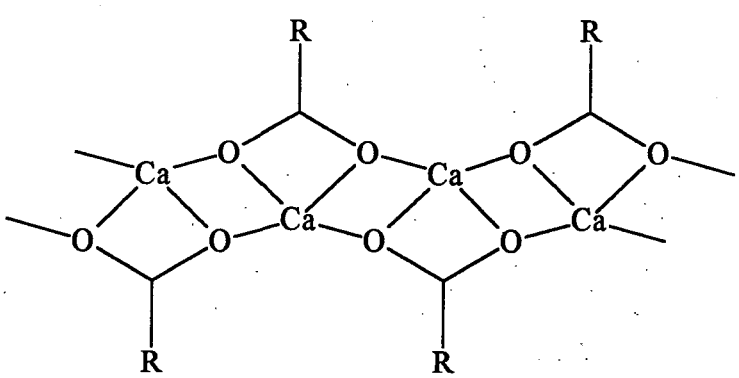


Figure 2.18 Calcium carboxylate chains in $CaH_2Mel \cdot 9H_2O$ $R=C_6(COO)_2(COOH)_2$

From the crystal structures given in table 2.4, three layer structures have been reported and one polymeric chain. It would appear that, like pyromellitate, polymeric layers are the common structure for crystals of metal(II) mellitates. For both pyromellitates and mellitates this observation can be rationalised by the geometry of the anion, viz. multiple (>2) carboxylate groups positioned around a planar, phenyl ring.

It was found that in the majority of the benzene dicarboxylates, the dianions bridged between two metals, forming polymeric chains. Layer structures were formed when the dianions coordinated to more than two metals. The only exception to this was $AgCu_2(pht)_2OH \cdot 5H_2O$, in which the dianion bridges between four metals but only formed chains.

Very few structures have been determined for benzene tricarboxylates, and only one of these had the fully deprotonated trianion. The structure found for this salt (disodium zinc trimesate) was a layer. One might expect the most common structure formed by the salts of the trianions to be polymeric layers because of the geometry of the anion (as discussed above). It was found from the dicarboxylate results that layer structures were normally formed when the anion coordinated to more than two metals. The trianions have a greater ability than the dicarboxylates to coordinate to more than two metal sites, making layer structures more probable.

For the same reasons as above, one would also expect the prevalent structure found for benzene pentacarboxylates to be layers.

### *2.2c Structural characterisation by vibrational spectroscopy*[24,70,71]

Because of the difficulty of growing single crystals of benzene polycarboxylates (>2 carboxylates) for structure determination, it is highly desirable to deduce structural features from the spectroscopy of powdered samples. Deacon and Phillips compared the IR spectra of 70 metal acetates with their structural features, as determined by single crystal XRD[70].

The IR spectrum of sodium acetate has been fully assigned[72] and the data are given in table 2.6. Although no XRD structure determination has been made for sodium acetate, or any other ionic acetate, the structure was deduced as ionic from its solution and solid state spectra.

| Type of vibration | Assignment | Wavenumber $cm^{-1}$ | Type of vibration | Assignment | Wavenumber $cm^{-1}$ |
|---|---|---|---|---|---|
| $A_1\ \nu_1$ | $CH_3$ sym. str. | 2936 | $B_1\ \nu_9$ | $CH_3$ def. | 1430 |
| $A_1\ \nu_2$ | $CH_3$ sym. def. | 1344 | $B_1\ \nu_{10}$ | $CH_3$ rock | 1009 |
| $A_1\ \nu_3$ | $CO_2$ sym. str. | 1414 | $B_1\ \nu_{11}$ | $CO_2$ rock | 460 |
| $A_1\ \nu_4$ | C-C str. | 924 | $B_2\ \nu_{12}$ | CH asym. str. | 3010 or 2989 |
| $A_1\ \nu_5$ | $CO_2$ sym. def. | 646 | $B_2\ \nu_{13}$ | $CH_3$ def. | 1443 |
| $A_2\ \nu_6$ | torsion | —— | $B_2\ \nu_{14}$ | $CH_3$ rock | 1042 |
| $B_1\ \nu_7$ | C-H asym. str. | 2989 or 3010 | $B_2\ \nu_{15}$ | $CO_2$ o.o.p. def. | 615 |
| $B_1\ \nu_8$ | $CO_2$ asym. str. | 1578 | | | |

Table 2.6 Assignments of frequencies in the IR spectrum of sodium acetate.

Metal coordination to the acetate anion will affect the $\nu$(C-O) frequencies $\nu_3$, $\nu_5$, $\nu_8$, $\nu_{11}$ and $\nu_{15}$. Studies have focused on the $\nu(CO_2)$ symmetric and asymmetric stretch

and in particular how the separation between these bands, $\Delta\nu_{(asym\text{-}sym)}$ is affected by the type of carboxylate coordination.

Deacon and Phillips concluded that compounds with $\Delta\nu_{(asym\text{-}sym)}$ significantly greater than ionic values (i.e. >200cm$^{-1}$; cf. Na($O_2$CMe), 164cm$^{-1}$) had monodentate carboxylate groups. It had previously been proposed that a monodentate carboxylate group may be thought of as a pseudo ester MO(R)C=O. This would increase the frequency for $\nu_{asym}(CO_2)$ and decrease that for $\nu_{sym}(CO_2)$ (compared to the absorptions for the free acetate ion), giving a greater $\Delta\nu_{(asym\text{-}sym)}$. But Deacon and Phillips found no correlation between $\Delta\nu_{(asym\text{-}sym)}$ of the monodentate carboxylates and either the OCO bond angle or C-O bond lengths to support this hypothesis.

It was found that $NaH(OOCMe)_2$ had a $\Delta\nu_{(asym\text{-}sym)}$ of 310cm$^{-1}$, suggesting monodentate coordination, but the acetate groups were not coordinated to any metal centres. In this compound the proton bridged between two acetate groups, figure 2.19, forming a very strong H-bond (O-H, 1.22Å). It would appear that the hydrogen acts as a pseudo metal, making the effective carboxylate coordination monodentate.

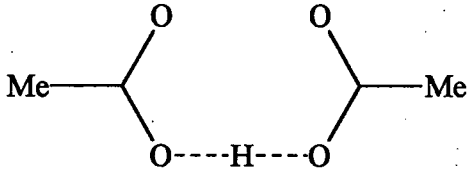


Figure 2.19 Very strong H-bond in $NaH(OOCMe)_2$. Hydrogen acts as a pseudo metal, coordinating to two acetate groups.

Values of $\Delta\nu_{(asym\text{-}sym)}$ significantly less than those for ionic acetate (i.e. values <150cm$^{-1}$) had either bridging or chelating acetates. In general it was found that values for $\Delta_{(chelating)}$ were less than those for $\Delta_{(bridging)}$, but there were a number of exceptions. Examples of both chelating and bridging were found with separations between 150-105cm$^{-1}$. Compounds with $\Delta\nu_{(asym\text{-}sym)} < 105cm^{-1}$ were mostly chelating acetates, but there were also some bridging examples. These examples were considered by the authors to be special cases because the acetates acted as a syn-syn bridge, and there was a very short metal-metal bond between the cations. Acetates with larger metal-metal bonds had $\Delta\nu_{(asym\text{-}sym)} > 105cm^{-1}$.

Values of $\Delta\nu_{(asym\text{-}sym)}$ close to that for the ionic sample (164cm$^{-1}$) were more ambiguous. There were no examples of monodentate coordination around this value but several bridging and one or two chelating. In summary:

| $\Delta\nu_{(asym-sym)}$ / $cm^{-1}$ | Carboxylate Coordination |
|---|---|
| >200 | monodentate |
| 164 | ionic (non coordinated) |
| 170-150 | ionic, bridging or chelating |
| <150 | bridging or chelating |
| <105 | chelating or syn-syn |

When extrapolating these findings to benzene polycarboxylates, one must remember that the changes in $\Delta\nu_{(asym-sym)}$ are relative to the separation found for the ionic anion. There are two further complications with assigning the IR spectra of benzene polycarboxylates: i) greater possibility of more than one type of carboxylate coordination; and ii) absorptions from the phenyl ring confusing this region of the spectrum. Luehrs *et al* compared the acetate results with the IR spectra of seventeen pyromellitate salts[24]. Unfortunately, only four of the pyromellitates had had their crystal structures determined. Table 2.7 gives values of $\Delta\nu_{(asym-sym)}$ and types of carboxylate coordination for these compounds.

| Compound | $\Delta\nu_{(asym-sym)}$ / $cm^{-1}$ | Carboxylate Coordination |
|---|---|---|
| $Tl_4PM$ | 180 | ionic |
| $Cu_2PM \cdot 10H_2O$ | 208 | monodentate |
| $CoH_2PM \cdot 6H_2O$ | 240 | pseudo monodentate[a] |
| $UO_2H_2PM \cdot 6H_2O$ | 150 | chelating |

Table 2.7 Spectroscopic and structural information for some selected pyromellitates. [a]Luehrs *et al* categorised the coordination as ionic.

Luehrs *et al* concluded that the pyromellitate salts of thallium (ionic), copper (monodentate) and uranium (chelating) had $\Delta\nu_{(asym-sym)}$ values in good agreement with those found for the metal acetates. However, cobalt dihydrogen pyromellitate hexahydrate has an ionic structure (discussed earlier, cf. section 2.2b) and a large value for $\Delta\nu_{(asym-sym)}$ of 240$cm^{-1}$. The authors concluded that the unusually large separation was due to H-bonding to water. Although they were correct in stating that the carboxylate groups were not coordinated to a metal centre, no account was taken of the intramolecular H-bond between adjacent carboxylate groups (O-H bond length 1.21Å, figure 2.20). The hydrogen can be viewed as a pseudo-metal, making the carboxylate coordination monodentate. This is analogous to the strong H-bonding found for $NaH(O_2CMe)_2$ discussed previously (figure 2.19).

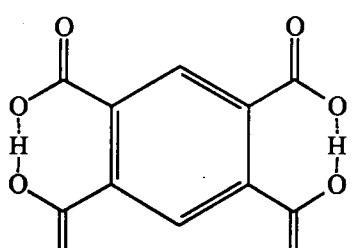

Figure 2.20 Very strong intramolecular H-bond found for the pyromellitate dianion in $CoH_2PM \cdot 6H_2O$.

The authors found that the IR spectrum of the cobalt salt had broad intense envelopes from 1800-900cm$^{-1}$, indicative of very strong H-bonds. However, no reference was made to the strong intramolecular H-bond that exists in the salt. Unusually strong H-bonding was also deduced for several other compounds: $Na_2H_2PM \cdot 2H_2O$, $(NH_4)_3HPM \cdot H_2O$ and $M(H_3PM)_2 \cdot 12H_2O$ (M = Zn, Fe, Ni). One can see that all of these compounds have acidic protons. It is not unreasonable to assume that these compounds also have intra- or intermolecular H-bonds similar to those found for the cobalt dihydrogen pyromellitate, and sodium hydrogen diacetate respectively. If intermolecular H-bonds exist, these will lead to either anionic dimers, oligomers or polymers, figure 2.21. However, considering the close proximity of adjacent carboxylate groups, one might expect an intramolecular H-bond to be more favourable.

Dimeric

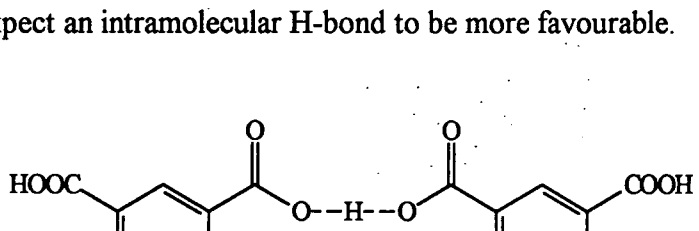

Polymeric

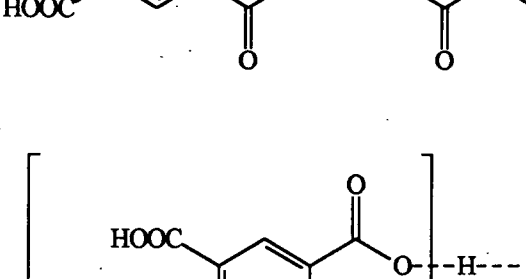

Figure 2.21 Intermolecular H-bonding possible for $H_3PM$ anion.

$\Delta\nu_{(asym\text{-}sym)}$ values were not given for the sodium and ammonium salts, but all the $M(H_3PM)_2 \cdot 12H_2O$ compounds had separations >200cm$^{-1}$, indicative of monodentate coordination. From the above information and examples it is reasonable to

predict that the crystal structure for the $M(H_3PM)_2 . 12H_2O$ salts would be ionic (i.e. no coordination between the metal and pyromellitate anion). The anion has three acidic protons and one of these is involved in a very strong intramolecular H-bond between adjacent carboxylates. The proton acts as a pseudo metal, making the carboxylate coordination monodentate. The cation is probably surrounded by six waters, forming an octahedral coordination sphere.

Luehrs *et al* concluded that $\Delta\nu_{(asym-sym)}$ could give information about the carboxylate coordination in pyromellitate salts, viz.:

| $\Delta\nu_{(asym-sym)}$ / $cm^{-1}$ | **Carboxylate Coordination** |
|---|---|
| >200 | monodentate |
| 180-170 | ionic (non coordinated) |
| 150-90 | chelating or bridging |

However, one should be cautious when assigning $\Delta\nu_{(asym-sym)}$ values for pyromellitates, as this correlation was based on only four compounds. Further, unambiguous examples are required to verify the correlation between $\Delta\nu_{(asym-sym)}$ and the carboxylate coordination for pyromellitate salts.

## 2.3 Thermal Decomposition of Metal Carboxylates.

Metals and metal oxides can be prepared by the thermal decomposition of metal carboxylates. Several areas of chemistry use thermal decomposition as a preparative route to metal/metal oxide systems (e.g. catalysis[73,74], thin film deposition[75], oxide supports[76] and ceramics[75,77] ). The type of carboxylate and the conditions of the thermal decomposition can affect the physical and chemical properties of the product. For example, Fields and Meyerson found that the surface area and porosity of silver produced by thermal decomposition of silver carboxylates was dependent on the carboxylate used[78].

| | | Surface area $m^2 g^{-1}$ | Pore diameter Å |
|---|---|---|---|
| silver trimesate | $\xrightarrow{\Delta}$ $Ag^0$ | 0.6 | 15-20 |
| silver mellitate | $\xrightarrow{\Delta}$ $Ag^0$ | 550 | 15-600 |

The thermal decomposition of solids is an important class of topochemical reaction. In a review of topochemistry Boldyrev[79] defined a topochemical reaction to be one in which:

i) the beginning of the reaction is associated with a definite site in the crystal. The site can be either a specific point in the unit cell or a lattice defect;
ii) there is feedback between the reaction and the properties of the solid in which the reaction proceeds (including reactivity); and
iii) there is a relationship between the thermodynamic and structural features of the starting material and the resulting product.

Thus in a topochemical reaction there is a preferential site where the reaction begins and also a localisation of the reaction around this nucleus. The zone in which the reaction preferentially proceeds is called the reaction interface. This interface is associated with the boundary of the nucleus. The nature of the reaction interface will influence the thermodynamic and structural relationship between the starting material and resulting product. In a review of the findings published by his research group[80], Galwey discussed the relationship between the type of nucleus and the resulting product. Many of the topochemical reactions studied were thermal decompositions, under vacuum, of metal carboxylates. The carboxylate anions included formate and a variety of dicarboxylates. The dicarboxylates are shown in figure 2.22. In their work Galwey *et al* encountered three types of nuclei: functional, fusion and fluid-flux.

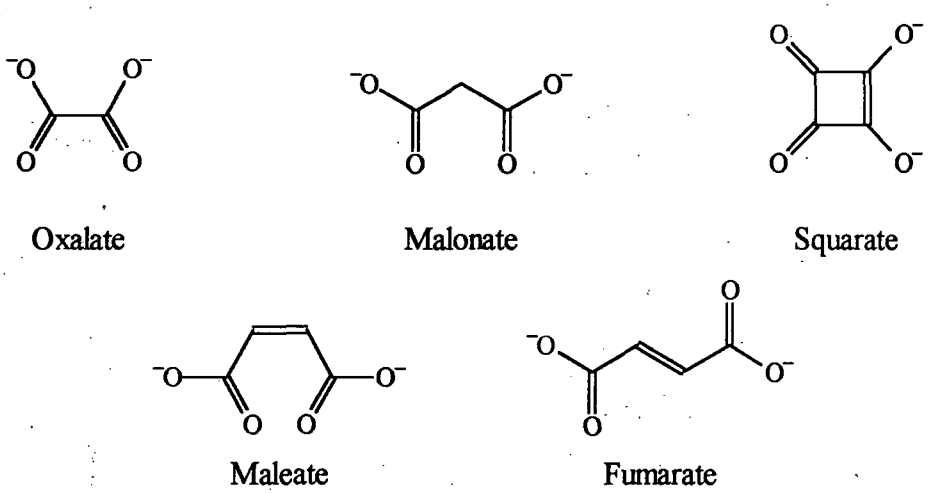


Figure 2.22 Carboxylate dianions studied by Galwey *et al*[80-88].

*1. Functional nuclei.* The product is also a catalyst of the reaction, making the process autocatalytic. Examples include the decomposition of nickel[81] and silver[82] squarate, and silver malonate[83].

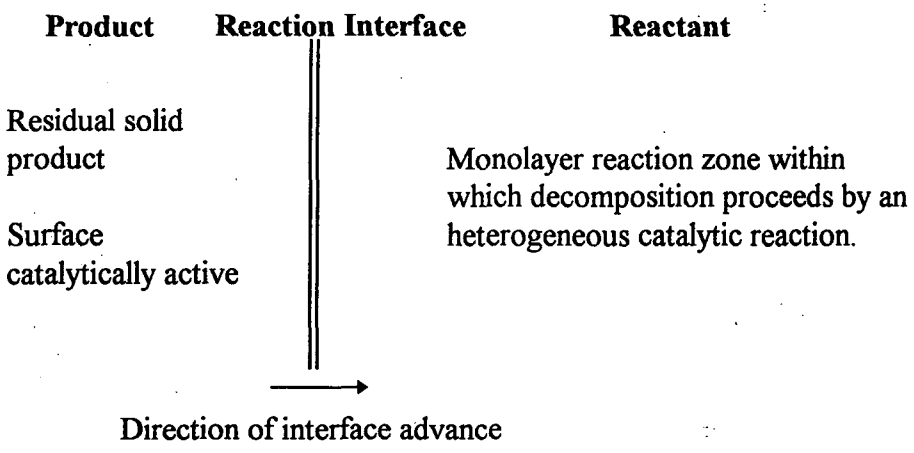


*2. Fusion nuclei.* The reaction interface is a region of temporary fusion, within which the reaction proceeds more readily. Melting was envisaged as a consequence of the production of a low melting point intermediate, or through the formation of a eutectic with the reactant.

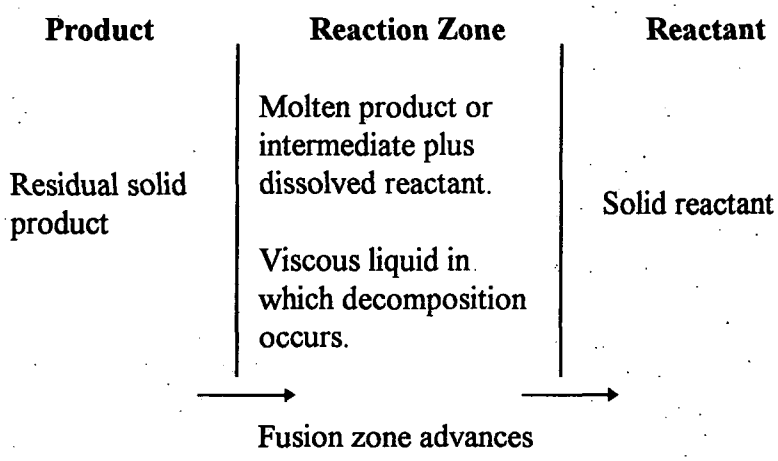


Copper(II) malonate thermally decomposed via fusion nuclei[84]. The reaction involved froth production identified with the occurrence of reaction in a viscous liquid. The nature of the liquid phase was not deduced, but it was found that the liquid phase was produced after the formation of an acetate intermediate.

$$2CH_2(CO_2)_2Cu \longrightarrow CH_2(CO_2Cu)_2 + 2CO_2 \quad [+ C + C_xH_y + (CH_3CO_2)_2Cu]$$

$$CH_2(CO_2Cu)_2 \longrightarrow Cu + 2CO_2\ [+ C_xH_y + C]$$

*3. Fluid-flux nuclei.* Such nuclei have special structures (normally a porous product) that can temporarily retain a condensable product. The condensed phase provides a medium within which the reaction preferentially proceeds. No metal carboxylate

decompositions have been reported with such nuclei. An example of fluid-flux nuclei is the reaction of potassium bromide with chlorine[80].

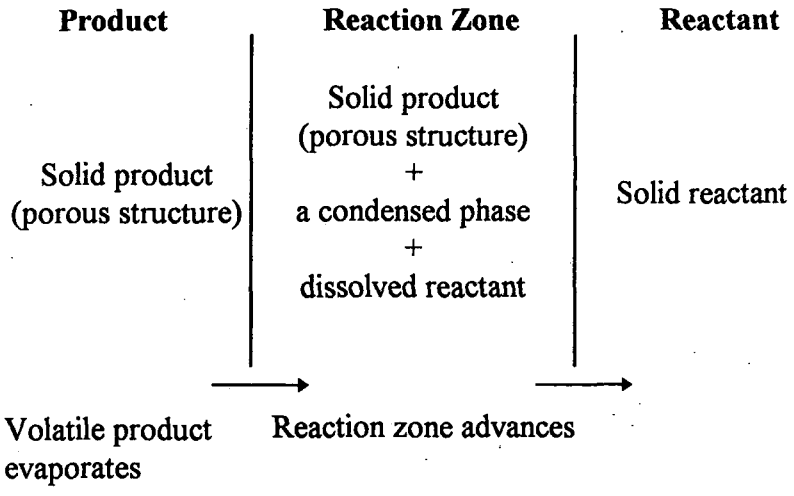


Liquid bromine was condensed at the reaction interface in the pores of the product. It was believed that chlorine reacted with potassium through ionic interactions in the homogenous phase.

$$KBr + Cl_2 \longrightarrow K[Br \cdot Cl_2] \{\text{in } Br_2 \text{ liquid}\} \longrightarrow KCl + BrCl$$

These three nuclei were the only ones encountered by Galwey *et al*, however, two further types of nuclei were envisaged.

*4. Furtive nuclei.* Very finely divided particles of product, dispersed throughout the reactant. Such nuclei could be difficult to identify and characterise.

*5. Fictive nuclei.* No residual product phase is formed, for example in the sublimation of a solid. Reactions involving these nuclei would not be classed as topochemical reactions as defined by Boldyrev (see above).

The thermal decompositions reported by Galwey *et al* were all carried out under vacuum. Other copper(II) carboxylates studied by the group include the maleate[85] and oxalate[86] salts. Both salts decomposed in a stepwise manner, $Cu^{2+} \rightarrow Cu^{+} \rightarrow Cu^{0}$. Temporary localised melting was detected with the first step (formation of a copper(I) salt), evidence of fusion nuclei. It was found that copper(II) maleate underwent an anionic isomerisation during the first step. The anion rearranged to the trans form, fumarate (see figure 2.22, p.28).

The second step (decomposition of the copper(I) salt) had a lower rate of reaction than the first step. There was no evidence of further melting, and it was concluded that the decomposition of the copper(I) salt proceeded in the solid state.

Copper(II) squarate[87], fumarate[85] and formate[88] were also studied. These salts decomposed via the stepwise reduction of the copper. Like the copper salts above, the rate of decomposition of the copper(I) salt was slower than the rate of reduction of the copper(II) salt. Due to insufficient data no conclusions were made about the type of reaction nuclei.

All of these decompositions yielded copper metal as the product. Carbon was also formed in the decompositions of copper(II) malonate and squarate. The product from the decomposition of the maleate and fumarate salts was copper supported on a polymeric carbonaceous residue.

The organic products formed during thermal decomposition under vacuum were studied by Taki *et al*[89]. It was shown that in some cases the rate of heating produced different yields of products. For example, the main organic product from the thermal decomposition of copper(II) fumarate and maleate was ethene. When the salts were rapidly heated using a laser, the main product was acetylene (the yield for both products was ~10%). It was proposed that this was due to rapid decarboxylation of the anion when heated by a laser, forming acetylene before the intermediate product was protonated.

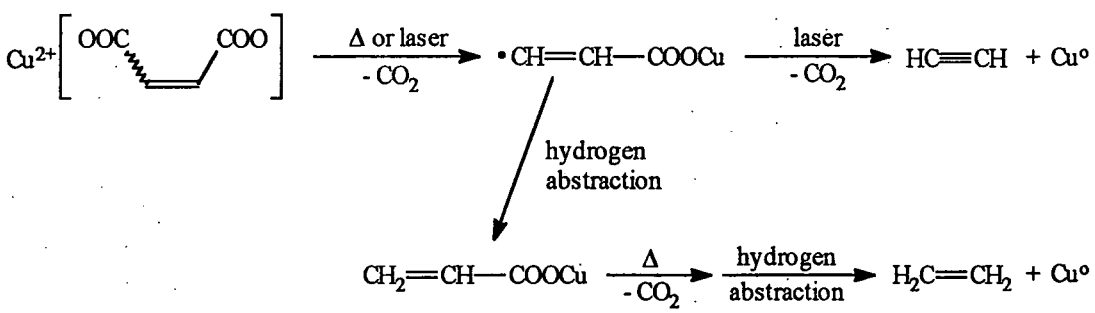


Taki *et al* also found that when physical mixtures of copper carboxylates were rapidly decomposed, they produced organic products (<1%) which were formed by the recombination of the radical intermediates. For example, the decomposition of copper benzoate in the presence of copper acetate, propionate and isobutyrate produced traces of toluene, ethyl benzene and isopropyl benzene respectively.

$$(PhCO_2)_2Cu + (RCO_2)_2Cu \xrightarrow{\Delta} PhR \quad (<1\%)$$

Fewer studies have been made of the thermal decompositions of zinc or copper benzene polycarboxylates. DTA-TG (differential thermal analysis – thermogravimetry)

results have been published for the decomposition under air for copper[90] and zinc[91] benzene dicarboxylates, and copper tricarboxylates[92].

The copper salts lost water of crystallisation by 200°C (an endothermic event) and all decomposed at 300-500°C. The decompositions were all exothermic and copper(II) oxide was the final product. Copper trimesate and hemimellitate (but not the trimellitate) formed some copper(I) oxide during decomposition when heated at a slower rate (5°C $min^{-1}$, cf. 10°C $min^{-1}$). The copper(I) oxide was subsequently oxidised. This was deduced from an increase in sample weight at the end of the decomposition ($Cu_2O \rightarrow 2CuO$).

Zinc benzene dicarboxylates all had similar DTA-TG's. Endotherms at 100-450°C were attributed to loss of water, but the weight loss did not account for all the water. The salts still had 0.5-1 water of crystallisation remaining. The decompositions occurred from ~400°C, continuing to ~700°C. The author stated that the decompositions were a one step process, forming zinc oxide. However, it was evident from the DTA-TG plots that the decomposition consisted of at least two events. First there was a very sharp loss of weight (~40%, ≅115m.u.) with a small endotherm. From the plots this looked like an endotherm occurring just after the start of an exotherm. A more gradual loss of weight followed (~15%, ≅45m.u.) and this second event was very exothermic. With no further results it is not possible to determine what these two events were. However, in the summary of chapter 6 (Thermal Decomposition of Zinc/Copper Trimellitates and Pyromellitates) two processes are proposed to explain these observations.

The decomposition under nitrogen of copper bis(hydrogen phthalate) dihydrate was reported by Goeta *et al*[93] (cf. table 2.1 for crystal structure information). They found that the decomposition involved three endothermic events (150, 200 and 310°C). The first event was attributed to loss of water. During the second endotherm phthalic anhydride was produced. It was proposed that this was due to proton transfer between the monoanions forming phthalate dianion, phthalic anhydride and water. The product from this was assumed to be copper(II) phthalate, which decomposed at 340°C, yielding metallic copper and a carbonaceous residue.

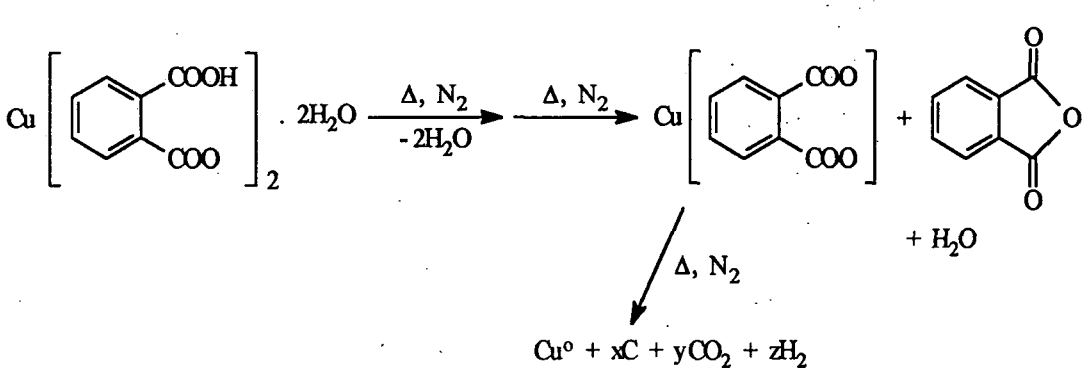

A versatile route for the formation of terephthalic acid is the Henkel reaction[94]. Potassium benzene carboxylates (mono and poly) can be converted into potassium terephthalate by heating the sample to 350-430°C under a carbon dioxide atmosphere. A zinc or cadmium catalyst is also required. The Henkel reaction is strictly the decarboxylation of a benzene carboxylate. However, rearrangement and carboxylation reactions also occur.

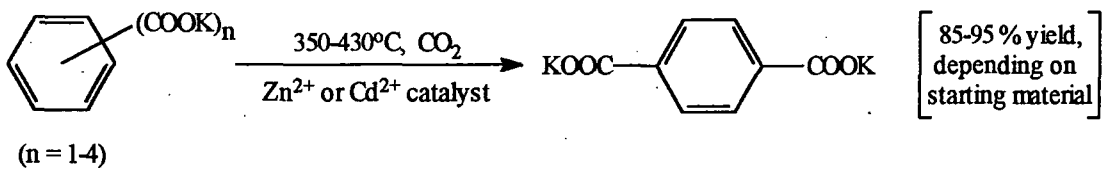


(n = 1-4)

Although not strictly thermal decomposition, this reaction shows the potential of benzene polycarboxylates to undergo thermal decarboxylations and rearrangements, to form the thermodynamically preferred product, terephthalate.

## 2.4 Uses of aromatic carboxylates

Metal carboxylates are an important class of industrial chemicals and have a large number of applications. A detailed review of these materials is beyond the scope of this thesis, but some illustrative examples of the uses of aromatic carboxylates are given below.

*a) Light and heat stabilisers.* Metal benzene carboxylates are often added to polymers to improve the stability of the polymers. Copper and lead salts have been used as stabilisers for siloxane rubbers[95] and polymers[96,97]. Transition metal salts of benzene dicarboxylates have also been used to improve the fading resistance of colour recording material[98]. Fire retardents is another large field of application. Zinc salts have been used as charring agents for polymers, including PVC[10,11] and polybromostyrene[12].

*b) Fungicides and herbicides.* Phthalic acid reacted with copper(II) in the presence of amines forms a fungicidal/herbicidal compound suitable for the control of apple canker and weeds[99]. Copper and zinc napheneates have been used as fungicides for the preservation of wood and textiles[100].

*c) Catalysts.* High surface area silver catalysts have been prepared by the thermal decomposition of silver aromatic polycarboxylates[13]. Silver is used as a heterogeneous catalyst for oxidation, cyclisation and cracking reactions. Cobalt pyromellitate has been shown to be a homogeneous catalyst for oxidation of acetic acid to peracetic acid[101].

*d) Magnetic exchange interactions.* There has been a great deal of interest in the unusual exchange interactions found in copper carboxylates[43,44]. More recently, some researchers have been studying the magnetic properties of benzene polycarboxylates[8,9].

*e) Detergents.* Sodium mellitate and pyromellitate have been used in the formation of detergents, replacing the sodium tripolyphosphates normally used. It was found that the detergents produced were comparable to those based on the phosphates[102].

*f) Other uses.* Cobalt, zinc and nickel salts of pyromellitic acid can be added to poly(ethylene terephthalate) melts to produce coloured polymers[103]. There has also been interest in the formation of one dimensional conductors, using benzene polycarboxylates to bridge between metal centres, forming polymeric chains[65].

# 3. PREPARATION OF ZINC/COPPER MIXED METAL HYDROXYCARBONATES

## 3.1 Introduction

This chapter describes work undertaken to identify the reaction conditions necessary to form single phase zinc/copper hydroxycarbonates. As will be demonstrated, the reaction between zinc/copper nitrate and sodium or potassium carbonate was not as straightforward as was first expected. The aim of the work reported here was to prepare suitable precursors for the synthesis of mixed metal carboxylates (i.e. single phase hydroxycarbonate). Consequently, it was not an exhaustive study of the preparation of zinc/copper hydroxycarbonates. The introduction gives a brief overview of the background of the study, and of the literature on the chemistry of hydroxycarbonates. This is followed by a discussion of the results and the conclusions from the work presented here. Finally the experimental details are given at the end of the chapter.

It was previously discovered[2,3] that the compositions of trimellitate and pyromellitate products, precipitated from an appropriate nitrate or sulphate solution, were highly dependent on pH (see section 1.2). To avoid forming mixed phases, zinc/copper hydroxycarbonates were used as intermediates, reacting them with trimellitic and pyromellitic acid to form the respective mixed metal salts[3]. The advantages of using hydroxycarbonates as intermediates were that:

i) they acted as templates for the formation of mixed metal carboxylates;
ii) they were pH buffers, helping to control the reaction conditions; and
iii) alkali metal salts of the acids were no longer required for the formation of mixed metal carboxylates, avoiding the inclusion of alkali metals in the product.

Zinc/copper hydroxycarbonates were precipitated from zinc/copper nitrate solutions by the addition of either sodium or potassium carbonate solution. Depending on the reaction conditions this produced one of several mineral phases or a mixture. For example:

$$(Zn,Cu)(NO_3)_2 + Na_2CO_3 \xrightarrow{H_2O} (Zn,Cu)_2CO_3(OH)_2$$

In the literature five mineral phases were commonly reported as resulting from similar preparations. There now follows a brief discussion of the different hydroxycarbonate phases, which is followed by a review of the literature on the preparation of hydroxycarbonates.

### *3.1a Hydroxycarbonate phases*

*Hydrozincite*, $Zn_5(CO_3)_2(OH)_6$ (colour: white), has a layer structure[104] consisting of zinc octahedra joined via 4 edges, forming a layer with $C_6$ symmetry, figure 3.1. Vacancies are located in alternate sites for alternate rows of octahedra. Tetrahedrally coordinated zinc atoms are situated above and below these vacancies. The ratio of tetrahedral to octahedral sites is 2:3. The layers are bridged by carbonate groups forming a 3-D lattice. Synthetic basic zinc carbonates always contain water, mostly adsorbed to the surface but some may be in channels situated between the rows of carbonate ions[104]. Synthetic hydrozincite can be deficient in carbonate groups leading to layer disorders. Ageing a deficient hydrozincite in carbonate solution will convert the solid to the ordered phase.

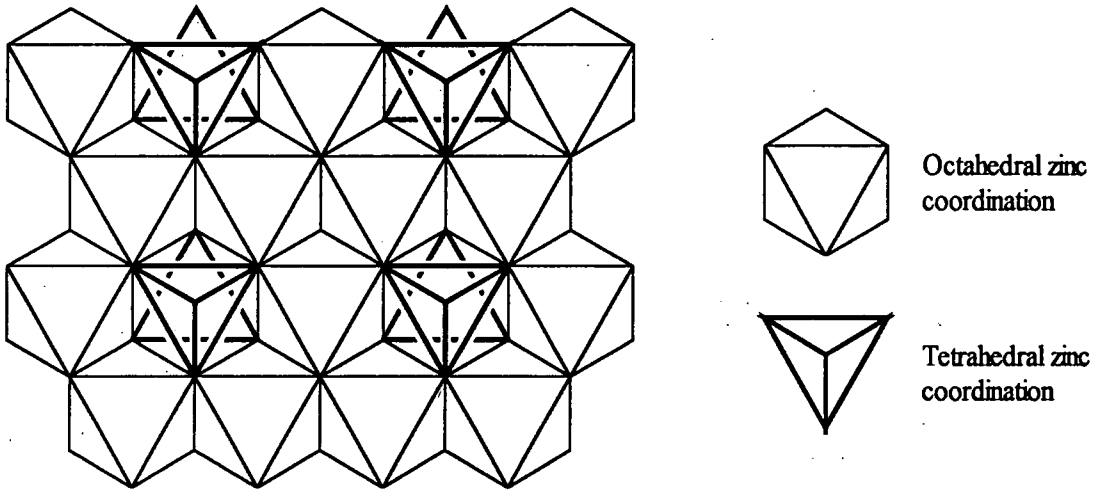


Figure 3.1 A single oxygen-zinc layer of hydrozincite. For clarity, the tetrahedral zinc coordination underneath the layer is not shown. This is located on the other side of the octahedral vacancy. The tetrahedra on either side of the vacancy do not share any oxygens.

*Aurichalcite*, $(Zn_xCu_{1-x})_5(CO_3)_2(OH)_6$ (colour: green-blue to light blue), has the same stoichiometry and a similar structure to hydrozincite[104,19], but there are distortions from the hydrozincite structure owing to the presence of $Cu^{2+}$. Copper preferentially occupies the octahedral sites, and because $Cu^{2+}$ has a $d^9$ electron configuration the copper sites have Jahn Teller distortions. The ratio of tetrahedral to octahedral sites is 2:3. It should in theory be possible to prepare aurichalcite for cation ratios of x = 1-0.4 (where x = Zn/(Zn + Cu)). Pure synthetic aurichalcite has only been reported[19] for x = 0.7. Products with greater zinc content had a hydrozincite impurity[19], while products richer in copper were found to be mixtures of aurichalcite and malachite[21,73].

*Malachite*, $Cu_2CO_3(OH)_2$ (colour: green, green-blue for zincian malachite), contains two crystallographically distinct copper sites, which are both distorted octahedra[105]. The coppers are bridged together by the anions, forming a complicated three dimensional structure. Zincian malachite has been formed[73] for cation ratios of $x \leq 0.3$.

*Georgite*, $Cu_2CO_3(OH)_2$ (colour: blue), is an amorphous phase with the same stoichiometry as malachite. Georgite has a different IR spectrum to malachite[106] and it was found during the current work that they also had different thermal stabilities. Pollard *et al*[20] found that depending on the ageing conditions in the mother liquor, synthetic georgite was converted to malachite or chalconatronite ($Na_2Cu(CO_3)_2 \cdot 3H_2O$).

*Gerhardtite*, $Cu_2NO_3(OH)_3$ (colour: green), is a hydroxynitrate and was another phase encountered in the experiments reported in this chapter. For simplicity, the term "hydroxycarbonate" has been used to cover gerhardtite, unless otherwise indicated. The crystal structure of gerhardtite has two distorted octahedral copper sites, the octahedra share 6 edges forming layers with $C_6$ symmetry[107]. The layers are similar to those in figure 3.1, except there are no vacancies and no tetrahedral sites. The layers are H-bonded together.

### *3.1b Preparation of hydroxycarbonates*

There were three methods reported in the literature for the preparation of zinc/copper hydroxycarbonates:

i) *precipitation*, by the addition of an alkali metal carbonate to zinc/copper nitrate solution until the pH is raised to 6.8-7.0 (the pH of 1.0M zinc/copper nitrate solution is ~2.5);

ii) *constant pH* is maintained during the precipitation by the controlled addition of both reagents; and

iii) *reverse precipitation*, by the addition of zinc/copper nitrate to an alkali metal carbonate solution. Often the carbonate is in excess to keep the pH constant. The carbonate solutions have a pH of ~11.

These methods have been used with varying degrees of success. Precipitation reactions at 85-90°C produced mixtures of malachite, aurichalcite and gerhardtite for copper-rich products, and predominantly aurichalcite (with some hydrozincite) for the zinc-rich[18,19]. Constant pH reactions[73] at 60°C yielded mixtures of malachite and aurichalcite (x=0.3), but ageing for 75mins or more converted the product to malachite. Reverse precipitations[21] at 60°C produced malachite for cation ratios of $x \leq 0.15$ and malachite/aurichalcite mixtures up to x=0.5. It was also shown that the phases within a mixture had different cation ratios. Pollard *et al*[74] obtained pure georgite using reverse

precipitation at 60°C, but had used sulphate solutions instead of nitrates. They collected the solid immediately because they had previously found[20] that the georgite phase, with continued stirring, aged to malachite (3 hours, 25°C). Without stirring, the georgite aged to $Na_2Cu(CO_3)_2 \cdot 3H_2O$, especially if the concentration of $Na_2CO_3$ was high.

Next is a discussion of the results, which is followed by the conclusion and the experimental details.

## 3.2 Discussion of Results

The aim of the work presented in this chapter was to prepare single phase, zinc/copper hydroxycarbonates. It was important to be able to identify the phases produced, especially for heterogeneous products. Because of the importance of the characterisation, the techniques used are discussed in a section of their own. Of the three preparative routes listed above, precipitation and constant pH experiments were attempted, but reverse precipitations were not. The results from these two routes are discussed individually after the section on the characterisation of the hydroxycarbonate.

### *3.2a Characterisation of hydroxycarbonates*

For this study several characterisation techniques were used to identify the hydroxycarbonate phases produced. Elemental analysis was used to calculate the cation ratio and (after the phase or phases were deduced) the relative amount of each phase in the product. The phases produced could normally be distinguished using powder XRD, the exceptions were georgite (which was amorphous) and hydrozincite. Hydrozincite was crystallographically very similar to aurichalcite, and it was found in the present study that it was not possible to unambiguously distinguish hydrozincite from aurichalcite. Himelfarb *et al* claim the identification is possible with very close examination of the diffraction patterns[19], but the quality of the XRD's obtained here precluded this.

The IR spectra for the minerals are shown in figure 3.2. Some of the distinctive features were: strong absorptions at 1415 and 1340$cm^{-1}$ from the nitrate group in gerhardtite; georgite had few absorptions below 1350$cm^{-1}$, except for a carbonate absorption at 838$cm^{-1}$; and OH absorptions at 3407, 3317$cm^{-1}$ for malachite. Although there were slight differences in the spectra obtained from hydrozincite and aurichalcite, it was not possible to determine whether such samples were a single phase.

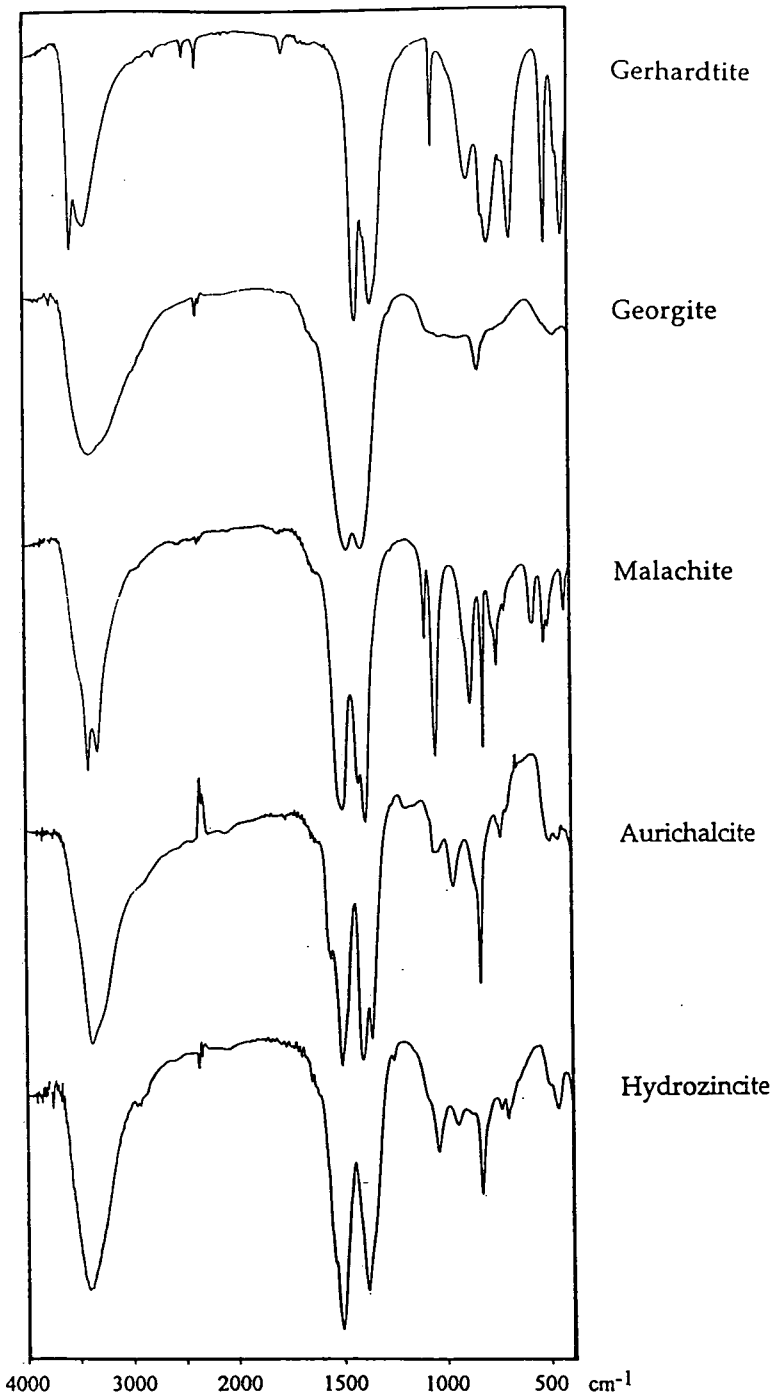


Figure 3.2 IR spectra of synthetically prepared zinc/copper hydroxycarbonates.

DSC was also used for some of the samples, and proved a sensitive technique for the identification of trace phases, as well as indicating the zinc/copper homogeneity for suspected single phase products. Most importantly, hydrozincite and aurichalcite had different thermal decomposition temperatures, table 3.1, and it was possible to easily identify hydrozincite present in aurichalcite samples.

| Mineral Phase | Decomposition Temperature (°C) |
|---|---|
| Gerhardtite (x=0.0) | 257 (endotherm) |
| Malachite (x=0.0) | 291 (endotherm) |
| Georgite (x≤0.5) | 400-450 (exo followed by an endotherm) |
| Aurichalcite (x=0.3) | 325 (endotherm) |
| Hydrozincite (x=1.0) | 241 (endotherm) |

Table 3.1 Thermal events deduced by DSC; x was the cation ratio Zn/(Zn+Cu)

The decomposition temperatures for hydrozincite and aurichalcite have posed some interesting questions. The two phases have similar crystal structures, but hydrozincite decomposed 80°C lower than an aurichalcite sample with a zinc/copper ratio of 2/1. One would expect that substituting copper into the zinc sites of a crystal would decrease the temperature of decomposition, as found for gerhardtite, malachite and aurichalcite. The greater thermal stability of aurichalcite compared with hydrozincite may result from aurichalcite having a more disordered structure.

A further observation was that some hydrozincite samples had a second endotherm at higher temperature (320-380°C), evidence of a second more stable phase, which was not identified by XRD or IR. It might be that the higher temperature endotherm was produced by an aurichalcite-like phase. If the greater thermal stability of aurichalcite was due to the disordering of the structure, this would suggest that similar distortions have occurred for some of the hydrozincite products. It was discussed earlier that hydrozincite deficient in carbonate groups had a more disordered structure[104]. This might be the reason for the higher temperature endotherm, but it was not, unfortunately, within the scope of the current study to address this problem.

### *3.2b Precipitation reactions*

Initially the hydroxycarbonates were prepared by the precipitation method. Potassium carbonate solution was slowly added to a boiling solution of zinc/copper nitrate, followed by a digestion period of a few hours. The products from these experiments are illustrated in figure 3.3. The phases produced from each experiment have been plotted against the cation ratio of the precipitate, where x = Zn/(Zn + Cu). The phases could not be separated, therefore x was calculated for the precipitate as a whole. The phases present were deduced by XRD and the amount of each phase was calculated from the elemental analysis.

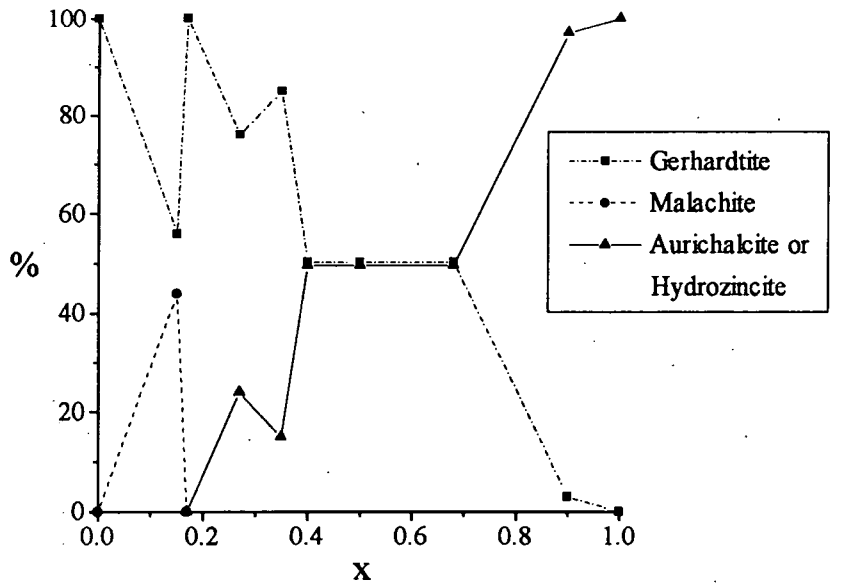


Figure 3.3 Hydroxycarbonate phases obtained from precipitation reactions at ~100°C; x is the cation ratio of the precipitate (Zn/(Zn+Cu)). x was not determined for each phase of a product, because the phases could not be separated.

Several problems were encountered under these reaction conditions, one being that the products were a mixture of phases (see figure 3.3). A predominant phase was the undesirable zinc/copper hydroxynitrate, gerhardtite*. If the addition of the carbonate was too fast or the pH of the reaction mixture exceeded 7, a grey impurity formed. The impurity was copper(II) oxide, which was formed by the hydrolysis of the hydroxycarbonate[108]. It was found that the hydrolysis could be reversed by adding more zinc/copper nitrate solution until the pH went below 7.

$$(Zn_xCu_{1-x})_2CO_3(OH)_2 \xrightarrow{H_2O,\ pH>7} CuO \underset{(Zn_xCu_{1-x})(NO_3)_2}{\overset{H_2O,\ pH>7}{\rightleftharpoons}} (Zn_xCu_{1-x})_2NO_3(OH)_3$$

For hydroxycarbonates to be used as "templates" for the reaction with carboxylic acids, they should ideally have a homogeneous zinc/copper distribution. If the hydroxycarbonates were not a single phase then the homogeneity of the cation distribution would be questionable, i.e. different phases may have different zinc/copper ratios. The formation of copper(II) oxide during some of the experiments also brings into question the homogeneity of the zinc/copper ratio. The formation of copper(II) oxide will produce a hydroxycarbonate phase with a deficiency in copper. Reacting

* A liquid nitrogen trap for condensables from a decomposition under vacuum exploded when warmed up. It was suspected that the cause of the explosion was an oxidising agent (e.g. $N_2O_3$) produced from a nitrate impurity reacting with organic residues in the trap. After this event, it was decided that gerhardtite was unsuitable as a starting material for the synthesis of mixed metal carboxylates.

copper(II) oxide with the nitrate solution will form a more copper-rich phase. A further problem with reacting the copper(II) oxide with zinc/copper nitrate solution is that this produced more gerhardtite. The formation of gerhardtite from copper(II) oxide has contributed to the predominant gerhardtite phases obtained for the copper-rich samples, as shown in figure 3.3.

The separation of the phases by aqueous extraction was attempted, but to no avail as the phases were insoluble. In one example a copper malachite/gerhardtite mixture was heated up in water, and the light blue powder went very dark brown. It was found that all of the gerhardtite and a third of the malachite had been hydrolysed, demonstrating that the gerhardtite phase was more readily hydrolysed than the malachite.

$$Cu_2(mal)_{0.75}(gerh)_{0.25} \xrightarrow{\Delta,\ H_2O} 0.5Cu_2(mal) + CuO$$

mal = malachite, $CO_3(OH)_2$
gerh = gerhardtite, $NO_3(OH)_3$

Figure 3.4 shows the phases obtained from precipitations at room temperature and ≤3°C. These graphs clearly show that as the temperature was decreased, the amount of gerhardtite formed also decreased. For the copper-rich samples ($x<0.3$) the predominant phase was now malachite. No copper(II) oxide was formed during these lower temperature precipitations. It would appear that reducing the temperature has alleviated the problem of hydrolysis.

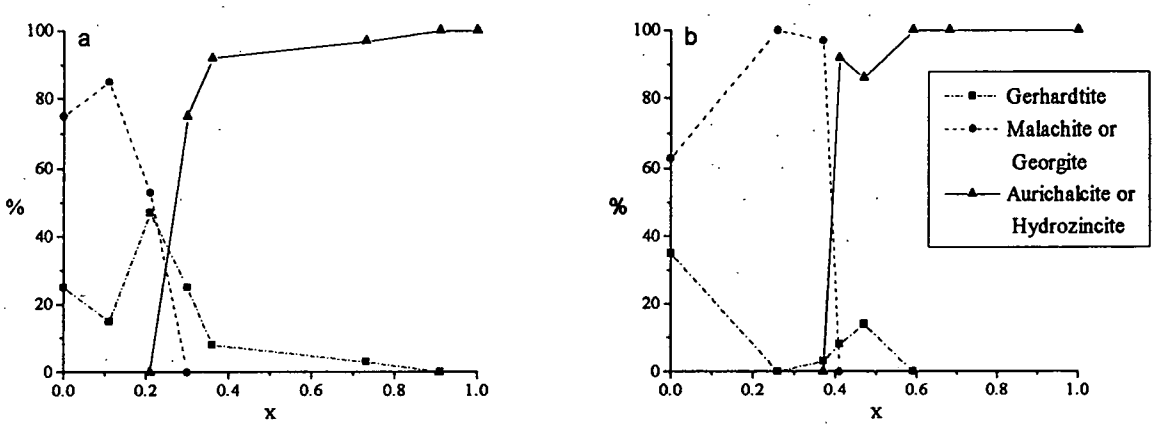


Figure 3.4 Hydroxycarbonate phases obtained from precipitation reactions at: a) 20°C and b) ≤3°C. x is the cation ratio of the precipitate (Zn/(Zn+Cu)).

The results from all the precipitation reactions (including results that were not shown in figures 3.2 and 3.3) have been compiled in the graph below, figure 3.5. For each experiment the reaction temperature has been plotted against the cation ratio of the precipitate. The symbol used to mark the data point identifies the phase or phases obtained.

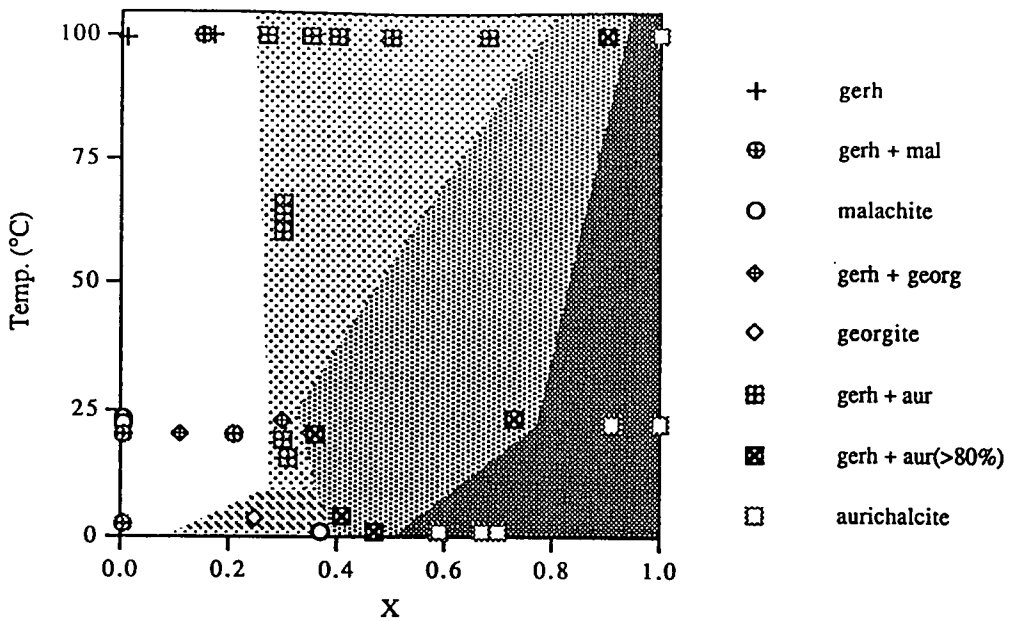


Figure 3.5 Graph showing the products obtained for precipitation reactions over a range of temperatures and cation ratios, x (Zn/(Zn+Cu)).

It is interesting to note that the mixed phases were either gerhardtite/malachite or gerhardtite/aurichalcite. A malachite/aurichalcite mixed phase was not produced in any of the experiments. As mentioned earlier, Porta *et al* obtained malachite/aurichalcite mixed phases for cation ratios of[21] $0.15< x \leq 0.5$. These products were obtained by reverse precipitations. However, it has also been reported that malachite/aurichalcite mixtures (x=0.3), produced by constant pH experiments, were converted to a malachite phase by ageing in the mother liquor for 75 minutes[73]. All the products in the present study were aged for at least an hour. If a malachite/aurichalcite phase was initially produced in any of these experiments, then that product has aged to either malachite or aurichalcite.

In order to determine the effect of pH on the reaction, several precipitations were carried out at 60°C, varying the final pH of the reaction mixture from 6 to 8. It was found that the amount of gerhardtite produced was not affected by the final pH (all the samples were ~40% gerhardtite). The precipitations with a final pH>6.9 underwent hydrolysis to differing extents, forming a copper(II) oxide impurity.

Significant reductions in gerhardtite were achieved by reducing the temperature of reaction. For x=0.3 the gerhardtite content was halved when prepared at room temperature compared to the precipitations at 60°C. At temperatures ≤3°C, single phase malachite and georgite products were formed.

It was also found that the speed of addition affected the amount of gerhardtite precipitated. Two rapid precipitation reactions were carried out at room temperature, preparing copper hydroxycarbonates. A solution of sodium carbonate was quickly

added to a copper nitrate solution. The amount of sodium carbonate used was stoichiometric for one of the reactions and 100% excess for the other. In both reactions a blue precipitate was immediately formed, but the colour of the precipitate went from blue to green upon ageing. The final products were both found to be malachite. The reaction with 100% excess of carbonate took a lot longer to age, 18 hours compared to 0.5 hours for the 1:1 reaction. It was suspected that georgite was formed first in the reaction (the blue precipitate), and that this was converted to malachite upon ageing. It would appear that the ageing process was affected by the pH of the mother liquor, taking much longer in the alkaline conditions for the reaction with excess carbonate (pH ~9). Similar results were reported for reverse precipitations, where it was found that georgite was the initial product and that this was converted to malachite after ageing for 3 hours at room temperature[20].

These results show that the amount of gerhardtite formed can be lowered by decreasing the reaction temperature and by increasing the speed of addition of the carbonate solution. The gerhardtite level does not appear to be affected by pH. Precipitations at ≤3°C produced single phase products for the zinc-rich hydroxycarbonates but, although there were some successes, this proved an unreliable method for the formation of single phase, copper-rich hydroxycarbonates.

### *3.2c Constant pH reactions*

To find satisfactory preparations for hydroxycarbonates with cation ratios of x≤ 0.5, a series of constant pH reactions with x=0.3 and 0.5 was undertaken. This method involved the simultaneous addition of both reagents, ensuring that the pH of the reaction remained constant. A variety of pH values was investigated and, for x=0.3, some reactions were carried out at 60°C as well as at room temperature. The results of these experiments are shown in figure 3.6. The phase produced for most of the reactions was georgite and no phase changes were observed when aged at room temperature for 2.5 hours. These results are very different to those reported by Waller *et al*[73]. As mentioned earlier, they initially produced a malachite/aurichalcite mixed phase by constant pH reactions at 60°C, pH 7.0 and x=0.33. They also found that the precipitate aged to a malachite phase after 75 minutes stirring at 60°C.

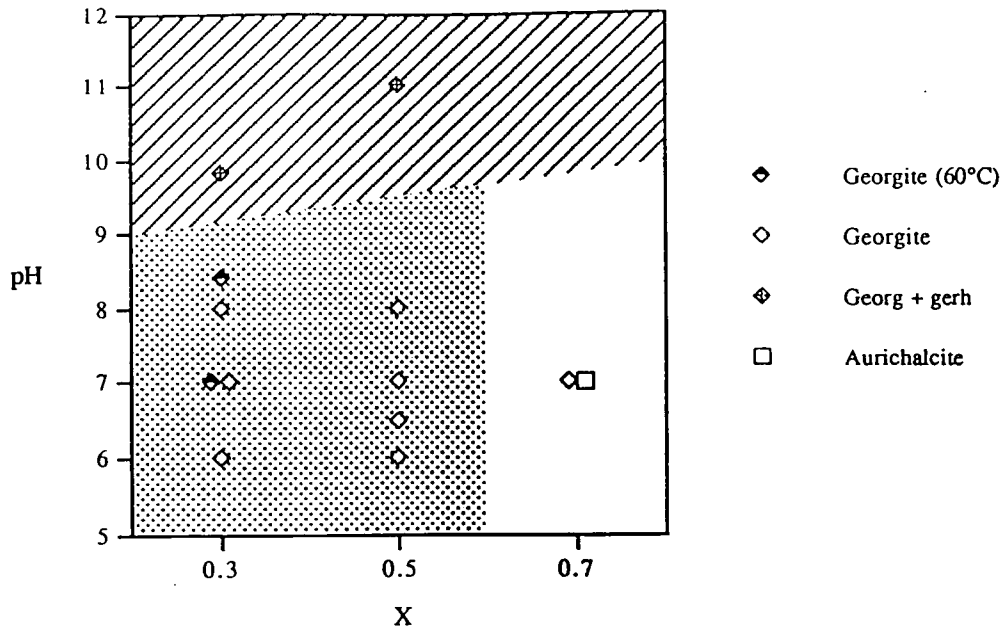


Figure 3.6 Graph showing the products obtained for constant pH reactions over a range of pH, x is the cation ratio of the product (Zn/(Zn+Cu)).

Low levels of gerhardtite were produced only under very alkaline conditions (pH>9.5; 11% gerhardtite for x=0.3 and 1% for x=0.5). The level of gerhardtite was lower for the product with greater zinc content, analogous to the precipitation reactions. No gerhardtite was formed with the reactions at 60°C and there was no hydrolysis of the products, even at pH 8.5. However, after collecting the product from the reaction at pH 11, the mother liquor was a clear blue colour (possibly[20] $Cu(CO_3)_2^{2-}$). The solution was heated up to reduce the volume, but instead of the solute precipitating out, a very dark brown, almost black deposit formed on the walls of the flask. The black deposit was assumed to be copper(II) oxide, formed by the hydrolysis of the dissolved copper salt.

A couple of reactions were investigated for x=0.7; both were carried out at room temperature and pH 7. The first produced georgite, which after 21 hours ageing was converted to aurichalcite. In a second reaction aurichalcite was initially produced and aged to georgite after 3 hours. This reaction was pursued no further as it appeared to be highly unreliable, and in any case there was already a satisfactory route to zinc-rich hydroxycarbonates.

It was decided that georgite was a satisfactory starting material for the preparation of copper-rich carboxylates, as all the products appeared homogeneous from their analyses and when observed under a microscope. Precipitation reaction at ≤3°C was found to be an acceptable method for the formation of zinc-rich aurichalcite samples and hydrozincite for zinc hydroxycarbonate. No hydrozincite was detected in the aurichalcite products prepared by cold precipitation. It was decided that it was

unnecessary to take the study any further (e.g. ageing at 60°C, formation of malachite, stability of the products to hydrolysis, reverse precipitations, etc.) as the aims of the hydroxycarbonate study had been accomplished, i.e. the preparation of single phase hydroxycarbonates for all cation ratios.

## 3.3 Conclusions

The scheme below illustrates the reactions deduced from the work reported in this chapter. A summary of the scheme follows, discussing each reaction path, I–V.

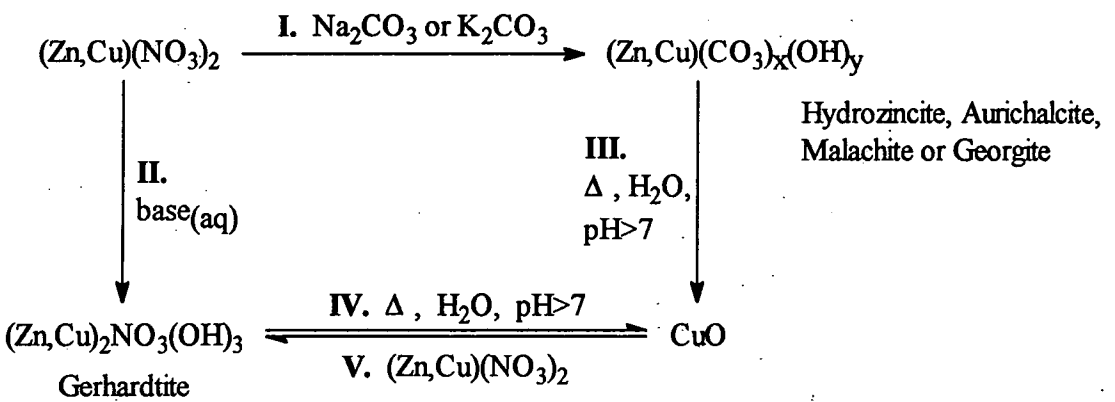


*Reaction I.* This was the desired reaction and was achieved by cold precipitations for zinc-rich products and by constant pH reactions (pH 6-8, T=20-60°C) for copper-rich products. It was found that the initial hydroxycarbonate phase formed could change on ageing. Phase changes identified in this work were: georgite → malachite; georgite → aurichalcite; and aurichalcite → georgite.

*Reaction II.* This was a side reaction of the precipitation experiments. The formation of gerhardtite was suppressed by decreasing the temperature of reaction. It was also found that this reaction became less favourable with increasing zinc/copper ratio. The precipitation experiment starts with an excess of zinc/copper nitrate solution, making reaction II more favourable. Gerhardtite was not formed during constant pH experiments (with pH = 6-8), because the route involved the simultaneous addition of both reagents, and hence there was never a large excess of zinc/copper nitrate (making reaction II less favourable).

The formation of gerhardtite was also affected by the speed of addition. For example gerhardtite was not formed when sodium carbonate solution was added rapidly to a copper nitrate solution at 20°C. These results also support the hypothesis that the formation of gerhardtite is related to the excess of zinc/copper nitrate. Providing there was adequate stirring, there would have been no excess of zinc/copper nitrate after the instantaneous addition of a stoichiometric amount of carbonate solution.

*Reactions III + IV.* Hydrolysis of the product, forming copper(II) oxide, was only a problem for the precipitation reactions at elevated temperatures. It occurred under basic conditions, i.e. if the end point was passed or the addition of carbonate solution was too fast. Hydrolysis also occurred when some samples were heated in water. It was found that gerhardtite hydrolysed more readily than the hydroxycarbonates, and may help to initiate III. This would help explain why hydrolysis did not occur during constant pH reactions under alkaline conditions, because no gerhardtite was produced.

*Reaction V.* It was found that copper(II) oxide formed by hydrolysis could be reacted with zinc/copper nitrate solution, forming gerhardtite. However, the gerhardtite phase formed will have a zinc/copper ratio smaller than that for the rest of the precipitate and thus lead to a heterogeneous product. It was therefore desirable to avoid hydrolysis of the precipitate (reactions III and IV)

The work discussed in this chapter has illustrated the complexity of the reaction between zinc/copper nitrate and potassium or sodium carbonate. The aim of the study was to determine the reaction conditions for the production of single phase zinc/copper hydroxycarbonates (i.e. reaction I). It was found that cold precipitation reactions formed single phase zinc-rich hydroxycarbonates ($x>0.5$), and that copper-rich hydroxycarbonates ($x\leq0.5$) were formed by constant pH precipitations.

## 3.4 Experimental Details

The hydroxycarbonates used for the preparation of zinc/copper trimellitates and pyromellitates have been cross referenced in those chapters to their experimental details here. Because of the number of reactions reported in this section an index has been compiled at the end of the chapter so that the details of specific experiments may be found more quickly. The reference code used for the index is also given in the heading to each experiment, e.g. BP(0.0/1.0).

### *3.4a Preparation of mixed metal hydroxycarbonates at ~100°C*

***a) Preparation of copper hydroxycarbonate*** BP(0.0/1.0)

A solution of potassium carbonate (31.50mls, 1.0M) was added, dropwise, to a boiling solution of copper nitrate (40.0mls, 1.0M). Initially a light blue solid precipitated along with a black solid impurity. The addition of carbonate was halted, and the reaction mixture was allowed to equilibrate. When the impurity had been reconverted the potassium carbonate addition was resumed, but at a much slower rate, allowing equilibration before each drop. After the addition of potassium carbonate solution the

pH of the reaction mixture had become neutral but the solid slowly changed colour to dark brown. Copper nitrate solution (8mls, 1.0M) was added until the colour of the solid started to get lighter and go green. The mixture was allowed to equilibrate for ~30mins after which suction filtration yielded 5.67g (98.4%) of a minty green powder. The product was characterised as follows.

*Elemental analysis (%):* Cu,53.1 C,0.0 H,1.8 N,5.6
Calculated: Cu,52.9 C,0.0 H,1.3 N,5.8
for $Cu_2NO_3(OH)_3$

*IR ($cm^{-1}$):* 3530, 3400(b), 1415(s), 1340(s), 1050, 880, 810(w),775, 665, 510(s), 420(w).
Gerhardtite.

*DSC (°C) [air, 10°C$min^{-1}$]:* 257(endo, s).

*Powder XRD:* The values of 4θ obtained for the sample correspond to the d spacings for gerhardtite. The first ten lines are shown below along with the data for gerhardtite.

| $Cu_2NO_3(OH)_3$ | | Gerhardtite | $Cu_2NO_3(OH)_3$ | | Gerhardtite |
|---|---|---|---|---|---|
| 4θ | d (Å) | d (Å) | 4θ | d (Å) | d (Å) |
| 25.85 | 6.89 | 6.91 | 64.45 | 2.79 | 2.80 |
| 43.50 | 4.11 | 4.12 | | | 2.74 |
| 49.35 | 3.63 | 3.54 | 67.55 | 2.67 | 2.67 |
| 51.95 | 3.45 | 3.45 | | | 2.62 |
| 59.00 | 3.04 | 3.04 | | | 2.60 |
| 59.75 | 3.01 | 3.01 | 71.65 | 2.52 | 2.52 |
| | | 2.94 | 73.50 | 2.46 | 2.49 |

***b) Preparation of $(Zn_{0.1}Cu_{0.9})$ hydroxycarbonate*** BP(0.15/0.85)

| 1.0M (Zn,Cu)$(NO_3)_2$ 40mls | | 1.0M $K_2CO_3$, 31.90mls |
|---|---|---|
| Temp, ~100°C | Final pH, 7 | Aged, 1hr |
| Product, 4.38g | Yield, 95.2% | Colour, mint green |

*Comments:*

The addition of potassium carbonate resulted in the immediate precipitation of a blue solid but, even with very slow addition, a black impurity started forming. The reaction temperature was decreased slightly so that the solution was no longer boiling and the addition was continued. The end point was overshot resulting in an alkaline, pH

11, solution with all the precipitate turning black. 1.0M $(Zn_{0.1}Cu_{0.9})(NO_3)_2$ solution was added until the reaction mixture became acidic, converting the suspension to a green solid.

*Elemental analysis (%):* Zn,9.2 Cu,51.3 C,1.9 H,1.1 N,3.7
Calculated: Zn,8.5 Cu,47.0 C,1.8 H,1.2 N,3.4
for $(Zn_{0.15}Cu_{0.85})_2(CO_3)_{0.34}(NO_3)_{0.56}(OH)_{2.76}$

*Powder XRD (4θ):* 25.85(G); 29.80(M); 35.35(M); 43.50(G); 48.50(M); 51.95(G); 67.55(G).

Only the strongest lines are given, malachite (M) and gerhardtite (G) diffractions accounted for all the lines.

A sample (1.44g) of the product was placed in a solvent extractor and water was passed over the sample for 16 hours. The sample did not appear to have changed colour except where some of the sample was outside the cold jacket. This had turned black, hydrolysed by the hot (~60°C) water vapour. There was insufficient hydrolysed sample to be characterised but the hydroxycarbonate was characterised as follows.

*Elemental analysis (%):* Zn,4.6 Cu,50.0 C,1.9 H,1.2 N,3.6

Approximately the same as before (although the Zn percentage is low).

***c) Preparation of $(Zn_{0.2}Cu_{0.8})$ hydroxycarbonate*** BP(0.17/0.83)

| | | |
|---|---|---|
| 1.0M $(Zn,Cu)(NO_3)_2$ 40mls | | 1.0M $K_2CO_3$, 25.10mls |
| Temp, ~100°C | Final pH, 7 | Aged, 3.5hrs |
| Product, 4.08g | Yield, 84.6% | Colour, light greenish-blue |

*Comments:*

The endpoint was slightly exceeded but no impurity was observed, to ensure hydrolysis did not occur 10mls of (Zn,Cu)nitrate solution was added and the mixture was allowed to equilibrate.

*Elemental analysis (%):* Zn,10.0 Cu,49.0 C,0.0 H,1.2 N,5.7
Calculated: Zn,9.2 Cu,43.8 C,0.0 H,1.3 N,5.8
for $(Zn_{0.17}Cu_{0.83})_2NO_3(OH)_3$

*Powder XRD (4θ):* 25.85(G); 43.50(G); 51.95(G); 67.55(G); 73.50(G).
Strongest lines shown; all the lines correspond to gerhardtite.

*DSC (°C) [air, 10°Cmin$^{-1}$]:* 260(endo, sh), 278(endo, s).

***d) Preparation of $(Zn_{0.3}Cu_{0.7})$ hydroxycarbonate*** BP(0.27/0.73)

| | | |
|---|---|---|
| 1.0M $(Zn,Cu)(NO_3)_2$ 30mls | | 1.0M $K_2CO_3$, 21.8mls |
| Temp, ~100°C | Final pH, 7 | Aged, 1.5hrs |
| Product, 3.21g | Yield, 91.4% | Colour, light greenish-blue |

*Elemental analysis (%):* Zn,15.2 Cu,39.7 C,0.8 H,1.2 N,4.5
Calculated: Zn,15.1 Cu,39.6 C,0.8 H,1.3 N,4.5
for $(Zn_{0.27}Cu_{0.73})_2(CO_3)_{0.16}(NO_3)_{0.76}(OH)_{2.92}$

*Powder XRD (4θ):* 25.85(G); 43.50(G); 51.95(G); 67.55(G); 73.50(G).

Strongest lines shown; also 3 very faint lines (4θ: 55.85, 61.80, 65.50) which were assigned to aurichalcite. All the other lines correspond to gerhardtite.

***e) Preparation of $(Zn_{0.33}Cu_{0.67})$ hydroxycarbonate*** BP(0.35/0.65)

| | | |
|---|---|---|
| 1.0M $(Zn,Cu)(NO_3)_2$ 360mls | | 1.0M $K_2CO_3$, 307mls |
| Temp, ~100°C | Final pH, 7 | Aged, 1hr |
| Product, 39.98g | Yield, 93.0% | Colour, grey-green |

*Elemental analysis (%):* Zn,18.7 Cu,34.1 C,0.8 H,1.1 N,4.9
Calculated: Zn,19.2 Cu,34.6 C,0.8 H,1.2 N,5.0
for $(Zn_{0.35}Cu_{0.65})_2(CO_3)_{0.16}(NO_3)_{0.85}(OH)_{2.83}$

*Powder XRD (4θ):* 25.60(G); 26.10; 32.15; 38.25; 43.20(G); 48.35; 51.50(G); 56.00; 57.90; 59.15; 61.95(A); 63.50.

There was a gerhardtite (G) and a faint aurichalcite (A) pattern present, but these two phases alone do not account for all the lines.

***f) Preparation of $(Zn_{0.4}Cu_{0.6})$ hydroxycarbonate*** BP(0.40/0.60)

| | | |
|---|---|---|
| 1.0M $(Zn,Cu)(NO_3)_2$ 32.9mls | | 1.0M $K_2CO_3$, 27.2mls |
| Temp, ~100°C | Final pH, 7 | Aged, 1hr |
| Product, 3.61g | Yield, 96.3% | Colour, grey-green |

*Comments:*

Because the endpoint was overshot, extra $(Zn_{0.4}Cu_{0.6})(NO_3)_2$ solution was added to convert the black impurity which had formed. However, after an hour's digestion the product was still slightly grey. Obviously the impurity had not been completely converted.

*Elemental analysis (%):* Zn,22.8 Cu,34.0 C,1.8 H,1.2 N,3.1
Calculated: Zn,23.0 Cu,33.5 C,1.8 H,1.2 N,3.1
for $(Zn_{0.40}Cu_{0.60})_2(CO_3)_{0.34}(NO_3)_{0.50}(OH)_{2.82}$

*Powder XRD (4θ):* 25.85(G); 43.50(G); 51.95(G); 67.55(G); 73.50(G).

Strongest lines shown; also 3 faint lines (4θ: 55.85, 61.80, 65.50) assigned to aurichalcite. All the other lines correspond to gerhardtite.

***g) Preparation of $(Zn_{0.5}Cu_{0.5})$ hydroxycarbonate*** BP(0.50/0.50)

| 1.0M $(Zn,Cu)(NO_3)_2$ 340mls | | 1.0M $K_2CO_3$, 290mls |
|---|---|---|
| Temp, ~100°C | Final pH, 7 | Aged, 1hr |
| Product, 38.27g | Yield, 98.6% | Colour, light blue |

*Elemental analysis (%):* Zn,28.9 Cu,27.8 C,1.8 H,1.2 N,3.1
Calculated: Zn,28.6 Cu,27.8 C,1.8 H,1.2 N,3.1
for $(Zn_{0.50}Cu_{0.50})_2(CO_3)_{0.34}(NO_3)_{0.50}(OH)_{2.82}$

*Powder XRD (4θ):* 25.85(G); 43.50(G); 51.95(G); 67.55(G); 73.50(G).

Strongest lines shown; also 3 faint lines (4θ: 55.85, 61.80, 65.50) assigned to aurichalcite. All the other lines correspond to gerhardtite.

*DSC (°C) [Ar, 5°Cmin$^{-1}$]:* 201(endo, s), 228(endo, w).

***h) Preparation of $(Zn_{0.67}Cu_{0.33})$ hydroxycarbonate*** BP(0.68/0.32)

| 1.0M $(Zn,Cu)(NO_3)_2$ 540mls | | 1.0M $K_2CO_3$, 461mls |
|---|---|---|
| Temp, ~100°C | Final pH, 7 | Aged, 1hr |
| Product, 61.1g | Yield, 98.0% | Colour, light grey-blue |

*Elemental analysis (%):* Zn,37.6 Cu,17.0 C,2.0 H,1.1 N,3.0
Calculated: Zn,38.5 Cu,17.6 C,2.1 H,1.2 N,3.1
for $(Zn_{0.68}Cu_{0.32})_2(CO_3)_{0.40}(NO_3)_{0.51}(OH)_{2.69}$

*Powder XRD (4θ):* 25.85(G); 43.50(G); 51.95(G); 67.55(G); 73.50(G).

Strongest lines shown; also 3 faint lines (4θ: 55.85, 61.80, 65.50) assigned to aurichalcite. All the other lines correspond to gerhardtite.

*DSC (°C) [Ar, 5°Cmin$^{-1}$]:* 201(endo, s), 228(endo, w).

***i) Preparation of $(Zn_{0.90}Cu_{0.10})$ hydroxycarbonate*** BP(0.90/0.10)

| 1.0M $(Zn,Cu)(NO_3)_2$ 30mls | | 1.0M $K_2CO_3$, 28.7mls |
|---|---|---|
| Temp, ~100°C | Final pH, 7 | Aged, 1hr |
| Product, 3.23g | Yield, 98.6% | Colour, pale blue |

*Elemental analysis (%):* Zn,53.6 Cu,5.6 C,3.7 H,1.3 N,0.2
Calculated: Zn,54.0 Cu,5.8 C,3.9 H,1.2 N,0.2
for $(Zn_{0.90}Cu_{0.10})_2(CO_3)_{0.70}(NO_3)_{0.03}(OH)_{2.57}$

*Powder XRD (4θ):* 25.85(G); 55.85(A); 61.80(A); 65.50(A); 67.55(G); 73.50(G).

The gerhardtite lines, G, were faint; A denotes diffractions assigned to aurichalcite.

***j) Preparation of zinc hydroxycarbonate*** BP(1.0/0.0)

| 1.0M $Zn(NO_3)_2$ 27mls | | 1.0M $K_2CO_3$, 30.2mls |
|---|---|---|
| Temp, ~100°C | Final pH, 7 | Aged, 1hr |
| Product, 2.89g | Yield, 97.4% | Colour, white |

*Elemental analysis (%):* Zn,63.2 C,3.9 H,1.2 N,0.0
Calculated: Zn,59.5 C,4.4 H,1.1
for $Zn_5(CO_3)_2(OH)_6$

*Powder XRD (4θ):* 55.85; 61.80; 65.50.

The three lines were very faint, but from the d spacings (3.21, 2.91, 2.75 Å respectively) the diffraction pattern was assigned to hydrozincite (3.14, 2.92, 2.72 Å).

*DSC (°C) [air, 10°Cmin$^{-1}$]:* 243(endo, s).

### *3.4b Preparation of mixed metal hydroxycarbonates at room temperature*

***a) Preparation of copper hydroxycarbonate***

i) RT(0.0/1.0)

| 1.0M $Cu(NO_3)_2$ 6mls | | 1.0M $K_2CO_3$, 6mls |
|---|---|---|
| Temp, RT | Final pH, - | Aged, 1hr |
| Product, 0.74g | Yield, 93% | Colour, blue |

*Comments:*

The solutions were added together and stirred; a blue solid formed and was characterised as follows.

*Elemental analysis (%):* Cu,47.3 C,3.7 H,1.4 N,1.3
Calculated: Cu,48.1 C,3.8 H,2.3 N,1.3
for $Cu_2(CO_3)_{0.83}(NO_3)_{0.25}(OH)_{2.09} . H_2O$

In an attempt to separate the hydroxynitrate from the hydroxycarbonate, water was added to the sample (0.74g, 2.8mmol). On heating the sample changed colour to dark green then greyish black and finally became a very dark (almost black) brown. Suction filtration yielded 0.51g (95%) of solid which was characterised as follows.

*Elemental analysis (%):* Cu,63.0 C,3.1 H,0.8 N,0.0
Calculated: Cu,63.8 C,3.0 H,1.0 N,0.0
for $0.5Cu_2(CO_3)(OH)_2 + CuO$

*IR ($cm^{-1}$):* 3407(s), 3317(s), 1508(s), 1427(w), 1389(s), 1097(w), 1050, 881, 819, 751(w), 573(w), 525(w), 431(w).
Malachite.

*Powder XRD (4θ):* 29.80; 35.35; 48.50.

Only the strongest lines are given; all the lines matched the d spacings for malachite. Unfortunately the strongest CuO lines (d spacing: 2.52, 2.32Å) both coincide with the malachite pattern. However, the corresponding lines (4θ: 71.55, 78.05) were both slightly more intense and more diffuse than expected, suggesting CuO was present.

Two experiments were carried out, quickly adding 10mls of 1.0M $Na_2CO_3$ solution to 5(ii) and 10mls (iii) of 1.0M $Cu(NO_3)_2$, and stirring vigorously for 2 hours. In 'ii' the precipitate was initially blue but after half an hour had become green, but in 'iii' the precipitate remained blue for the first couple of hours' stirring. Stirring was continued for 'iii' and after 18 hours the mixture had become a minty green. The products were analysed as follows.

ii) P45

| | | |
|---|---|---|
| Product, 0.423g | Yield, 73.5% | Colour, mint green |

*Elemental analysis (%):* Cu,54.8 C,5.3 H,1.1 N,0.0
Calculated: Cu,55.2 C,5.2 H,1.3 N,0.0
for $Cu_2CO_3(OH)_2 \cdot 0.5H_2O$

*IR ($cm^{-1}$):* 3600-3000(b), 1490(s), 1385(s), 1097(w), 1050, 870, 815, 750, 575(w), 520(w), 505(sh), 430(w).
Malachite.

*Powder XRD:* Malachite.

*DSC (°C) [Ar, 5°C$min^{-1}$]:* endotherm at 291.

iii) P44

| | | |
|---|---|---|
| Product, 1.093g | Yield, 95.0% | Colour, mint green |

*Elemental analysis (%):* Cu,58.0 C,5.4 H,1.1 N,0.0
Calculated: Cu,55.2 C,5.2 H,1.3 N,0.0
for $Cu_2CO_3(OH)_2 \cdot 0.5H_2O$

*IR ($cm^{-1}$):* 3600-3000(b), 1490(s), 1385(s), 1097(w), 1045, 875, 820, 750, 575(w), 520(w), 505(w), 430(w).
Malachite.

*Powder XRD:* Malachite.

*DSC (°C) [Ar, 5°C$min^{-1}$]:* endotherm at 292.

***b) Preparation of $(Zn_{0.1}Cu_{0.9})$ hydroxycarbonate*** RT(0.11/0.89)

| | | |
|---|---|---|
| 1.0M $(Zn,Cu)(NO_3)_2$ 10mls | | 1.0M $K_2CO_3$, 10mls |
| Temp, RT | Final pH, - | Aged, 1hr |
| Product, 1.18g | Yield, 96.8% | Colour, light blue |

*Comments:*

The reagents were quickly added together, and stirred (but not vigorously).

*Elemental analysis (%):* Zn,6.0 Cu,46.1 C,4.3 H,1.5 N,0.9
Calculated: Zn,5.9 Cu,46.5 C,4.3 H,0.9 N,1.7
for $(Zn_{0.11}Cu_{0.89})_2(CO_3)_{0.88}(NO_3)_{0.15}(OH)_{2.09} \cdot H_2O$

*IR ($cm^{-1}$):* 3600-3000(b), 1474, **1420**, **1384**, **1047(w)**, 832(w), **510(w)**, **430(w)**.
Georgite plus weak gerhardtite absorptions (**bold**).

*Powder XRD:* Gave no diffraction pattern.

***c) Preparation of ($Zn_{0.2}Cu_{0.8}$) hydroxycarbonate*** RT(0.21/0.79)

| 1.0M (Zn,Cu)$(NO_3)_2$ 20mls | | 1.0M $K_2CO_3$, 20.9mls |
|---|---|---|
| Temp, RT | Final pH, 7 | Aged, 0hrs |
| Product, 2.28g | Yield, 94.8% | Colour, light blue |

*Elemental analysis (%):* Zn,11.6 Cu,41.6 C,2.7 H,1.4 N,2.7
Calculated: Zn,11.4 Cu,41.8 C,2.7 H,1.4 N,2.7
for $(Zn_{0.21}Cu_{0.79})_2(CO_3)_{0.54}(NO_3)_{0.47}(OH)_{2.45} \cdot 0.5H_2O$

*IR ($cm^{-1}$):* 3533, 3400(b), **1478(sh)**, 1421(s), **1384**, 1341, 1047(w), 837(w), 811(w), 783(w), 677(w), 510, 433.
Gerhardtite and malachite (**bold**).

*Powder XRD (4θ):* 25.85; 43.50; 51.95; 67.55; 73.50.
Only the strongest lines are shown; all the lines correspond to gerhardtite.

***d) Preparation of ($Zn_{0.3}Cu_{0.7}$) hydroxycarbonate***

i) RT(0.30/0.70)

| 1.0M (Zn,Cu)$(NO_3)_2$ 20mls | | 1.0M $K_2CO_3$, 19.9mls |
|---|---|---|
| Temp, 19°C | Final pH, 7.3 | Aged, 0hrs |
| Product, 2.34g | Yield, 95.1% | Colour, light blue |

*Elemental analysis (%):* Zn,16.3 Cu,36.5 C,3.3 H,1.5 N,1.7
Calculated: Zn,16.0 Cu,36.2 C,3.3 H,1.8 N,1.7
for $(Zn_{0.30}Cu_{0.70})_2(CO_3)_{0.68}(NO_3)_{0.30}(OH)_{2.34} \cdot H_2O$

*Powder XRD (4θ):* 25.85(G); 43.50(G); 51.95(G); 67.55(G); 73.50(G).
Only the strongest lines are shown; also 3 faint lines (4θ: 55.85, 61.80, 65.50) assigned to aurichalcite, all the other lines correspond to gerhardtite, G.

ii) RT(0.31/0.69)

| 1.0M (Zn,Cu)$(NO_3)_2$ 310mls | | 1.0M $K_2CO_3$, 234.5mls |
|---|---|---|
| Temp, 15.4°C | Final pH, 6.9 | Aged, 0hrs |
| Product, 34.82g | Yield, 99.9% | Colour, light blue |

*Elemental analysis (%):* Zn,17.0 Cu,36.8 C,1.4 H,1.3 N,3.8
Calculated: Zn,17.5 Cu,37.8 C,1.4 H,1.2 N,3.9
for $(Zn_{0.31}Cu_{0.69})_2(CO_3)_{0.27}(NO_3)_{0.64}(OH)_{2.82}$

*Powder XRD (4θ):* 25.85(G); 43.50(G); 51.95(G); 67.55(G); 73.50(G).

Only the strongest lines are shown; 3 faint lines (4θ: 55.85, 61.80, 65.50) assigned to aurichalcite, all the other lines correspond to gerhardtite, G.

***e) Preparation of $(Zn_{0.4}Cu_{0.6})$ hydroxycarbonate*** RT(0.36/0.64)

| 1.0M $(Zn,Cu)(NO_3)_2$ 10mls | | 1.0M $K_2CO_3$, 8.75mls |
|---|---|---|
| Temp, RT | Final pH, 7 | Aged, 0hrs |
| Product, 1.07g | Yield, 89.6% | Colour, light blue |

*Elemental analysis (%):* Zn,19.7 Cu,33.7 C,4.8 H,1.5 N,0.5
Calculated: Zn,19.8 Cu,34.1 C,4.8 H,1.5 N,0.5
for $(Zn_{0.36}Cu_{0.64})_2(CO_3)_{0.95}(NO_3)_{0.08}(OH)_{2.02} \cdot 0.75H_2O$

*IR ($cm^{-1}$):* 3600-2900(b), 1510(s), 1415(s), 1384(sh), **1050(w)**, 1047(w), 968(w), 836, 749(w), **668(w)**, **510(sh)**, 475(w).
Mainly aurichalcite, trace of gerhardtite (**bold**).

*Powder XRD:* Amorphous

***f) Preparation of $(Zn_{0.8}Cu_{0.2})$ hydroxycarbonate*** RT(0.73/0.27)

| 1.0M $(Zn,Cu)(NO_3)_2$ 20mls | | 1.0M $K_2CO_3$, 21.4mls |
|---|---|---|
| Temp, 23.5°C | Final pH, 7.2 | Aged, 0hrs |
| Product, 2.27g | Yield, 100% | Colour, pale blue |

*Elemental analysis (%):* Zn,43.0 Cu,15.2 C,4.2 H,1.2 N,0.4
Calculated: Zn,43.2 Cu,15.5 C,4.2 H,1.1 N,0.4
for $(Zn_{0.73}Cu_{0.27})_2(CO_3)_{0.78}(NO_3)_{0.06}(OH)_{2.38}$

*Powder XRD:* The pattern was faint but the values of d obtained matched those for aurichalcite, see below.

| Sample | | Aurichalcite | Sample | | Aurichalcite |
|---|---|---|---|---|---|
| 4θ | d (Å) | d (Å) | 4θ | d (Å) | d (Å) |
| 26.00 | 6.85 | 6.78 | 71.35 | 2.53 | 2.50 |
| 43 - 44 | 4.16 - 4.06 | 4.02 | 77.55 | 2.33 | 2.33 |
| 48.35 | 3.70 | 3.68 | 84.50 | 2.15 | 2.15 |
| 55.85 | 3.21 | 3.19 | 94.20 | 1.94 | 1.95 |
| 61.80 | 2.91 | 2.89 | 115.60 | 1.60 | 1.60 |
| 65.50 | 2.75 | 2.72 | 119.20 | 1.56 | 1.56 |
| 67.70 | 2.66 | 2.61 | | | |

### *g) Preparation of ($Zn_{0.9}Cu_{0.1}$) hydroxycarbonate*

i) RT(0.91/0.09)

| 1.0M (Zn,Cu)$(NO_3)_2$ 20mls | | 1.0M $K_2CO_3$, 21.2mls |
|---|---|---|
| Temp, 22.5°C | Final pH, 6.85 | Aged, 0hrs |
| Product, 2.18g | Yield, 98.6% | Colour, pale blue |

*Elemental analysis (%):* Zn,53.7 Cu,5.4 C,4.0 H,1.4 N,0.0

Calculated: Zn,53.8 Cu,5.2 C,4.0 H,1.2

for $(Zn_{0.91}Cu_{0.09})_2(CO_3)_{0.73}(OH)_{2.54}$

*Powder XRD (4θ):* 26.00; 55.85; 61.80; 65.50; 67.70 .
Aurichalcite.

ii) A112

| 1.0M (Zn,Cu)$(NO_3)_2$ 200mls | | 1.0M $K_2CO_3$, ~200mls |
|---|---|---|
| Temp, 22°C | final pH, ~7 | Aged, 0hrs |
| Product, 21.86g | Yield, 99.3% | Colour, light blue |

*Elemental analysis (%):* Zn,52.7 Cu,5.7 C,4.0 H,1.2 N,0.0

Calculated: Zn,52.0 Cu,5.6 C,4.2 H,1.4 N,0.0

for $(Zn_{0.9}Cu_{0.1})_5(CO_3)_2(OH)_6 \cdot H_2O$

*IR ($cm^{-1}$):* 3600-2900(b), 1507(s), 1394(s), 1045, 961, 839(s), 740(w), 709(w), 496(w).
Aurichalcite.

*Powder XRD:* Aurichalcite.

*DSC (°C) [air, 10°Cmin$^{-1}$]:* 61(endo, w), 286(endo, s), 381(endo, vw).

***h) Preparation of zinc hydroxycarbonate***

i) RT(1.0/0.0)

| 1.0M $Zn(NO_3)_2$ 350mls | | 1.0M $K_2CO_3$, 358mls |
|---|---|---|
| Temp, 22.2°C | Final pH, 6.35 | Aged, 0hrs |
| Product, 46.41g | Yield, 100% | Colour, white |

*Elemental analysis (%):* Zn,50.4 C,5.7 H,1.0 N,0.0

Calculated: Zn,49.9 C,5.6 H,1.9

for $Zn_2(CO_3)_{1.23}(OH)_{1.54} \cdot 1.75H_2O$

*Powder XRD (4θ):* The values of d obtained correspond well with those for hydrozincite. Only the strongest lines are shown.

| Sample | | Hydrozincite | Sample | | Hydrozincite |
|---|---|---|---|---|---|
| 4θ | d (Å) | d (Å) | 4θ | d (Å) | d (Å) |
| 26.00 | 6.85 | 6.77 | 103.05 | 1.78 | 1.77 |
| 50.20 | 3.57 | 3.66 | 107.80 | 1.71 | 1.69 |
| 65.30 | 2.76 | 2.74 | 124.55 | 1.50 | 1.50 |
| 77.55 | 2.33 | 2.34 | | | |
| 85.85 | 2.12 | 2.08 | | | |
| 93.50 | 1.95 | 1.94 | | | |

ii) P52

| 1.0M $Zn(NO_3)_2$ 290mls | | 1.0M $K_2CO_3$, ~291mls |
|---|---|---|
| Temp, 22°C | final pH, 6.19 | Aged, 21hrs |
| Product, 32.64g | Yield, 99.3% | Colour, white |

*Comments:*

The mixture was left stirring overnight to equilibrate. At the beginning of the next day the pH was 6.8, this slowly increased to 7.0, when it was collected.

*Elemental analysis (%):* Zn,59.7 C,5.1 H,1.1 N,0.0

Calculated: Zn,57.7 C,4.2 H,1.4 N,0.0

for $Zn_5(CO_3)_2(OH)_6 \cdot H_2O$

*IR (cm$^{-1}$):* 3600-3000(b), 1600-1300(b), 1040(w), 950(w), **870**, 835, 740(w), 705(w), 470(w).

Hydrozincite plus an extra absorption (in **bold**).

*Powder XRD:* Hydrozincite.

*DSC (°C) [Ar, 5°Cmin$^{-1}$]:* 241(endo), 321(endo, w).

iii) A102

| | | |
|---|---|---|
| 1.0M $Zn(NO_3)_2$ 46.5mls | | 1.0M $K_2CO_3$, 49.4mls |
| Temp, 22°C | final pH, 6.83 | Aged, 18hrs |
| Product, 5.163g | Yield, 97.9% | Colour, white |

*Comments:*

After the addition of carbonate the pH slowly increased, to allow the mixture to equilibrate it was left stirring overnight. At the beginning of the next day the pH had settled at 8.63.

*Elemental analysis (%):* Zn,56.9 C,4.0 H,1.3 N,0.0
Calculated: Zn,57.7 C,4.2 H,1.4 N,0.0
for $Zn_5(CO_3)_2(OH)_6 \cdot H_2O$

*IR (cm$^{-1}$):* 3600-2700(b), 1500-1380(b), 1045, 950(w), 835, 740(w), 705(w), 470(w). Hydrozincite.

*Powder XRD:* Hydrozincite.

*DSC (°C) [Ar, 5°Cmin$^{-1}$]:* 241(endo).

### *3.4c Preparation of mixed metal hydroxycarbonates at <4°C*

***a) Preparation of copper hydroxycarbonate*** IB(0.0/1.0)

| | | |
|---|---|---|
| 1.0M $Cu(NO_3)_2$ 350mls | | 1.0M $K_2CO_3$, 351mls |
| Temp, 2.5°C | Final pH, 7.2 | Aged, 0hrs |
| Product, 40.61g | Yield, 94.9% | Colour, light green |

*Elemental analysis (%):* Cu,52.1 C,3.5 H,1.1 N,2.3
Calculated: Cu,51.9 C,3.5 H,1.5 N,2.2
for $Cu_2(CO_3)_{0.71}(NO_3)_{0.39}(OH)_{2.19} \cdot 0.75H_2O$

*Powder XRD (4θ):* 25.85(G); 29.80(M); 35.35(M); 43.50(G); 48.50(M); 51.95(G); 67.55(G); 73.50(G).

Malachite, M, and gerhardtite, G, were the only phases observed.

*DSC (°C) [Ar, 5°Cmin$^{-1}$]:* 196(endo, s), 227(endo).

***b) Preparation of ($Zn_{0.3}Cu_{0.7}$) hydroxycarbonate*** IB(0.37/0.63)

| 1.0M (Zn,Cu)$(NO_3)_2$ 20mls | | 1.0M $K_2CO_3$, 20.75mls |
|---|---|---|
| Temp, 1°C | Final pH, 6.9 | Aged, 0hrs |
| Product, 2.39g | Yield, 78.9% | Colour, pale green |

*Comments:*

The yield was low because some of the solid passed through the filter.

*Elemental analysis (%):* Zn,14.9 Cu,24.6 C,4.7 H,2.1 N,0.1

Calculated: Zn,16.0 Cu,26.4 C,5.0 H,2.5 N,0.1

for $(Zn_{0.37}Cu_{0.63})_2(CO_3)_{1.27}(NO_3)_{0.03}(OH)_{1.43} \cdot 3H_2O$

*IR (cm$^{-1}$):* 3600-3000(b), 1505(s), 1395(s), 1100, 1050, 870, 820(s), 745, 705(w), 575(w), 495(w), 410(w).

Malachite.

*Powder XRD:* Amorphous.

***c) Preparation of ($Zn_{0.4}Cu_{0.6}$) hydroxycarbonate*** IB(0.41/0.59)

| 1.0M (Zn,Cu)$(NO_3)_2$ 20mls | | 1.0M $K_2CO_3$, 20.6mls |
|---|---|---|
| Temp, 4.0°C | Final pH, 6.9 | Aged, 0hrs |
| Product, 2.12g | Yield, 93.9% | Colour, pale blue |

*Elemental analysis (%):* Zn,22.9 Cu,31.7 C,3.9 H,1.6 N,0.5

Calculated: Zn,22.5 Cu,31.5 C,3.9 H,1.9 N,0.5

for $(Zn_{0.41}Cu_{0.59})_2(CO_3)_{0.77}(NO_3)_{0.08}(OH)_{2.38} \cdot H_2O$

*IR (cm$^{-1}$):* 3600-2800(b), 1509(s), 1414(s), 1384, 972(w), 837, 746(w), 506(w), 475(w).

Aurichalcite.

*Powder XRD:* Amorphous.

In an attempt to enlarge the particle size of the powder, in order to obtain a diffraction pattern, a small sample of the product (~0.2g) was added to water (4mls) and left for 17 days. The solid was collected and it was observed that its colour had changed to a minty green. The solid was characterised as follows.

*Elemental analysis (%):* Zn,22.6 Cu,33.7 C,4.2 H,1.2 N,0.0
Calculated: Zn,22.5 Cu,34.2 C,4.3 H,1.5
for $(Zn_{0.39}Cu_{0.61})_2(CO_3)_{0.81}(OH)_{2.38} \cdot 0.5H_2O$

*IR ($cm^{-1}$):* 3600-2800(b), 1509(s), 1394(s), 1101(w), 1054, 972(w), 870, 838, 745(w), 478(w).
Aurichalcite.

*Powder XRD (4θ):* 35.10; 55.85; 61.80; 65.50.
The sample gave a faint diffraction pattern corresponding to aurichalcite.

***d) Preparation of $(Zn_{0.5}Cu_{0.5})$ hydroxycarbonate*** IB(0.47/0.53)

| 1.0M $(Zn,Cu)(NO_3)_2$ 20mls | | 1.0M $K_2CO_3$, 18.4mls |
|---|---|---|
| Temp, 1°C | Final pH, 7.1 | Aged, 0hrs |
| Product, 2.08g | Yield, 92.2% | Colour, pale blue |

*Elemental analysis (%):* Zn,27.3 Cu,29.7 C,3.6 H,1.4 N,0.9
Calculated: Zn,27.3 Cu,29.9 C,3.6 H,1.3 N,0.9
for $(Zn_{0.47}Cu_{0.53})_2(CO_3)_{0.68}(NO_3)_{0.14}(OH)_{2.50} \cdot 0.25H_2O$

*Powder XRD (4θ):* 25.85(G); 51.95(G); 55.85(A); 61.80(A); 65.50(A).
A very faint gerhardtite, G, pattern (only 2 lines were detected) and aurichalcite, A, account for all the lines.

***e) Preparation of $(Zn_{0.6}Cu_{0.4})$ hydroxycarbonate*** IB(0.59/0.41)

| 1.0M $(Zn,Cu)(NO_3)_2$ 20mls | | 1.0M $K_2CO_3$, 18mls |
|---|---|---|
| Temp, 1°C | Final pH, 7.5 | Aged, 0hrs |
| Product, 2.19g | Yield, 97.0% | Colour, pale green-blue |

*Elemental analysis (%):* Zn,33.9 Cu,23.3 C,4.5 H,1.3 N,0.0
Calculated: Zn,34.2 Cu,23.1 C,4.5 H,1.3
for $(Zn_{0.59}Cu_{0.41})_2(CO_3)_{0.85}(OH)_{2.30} \cdot 0.35H_2O$

*Powder XRD (4θ):* 55.85; 61.80; 65.55.

Aurichalcite.

### *f) Preparation of ($Zn_{0.7}Cu_{0.3}$) hydroxycarbonate*

i) IB(0.68/0.32)

| | | | | | |
|---|---|---|---|---|---|
| 1.0M $(Zn,Cu)(NO_3)_2$ | 20mls | | | 1.0M $K_2CO_3$, | 19.8mls |
| Temp, | 0.6°C | Final pH, | 7.0 | Aged, | 0hrs |
| Product, | 2.17g | Yield, | 95.4% | Colour, | pale green-blue |

*Elemental analysis (%):* Zn,39.2 Cu,17.6 C,4.0 H,1.3 N,0.0
Calculated: Zn,39.2 Cu,17.9 C,4.1 H,1.5
for $(Zn_{0.68}Cu_{0.32})_2(CO_3)_{0.78}(OH)_{2.44} \cdot 0.5H_2O$

*Powder XRD (4θ):* 55.85(A); 61.80(A); 65,50(A).
Aurichalcite.

ii) P75

| | | | | | |
|---|---|---|---|---|---|
| 1.0M $(Zn,Cu)(NO_3)_2$ | 200mls | | | 1.0M $K_2CO_3$, | ~200mls |
| Temp, | 1.1-1.5°C | final pH, | 7.14 | Aged, | 2hrs |
| Product, | 20.96g | Yield, | 96.0% | Colour, | light blue-green |

*Elemental analysis (%):* Zn,36.8 Cu,17.8 C,3.9 H,1.3 N,0.0
Calculated: Zn,37.6 Cu,18.0 C,4.1 H,1.7 N,0.0
for $(Zn_{0.67}Cu_{0.33})_5(CO_3)_2(OH)_6 \cdot 2H_2O$

*IR ($cm^{-1}$):* 3600-2900(b), 1561(sh), 1509(s), 1410(s), 1380(sh), 1047(w), 967, 838(s), 740(w), 503(w), 474(w).
Aurichalcite.

*Powder XRD:* Aurichalcite.

*DSC (°C) [air, 10°C$min^{-1}$]:* 316(endo, b).

## *3.4d Preparation of ($Zn_{0.3}Cu_{0.7}$) hydroxycarbonate*

Several experiments were carried out to explore the effect of temperature and final pH (the pH after addition) when preparing ($Zn_{0.3}Cu_{0.7}$) hydroxycarbonate by the slow addition of 1.0M $K_2CO_3$ to 20mls of 0.5M $(Zn,Cu)(NO_3)_2$ solution. Some coprecipitation experiments were also undertaken, slowly adding the two reagents

(10mls of 0.5M nitrate solution added with 1.0M $K_2CO_3$) keeping the pH constant (±0.2).

***Precipitation preparations of $(Zn_{0.3}Cu_{0.7})$ hydroxycarbonate***

i) P32

| | | | | | |
|---|---|---|---|---|---|
| 0.5M (Zn,Cu)$(NO_3)_2$ | 20mls | | | 1.0M $K_2CO_3$, | 8.70mls |
| Temp, | 60-62°C | Final pH, | 8.1 | Aged, | 3.5hrs |
| Product, | 1.065g | Yield, | 95.5% | Colour, | grey-brown |

*Comments:*

During the addition a greenish-blue precipitate was formed, the pH increased steadily to ~5.5 where it remained until just before the end point, when the pH rose dramatically with just a few drops of carbonate solution. The final pH was 8.1 but on ageing this steadily decreased levelling off at 6.5, during the ageing the precipitate started going grey eventually becoming dark brown.

*Elemental analysis (%):* Zn,16.1 Cu,39.8 C,1.9 H,1.1 N,2.3
Calculated: Zn,17.6 Cu,41.1 C,1.9 H,1.3 N,2.3
for $(Zn_{0.3}Cu_{0.7})_2(CO_3)_{0.36}(NO_3)_{0.38}(OH)_{2.90}$

*Powder XRD:* Gerhardtite and faint aurichalcite patterns.

*DSC (°C) [Ar, 5°Cmin$^{-1}$]:* endotherms at 221 and 250.

ii) P33

| | | | | | |
|---|---|---|---|---|---|
| 0.5M (Zn,Cu)$(NO_3)_2$ | 20mls | | | 1.0M $K_2CO_3$, | 8.72mls |
| Temp, | 64-65°C | Final pH, | 7.8 | Aged, | 3hrs |
| Product, | 1.082g | Yield, | 97.8% | Colour, | grey-brown |

*Comments:*

Similar to before except this time the pH settled at 6.25.

*Elemental analysis (%):* Zn,16.6 Cu,37.1 C,2.1 H,1.2 N,2.4
Calculated: Zn,17.4 Cu,39.4 C,2.2 H,1.2 N,2.5
for $(Zn_{0.3}Cu_{0.7})_2(CO_3)_{0.42}(NO_3)_{0.41}(OH)_{2.75}$

*Powder XRD:* Gerhardtite and faint aurichalcite patterns.

*DSC (°C) [Ar, 5°Cmin$^{-1}$]:* endotherms at 220 and 249.

iii) P34

| 0.5M (Zn,Cu)$(NO_3)_2$ | 20mls | 1.0M $K_2CO_3$, | 8.70mls |
|---|---|---|---|
| Temp, 60-63°C | Final pH, 6.95 | Aged, | 3hrs |
| Product, 1.091g | Yield, 97.2% | Colour, | grey-green |

*Comments:*

After addition of carbonate the precipitate was a light greenish-blue, but upon ageing the pH slowly increased up to 8.05, accompanied by a colour change to grey-green, during the first 1.5 hours. The sample was collected after 3 hours ageing, by which time the pH had dropped to 6.64.

*Elemental analysis (%):* Zn,17.0 Cu,39.6 C,2.2 H,1.2 N,2.4
Calculated: Zn,17.5 Cu,39.6 C,2.2 H,1.2 N,2.4
for $(Zn_{0.3}Cu_{0.7})_2(CO_3)_{0.42}(NO_3)_{0.39}(OH)_{2.77}$

*Powder XRD:* Gerhardtite and faint aurichalcite patterns.

*DSC (°C) [Ar, 5°Cmin$^{-1}$]:* endotherms at 220 and 249.

iv) P36

| 0.5M (Zn,Cu)$(NO_3)_2$ | 20mls | 1.0M $K_2CO_3$, | 8.55mls |
|---|---|---|---|
| Temp, 60-62°C | Final pH, 6.15 | Aged, | 2.5hrs |
| Product, 1.092g | Yield, 96.3% | Colour, | light turquoise |

*Comments:*

With the addition of carbonate a greenish-blue solid precipitated, the addition was stopped when the pH reached 6.15. After 1.5 hours ageing the pH had increased to 7.45 where it remained until the sample was collected.

*Elemental analysis (%):* Zn,16.9 Cu,39.1 C,2.0 H,1.2 N,2.8
Calculated: Zn,17.3 Cu,39.2 C,2.0 H,1.2 N,2.8
for $(Zn_{0.3}Cu_{0.7})_2(CO_3)_{0.36}(NO_3)_{0.38}(OH)_{2.90}$

*IR (cm$^{-1}$):* 3600-3100(b), **1485(w)**, 1420, **1390(sh)**, 1350, 1050(w), **840(w)**, 820(w), 780(b), 670(w), 515, 430(w).
Gerhardtite absorptions plus less intense aurichalcite (**bold**).

*Powder XRD:* Gerhardtite and faint aurichalcite patterns.

*DSC (°C) [Ar, 5°Cmin$^{-1}$]:* endotherms at 219 and 248.

v) P37

| 0.5M (Zn,Cu)$(NO_3)_2$ 20mls | | 1.0M $Na_2CO_3$, 8.47mls |
|---|---|---|
| Temp, 60-63°C | Final pH, 6.15 | Aged, 2.5hrs |
| Product, 1.113g | Yield, 98.0% | Colour, grey-green |

*Comments:*

The previous experiment was repeated using $Na_2CO_3$, to see if a different carbonate would affect the reaction. A blue-green solid precipitated, after 1hr ageing the solid had become more green in colour and the pH had risen to 7.35. After 2 hours the pH had fallen to 7.40 having peaked at 7.55, and the solid was becoming grey, eventually turning a grey-green colour.

*Elemental analysis (%):* Zn,16.3 Cu,37.1 C,1.9 H,1.1 N,2.8
Calculated: Zn,17.3 Cu,39.1 C,2.0 H,1.2 N,2.9
for $(Zn_{0.3}Cu_{0.7})_2(CO_3)_{0.38}(NO_3)_{0.47}(OH)_{2.77}$

*Powder XRD:* Gerhardtite and faint aurichalcite patterns.

*DSC (°C) [Ar, 5°Cmin$^{-1}$]:* endotherms at 221 and 256.

vi) P42

| 0.5M (Zn,Cu)$(NO_3)_2$ 20mls | | 1.0M $K_2CO_3$, 10mls |
|---|---|---|
| Temp, 3°C | Final pH, 6.40 | Aged, 4hrs |
| Product, 1.145g | Yield, 95.3% | Colour, blue turquoise |

*Comments:*

After the addition of carbonate, the pH slowly rose to 6.80, the solid remained a light blue colour and was collected after 4 hours.

*Elemental analysis (%):* Zn,14.2 Cu,41.0 C,5.0 H,1.5 N,0.0
Calculated: Zn,16.3 Cu,37.0 C,5.0 H,1.7 N,0.0
for $(Zn_{0.3}Cu_{0.7})_2(CO_3)(OH)_2 \cdot H_2O$

*IR (cm$^{-1}$):* 3600-2600(b), 1600-1300(b), 830(w), 480(w b).
Georgite.

*Powder XRD:* Amorphous.

*DSC (°C) [air, 10°Cmin$^{-1}$]:* 62(endo, w), 109(endo, w), 397(endo, w), 437(exo, vw).

vii) P43

| 0.5M (Zn,Cu)$(NO_3)_2$ 20mls | | 1.0M $K_2CO_3$, ~10mls |
|---|---|---|
| Temp, 22-25°C | Final pH, 6.80 | Aged, 4hrs |
| Product, 1.175g | Yield, 99.4% | Colour, light turquoise |

*Comments:*

After the addition of carbonate, the mixture was stirred for 4 hours, the pH slowly rose to 8.00, but the solid remained a light blue turquoise.

*Elemental analysis (%):* Zn,16.0 Cu,33.2 C,3.5 H,1.4 N,1.4
Calculated: Zn,16.6 Cu,37.6 C,3.9 H,1.2 N,1.5
for $(Zn_{0.3}Cu_{0.7})_2(CO_3)_{0.77}(NO_3)_{0.25}(OH)_{2.21} \cdot 0.5H_2O$

*IR (cm$^{-1}$):* **3600-2900(b)**, **1600-1300(b)**, 1045(w), **835(w)**, 805(w), 770(w), 690(w), 510(w), 430(w).
Georgite absorptions (**bold**) plus less intense gerhardtite.

*Powder XRD:* Gerhardtite pattern.

*DSC (°C) [Ar, 5°Cmin$^{-1}$]:* endotherms at 214 and 229(w).

***Constant pH preparations of $(Zn_{0.3}Cu_{0.7})$ hydroxycarbonate***

viii) P47

| 0.5M (Zn,Cu)$(NO_3)_2$ 10mls | | 1.0M $K_2CO_3$, ~5mls |
|---|---|---|
| Temp, 27°C | Const. pH, 7.0 | Aged, 2.5hrs |
| Product, 0.579g | Yield, 96% | Colour, darker turquoise |

*Comments:*

The two reagents were carefully added at such a rate to keep the pH at 7.0 ±0.2. A blue solid precipitated and the pH after the addition was 7.01, at this stage a small sample (0.024g) was taken to compare with the aged product. After 2.5 hours stirring the pH had risen to 8.56 but there was no obvious physical change to the mixture.

Unaged sample:
*IR (cm$^{-1}$):* 3600-2800(b), 1550-1300(b), 830(w), 480(w b).

Georgite.

*Powder XRD:* Amorphous.

*DSC (°C) [air, 10°Cmin$^{-1}$]:* 110(endo, w), 467(endo, w), 480(exo, w).

Aged sample:
*Elemental analysis (%):* Zn,15.3 Cu,35.1 C,4.5 H,1.7 N,0.0
Calculated: Zn,16.3 Cu,37.0 C,5.0 H,1.7 N,0.0
for $(Zn_{0.3}Cu_{0.7})_2(CO_3)(OH)_2 . H_2O$

*IR (cm$^{-1}$):* 3600-2800(b), 1600-1300(b), 835(w), 470(w b).
Georgite.

*Powder XRD:* Amorphous.

*DSC (°C) [$N_2$, 10°Cmin$^{-1}$]:* 118(endo, w), 270(endo, vw), 476(endo, w) and 494 (exo, w).

ix) P48

| | | | | | |
|---|---|---|---|---|---|
| 0.5M $(Zn,Cu)(NO_3)_2$ | ~10mls | | | 1.0M $K_2CO_3$, | 5.40mls |
| Temp, | 60°C | Const. pH, | 7.0 | Aged, | 0hrs |
| Product, | 0.509g | Yield, | 85% | Colour, | light blue |

*Comments:*

The precipitate was a light blue-turquoise during the whole of the reaction, and was collected immediately with no ageing. The yield was low because slightly less than 10mls of nitrate solution was used.

*Elemental analysis (%):* Zn,14.5 Cu,38.7 C,4.6 H,1.5 N,0.0
Calculated: Zn,16.3 Cu,37.0 C,5.0 H,1.7 N,0.0
for $(Zn_{0.3}Cu_{0.7})_2(CO_3)(OH)_2 . H_2O$

*IR (cm$^{-1}$):* 3600-2800(b), 1475 + 1400(b), 1260(w), 830(w), 440(w b).
Georgite.

*Powder XRD:* Amorphous.

*DSC (°C) [$N_2$, 10°Cmin$^{-1}$]:* 237(endo, b), and 509(exo, w).

x) P49

| 0.5M (Zn,Cu)$(NO_3)_2$ | 10.0mls | 1.0M $K_2CO_3$, Xs |
|---|---|---|
| Temp, 23°C | Const. pH, 9.8 | Aged, 0hrs |
| Product, 0.583g | Yield, 96% | Colour, rich blue |

*Comments:*

The precipitate was a rich blue during the whole of the reaction, and was collected immediately with no ageing.

*Elemental analysis (%):* Zn,14.9 Cu,37.1 C,4.3 H,1.5 N,0.6
Calculated: Zn,16.1 Cu,36.7 C,4.4 H,1.3 N,0.6
for $(Zn_{0.3}Cu_{0.7})_2(CO_3)_{0.89}(NO_3)_{0.11}(OH)_{2.11} \cdot H_2O$

*IR ($cm^{-1}$):* 3600-2900(b), 1470 + 1400(b), 840(w), 450(w b).
Georgite.

*Powder XRD:* Amorphous.

*DSC (°C) [$N_2$, 10°C$min^{-1}$]:* 116(endo, w), ~210(endo, b w), 420(endo, w), 445 (exo, w).

xi) P50

| 0.5M (Zn,Cu)$(NO_3)_2$ | 10.0mls | 1.0M $K_2CO_3$, 5.40mls |
|---|---|---|
| Temp, 58°C | Const. pH, 8.4 | Aged, 0.1hrs |
| Product, 0.565g | Yield, 94% | Colour, turquoise |

*Comments:*

The final pH was 8.39 and the mixture was stirred for a further 5 mins, there was no change in pH so the sample was collected.

*Elemental analysis (%):* Zn,15.5 Cu,37.3 C,4.8 H,1.4 N,0.0
Calculated: Zn,16.3 Cu,37.0 C,5.0 H,1.7 N,0.0
for $(Zn_{0.3}Cu_{0.7})_2(CO_3)(OH)_2 \cdot H_2O$

*IR ($cm^{-1}$):* 3600-2800(b), 1470 + 1400(b), 835(w), 450(w b).
Georgite.

*Powder XRD:* Amorphous.

*DSC (°C) [$N_2$, 10°Cmin$^{-1}$]:* 175(endo, b w), 440(endo, w), 489(exo, w).

xii) P51

| | | |
|---|---|---|
| 0.5M (Zn,Cu)$(NO_3)_2$ 10.0mls | | 1.0M $K_2CO_3$, 5.20mls |
| Temp, 25°C | Const. pH, 6.0 | Aged, 0hrs |
| Product, 0.512g | Yield, 85% | Colour, darker turquoise |

*Comments:*

A blue precipitate formed on addition of the reagents; the yield was slightly low owing to some product going through the filter.

*Elemental analysis (%):* Zn,13.6 Cu,41.2 C,4.5 H,1.5 N,0.0
Calculated: Zn,16.3 Cu,37.0 C,5.0 H,1.7 N,0.0
for $(Zn_{0.3}Cu_{0.7})_2(CO_3)(OH)_2 \cdot H_2O$

*IR (cm$^{-1}$):* 3600-2800(b), 1470 + 1400(b), 840(w), 450(w b).
Georgite.

*Powder XRD:* Amorphous.

*DSC (°C) [air, 10°Cmin$^{-1}$]:* 125(endo, w), 455(endo, w), 480(endo, w).

xiii) P58

| | | |
|---|---|---|
| 0.5M (Zn,Cu)$(NO_3)_2$ 10.0mls | | 1.0M $K_2CO_3$, 7.00mls |
| Temp, 22°C | Const. pH, 8.2 | Aged, 0hrs |
| Product, 0.555g | Yield, 92% | Colour, light blue |

*Comments:*

It was much harder to keep the pH constant, it ranged from 7.9-8.4.

*Elemental analysis (%):* Zn,15.4 Cu,38.8 C,4.7 H,1.5 N,0.0
Calculated: Zn,16.3 Cu,37.0 C,5.0 H,1.7 N,0.0
for $(Zn_{0.3}Cu_{0.7})_2(CO_3)(OH)_2 \cdot H_2O$

*IR (cm$^{-1}$):* 3600-2800(b), 1470 + 1400(b), 835(w), 460(w b).
Georgite.

*Powder XRD:* Amorphous.

*DSC (°C) [air, 10°Cmin$^{-1}$]:* 112(endo, w), 423(endo, w), 454(exo, vw).

xiv) P62

| 0.5M $(Zn,Cu)(NO_3)_2$ 200mls | | 1.0M $K_2CO_3$, ~200mls |
|---|---|---|
| Temp, 20°C | Const. pH, 7.0 | Aged, 0hrs |
| Product, 11.77g | Yield, 98.0% | Colour, light blue (hint of green) |

*Comments:*

200mls of 0.5M $(Zn_{0.3}Cu_{0.7})(NO_3)_2$ solution was slowly added to the reaction flask along with 1.0M $K_2CO_3$, keeping the pH at 7.0 ±0.3. Unfortunately the reaction had to be left overnight leaving >100mls of nitrate unreacted. To prevent further reaction or phase changes in the mother liquor the solid was filtered off. The next day a small sample was removed (a, 0.077g) for analysis, and the rest of the solid was added to the mother liquor and the reaction was continued. Half way through the addition the pH was accidentally allowed to rise to 9.6; only nitrate was added until the pH reached 7.0. The mixture was allowed to equilibrate and the solid was collected (b, 6.893g). Slightly less than 100mls of nitrate solution still remained, this was subsequently reacted with $K_2CO_3$ at a pH of 7.0 and the solid was collected (c, 4.799g). All the samples were similar in appearance, light blue powders (with a hint of green), and they all analysed as georgite as shown below.

**a.**

*IR (cm$^{-1}$):* 3600-2800(b), 1475 + 1408(b), 835(w), 476(w b).
Georgite.

*DSC (°C) [air, 10°Cmin$^{-1}$]:* 122(endo, w), 442(endo, w), 460(exo, w).

**b.**

*Elemental analysis (%):* Zn,16.9 Cu,35.3 C,4.8 H,1.7 N,0.0
Calculated: Zn,16.3 Cu,37.0 C,5.0 H,1.7 N,0.0
for $(Zn_{0.3}Cu_{0.7})_2(CO_3)(OH)_2 \cdot H_2O$

*IR (cm$^{-1}$):* 3600-2800(b), 1475 + 1400(b), 836(w), 472(w b).
Georgite.

*DSC (°C) [air, 10°Cmin$^{-1}$]:* 147(endo, b), 439(endo, w), 458(exo, w).

c.

*Elemental analysis (%):* Zn,18.0 Cu,34.6 C,4.8 H,1.6 N,0.0
Calculated: Zn,16.3 Cu,37.0 C,5.0 H,1.7 N,0.0
for $(Zn_{0.3}Cu_{0.7})_2(CO_3)(OH)_2 . H_2O$

*IR ($cm^{-1}$):* 3600-2800(b), 1476 + 1408(b), 836(w), 477(w b).
Georgite.

*DSC (°C) [air, 10°C$min^{-1}$]:* 126(endo, w), 451(endo, w), 465(exo, w).

### *3.4e Constant pH preparations of ($Zn_{0.5}Cu_{0.5}$) hydroxycarbonate*

The following experiments were undertaken to find the best conditions for the preparation of $(Zn_{0.5}Cu_{0.5})$ hydroxycarbonate. Constant pH precipitations were carried out with 10ml aliquots of 0.5M $(Zn_{0.5}Cu_{0.5})(NO_3)_2$ solution, at room temperature over a range of different pH's.

i) P69

| 0.5M (Zn,Cu)$(NO_3)_2$ 10.0mls | | 1.0M $K_2CO_3$, ~5mls |
|---|---|---|
| Temp, 20°C | Const. pH, 6.0 | Aged, 0hrs |
| Product, 0.467g. | Yield, 77% | Colour, dark turquoise |

*Elemental analysis (%):* Zn,23.2 Cu,30.4 C,4.5 H,1.6 N,0.0
Calculated: Zn,27.1 Cu,26.4 C,5.0 H,1.7 N,0.0
for $(Zn_{0.5}Cu_{0.5})_2(CO_3)(OH)_2 . H_2O$

*IR ($cm^{-1}$):* 3600-2700(b), 1477 + 1402(b), 836, 471(w b).
Georgite.

*Powder XRD:* Amorphous.

*DSC (°C) [air, 10°C$min^{-1}$]:* 69(endo, w), 118(endo, w), 460(endo, w), 481(exo, w).

ii) P66

| 0.5M (Zn,Cu)$(NO_3)_2$ 10.0mls | | 1.0M $K_2CO_3$, 6.55mls |
|---|---|---|
| Temp, 22°C | Const. pH, 7.0 | Aged, 0hrs |
| Product, 0.579g | Yield, 96% | Colour, light blue |

*Elemental analysis (%):* Zn,25.8 Cu,24.5 C,4.6 H,1.7 N,0.0
Calculated: Zn,27.1 Cu,26.4 C,5.0 H,1.7 N,0.0
for $(Zn_{0.5}Cu_{0.5})_2(CO_3)(OH)_2 . H_2O$

*IR ($cm^{-1}$):* 3600-2700(b), 1478(s), 1386(s), 836(w), 476(w b).
Georgite.

*Powder XRD:* Amorphous.

*DSC (°C) [air, 10°C$min^{-1}$]:* 106(endo, w), 441(endo, w), 470(exo, w).

iii) P67

| 0.5M (Zn,Cu)$(NO_3)_2$ 10.0mls | | 1.0M $K_2CO_3$, ~10mls |
|---|---|---|
| Temp, 20°C | Const. pH, 8.0 | Aged, 0hrs |
| Product, 0.613g | Yield, 98% | Colour, light blue |

*Elemental analysis (%):* Zn,26.5 Cu,25.2 C,4.6 H,1.7 N,0.0
Calculated: Zn,26.2 Cu,25.4 C,4.8 H,2.0 N,0.0
for $(Zn_{0.5}Cu_{0.5})_2(CO_3)(OH)_2 . 1.5H_2O$

*IR ($cm^{-1}$):* 3600-2700(b), 1474 + 1384(b), 838(w), 476(w b).
Georgite.

*Powder XRD:* Amorphous.

*DSC (°C) [air, 10°C$min^{-1}$]:* 50(endo, w), 116(endo, w), 420(endo, w).

iv) P68

| 0.5M (Zn,Cu)$(NO_3)_2$ 10.0mls | | 1.0M $K_2CO_3$, Xs |
|---|---|---|
| Temp, 19°C | Const. pH, 11.0 | Aged, 0hrs |
| Product, 0.513g | Yield, 96% | Colour, light blue |

*Comments:*

The solid was collected when the addition of nitrate solution had finished, the mother liquor was clear, but blue in colour. The solution was heated up to reduce the volume of liquid but instead of the solute precipitating out, a black (very dark brown) deposit formed on the walls of the flask. Unfortunately, there was not enough for analysis.

*Elemental analysis (%):* Zn,30.8 Cu,27.6 C,2.6 H,1.8 N,0.5
Calculated: Zn,30.7 Cu,29.8 C,2.7 H,1.4 N,0.5
for $(Zn_{0.5}Cu_{0.5})_2(CO_3)_{0.47}(NO_3)_{0.07}(OH)_{2.99}$

*IR ($cm^{-1}$):* 3600-2700(b), 1623(w), 1474(s), **1415**(s), 1383, **1044**(w), 841(w), 460(w b).
Georgite absorptions plus less intense gerhardtite (**bold**).

*Powder XRD:* Amorphous.

*DSC (°C) [air, 10°C$min^{-1}$]:* 109(endo, w), 224(endo, w).
Peak at 224°C was due to a phase other than georgite.

v) P70

| 0.5M $(Zn,Cu)(NO_3)_2$ 360mls | | 1.0M $K_2CO_3$, ~175mls |
|---|---|---|
| Temp, 20°C | Const. pH, 6.5 | Aged, 0hrs |
| Product, 20.47g | Yield, 94.4% | Colour, blue |

*Elemental analysis (%):* Zn,25.9 Cu,27.5 C,4.7 H,1.5 N,0.0
Calculated: Zn,27.1 Cu,26.4 C,5.0 H,1.7 N,0.0
for $(Zn_{0.5}Cu_{0.5})_2(CO_3)(OH)_2 \cdot H_2O$

*IR ($cm^{-1}$):* 3600-2700(b), 1475(s), 1405(s), 838(w), 458(w b).
Georgite.

*Powder XRD:* Amorphous.

*DSC (°C) [air, 10°C$min^{-1}$]:* 104(endo, w), 473(endo, w), 489(exo, w).

### *3.4f Constant pH preparations of $(Zn_{0.7}Cu_{0.3})$ hydroxycarbonate*

A few experiments were undertaken to find the best conditions for the preparation of $(Zn_{0.7}Cu_{0.3})$ hydroxycarbonate. Constant pH precipitations were carried out to see how they compared to normal precipitations (aurichalcite was formed for zinc-rich precipitations at ≤3°C).

i) P74

| 0.5M $(Zn,Cu)(NO_3)_2$ 10.0mls | | 1.0M $K_2CO_3$, ~5mls |
|---|---|---|
| Temp, 23°C | Const. pH, 7.0 | Aged, various |
| Product, n/a | Yield, n/a | Colour, light blue |

*Comments:*

The reaction yielded a light blue solid, a sample was taken and characterised by IR. The rest of the product was stirred at room temperature, and samples were subsequently analysed at regular intervals; the pH of the mixture was also noted.

Unaged:

*Sample:* light blue powder. *pH of reaction mixture* = 6.94

*IR ($cm^{-1}$):* 3600-2900(b), 1478(s), 1406(s), 838(w).
Georgite.

Aged for 2 hours:

*Sample:* light blue powder. *pH of reaction mixture* = 8.42

*IR ($cm^{-1}$):* 3600-2900(b), 1476(s), 1406(s), 838(w).
Georgite.

Aged for 3.5 hours:

*Sample:* light blue powder. *pH of reaction mixture* = 8.62

*IR ($cm^{-1}$):* 3600-2900(b), 1476(s), 1406(s), 838(w).
Georgite.

Aged for 5 hours:

*Sample:* light blue powder. *pH of reaction mixture* = 8.77

*IR ($cm^{-1}$):* 3600-2900(b), 1476(s), 1406(s), 837(w).
Georgite.

Aged for 21 hours:

*Sample:* light green powder. *pH of reaction mixture* = 9.01

*IR ($cm^{-1}$):* 3600-2700(b), 1561, 1509(s), 1414(s), 1364, 1190(w), 1061(w), 970(w), 838(s), 739(w), 506(w), 463(w).
Aurichalcite.

ii) P72

| | | |
|---|---|---|
| 1.0M $(Zn,Cu)(NO_3)_2$ 180mls | | 1.0M $K_2CO_3$, ~175mls |
| Temp, 21°C | Const. pH, 7.0 | Aged, 0hrs |

| | | |
|---|---|---|
| Product, 19.11g | Yield, 97.2% | Colour, light blue |

*Comments:*

Prior to collecting the product a small sample of the reaction mixture was removed (precipitate and liquor) and stirred for a further 3 hours to see if ageing had any affect. The aged precipitate was collected (0.291g) this was a light blue powder similar to the unaged sample.

Unaged:

*Elemental analysis (%):* Zn,40.0 Cu,16.8 C,4.1 H,1.2 N,0.0

Calculated: Zn,40.6 Cu,16.9 C,4.3 H,1.4 N,0.0

for $(Zn_{0.7}Cu_{0.3})_5(CO_3)_2(OH)_6 \cdot H_2O$

*IR ($cm^{-1}$):* 3600-2700(b), 1561(sh), 1510(s), 1410(s), 1365, 1047, 970, 838(s), 740(w), 504(w), 474(w).
Aurichalcite.

*DSC (°C) [air, 10°C$min^{-1}$]:* 326(endo, b).

Aged:

*Elemental analysis (%):* Zn,38.4 Cu,15.8 C,5.2 H,1.4 N,0.0

Calculated: Zn,37.9 Cu,15.8 C,5.0 H,1.7 N,0.0

for $(Zn_{0.7}Cu_{0.3})_2(CO_3)(OH)_2 \cdot H_2O$

*IR ($cm^{-1}$):* 3600-2700(b), 1479(s), 1406(s), 837.
Georgite.

*DSC (°C) [air, 10°C$min^{-1}$]:* 112(endo, w), 438(endo, w), 477(exo, w).

To study the effect of ageing in water a sample (0.193g) of the unaged product was added to a flask with ~15mls of water and stirred for 3 hours at room temperature. A light green-blue powder was filtered off, 0.181g (94%) and was characterised as follows.

*IR ($cm^{-1}$):* 3600-3000(s), 1560(sh), 1510(s), 1411(s), 1366, 1049(w), 971(w), 838(s), 740(w), 507(w), 471(w).
Aurichalcite.

*DSC (°C) [air, 10°C$min^{-1}$]:* 340(endo, b).

## 3.5 Experiment Index



N.B. the prefixes BP, RT and IB indicate boiling point, room temperature and ice-bath reaction conditions. The ratio in parentheses was the cation ratio for the product.

# 4. PREPARATION OF ZINC/COPPER MIXED METAL TRIMELLITATES

## 4.1 Introduction

This chapter describes the preparation and characterisation of zinc/copper mixed metal trimellitates. The introduction is an overview of previous work on trimellitates, and a summary of the aims for the project. A discussion of the results and conclusions follow this section and the experimental details are given at the end of the chapter.

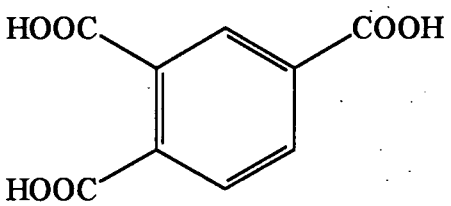


Figure 4.1 Trimellitic acid

The preparation of copper trimellitate was previously reported in the literature. The salt was prepared by adding equivalent quantities of 0.1M copper nitrate solution to a hot solution of 0.1M ammonium trimellitate[109]. A pH of 5.5 was quoted but it was unclear whether this referred to the pH of the reaction mixture throughout the experiment or at the end of it.

$$3Cu(NO_3)_2 + 2(NH_4)_3TM \longrightarrow Cu_3TM_2 . 5H_2O$$

It was found that the product was barely soluble in water, ~$6.0 \times 10^{-5}$ mol $dm^{-3}$. IR and XRD data for the salt were also given.

It was previously found by this research group[2,3] that the products precipitated by the addition of aqueous solutions of aromatic polycarboxylates to copper nitrate solution were dependent on pH (discussed in more detail in section 1.2). If the pH was not controlled, a range of products was obtained as the reaction mixture became less acidic (the pH of 1.0M solution of copper nitrate was ~2.5, as the nitrate was reacted so the pH of the system became less acidic). Experiments were undertaken keeping the pH constant by the controlled addition of the two reagents. Because of the limited solubility of trimellitic acid, the soluble sodium or potassium salts were used[3]. These experiments resulted in the formation of $CuNa_2H_2TM_2 . 4H_2O$ and the analogous $CuK_2H_2TM_2 . 2H_2O$. The inclusion of the alkali metal in the product meant that this was an unsatisfactory route to zinc/copper trimellitates.

$$Cu(NO_3)_2 + 2Na_3TM \xrightarrow{H_2O} CuNa_2H_2TM_2 . 4H_2O + 2NaNO_3 + 2NaOH$$

In order to use the free acid, and thus exclude alkali metals from the product, reactions were undertaken with zinc/copper hydroxycarbonates. As has already been mentioned (chapter 1) several advantages were seen in using these solids:

i) exclusion of alkali metal;
ii) buffer effect, controlling the pH of the reaction mixture; and
iii) the hydroxycarbonates acting as templates for the formation of mixed metal, zinc/copper trimellitates.

An aqueous solution of trimellitic acid reacted almost quantitatively with zinc/copper hydroxycarbonate, forming a basic mixed metal salt. The reaction involved the conversion of one solid into another, because both the hydroxycarbonate and the trimellitate were insoluble. This meant there was a suspension during the whole of the reaction. It was assumed that the trimellitate product was a member of the solid solution series $((Zn_xCu_{1-x})OH)_3TM . 3H_2O$.

$$(Zn_{0.75}Cu_{0.25})_2(OH)_2CO_3 + 2H_3TM \longrightarrow ((Zn_{0.75}Cu_{0.25})OH)_3TM . 3H_2O + 3CO_2$$

The aims of the work reported here were to prepare other trimellitates of this solid solution series using the hydroxycarbonate route and covering a range of zinc/copper ratios; to characterise the series (including the crystal structure); and to investigate the thermal decomposition of the salts (the subject of chapter 6). Next is a discussion of the results followed by the conclusions and experimental details.

## 4.2 Discussion of Results

In principle, tribasic acids like trimellitic acid can form neutral ($m_3TM$, where m represents a single metal valency), acidic ($mH_2TM$ or $m_2HTM$) or basic ($m_4TMOH$, etc.) salts. All three types of salts were prepared via the hydroxycarbonate route and the type of salt formed depended on the amount of acid used. Some experiments were also undertaken to prepare trimellitates by reacting brass with trimellitic acid, but these only resulted in acidic salts. First the basic trimellitates will be discussed, followed by the neutral and then the acidic salts (i.e. in order of decreasing metal content).

### *4.2a Basic trimellitates*

In attempting to prepare members of the solid solution series, it became apparent that the stoichiometry calculated for the series was misleading, and that the maximum number of metals that could be incorporated was 2.5 per trimellitate group, as opposed to 3. Incomplete reactions occurred if the ratio of metal to trimellitate was greater than 2.5. The general formula for the trimellitate solid solution series is given in the reaction scheme below.

$$5(Zn_xCu_{1-x})_2(OH)_2CO_3 + 4H_3TM \longrightarrow 4(Zn_xCu_{1-x})_{1.5+y}(OH)_{2y}TM \cdot 2H_2O$$

$$x > 0.5; \quad y = 0.5\text{-}1$$

Basic trimellitates of the above series were prepared with cation ratios of x=1.0, 0.9, 0.67 and 0.5. The compound previously prepared with x=0.75 (discussed in section 4.1) was re-analysed and found to be a member of the series. The series was non stoichiometric and could accommodate between 2 to 2.5 metals per trimellitate group (i.e. y=0.5-1), although the products obtained from the reactions with zinc/copper hydroxycarbonates usually had 2.5 metals. Only salts with cation ratios of x≥0.5 were obtained, attempts to prepare copper-rich trimellitates always produced mixtures of basic and neutral salts (these will be discussed later).

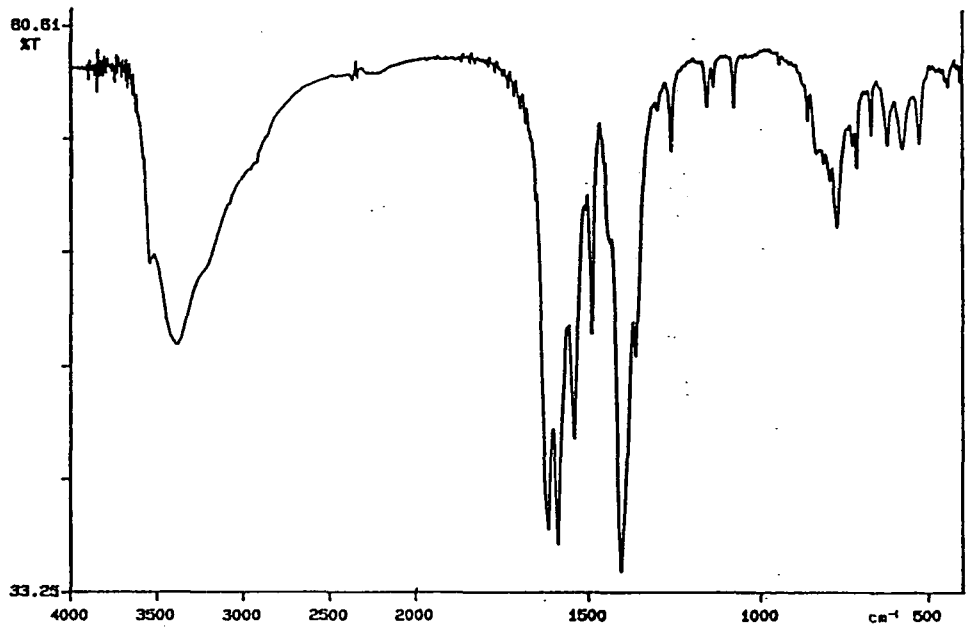


Figure 4.2 IR spectrum of zinc/copper basic trimellitate, $(Zn_xCu_{1-x})_{2.5}(OH)_2TM \cdot 2H_2O$ (for the spectrum shown x=0.9, y=1).

The basic zinc/copper trimellitates were insoluble light blue powders (the zinc salt was white), and were easy to handle as they were both air and moisture stable. The IR spectra for the salts (figure 4.2) were dominated by $\nu(CO_2)$ absorptions at ~1600 from

the carboxylate groups and 1395cm$^{-1}$, and ν(O-H) absorptions at 3600-2900cm$^{-1}$ from water and hydroxyl groups. The absorption at 1490cm$^{-1}$ was due to ring deformations of the phenyl group. The aromatic hydrogen in plane bending vibrations were at 1156, 1137 and 1078cm$^{-1}$, and out of plane bending vibration at 774cm$^{-1}$.

Powder X-ray diffraction was found to be very useful for the identification of the phases produced. Table 4.1 gives the 4θ and d spacings obtained for the zinc salt. All the mixed salts of the series had similar diffraction patterns.

| 4θ | d (Å) | 4θ | d (Å) |
|---|---|---|---|
| 16.95 | 10.49(4) | 35.45 | 5.03(1) |
| 23.50 | 7.57(3) | 41.80 | 4.27(1) |
| 24.80 | 7.18(3) | 44.35 | 4.03(1) |
| 31.90 | 5.59(2) | 45.10 | 3.96(1) |
| 32.45 | 5.49(2) | 45.70 | 3.91(1) |
| 34.60 | 5.15(1) | 48.30 | 3.71(1) |

Table 4.1 XRD results (4θ <50°) for $Zn_{2.5}(OH)_2TM \cdot 2H_2O$. Estimated standard deviations for the d spacings are in parentheses.

As was previously mentioned, the basic trimellitates were insoluble, making recrystallisation impossible. The only way found to produce crystals was by the slow reaction of the reagents. The gel method[16] was used to slowly react zinc/copper nitrate solutions with sodium trimellitate solution. This involved impregnating a silica gel with the nitrate solution, then adding a weak trimellitate solution on top of the gel. The silica gel slows down the transportation of the reagents, encouraging the formation of isolated single crystals. The reactions occurred over a period of days to weeks. This route was successful in producing crystals of $Zn_2OH(TM) \cdot 2H_2O$ (colourless prisms) and $ZnCuOH(TM) \cdot 2H_2O$ (green, distorted octahedra). Both compounds had the same powder diffraction patterns as the basic trimellitate solid solution series. However, the metal content was lower than that normally found for the hydroxycarbonate preparations (cf. 2.5 metals per trimellitate). The structure was determined for both compounds. The zinc salt will be discussed first and then the mixed metal salt will be compared with it. Full data for these structures are given at the end of the chapter with the experimental details.

*Crystal structure of $Zn_2OH(TM) \cdot 2H_2O$*

The crystal structure of basic zinc trimellitate had two metal sites in a 1:1 ratio (figure 4.3), and surprisingly both sites were square based pyramidal. There were only a few structures reported in the literature with zinc coordinated to five oxygens[27,110-117] and of these only three structures had square based pyramidal zinc[110,112], the others being trigonal bipyramidal.

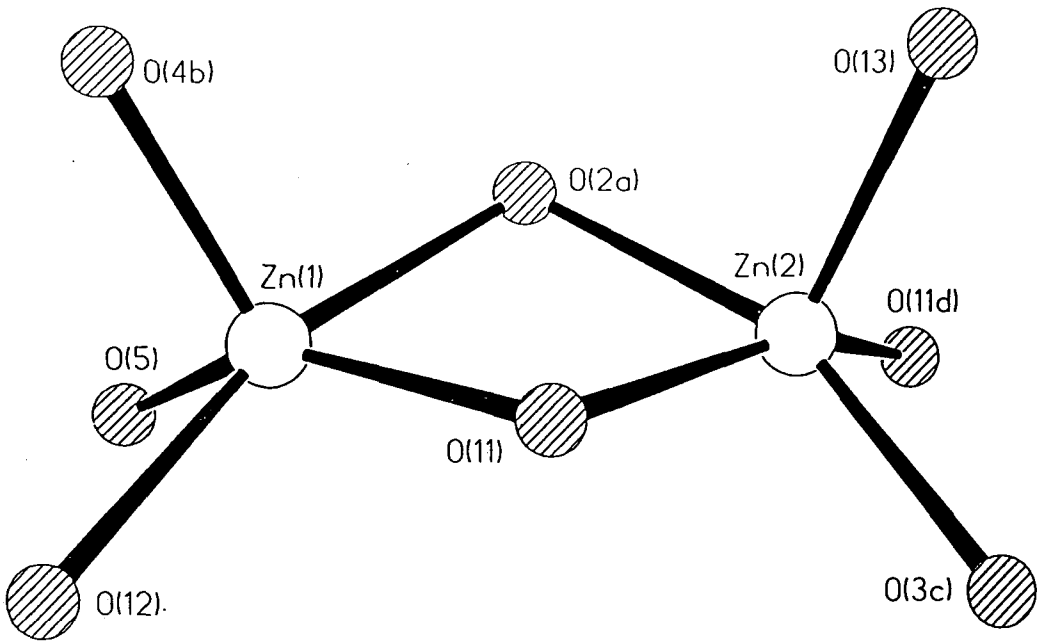


Figure 4.3 Metal coordination for $Zn_2OH(TM) . 2H_2O$.

Zn(1) was coordinated to 3 carboxyl oxygens, 1 water and 1 hydroxyl oxygen (O(12) and O(11) respectively). The oxygen at the apex of the pyramid, O(4b), was from a carboxyl group. The bond lengths ranged from 1.955-2.126Å (table 4.2), and the zinc atom was slightly above the mean plane of the base (0.415Å). The two zinc sites shared a basal edge and the angle between the planes of the bases was 132.0°. The distance between the metals was 3.178Å. Zn(2) was coordinated to 2 carboxyl, 1 water and 2 hydroxyl oxygens, forming a less distorted pyramid (i.e. excluding the apical oxygen, O(13), the distances from the mean basal plane were closer to zero, table 4.2). The hydroxyl oxygens, O(11) and O(11d), were trans in the base and a water molecule, O(13), occupied the apical site. The Zn-O bond lengths ranged from 2.033-2.068Å and the metal was 0.383Å above the plane of the base.

| **Zn(1) coordination** | | | **Zn(2) coordination** | | |
|---|---|---|---|---|---|
| | **Zn-O (Å)** | **Height from base (Å)** | | **Zn-O (Å)** | **Height from base (Å)** |
| Zn(1) | — | 0.415 | Zn(2) | — | 0.383 |
| O(4b) | 1.966(4) | 2.376 | O(13) | 2.060(4) | 2.433 |
| O(2a) | 2.126(4) | 0.163 | O(2a) | 2.065(4) | 0.070 |
| O(5) | 1.955(4) | -0.148 | O(3a) | 2.033(4) | 0.064 |
| O(11) | 1.999(4) | -0.166 | O(11) | 2.068(4) | -0.074 |
| O(12) | 2.094(4) | 0.151 | O(11a) | 2.039(4) | -0.060 |

Table 4.2 Distances from the mean basal plane and bond lengths for the zinc sites in $Zn_2OH(TM) . 2H_2O$. Standard deviations are given for the bond lengths (in parentheses) but were not calculated for the heights from the base.

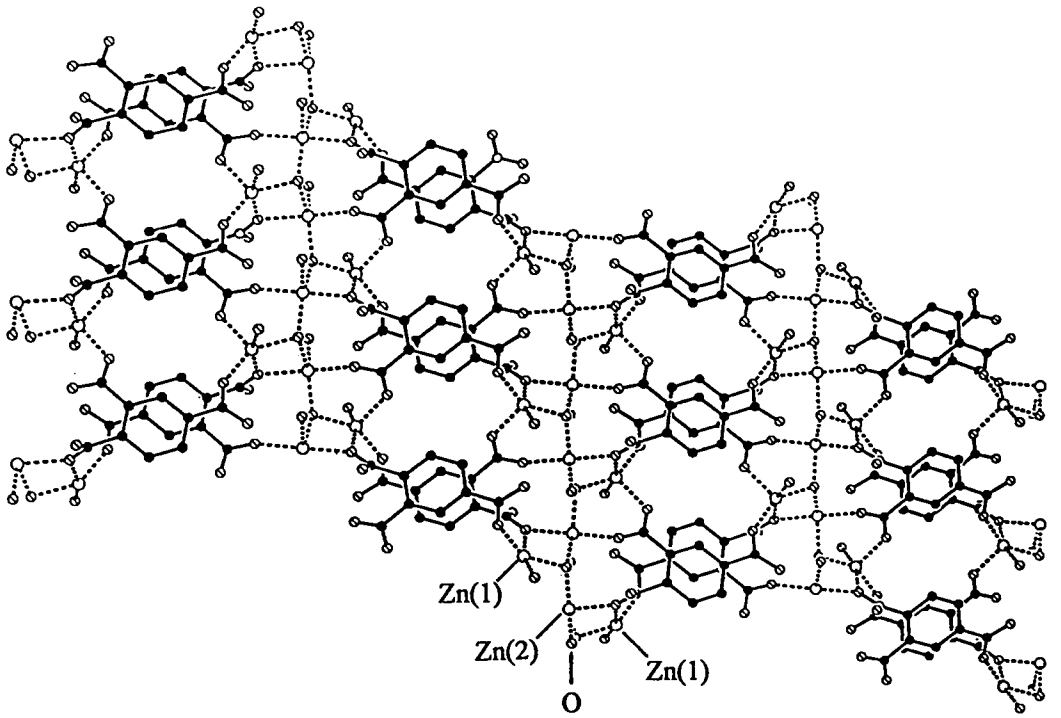


Figure 4.4 View down the z axis of $Zn_2OH(TM) . 2H_2O$.

Figure 4.4 is the view along the z axis; broken lines have been used to highlight the metal coordination. The backbone of the metal oxygen chains which ran parallel to the y axis was -Zn(2)-O(11)-Zn(2)-O(11)-. The Zn(1) pyramids were situated on either side of the chain, and coordinated to three different trimellitate groups. The chains were bridged by trimellitate groups, forming layers. The Zn(2) atoms were bridged by the hydroxyl oxygens (O(11) was coordinated to 3 metals), forming chains of 5 coordinate zincs along the y axis, figure 4.4. The metal-metal distance between neighbouring Zn(2) sites was 3.325Å and between Zn(1)-Zn(2b) was 3.399Å (Zn(2b) was the next nearest Zn(2) site to Zn(1); the metals were bridged by the hydroxyl oxygen O(11)).

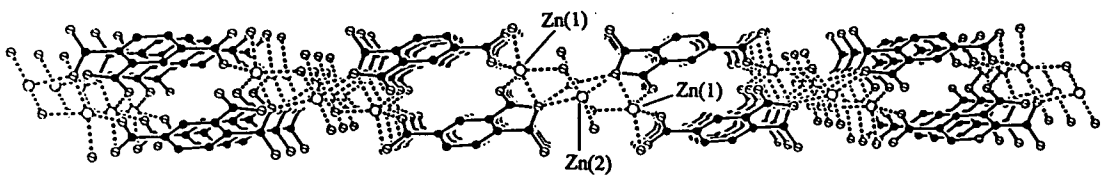


Figure 4.5 View down the y axis of $Zn_2OH(TM) . 2H_2O$.

The trimellitates were paired, one above and one below the metal chains, as shown in figure 4.5. These groups were angled such that the upper trimellitate was approximately coplanar with the lower trimellitate of the next pair (figure 4.6). The trimellitates on the other side of the chain were orientated in the opposite direction. The

angle between the planes of the phenyl rings either side of the chain was 53.7°. The angle calculated was that between the normal for each plane.

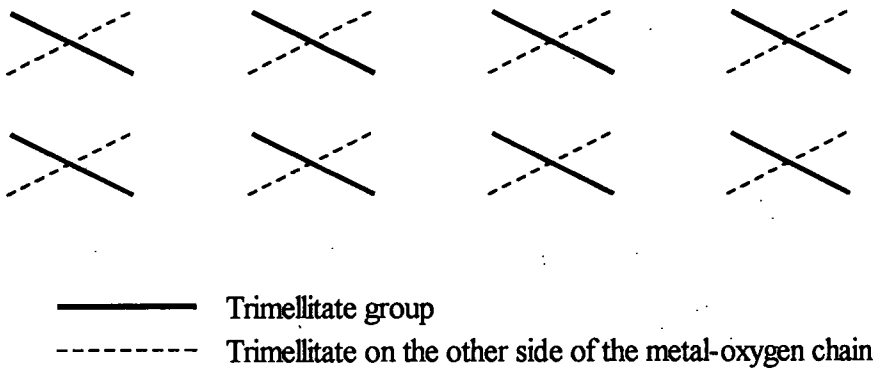


Figure 4.6 Orientation of the trimellitate groups within a layer for $Zn_2OH(TM)$ . $2H_2O$. The view is along the x axis, i.e. orthogonal to the metal-oxygen chains.

*Crystal structure of ZnCuOH(TM) . $2H_2O$*

The crystal structure of ZnCuOH(TM) . $2H_2O$ was very similar to that for the zinc salt, but some differences were found for the metal coordinations. Zinc and copper cations were indistinguishable by x-ray diffraction because they have very similar numbers of electrons. However, the position of the copper was deduced from the M-O bond lengths (table 4.3 and figure 4.7). The distances for the site assumed to be Zn(1) corresponded well with those found for the zinc salt, but the coordination around the other site was notably different.

| **Zn(1) coordination** | | | **Cu coordination** | | |
|---|---|---|---|---|---|
| | **Zn-O (Å)** | **Height from base (Å)** | | **Cu-O (Å)** | **Height from base (Å)** |
| Zn(1) | — | 0.345 | Cu | — | 0.123 |
| O(4b) | 1.981(8) | 2.330 | O(13) | 2.362(9) | 2.481 |
| O(2a) | 2.116(8) | 0.104 | O(2a) | 1.996(7) | -0.014 |
| O(5) | 1.928(8) | -0.094 | O(3a) | 1.945(9) | -0.013 |
| O(11) | 2.012(8) | -0.105 | O(11) | 2.024(8) | 0.015 |
| O(12) | 2.068(9) | 0.095 | O(11a) | 1.981(8) | 0.012 |

Table 4.3 Distances from the mean basal plane and bond lengths for the metal sites in CuZnOH(TM) . $2H_2O$. Standard deviations are given for the bond lengths (in parentheses) but were not calculated for the heights from the base.

In comparison with the Zn(2) site for basic zinc trimellitate, the square based pyramid was less distorted and the apical bond (to a water molecule) was significantly longer, 2.362Å. A long apical bond is characteristic of copper square based

pyramids[28,29,50,55,64]. Hence, it was deduced that the copper had preferentially filled the "Zn(2)" site, as opposed to being randomly distributed through the structure.

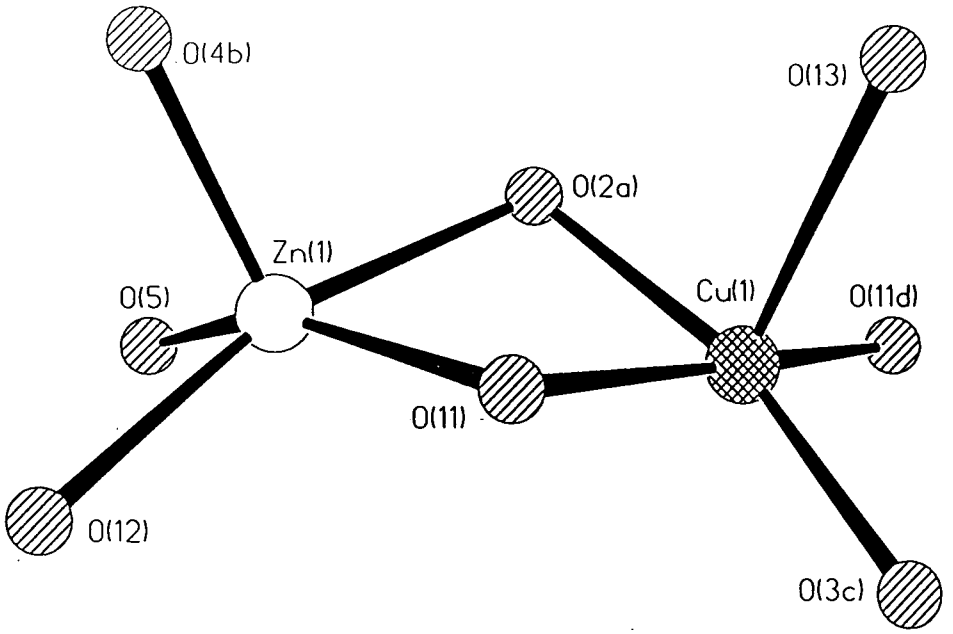


Figure 4.7 Metal coordination for ZnCuOH(TM) . $2H_2O$.

The metal-metal distances were slightly different, Cu-Cu was 3.237(3)Å (cf. Zn(2)-Zn(2), 3.325Å) and the shortest Zn-Cu distance (see figure 4.7) was 3.069(2)Å (cf. Zn(1)-Zn(2), 3.178Å). The angle between the basal planes (shown in figure 4.7) was slightly larger than that found for the zinc salt, 134.4° (cf. 132.0°).

Despite these differences in the metal coordination the overall layer structure was very similar to that for the zinc salt, figures 4.4–4.6, except that copper occupies the Zn(2) sites in these diagrams. The copper atoms were bridged by hydroxyl groups, O(11), forming metal-oxygen chains along the y axis. Coordinated to either side of these chains were zinc square based pyramids. The trimellitate groups bridged between the chains, forming layers.

The two crystal structures illustrate that for the basic trimellitate solid solution series, $(Zn_xCu_{1-x})_{1.5+y}(OH)_{2y}TM$, copper was substituted for zinc in the Zn(2) sites of the zinc trimellitate structure. It would appear that copper was unable to substitute for the zinc occupying the other site, because attempts to prepare copper-rich samples of the solid solution series were unsuccessful. The main difference between the copper and zinc coordinations was the length of the apical bond, 2.362 and 2.060Å respectively. For the Zn(2) site the apex of the pyramid was formed by a water molecule, O(13). This water molecule was not involved in any framework bonding for the layer, and lengthening the apical bond to this site did not affect the overall layer structure. However, the apical bond of the Zn(1) site was to a carboxylate group. If this bond was lengthened, owing to copper substitution, this would distort the layer structure. It is therefore postulated that zinc in the Zn(1) position cannot be replaced by copper because this would distort the layer structure too much. However, the copper can replace zinc in

the Zn(2) site because this does not significantly distort the layer. As there was an equivalent number of Zn(1) and Zn(2) sites, the maximum copper substitution expected for the solid solution series is a 1:1 zinc, copper ratio, as was found experimentally.

The stoichiometry for the crystals was $M_2OH(TM)$, and for the precipitates was $M_{2.5}(OH)_2TM$. Although these products had different stoichiometries they all produced similar powder XRD patterns, i.e. they had similar structures. The crystal structures reported here gave little indication of how extra metals and hydroxides (of the precipitated salts) were accommodated within them. Considering that the oxygen atoms were positioned along the metal chains (see figure 4.5), one would expect extra cations to be situated above or below the chains so that they could interact with the oxygen atoms. The extra hydroxyl groups, required to balance the charge, may interact with the zinc cations in the chains, making them 6 coordinate (i.e. octahedral).

It was discussed in the literature review, section 2.2c, that the separation between the asymmetric and symmetric $\nu(CO_2)$ absorptions, $\Delta\nu_{(asym\text{-}sym)}$, was dependent on the type of carboxylate coordination. Most of the work has centred on acetate salts[70,71], but there was one article concerned with pyromellitate compounds[24]. It was found for the acetates that:

| $\Delta\nu_{(asym\text{-}sym)}$ / $cm^{-1}$ | Carboxylate Coordination |
|---|---|
| >200 | monodentate |
| 164 | ionic (non coordinated) |
| 170-150 | ionic, bridging or chelating |
| <150 | bridging or chelating |
| <105 | chelating or syn-syn |

Other carboxylates are expected to have similar correlations, but the $\Delta\nu_{(asym\text{-}sym)}$ values will be relative to those for the ionic salts. For the present work it was assumed that $\Delta\nu_{(asym\text{-}sym)}$ for an ionic trimellitate salt was the same as pyromellitate[24], 180$cm^{-1}$.

| $\nu(CO_2)_{asym}$ / $cm^{-1}$ | $\nu(CO_2)_{sym}$ / $cm^{-1}$ | $\Delta\nu_{(asym\text{-}sym)}$ / $cm^{-1}$ | Carboxylate Coordination |
|---|---|---|---|
| **$Zn_2OH(TM) . 2H_2O$** | | | |
| 1617 (s) | 1397 (s) | 220 | monodentate |
| 1588 (s) | 1362 (m) | 226 | monatomic bridge |
| 1541 (m) | 1397 (s) | 144 | bridging |
| **$ZnCuOH(TM) . 2H_2O$** | | | |
| 1617 (s) | 1400 (s) | 217 | monodentate |
| 1592 (s) | 1354 (m) | 238 | monatomic bridge |
| 1541 (m) | 1400 (s) | 141 | bridging |

Table 4.4 IR and crystal structure data for $ZnCuOH(TM) . 2H_2O$ and $Zn_2OH(TM) . 2H_2O$.

IR and crystal structure data are given in table 4.4 for the two trimellitate crystals. Assignments of $\nu(CO_2)$ are often more difficult for polycarboxylates because there can be more than one type of carboxylate coordination. The trimellitate crystals discussed here had three different types of carboxylate coordination. For the two salts three absorptions were assigned to asymmetrical vibrations and two for symmetrical vibrations (i.e. two of the carboxylate coordinations had similar $\nu(CO_2)_{sym}$ absorptions). It was assumed that the absorption at $1397cm^{-1}$ was from $\nu(CO_2)_{sym}$ for two different carboxylate groups because it was a much stronger absorption (cf. IR spectrum for basic metal trimellitate, figure 4.2).

What still required to be ascertained was which $\nu(CO_2)_{asym}$ absorption was associated with the $\nu(CO_2)_{sym}$ absorption at $1362cm^{-1}$. This was deduced by comparing the IR absorptions for both salts. Only two absorptions for the mixed metal salt were notably different to those for the zinc salt, 1592 and $1354cm^{-1}$. (cf. 1588 and $1362cm^{-1}$ respectively). This suggested that only one carboxylate group was significantly affected by the substitution of copper and that this carboxylate group absorbs at 1588 and $1362cm^{-1}$ for basic zinc trimellitate, and 1592 and $1354cm^{-1}$ for basic zinc copper trimellitate.

The values of $\Delta\nu_{(asym-sym)}$ are given in table 4.4 along with the assignments for the carboxylate coordination. A $\Delta\nu_{(asym-sym)}$ value of $\sim 140cm^{-1}$ was from the bridging carboxylate. There were two separations $>200cm^{-1}$, which are normally associated with monodentate coordinations. The coordinations were monodentate and monatomic bridge (for which no values of $\Delta\nu_{(asym-sym)}$ had previously been assigned). It would therefore appear to be more appropriate to define values $>200cm^{-1}$ as mono-hapto carboxylates. The larger separation was assigned to monatomic bridging carboxylate because the $\nu(CO_2)$ absorptions were the ones affected by copper substitution. The monatomic bridge was coordinated to zinc and copper atoms for the mixed salt. The monodentate carboxylate was coordinated to zinc for both salts, and one would not expect the IR absorptions for this group to differ greatly between the two salts.

To summarise, it was deduced that these two trimellitate salts had $\Delta\nu_{(asym-sym)}$ values of 226 and $238cm^{-1}$ from monatomic bridging carboxylates, 220 and 217 from monodentate, and 144 and 141 from bridging carboxylate groups. It was also found that monatomic bridges have separations comparable to those found for monodentate carboxylates.

### *4.2b Neutral trimellitates*

Neutral salts of copper and zinc were formed by increasing the amount of acid reacting with the hydroxycarbonate.

$$3M_2(OH)_2CO_3 + 4H_3TM \longrightarrow 4M_{1.5}TM \cdot 2H_2O + 3CO_2 + H_2O$$

As mentioned previously, the attempted preparations of copper-rich basic trimellitates always produced either incomplete reactions or mixtures. The mixtures consisted of two or more the following three phases (deduced by XRD):

i) basic trimellitate solid solution series;

ii) basic copper salt (the stoichiometry was not deduced because the phase was never isolated); and

iii) neutral copper phase.

The zinc/copper ratio for each phase in a mixture could not be determined because the phases were inseparable.

When sufficient acid was present, mixed salts with the same structure as the neutral copper salt were obtained, and had the general formula $(Zn_xCu_{1-x})_{1.5-1.9}(OH)_{0-0.8}TM \cdot 2H_2O$. This series had a very limited substitution ($x<0.2$), but it was possible to increase the metal content to 1.9 (i.e. creating a basic salt).

Powder XRD was invaluable in determining the phases present. The 4θ and d spacings for zinc and copper neutral salts and the basic copper trimellitate (phase "ii" above) are given in table 4.5.

| $Cu_{1.5}TM \cdot 2H_2O$ | | Basic copper salt | | $Zn_{1.5}TM \cdot 2H_2O$ | |
|---|---|---|---|---|---|
| 4θ | d (Å) | 4θ | d (Å) | 4θ | d (Å) |
| 16.50 | 10.77(4) | 18.30 | 9.72(4) | 11.90 | 14.93(12) |
| 25.20 | 7.06(3) | 23.45 | 7.59(3) | 18.15 | 9.80(4) |
| 29.20 | 6.10(2) | 24.70 | 7.20(3) | 29.35 | 6.07(2) |
| 30.25 | 5.89(2) | 27.40 | 6.50(2) | 30.20 | 5.90(2) |
| 33.40 | 5.34(2) | 34.85 | 5.12(1) | 33.65 | 5.30(2) |
| 34.00 | 5.24(2) | 43.40 | 4.12(1) | 41.45 | 4.31(1) |
| 38.10 | 4.68(1) | 49.10 | 3.64(1) | 45.45 | 3.93(1) |
| 38.90 | 4.59(1) | | | 46.70 | 3.83(1) |
| 40.80 | 4.38(1) | | | 48.75 | 3.67(1) |
| 43.85 | 4.08(1) | | | | |
| 44.95 | 3.98(1) | | | | |
| 46.40 | 3.85(1) | | | | |
| 46.85 | 3.82(1) | | | | |
| 47.55 | 3.76(1) | | | | |

Table 4.5 XRD results for $Cu_{1.5}TM \cdot 2H_2O$, basic copper salt (stoichiometry not known), and $Zn_{1.5}TM \cdot 2H_2O$. Estimated standard deviations for the d spacings are in parentheses.

IR was of limited use as the spectra of the basic and neutral trimellitate salts were all similar. For example the main difference of the copper-rich trimellitate spectrum from that for basic zinc trimellitate, figure 4.2, was that the carboxylate absorptions at 1569 and 1391cm$^{-1}$ were only accompanied by one other absorption, at 1490 cm$^{-1}$ (cf. figure 4.2: 1617, 1589, 1542, 1490, 1408, 1364cm$^{-1}$).

It was mentioned in the introduction to this chapter that the preparation of $Cu_3TM_2$ . $5H_2O$ was reported in the literature. Although this compound has a similar stoichiometry to the copper trimellitate reported here, the two salts had different XRD patterns. Hence, the two compounds were different phases of copper trimellitate.

No attempt was made to substitute copper into $Zn_{1.5}TM$ . $2H_2O$ because there was already a suitable solution series for the zinc-rich trimellitates. Like the previous trimellitates this white powder was insoluble, but was air and moisture stable. The IR spectrum was similar to that of the neutral copper salt except that the carboxylate bands were at 1574 and 1402cm$^{-1}$ (both peaks were broad).

The $\Delta\nu_{(asym-sym)}$ values for copper and zinc trimellitate were 178 and 172cm$^{-1}$ respectively. These values are very close to the 180cm$^{-1}$ assumed for ionic coordination. However, it is unlikely that these salts were ionic, because one would expect them to have had a greater water content in order to fulfil the coordination for the cations. The carboxylates were more likely to be either bridging or chelating. It was found for the acetates that bridging carboxylates often had separations close to that found for ionic carboxylates. Whether the carboxylate groups were bridging or chelating, the structure for the salts will be polymeric (most likely to be a layer), because the anion was a polycarboxylate with all the carboxylates coordinated to metal centres.

### *4.2c Acidic trimellitates*

CuHTM . $2.5H_2O$ was prepared by the hydroxycarbonate route when a large excess of trimellitic acid was used, but only as part of a mixture of trimellitates. Acidic salts were also formed by reacting brass with trimellitic acid. Several experiments were undertaken to explore the possibility of using brass (30/70 zinc copper ratio) as a source of copper and zinc for the formation of mixed metal salts. No reaction was observed when brass turnings were added to a boiling aqueous solution of trimellitic acid, but when left to stand for a few days, blue spherulites formed on the brass as well as a small amount of blue and white precipitates. The blue powder and the spherulites were characterised as $Cu_{0.5}H_2TM$ . $2H_2O$ (with up to 1-2% zinc incorporation). The white powder was originally presumed to be unreacted trimellitic acid and was not analysed. In the light of the electrolysis experiments (discussed next) it is highly likely that the white precipitate was $Zn_{0.5}H_2TM$ . $2H_2O$.

$$\text{Zn/Cu (brass)} + H_3TM \xrightarrow{\text{RT, 48hrs}} Zn_{0.5}H_2TM \cdot 2H_2O \quad (2\text{-}4\%) + Cu_{0.5}H_2TM \cdot 2H_2O \quad (2\text{-}4\%)$$

A small amount of green solid later developed on the brass. This was characterised as $(Zn_{0.3}Cu_{0.7})HTM \cdot 3H_2O$ and gave the same diffraction pattern as that for the copper monohydrogen salt, but again was obtained in very low yield.

Some electrolysis experiments were carried out to try and improve the yield for the brass reactions. The cell had a brass anode and used a solution of trimellitic acid as the electrolyte. The experiments did produce gram quantities of trimellitates, but the products were a mixture of zinc dihydrogen and copper mono- and di-hydrogen salts. It was hoped that the metals would substitute all the acidic protons, however, this was not achieved.

$$\text{Zn/Cu (brass)} + H_3TM \xrightarrow{e^-} Zn_{0.5}H_2TM \cdot 2H_2O + Cu_{0.5}H_2TM \cdot 2H_2O + CuHTM \cdot 2H_2O$$

| $CuHTM \cdot 2.5H_2O$ | | $Cu_{0.5}H_2TM \cdot 2H_2O$ | | $Zn_{0.5}H_2TM \cdot 2H_2O$ | |
|---|---|---|---|---|---|
| 4θ | d (Å) | 4θ | d (Å) | 4θ | d (Å) |
| 14.90 | 11.93(8) | 17.70 | 10.04(4) | 14.80 | 12.01(8) |
| 27.90 | 6.38(2) | 25.55 | 6.97(3) | 20.40 | 8.72(4) |
| 29.85 | 5.97(2) | 26.35 | 6.76(3) | 28.05 | 6.35(2) |
| 31.30 | 5.69(2) | 30.05 | 5.93(2) | 29.05 | 6.13(2) |
| 32.15 | 5.54(2) | 34.10 | 5.23(2) | 34.35 | 5.19(1) |
| 33.80 | 5.27(2) | 36.10 | 4.94(1) | 37.25 | 4.79(1) |
| 34.65 | 5.15(1) | 38.00 | 4.70(1) | 41.00 | 4.36(1) |
| 38.60 | 4.62(1) | 41.80 | 4.27(1) | 42.25 | 4.23(1) |
| 43.40 | 4.12(1) | 47.45 | 3.77(1) | 45.00 | 3.97(1) |
| 46.15 | 3.87(1) | 48.85 | 3.66(1) | 46.80 | 3.82(1) |
| 46.85 | 3.82(1) | | | 47.80 | 3.74(1) |
| 48.85 | 3.66(1) | | | 48.85 | 3.66(1) |
| | | | | 49.85 | 3.59(1) |

Table 4.6 XRD results ($4\theta<50°$) for $CuHTM \cdot 2.5H_2O$, $Cu_{0.5}H_2TM \cdot 2H_2O$, and $Zn_{0.5}H_2TM \cdot 2H_2O$. Estimated standard deviations for the d spacings are in parentheses.

The acidic salts were sparingly soluble, but attempts to recrystallise them from water resulted in the samples disproportionating, producing a mixture of neutral,

$M_{1.5}TM \cdot 2H_2O$, and acidic salts. Suitable crystals for x-ray structural determination were not obtained by recrystallisation. Figure 4.8 shows the IR spectra for the acidic salts and table 4.6 gives the XRD results.

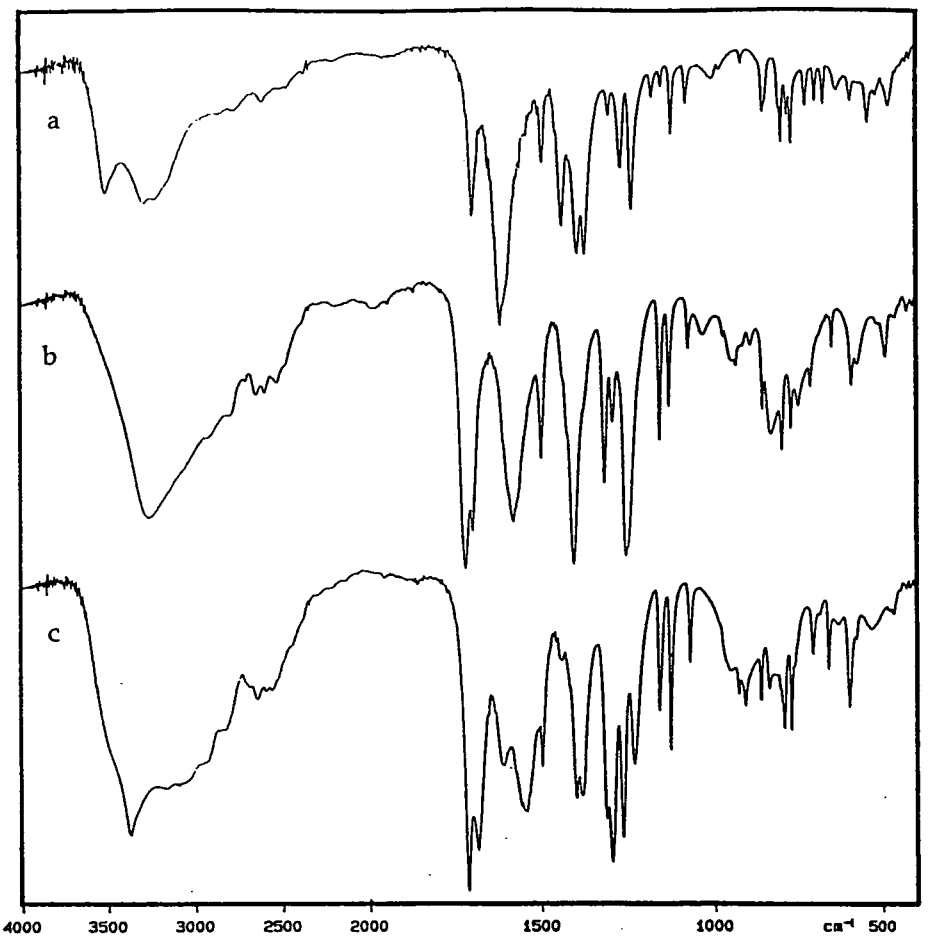


Figure 4.8 IR spectra for (a-c) $CuHTM \cdot 2.5H_2O$, $Cu_{0.5}H_2TM \cdot 2H_2O$, and $Zn_{0.5}H_2TM \cdot 2H_2O$.

The IR spectra for these salts had $\nu(CO)$ carbonyl absorptions at ~1700cm$^{-1}$, the intensity of which was greater for the dihydrogen salts, $M(H_2TM)_2$ (for these salts there were two $\nu(CO)$ peaks). As one would expect, the carboxylate bands (~1600 and ~1400cm$^{-1}$) were less intense for the salts with more carboxylic groups. At ~1400cm$^{-1}$ there was also a $\nu(CO_2)$ absorption from the carboxylic groups (the IR spectrum for trimellitic acid had a carboxylate $\nu(CO_2)$ absorption at 1410cm$^{-1}$).

Data for $\nu(CO_2)$ carboxylate absorptions are collated in table 4.7. Copper hydrogen trimellitate had $\Delta\nu_{(asym-sym)}$ values of 246 and 180cm$^{-1}$. It was deduced from these values that the compound had a monodentate carboxylate group and a bridging/chelating carboxylate group, respectively. A $\Delta\nu_{(asym-sym)}$ value of 180cm$^{-1}$ could also be for an ionic/non coordinated carboxylate group, but considering the low number of donor sites, 2.5 water molecules and 1 monodentate carboxylate group (assuming that the carboxylic group did not coordinate to copper), it is more probable that both carboxylate groups were coordinated to copper.

| $\nu(CO_2)_{asym}$ / $cm^{-1}$ | $\nu(CO_2)_{sym}$ / $cm^{-1}$ | $\Delta\nu_{(asym-sym)}$ / $cm^{-1}$ | Carboxylate Coordination |
|---|---|---|---|
| **$CuHTM \cdot 2.5H_2O$** | | | |
| 1619 | 1439 | 180 | bridging/chelating |
| 1619 | 1373 | 246 | monodentate |
| **$Cu_{0.5}H_2TM \cdot 2H_2O$** | | | |
| 1579 | 1404 | 175 | bridging/chelating or non coordinated |
| **$Zn_{0.5}H_2TM \cdot 2H_2O$** | | | |
| 1610 | 1385 | 225 | monodentate |
| 1544 | 1401 (1385) | 143 (159) | bridging/chelating |

Table 4.7 IR data for $CuHTM \cdot 2.5H_2O$, $Cu_{0.5}H_2TM \cdot 2H_2O$, and $Zn_{0.5}H_2TM \cdot 2H_2O$.

Copper dihydrogen trimellitate had a $\Delta\nu_{(asym-sym)}$ value of 175 $cm^{-1}$. It could not be determined whether the carboxylate coordination was bridging/chelating or non coordinated because there were sufficient water molecules per copper to form an ionic structure of hydrated copper cations and trimellitate monoanions.

Although the zinc dihydrogen salt had the same stoichiometry as the copper salt it was deduced from the IR spectra for the salts that they had different structures. Two carboxylate coordinations were deduced for the zinc salt, monodentate and bridging/chelating. A second $\Delta\nu_{(asym-sym)}$ value is given in parentheses for the bridging/chelating carboxylate because it was not evident which peak was the corresponding $\nu(CO_2)_{asym}$. However, either value of $\Delta\nu_{(asym-sym)}$ is associated with bridging/chelating carboxylate groups.

The experiments using brass proved to be a less than satisfactory route to the trimellitates, producing low yields of trimellitates of low metal content (i.e. only acidic salts were formed). Also the majority of the products formed were single metal salts and not mixed metal trimellitates. However, these experiments have helped to isolate and characterise three new trimellitate phases. The dihydrogen salts, $M(H_2TM)_2$, always coprecipitated as the single metal salts and appeared to have little tolerance for the substitution of the other cation (less than 2% zinc substitution in the copper salt and no copper in the zinc salt). Monohydrogen trimellitate, MHTM, was normally obtained as the copper salt, but it was found that the copper could be replaced by zinc, at least up to 30%.

All the acidic salts have limited solubility in water but recrystallisation failed to produce single crystals. However, gel experiments using a copper nitrate/nitric acid solution, produced crystals of $CuHTM \cdot 2.5H_2O$ (blue hexagonal plates) suitable for

crystal structure determination. A second phase ($Cu_{0.5}$NaHTM . $2H_2O$) later developed in the gel, but the crystals were not suitable for x-ray analysis.

*Crystal structure of CuHTM . 2.5$H_2O$*

As with other copper aromatic carboxylates[28,29,50,55,64] the metal coordination in CuHTM . 2.5$H_2O$ was square based pyramidal (figure 4.9). The base consisted of a water molecule and 3 carboxyl oxygens (bond lengths ranged from 1.946-1.959Å). The apical water molecule (Cu-O(13), 2.501(3)Å) also capped another copper site. The Cu-O(13)-Cu angle was 117.4° and the distance between the metals was 4.274Å (this was not the shortest Cu-Cu distance). There were two hydrogen bonds as well between O(12) and O(2) from neighbouring bases (O···O distance was 2.710(5) Å).

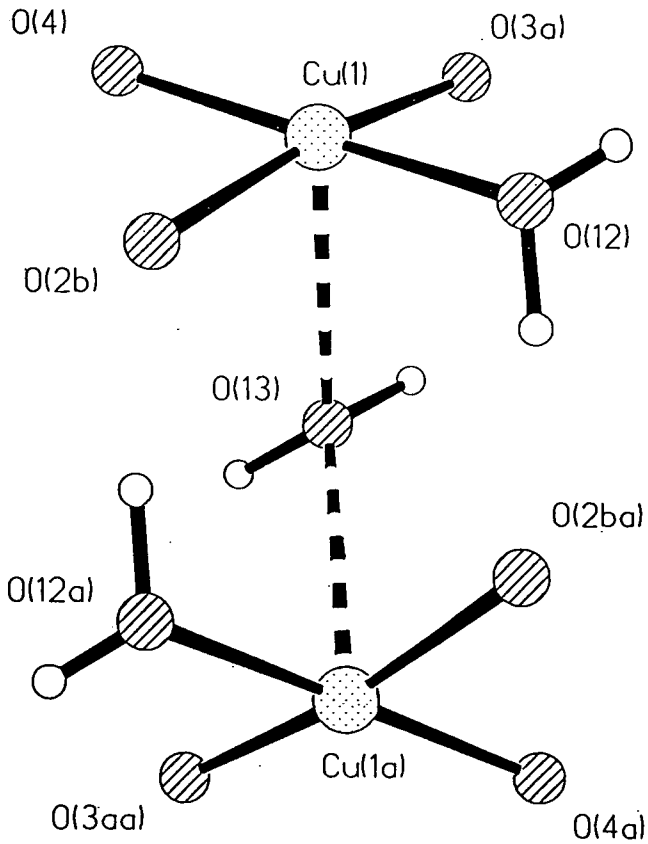


Figure 4.9 Metal coordination for CuHTM . 2.5$H_2O$.

Figure 4.10 shows how the copper centres were bridged by the trimellitate groups to form chains. For clarity the apical water molecules have been omitted from this and subsequent figures. The copper atoms that share apical sites with the metals in figure 4.10 are not shown, but are situated above and below the plane of the diagram. The orthogonal copper bases were bridged by two carboxyl groups, illustrated in figure 4.10. These coppers were much closer together (3.537Å) than those with a common apex.

The trimellitate group had two carboxylate coordinations. The carboxylate meta to the acid group was bridging (syn-anti), and the para carboxylate was monodentate. These were the coordinations deduced from the IR spectrum for the salt.

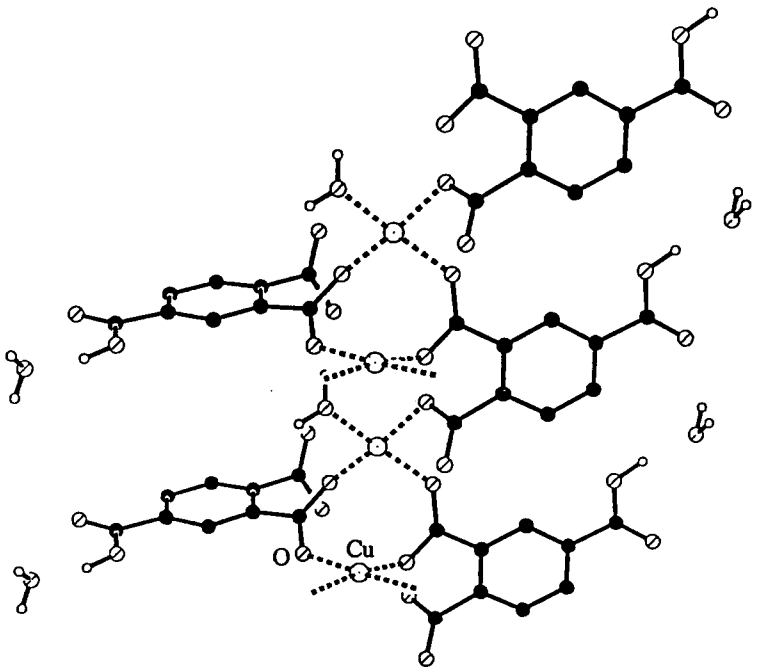


Figure 4.10 Copper trimellitate chain for CuHTM . $2.5H_2O$.

The copper trimellitate chains intersect to form layer networks, illustrated in figures 4.10 and 4.11. Dotted lines have been used to highlight the metal coordination. The angle between the chains was 83.4°.

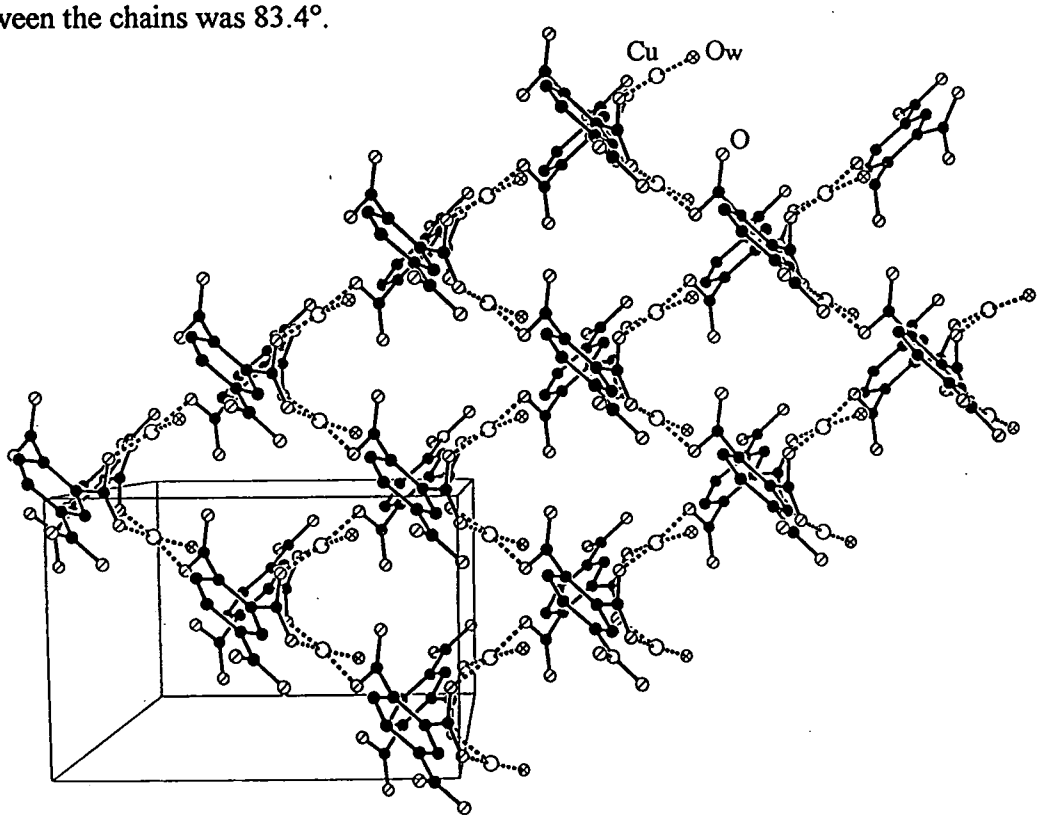


Figure 4.11 View down the z axis for CuHTM . $2.5H_2O$.

In figure 4.11 the phenyl rings on the near side of the layer are sticking out of the page and are all in the same orientation. The rings on the other side of the layer were almost orthogonal to the other rings, and are pointing into the page.

Figure 4.12 is the view down the x axis and shows the trimellitate groups either side of the layer. Half of the unit cell in this diagram appears to be empty because, for clarity, the layer occupying this half was omitted.

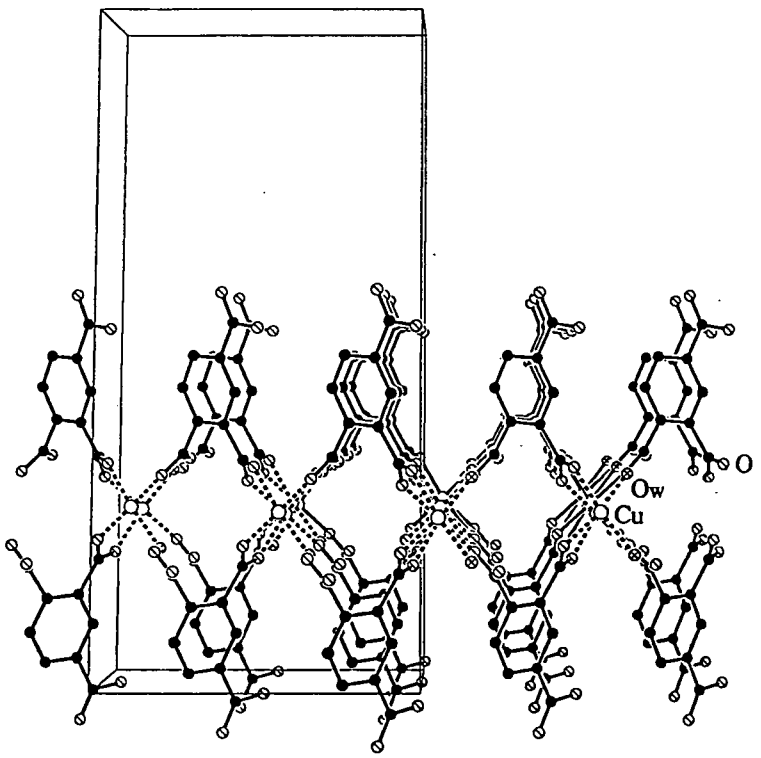


Figure 4.12 View down the x axis for CuHTM . $2.5H_2O$.

The trimellitate groups on either side of the layers interlock to give a closely packed structure. This was held together by strong H-bonding. Figure 4.13 shows the chains from three adjacent layers, and illustrates the intermeshing of the trimellitate groups. The protonated carboxyl groups were situated between the phenyl rings from the adjacent layer. The water situated between the layers was involved in strong H-bonding with the acidic proton from one layer (O···O distance, 2.591(6)Å) and the carboxyl groups from the other (O···O distance, 2.705(6) and 2.917(6)Å). There was also H-bonding between the water from the base of the copper coordination and the carbonyl oxygen of the acidic carboxyl group from the adjacent layer (O···O distance, 2.709(5)Å).

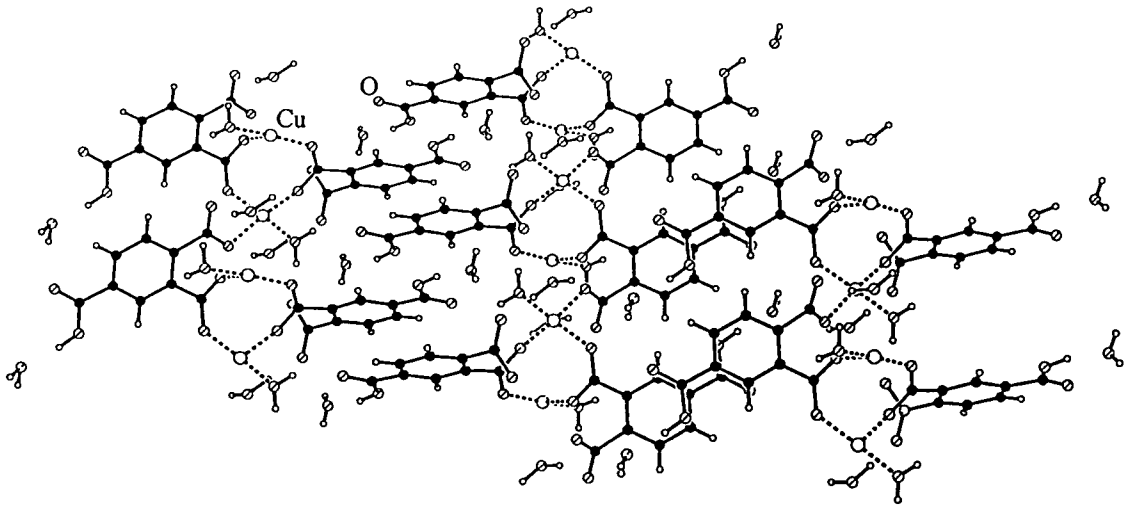


Figure 4.13 The close interaction between the layers in CuHTM . $2.5H_2O$.

Full data for the structure are given with the experimental details at the end of the chapter.

## 4.3 Conclusions

The aims for the work reported in this chapter were to establish the limits of the basic trimellitate solid solution series, and to deduce its crystal structure. This work has shown that the solution series has the general formula:

$$(Zn_xCu_{1-x})_{1.5+y}(OH)_{2y}TM \cdot 2H_2O$$

Reacting zinc/copper hydroxycarbonates with trimellitic acid produced mixed metal salts of the series, with y=1 and $x \geq 0.5$.

Prior to this thesis, no crystal structures of metal(II) trimellitates had been reported. In the course of the present study, the crystal structures of three salts were determined, of which two were members of the above solid solution series (with cation ratios of x=1 and x=0.5). The crystals of the basic trimellitates had a polymeric layer structure. There were two metal sites in a 1:1 ratio and both sites were square based pyramidal (an unusual coordination for zinc). From the structures it was deduced that the copper preferentially occupied the Zn(2) position of the zinc salt, causing little distortion to the structure. It was discussed how substituting copper for zinc in the Zn(1) site would lengthen the apical bond, part of the layer framework, leading to distortions of the crystal structure. It was postulated that this was the reason why the substitution of copper into the solid solution was limited (preparations for products with $x<0.5$ were unsuccessful).

For the copper-rich products, trimellitates based on $Cu_{1.5}TM \cdot 2H_2O$ were prepared. Zinc could be substituted into this structure up to x=0.2, and it was possible to increase the metal content (y<0.4 using the general formula above). Unfortunately no crystals were obtained for this phase.

Reactions between brass and trimellitic acid gave poor yields of acidic metal salts (i.e. low metal content). Zinc and copper from brass did not readily react with the acid and the brass did not act as a template for the formation of mixed metal trimellitates. The slow reaction with trimellitic acid allowed the acidic salts formed to be dissolved, the single metal salts were coprecipitated when the solution became saturated. One of the reasons why the hydroxycarbonate route was so successful was because the starting material readily reacted with the acid. Insoluble mixed metal compounds were formed rather than soluble salts that could coprecipitate as single metal salts.

The reaction between hydroxycarbonate and trimellitic acid involved the conversion of one solid into another. It was surprising that this was achieved in a relatively short time (one hour refluxing was sufficient). One postulation is that the reaction actually proceeded via a slightly soluble intermediate (maybe an acidic salt), allowing the hydroxycarbonate particles to be broken down and formed into trimellitate particles. Therefore, as the surface of the hydroxycarbonate particle reacted, the product temporarily dissolved, revealing fresh hydroxycarbonate for reaction. The opposite scenario is that the surface of the hydroxycarbonate reacted with the acid but the product remained attached to the particle. This would lead to a heterogeneous product, consisting of hydroxycarbonate encapsulated in zinc/copper trimellitate. Further work is required to establish why the reaction was so efficient.

The crystal structure of copper monohydrogen trimellitate was determined. The 5 coordinate copper atoms were bridged by trimellitate groups, forming layers. The layers were closely packed, and strong H-bonding existed between them.

It was shown that the separation between the asymmetric and symmetric $\nu(CO_2)$ frequencies was dependent on the type of carboxylate coordination. The $\Delta\nu_{(asym\text{-}sym)}$ values appear to have a similar trend to that found for acetate salts[70]. However, the work reported here has been limited to three solved crystal structures. Further results are required to ascertain the coordinations associated with specific $\Delta\nu_{(asym\text{-}sym)}$ values. However, the present results suggest that carboxylate coordinations for trimellitate compounds can be cautiously assigned using the results reported for the acetate salts.

For future work aimed at preparing catalysts, the acidic salts are of lesser importance, having low metal contents. However, it would be interesting to determine how much copper can be substituted into the neutral zinc salt. Of course, it would be desirable to obtain crystals of both zinc and copper neutral trimellitates, but the gel method (which has been instrumental in growing crystals of trimellitates and pyromellitates) is unpredictable, and results are not certain. For example, most attempts to form copper trimellitate produced powders. Progress might be made using a weaker

solution of sodium trimellitate, adding the first aliquot to seed some micro-crystals, then replacing the supernatant solution with another aliquot of trimellitate solution to enlarge these crystals, and continuing until crystals of suitable size are obtained. Some gel experiments could also be tried using a trimellitic acid solution as the supernatant liquid (enough acid can be dissolved to make a suitable reagent).

In summary, several zinc/copper trimellitates were prepared and characterised. The crystal structures for three salts were deduced, the first metal(II) trimellitate structures reported. The structures were all polymeric layers. It was also shown that, like acetate salts, the separation between asymmetric and symmetric $\nu(CO_2)$ absorptions were related to the carboxylate coordination.

## 4.4 Experimental Details

Details of the hydroxycarbonates reported here can be found in the experimental section of chapter 3, Preparation of Zinc/Copper Hydroxycarbonates (there is an experiment index at the end of the chapter). The hydroxycarbonates have been given a reference (e.g. RT(1.0/0.0) and A112), and their experimental details can be found using the index at the end of chapter 3.

Trimellitic acid was prepared by refluxing a solution of the anhydride (solid anhydride purchased from Aldrich, 97% purity, the remainder was free acid) for an hour, ensuring that all the solid had dissolved. The acid crystallised from the solution as it cooled.

It should be pointed out that the percentage yields calculated for the experiments below, have been deduced from the elemental analyses for both the hydroxycarbonate starting material and the trimellitate end product. Hence, there may be greater errors associated with the yields than would normally be expected, because both compounds were non-stoichiometric and the actual elemental compositions were not known.

### *4.4a Scaled up preparations of zinc/copper trimellitates*

#### *a) Zinc trimellitate*

The solid hydroxycarbonate RT(1.0/0.0) (37.5g, 143mmol) was added to a hot aqueous solution of trimellitic acid (25.43g, 121mmol, in 200mls of water). On addition a gas was evolved ($CO_2$) and the resultant suspension was stirred. The liquid phase was brought to the boil and refluxed for 1 hour. A solid phase was present throughout the experiment. Suction filtration yielded 56.06g (93.0%) of white powder which was characterised as follows.

*Elemental analysis (%):* Zn,36.6 C,24.6 H,1.8

Calculated for $Zn_{2.5}(OH)_2TM \cdot 2H_2O$: Zn,37.1 C,24.5 H,2.0

*IR ($cm^{-1}$):* 3540, 3361(b), 1615, 1588(s), 1543, 1492, 1398(s), 1364, 1301(w), 1260, 1156, 1135(w), 1078, 946, 861, 836, 804(w), 774, 760, 730(w), 716(w), 670, 608, 572, 525.

*Powder XRD (4θ):* 16.95; 23.50; 24.80; 31.90; 32.45; 34.60; 35.45; 41.80; 44.35; 45.10; 45.70; 48.30.

***b) $(Zn_{0.90}Cu_{0.10})$ trimellitate***

A slurry of finely ground hydroxycarbonate A112 (17.93g, 31.7mmol) was added to a warmed aqueous solution of trimellitic acid (15.30g, 72.8mmol, in 100mls of water). A rich blue suspension formed, but after 10-15 minutes the solid had become lighter in colour. The mixture was left stirring overnight at room temperature. Suction filtration yielded 29.48g (95.3%) of light blue powder which was characterised as follows.

*Elemental analysis (%):* Zn,33.6 Cu,3.4 C,26.9 H,2.0
Calculated for
$(Zn_{0.90}Cu_{0.10})_{2.5}(OH)_2TM \cdot 2H_2O$: Zn,33.4 Cu,3.6 C,24.5 H,2.0
$(Zn_{0.90}Cu_{0.10})_{2.3}(OH)_{1.6}TM \cdot H_2O$: Zn,33.6 Cu,3.6 C,26.8 H,1.6

*IR ($cm^{-1}$):* 3544, 3383(b), 1617(s), 1589(s), 1542, 1490, 1408(s), 1363, 1260(w), 1156(w), 1137(w), 1078(w), 861(w), 774, 715(w), 671(w), 622(w), 577(w), 526(w).

*Powder XRD (4θ):* Basic zinc phase.

***c) $(Zn_{0.75}Cu_{0.25})$ trimellitate***

30g of the trimellitate had been previously made[3], it was characterised as follows.

*Elemental analysis (%):* Zn,27.8 Cu,9.3 C,23.9 H,2.0
Calculated for
$(Zn_{0.75}Cu_{0.25})_{2.5}(OH)_2TM \cdot 2H_2O$: Zn,27.9 Cu,9.0 C,24.6 H,2.0

*IR ($cm^{-1}$):* 3374(b), 1616(s), 1590(s), 1542, 1490, 1406(s), 1363(sh), 1259(w), 1155(w), 1136(w), 1078(w), 860(w), 837(w), 774, 714(w), 670(w), 625(w), 582(w), 527(w).

*Powder XRD (4θ):* 16.25; 23.70; 24.80; 26.00; 31.80; 32.30; 34.75; 35.45; 41.75; 44.40; 45.20; 45.85; 48.25.
Basic zinc phase.

***d) $(Zn_{0.67}Cu_{0.33})$ trimellitate***

The same procedure as 'a' was used reacting BP(0.67/0.33) (30.6g, 132mmol) with trimellitic acid (20.0g, 95.1mmol) dissolved in 200mls of water. The suspension

was stirred under reflux conditions for 1 hour. Suction filtration yielded 41.4g (92.9%) of light blue powder which was characterised as follows.

*Elemental analysis (%):* Zn,25.8 Cu,13.1 C,21.9 H,1.8
Calculated for
$((Zn_{0.66}Cu_{0.34})OH)_3TM \cdot 3H_2O$: Zn,25.8 Cu,12.5 C,21.3 H,2.4
$((Zn_{0.66}Cu_{0.34})OH)_3TM \cdot 2H_2O$: Zn,26.5 Cu,13.3 C,22.1 H,2.5

*IR($cm^{-1}$):* 3421(b), 1616(s), 1591(s), 1542, 1490, 1406(s), 1363(sh), 1259(w), 1155(w), 1078(w), 861(w), 772, 713(w), 671(w), 625(w), 581(w), 527(w).

*Powder XRD (4θ):* 16.25; 23.65; 24.85; 25.65; 29.85; 31.90; 32.45; 34.75; 35.50; 37.35; 41.80; 44.45; 45.35; 45.85; 48.35; 49.15.

Basic zinc phase plus some starting material; line at 4θ=25.65 due to hydroxycarbonate.

***e) $(Zn_{0.5}Cu_{0.5})$ trimellitate***

The same procedure as before was used reacting BP(0.50/0.50) (37.1g, 163mmol) with trimellitic acid (24.0g, 114mmol) dissolved in 200mls of water. The suspension was stirred under reflux conditions for 3 hours. Suction filtration yielded 52.6g of a heterogeneous solid, consisting of light blue and light green powder which was analysed as follows.

Elemental analysis (%): Zn,17.0 Cu,20.1 C,24.7 H,1.8 N,0.4

*Powder XRD (4θ):* Basic zinc phase plus a faint gerhardtite pattern

From the XRD, it was deduced that the hydroxycarbonate was not completely reacted. The product was refluxed with further acid (10.0g, 48mmol) for 3 hours. Suction filtration yielded 47.1g (53.9%) of light greenish blue powder which was characterised as follows.

*Elemental analysis (%):* Zn,12.5 Cu,17.7 C,31.0 H,2.0 N,0.0
Calculated for
$(Zn_{0.41}Cu_{0.59})_{1.6}(OH)_{0.2}TM \cdot 2H_2O$: Zn,12.2 Cu,17.2 C,30.9 H,2.1

*IR ($cm^{-1}$):* 3700-2900(b), 1552(s), 1491, 1403(s), 1301(w), 1258, 1153(w), 1135(w), 1065(w), 917(w), 860, 821, 805, 772, 731, 673(w), 635(w), 597(w), 524.

*Powder XRD (4θ):* 16.25; 16.60; 23.60; 24.80; 29.30; 31.90; 32.50; 33.30; 34.00; 34.70; 35.55; 38.05; 38.95; 40.90; 41.85; 44.55; 45.20; 45.80; 46.60.
A mixture of copper and basic zinc phase .

***f) Attempted preparation of ($Zn_{0.35}Cu_{0.65}$) trimellitate***

The same procedure as before was used reacting BP(0.35/0.65) (37.1g, 155mmol) with trimellitic acid (25.7g, 122mmol) dissolved in 200mls of water. The suspension was stirred under reflux conditions for 1 hour. Suction filtration yielded 46.1g (97.6%) of light green powder which was characterised as follows.

*Elemental analysis (%):* Zn,5.8 Cu,27.2 C,29.3 H,1.8
Calculated for
$(Zn_{0.17}Cu_{0.83})_{1.9}(OH)_{0.8}TM \cdot 1.5H_2O$: Zn,5.7 Cu,27.2 C,29.3 H,1.8

*IR ($cm^{-1}$):* 3420(b), 1560(s), 1491, 1396(s), 1253(w), 1133(w), 1073(w), 969(w), 924(w), 821, 765, 731(w), 673(w), 640(w), 598(w), 525.

*Powder XRD (4θ):* 16.50; 28.70; 29.25; 33.35; 34.00; 34.80; 38.05; 38.95; 43.75; 44.85; 46.60; 47.50.
Cu trimellitate phase.

***g) Attempted preparation of ($Zn_{0.3}Cu_{0.7}$) trimellitate***

The same procedure as before was used reacting RT(0.31/0.69) (29.25g, 126mmol) with trimellitic acid (27.24g, 130mmol) dissolved in 200mls of water. The suspension was stirred under reflux conditions for 3 hours. Suction filtration yielded 44.62g (97.0%) of light blue powder which was characterised as follows.

*Elemental analysis (%):* Zn,5.6 Cu,24.3 C,31.0 H,2.2 N0.1
Calculated for
$(Zn_{0.18}Cu_{0.82})_{1.6}(OH)_{0.2}TM \cdot 2H_2O$: Zn,5.3 Cu,23.9 C,31.0 H,2.1
$(Zn_{0.18}Cu_{0.82})_{1.5}TM \cdot 2H_2O$: Zn,5.2 Cu,23.1 C,31.9 H,2.1

*IR ($cm^{-1}$):* 3567, 3420(b), 1560(s), 1491, 1391(s), 1252(w), 1152(w), 1136(w), 1065(w), 864(w), 822(w), 773, 730(w), 674(w), 638(w), 598(w), 523.

*Powder XRD (4θ):* 16.55; 29.15; 29.65; 30.20; 33.35; 33.95; 38.00; 38.95; 40.85; 43.80; 44.90; 46.55; 47.00; 47.65.
Cu trimellitate phase.

***h) Cu trimellitate***

The same procedure as before was used reacting IB(0.0/1.0) (38.00g, 155mmol) with trimellitic acid (23.95g, 114mmol) dissolved in 200mls of water. The suspension was stirred under reflux conditions for 1 hour. Suction filtration yielded 53.0g of a heterogeneous solid which consisted of light green and light blue powder which analysed as follows.

*Elemental analysis (%):* Cu,35.7 C,24.1 H,1.9 N,0.5

*Powder XRD (4θ):* **16.60**; 18.30; 23.45; 24.70; 25.80; 27.40; **29.35**; **29.85**; **33.35**; **34.00**; 34.85; **38.15**; **39.00**; 43.40; **44.85**; **46.35**; **47.05**; 49.10.

A mixture of two copper trimellitate phases, $Cu_{1.5}TM$ (**bold**) plus another copper salt. The latter phase was probably a basic trimellitate, deduced from the high copper percentage obtained for the elemental analysis. The line at 25.80 coincides with the strongest diffraction for gerhardtite (a component of IB(0.0/1.0)).

In order to obtain a single phase the solid (48.37g) was refluxed with further acid (19.26g, 91.6mmol) for 2 hours. Suction filtration yielded 61.66g (96.6%) of light blue powder which was characterised as follows.

*Elemental analysis (%):* Cu,27.3 C,32.2 H,2.2 N,0.0
Calculated for $Cu_{1.5}TM \cdot 2H_2O$: Cu,28.2 C,31.9 H,2.1

*IR ($cm^{-1}$):* 3568, 3220(b), 1569(s), 1490, 1391(s), 1301(w), 1252(w), 1152(w), 1136(w), 1094(w), 1066, 865(w), 822, 773, 730, 675(w), 639(w), 600(w), 523.

*Powder XRD (4θ):* 16.60; 25.20; 29.30; 29.60; 30.25; 33.35; 33.95; 38.10; 38.90; 40.95; 43.95; 44.85; 46.45; 46.80; 47.50; 48.65.
Copper trimellitate

### *4.4b Limits of solution series*

#### *a) Reaction of zinc hydroxycarbonate with $H_3TM$*

The hydroxycarbonate BP(1.0/0.0) (1.895g, 3.5mmol) was added to a hot aqueous solution of trimellitic acid (2.808g, 13.4mmol, in 25mls of water). On addition a gas was evolved ($CO_2$). The mixture was refluxed for 1 hour. Suction filtration yielded 3.13g (80.8%) of white powder which was characterised as follows.

*Elemental analysis (%):* Zn,27.2 C,32.5 H,1.6
Calculated for $Zn_{1.5}TM \cdot 2H_2O$: Zn,28.7 C,31.6 H,2.1

*IR ($cm^{-1}$):* 3404(b), 2936(b), 1574(s), 1498, 1402(s), 1299(w), 1257(w), 1180(w), 1126(w), 1080(w), 921, 844, 810, 767, 731, 670(w), 615(w), 569(w), 533.

*Powder XRD (4θ):* 11.90; 18.15; 29.35; 30.20; 33.65; 41.45; 45.45; 46.70; 48.75.
The pattern was quite diffuse and was different to that for the previously prepared basic zinc trimellitate.

***b) Reaction of copper hydroxycarbonate with $H_3TM$***

The same procedure as before was used reacting the hydroxycarbonate BP(0.0/1.0) (5.502g, 22.9mmol) with trimellitic acid (3.609g, 17.2mmol, in 30mls water) and refluxing for 1 hour. Suction filtration yielded 7.42g (69.9%) of a heterogeneous powder consisting of light blue and green solid. They were characterised as follows.

Light blue solid:
*Elemental analysis (%):* Cu,26.9 C,30.8 H,2.0 N,0.1
Calculated for $Cu_{1.5}TM \cdot 2.5H_2O$: Cu,27.4 C,31.1 H,2.3

Green solid:
*Elemental analysis (%):* Cu,39.6 C,17.1 H,1.5 N,2.2

From the high percentage of copper, it was deduced that the solid was a mixture of trimellitate and gerhardtite.

The starting material had not completely reacted. The blue solid was trimellitate and the green solid unconverted starting material. The mixture was refluxed with further acid (1.80g, 8.6mmol, in 30mls of water) for 1 hour. Suction filtration yielded 7.42g (69.9%) of light blue powder which was characterised as follows.

*Elemental analysis (%):* Cu,26.6 C,31.8 H,2.2 N,0.0
Calculated for $Cu_{1.5}TM \cdot 2.5H_2O$: Cu,27.4 C,31.1 H,2.3

*IR ($cm^{-1}$):* 3568, 3220(b), 1569(s), 1490, 1391(s), 1252(w), 1152(w), 1136(w), 1094(w), 1066, 865(w), 822, 773, 730(w), 675(w), 600(w), 523.

*Powder XRD (4θ):* 16.50; 25.20; 29.20; 30.25; 33.40; 34.00; 38.10; 38.90; 40.80; 43.85; 44.95; 46.40; 46.85; 47.55.
Same as previous copper trimellitate.

***c) Reaction of $(Zn_{0.1}Cu_{0.9})$hydroxycarbonate with $H_3TM$***

The same procedure as before was used reacting the hydroxycarbonate RT(0.11/0.89) (0.486g, 2.0mmol) with trimellitic acid (1.92g, 9.1mmol, in 25mls of water) and refluxing for 2 hours. Suction filtration yielded 0.885g (67.9%, the filtrate was cloudy) of pale blue powder which was characterised as follows.

*Elemental analysis (%):* Zn,0.4 Cu,25.5 C,32.4 H,2.4
Calculated for
$(Zn_{0.02}Cu_{0.98})_{1.35}H_{0.3}(TM) \cdot 2H_2O$: Zn,0.5 Cu,25.5 C,32.8 H,2.2

*IR ($cm^{-1}$):* 3568, **3504**, 3220(b), **1699**, 1561(s), 1491, 1394(s), 1266(w), **1235(w)**, **1175(w)**, 1151(w), 1136(w), **1121(w)**, 1066, 856(w), 822, **800(w)**, 772, 728(w), 674(w), 600(w), 523.
Similar absorptions to $Cu_{1.5}TM$ plus peaks for CuHTM (**bold**).

*Powder XRD (4θ):* **15.00**; 16.70; 29.40; 33.45; 34.15; **34.70**; 39.00; 41.00; **43.55**; 46.45; 46.95; 47.75; **48.95**.
$Cu_{1.5}$TM plus a faint CuHTM (**bold**) pattern.

***d) Reaction of $(Zn_{0.2}Cu_{0.8})$hydroxycarbonate with $H_3TM$***

The same procedure as before was used reacting the hydroxycarbonate RT(0.21/0.79) (0.703g, 2.9mmol) with trimellitic acid (0.51g, 2.4mmol, in 20mls of water) under reflux conditions for 1 hour. Suction filtration yielded 0.699g (56.8%, low yield because it was a fine powder and some went through the filter paper) of light turquoise powder which was characterised as follows.

*Elemental analysis (%):* Zn,3.6 Cu,22.9 C,27.6 H,1.9
Calculated for
$(Zn_{0.13}Cu_{0.87})_{1.6}(OH)_{0.2}TM \cdot 4H_2O$: Zn,3.5 Cu,23.0 C,28.0 H,2.9

*IR ($cm^{-1}$):* 3420(b), 1521(s), 1491, 1399(s), 1256(w), 1136(w), 1076(w), 823(w), 764, 7278(w), 671(w), 600(w), 546.

*Powder XRD (4θ):* 16.45(c, bz); 18.20(z); 23.40(bz); 24.75(bz); 25.75; 27.40; 29.75; 33.35(c); 34.05(c); 39.10(c); 49.20.

Three phases were identified, copper trimellitate (c), zinc trimellitate (z), and the basic zinc salt (bz). The lines were weak and many were not positively assigned to a phase.

***e) Reaction of $(Zn_{0.3}Cu_{0.7})$hydroxycarbonate with $H_3TM$***

The same procedure as before was used reacting the hydroxycarbonate RT(0.31/0.69) (2.0g, 8.6mmol) with trimellitic acid (1.47g, 7.0mmol, in 20mls of water) under reflux conditions for 1 hour. Suction filtration yielded 2.86g (95.0%) of light green powder, characterised as follows.

*Elemental analysis (%):* Zn,6.6 Cu,25.9 C,27.2 H,2.0 N,0.1
Calculated for
$(Zn_{0.20}Cu_{0.80})_{2.0}OH(TM) \cdot 2H_2O$: Zn,6.7 Cu,26.2 C,27.8 H,2.1

*IR ($cm^{-1}$):* 3384(b), 1570(s), 1490, 1390(s), 1255(w), 1152(w), 1135(w), 1067, 821, 771, 728(w), 673(w), 598(w), 523.

*Powder XRD (4θ):* 16.25; **16.60**; 23.65; 24.80; 25.85; **29.35**; **30.25**; **33.35**; **34.05**; 34.75; 35.60; **38.15**; **38.95**; **40.80**; 41.85; **44.55**; **44.85**; **46.65**; **47.00**.
Mixture of neutral copper (**bold**) and basic zinc salt.

***f) Reaction of $(Zn_{0.3}Cu_{0.7})$hydroxycarbonate with $H_3TM$***

The same procedure as before was used, reacting the hydroxycarbonate P48 (0.100g, 0.416mmol) with trimellitic acid (0.118g, 0.562mmol, in 20mls of water) under reflux conditions for 1.5 hours. The addition produced a small amount of green solid suspended in a blue solution, but after 10 minutes the solution had lost its colour and there appeared to be an increase in the volume of solid. Suction filtration yielded 0.0847g (53%) of turquoise powder, characterised as follows.

*Elemental analysis (%):* Zn,2.1 Cu,31.3 C,28.3 H,2.0 N,0.0
Calculated for
$(Zn_{0.06}Cu_{0.94})_{2.0}OH(TM) . 2H_2O$: Zn,2.0 Cu,30.8 C,27.9 H,2.1

*IR ($cm^{-1}$):* 3421(b), 3259(b), 1559(s), 1553(s), 1493, 1403(s), 1257(w), 1137(w), 1078, 780, 734(w), 715(w), 675(w), 600(w), 541(w), 473(w).

*Powder XRD (4θ):* Basic copper trimellitate (see the scaled up copper trimellitate preparation), plus a faint $Cu_{1.5}TM$ pattern.

***g) Reaction of $(Zn_{0.35}Cu_{0.65})$hydroxycarbonate with $H_3TM$***

The same procedure as before was used reacting the hydroxycarbonate RT(0.36/0.64) (0.706g, 3.0mmol) with trimellitic acid (1.89g, 9.0mmol, in 25mls of water) under reflux conditions for 1.5 hours. Suction filtration yielded 0.896g (74.1%) of light blue powder which was characterised as follows.

*Elemental analysis (%):* Zn,3.1 Cu,19.7 C,33.0 H,2.7 N,0.0
Calculated for
$(Zn_{0.13}Cu_{0.87})_{1.2}H_{0.6}TM . 2.5H_2O$: Zn,3.1 Cu,20.1 C,32.8 H,2.6

*IR ($cm^{-1}$):* **3504**, 3287(b), **1700**, 1616, 1594(s), 1494, 1436, 1395(s), 1374, 1302(w), 1266, **1234**, **1175(w)**, 1150(w), **1120(w)**, 1079, 855(w), **800(w)**, 727(w), 698(w), 674(w), 594(w), 542(w).
Similar absorptions to $Cu_{1.5}TM$ plus peaks for CuHTM (**bold**).

*Powder XRD (4θ):* 14.95; **16.70**; 27.90; **29.30**; 30.00; **30.50**; 31.30; 32.25; **33.45**; **33.95**; 34.65; 35.33; **38.55**; **40.05**; 43.45; **44.95**; **46.50**; **47.00**; 48.95.
Mixture of neutral copper salt (**bold**) and copper monohydrogen trimellitate.

***4.4c Reactions between brass and $H_3TM$***

Brass (1.00g 15.6mmol) was added to an aqueous solution of trimellitic acid (3.44g, 16.4mmol, in 50mls of water). The solution was refluxed for 24 hours, but no

change was observed. On leaving the mixture to stand for a couple of days, the solution became a light golden colour. A light blue and a white solid had been precipitated. On warming the flask the white solid (assumed to be acid) dissolved and suction filtration yielded a small amount of blue powder (~0.05g).

In an attempt to prepare some more product the brass was added to another solution of acid. After 16 hours at room temperature the flask contained a golden solution with a very small amount of blue and white solid. The mixture was refluxed for one hour, this dissolved all the solid and the brass regained its metallic lustre. The solution was cooled and left at room temperature for a week, during which light greenish blue spherulites formed on the brass and a powder had settled on the bottom of the flask. The bulk of the brass was still unreacted. ~0.1g of product was collected, upon analysis the spherulites and powder were found to be the same product, characterised as follows.

*Elemental analysis (%):* Zn,0.1 Cu,11.1 C,39.0 H,3.2
Calculated for
$(Zn_{0.01}Cu_{0.99})_{0.5}H_{2.0}TM \cdot 2H_2O$: Zn,0.1 Cu,11.4 C,39.0 H,3.3

*Powder XRD (4θ):* 17.65; 25.45; 26.35; 30.05; 34.05; 36.05; 37.90; 41.75; 47.25; 48.85.

A small amount of green solid later developed on the brass turnings, this was collected and analysed as follows

*Elemental analysis (%):* Zn,6.7 Cu,15.3 C,32.6 H,3.1
Calculated for
$(Zn_{0.30}Cu_{0.70})HTM \cdot 3H_2O$: Zn,5.8 Cu,13.6 C,33.1 H,3.0
$(Zn_{0.30}Cu_{0.70})_{1.1}H_{0.8}TM \cdot 3H_2O$: Zn,6.5 Cu,14.7 C,32.4 H,2.9

*IR ($cm^{-1}$):* 3377(b), 1701, 1560(s), 1496, 1386(s), 1296, 1262, 1229(w), 1156(w), 1126(w), 1072(w), 794(w), 772, 600(w).

*Powder XRD (4θ):* Very faint CuHTM pattern.

### *4.4d Electrochemical reaction between $H_3TM$ and brass or copper*

a)

A sacrificial brass (30% Zn, 70% Cu) anode was immersed in 20mls of saturated trimellitic acid solution. Current was passed until the anode was no longer functional, because of the formation of a blue solid on the electrode. The solid on the electrode was light blue on the top half and a darker blue on the bottom, samples from the two regions were analysed. There was also a light blue precipitate, unfortunately this solid was

mixed with Cu which had formed and fallen from the cathode. The products were characterised as follows (elemental analysis was not carried out because the products were contaminated with each other and with copper).

Light blue solid on electrode:
*Powder XRD (4θ):* 15.00; **17.65**; **25.45**; **26.35**; 27.75; **29.85**; **34.05**; **36.05**; 38.45; **41.75**; 43.25; **47.25**; **48.75**.
Copper dihydrogen salt (**bold**), plus a faint monohydrogen pattern.

Darker blue solid on electrode:
*Powder XRD (4θ):* **15.00**; 17.65; 25.45; 26.35; **27.75**; 29.85; **31.10**; **31.95**; 34.10; **34.55**; 36.05; **38.45**; 41.75; **43.25**; 48.75.
Copper monohydrogen salt (**bold**), plus a faint copper dihydrogen pattern.

Light blue precipitate:
*Powder XRD (4θ):* 15.00; **17.65**; **25.45**; **26.35**; 27.75; **29.85**; **34.05**; **36.05**; 38.45; **41.75**; 43.25; **47.25**; **48.75**.
Copper dihydrogen salt (**bold**), plus a faint monohydrogen pattern.

The filtrate was kept, and on standing light greenish blue spherulites and small clear needle crystals formed. It was possible to separate enough of each sample for analysis.

Spherulites:
*Elemental analysis (%):* Zn,0.2 Cu,11.1 C,39.2 H,3.2
Calculated for $(Zn_{0.01}Cu_{0.99})_{0.5}H_{2.0}TM \cdot 2H_2O$: Zn,0.1 Cu,11.4 C,39.0 H,3.3

*IR ($cm^{-1}$):* 3261(b), 2646, 2597, 2526, 1719(s), 1698(s), 1579(s), 1498, 1404(s), 1316(s), 1293, 1252(s), 1156, 1129, 1076(w), 1034(w), 938(w), 895(w), 857, 832, 799, 772, 750, 713, 650(w), 592, 575(w), 491.

*Powder XRD (4θ):* 17.70; 25.55; 26.35; 30.05; 34.10; 36.10; 38.00; 41.80; 47.45; 48.85.
Pattern for copper dihydrogen salt.

Clear crystals:
*Elemental analysis (%):* Zn,9.8 C,36.5 H,3.7
Calculated for $Zn_{0.5}H_2TM \cdot 3H_2O$: Zn,11.0 C,36.5 H,3.7
Calculated for $Zn_{0.45}H_{2.1}TM \cdot 3H_2O$: Zn,10.1 C,36.9 H,3.8

*IR ($cm^{-1}$):* 3373(b), 2645, 2597, 1714(s), 1685(s), 1610, 1555(s), 1498, 1401(s), 1385(s), 1313(s), 1296, 1264(s), 1230, 1158, 1126, 1072(w), 930, 911, 864, 840, 794, 773, 708(w), 662(w), 600, 540(w).

*Powder XRD (4θ):* 14.80; 20.40; 28.05; 29.05; 34.35; 37.25; 41.00; 42.25; 45.00; 46.80; 47.80; 48.85; 49.85.
A different XRD pattern to previous zinc trimellitates.

The precipitate (0.154g) was refluxed in 50mls of water for 26 hours. The solid remaining was collected (48mg of light greenish blue powder) and the filtrate, which had a slight blue tinge, was left to evaporate. A mixture of phases crystallised out of the filtrate (86mg), mostly turquoise spherulites, but also some clear needles and a tiny amount of blue solid. The undissolved solid and the phases from the filtrate were characterised as follows.

Undissolved solid:
*Elemental analysis (%):* Zn,0.1 Cu,27.1 C,31.9 H,2.1
Calculated for $(Zn_{0.01}Cu_{0.99})_{1.5}TM \cdot 2H_2O$: Zn,0.3 Cu,27.8 C,31.9 H,2.1

*Powder XRD (4θ):* Same pattern as neutral copper trimellitate.

Solid from filtrate:
*IR ($cm^{-1}$):* 3258(b), 2649, 2597, 2535, 1718(s), 1698(s), 1577(s), 1498, 1405(s), 1316(s), 1294, 1253(s), 1156, 1129, 1072(w), 1034(w), 937, 857, 834, 798, 772, 750, 713, 661(w), 650(w), 592, 575(w), 492(w).
Similar to copper dihydrogen salt.

*Powder XRD (4θ):* Copper dihydrogen plus faint monohydrogen and zinc dihydrogen phases.

b)

The electrolysis reaction was repeated using a sacrificial copper anode and platinum cathode immersed in an aqueous solution of trimellitic acid. The anodic and cathodic chambers were separated by a sintered frit using a H shaped cell. Initially 2.9V, 7mA was passed through the cell, but after 70 hours the anode had become coated in a light blue solid (0.316g), which had increased the resistance of the cell causing the circuit to overload, i.e. the current could no longer be maintained at 7mA; the voltage had risen to 50V. A light blue solid had precipitated (0.229g) and the platinum electrode had a copper coating (8mg of copper, 99% selectivity, where selectivity = moles of copper reacted/moles of copper lost from cathode). No copper had fallen from the electrode.

Solid on the electrode:
*Elemental analysis (%):* Cu,12.2 C,39.3 H,3.3
Calculated for $Cu_{0.5}H_{2.0}TM \cdot 2H_2O$: Cu,11.4 C,39.0 H,3.2

*Powder XRD (4θ):* Copper dihydrogen salt.

Precipitate:
*Elemental analysis (%):* Cu,12.2 C,39.3 H,3.2
Calculated for $Cu_{0.5}H_{2.0}TM \cdot 2H_2O$: Cu,11.4 C,39.0 H,3.2

*Powder XRD (4θ):* Copper dihydrogen salt.

c)

The previous experiment was repeated using a brass (36% zinc, 64% copper) anode; the galvanometer overloaded after 7 hours. A light blue precipitate had formed (68mg) and the electrode was covered in a light blue solid (158mg), clear needle crystals were interspersed in the blue product. This was observed under a microscope. The surface of the electrode, after the solid had been removed, was pitted and had gold and red-gold regions. The platinum electrode had become coated in metal (4.1mg, 86% selectivity) which was removed with nitric acid. This solution was analysed and found to contain Cu, 80ppm, and Zn, 1.0ppm. The products were analysed as follows.

Precipitate:
*Elemental analysis (%):* Zn,0.1 Cu,11.2 C,38.9 H,3.2
Calculated for
$(Zn_{0.02}Cu_{0.98})_{0.5}H_{2.0}TM \cdot 2H_2O$: Zn,0.2 Cu,11.2 C,39.0 H,3.2

*Powder XRD (4θ):* Copper dihydrogen phase.

Solid from electrode:
*Elemental analysis (%):* Zn,0.3 Cu,11.2 C,38.8 H,3.3
Calculated for $(Zn_{0.02}Cu_{0.98})_{0.5}H_{2.0}TM \cdot 2H_2O$: Zn,0.2 Cu,11.1 C,39.0 H,3.2

*Powder XRD (4θ):* Copper dihydrogen pattern plus a very faint line at 4θ ~14.9, which could be either a zinc dihydrogen or copper monohydrogen phase.

### *4.4e Gel crystal growth experiments and crystal structure determinations*

Because it was so difficult to grow crystals of the trimellitates (only the acidic salts were slightly soluble but clusters were always obtained after slow evaporation) a series of gel experiments was undertaken. Silica gels were made by slowly adding 2M sodium silicate solution (~6.5mls) to 30mls of 1M nitric acid, stirred at room temperature, until a pH of 4.5-5 was reached. Care had to be taken as the end point was very sharp, Hydrion multirange indicator paper was used to check the pH. The solution was then quickly dispensed into 5 test tubes. Gelling started after ~5 minutes and the gels were left to settle, ~24 hours. Each gel was primed by adding 6mls of a 0.5M zinc/copper nitrate solution to the test tube, taking care not to damage the gel, and

leaving for 1-2 weeks. The supernatant solution was then changed for a 0.1M solution of sodium trimellitate which slowly reacted with the Zn/Cu cations. Not all the experiments were successful, some only formed powders. Others initially produced powders, but later developed crystals. Only the successful experiments are documented below.

***a) Copper nitrate - gel***

Because previous experiments to form copper trimellitate had failed, the gel was primed with an acidified nitrate solution in an attempt to form the more soluble CuHTM. A 1:1 mixture of copper nitrate and nitric acid solution was used, replaced after a couple of weeks with a 0.1M sodium trimellitate solution. After a week navy blue spherical clusters and lighter crystals had formed on top of the gel. Under a microscope three phases were identified:

i) light turquoise thin narrow plates normally radiating from a central point;
ii) clusters of blue rhombohedral plates; and
iii) spherical clusters of navy blue rectangular plates.

The crystals of phase "iii" were of poor morphology, and the centres of these large cluster were found to be much lighter in colour. Due to the lack of sample "i" it was only characterised by powder XRD.

i) light turquoise crystals:
*Powder XRD (4θ):* 14.80; 29.55; 30.35; 32.20; 33.45; 34.20; 35.40; 40.00; 45.10.
The XRD pattern had not been encountered before.

ii) blue crystals:
*Elemental analysis (%):* Cu,19.5 C,34.1 H,2.9 Na,0.4 N,0.0
Calculated for CuHTM . $2.5H_2O$: Cu,20.1 C,34.1 H,2.8

*IR ($cm^{-1}$):* 3505, 3288(b), 2613, 1698(s), 1619(s), 1495, 1439(s), 1395(s), 1373(w), 1303(w), 1267, 1236(s), 1176(w), 1150(w), 1121, 1080(w), 1009(w), 920(w), 854, 800, 770, 727, 698, 673, 635(w), 594, 542, 480.

*Powder XRD (4θ):* 14.90; 27.90; 29.85; 31.30; 32.15; 33.80; 34.65; 38.60; 43.40; 46.15; 46.85; 48.85

iii) navy blue crystals
*Elemental analysis (%):* Cu,11.2 Na,7.0 C,36.3 H,2.7 N,0.0
Calculated for $Cu_{0.5}$NaHTM . $2H_2O$: Cu,10.6 Na,7.7 C,36.2 H,2.7

*IR ($cm^{-1}$):* 3610, 3426(b), 3216(sh), 2897, 2641, 1710(s), 1640(s), 1607, 1565(s), 1497, 1420(s), 1397, 1347(s), 1302, 1277, 1240(s), 1168, 1120, 1077, 994(w), 976(w), 921(w), 854, 810, 799, 772, 730(w), 704, 674(w), 589, 539, 473(w).

*Powder XRD (4θ):* **14.75**; 15.80; 27.75; 31.15; 34.00; 35.45; 36.70; 38.65; 41.65; 44.45; 47.30.

The first line **(bold)** was faint and probably due to a small amount of CuHTM . $2.5H_2O$ impurity.

Large cluster (navy blue plus lighter blue centre):
*Powder XRD (4θ):* Mixture of ii and iii.

The supernatant liquid was replaced with a weaker solution of sodium trimellitate (3.5mls, 0.07M), after two weeks a few specks could be seen under the microscope. It was assumed that all the trimellitate had been used up, so 0.5mls of 0.1M sodium trimellitate was added in the hope that the crystallites that had formed would act as seeds for the growth of single crystals. The next day there were numerous isolated crystals on the surface of the gel and on the wall of the test tube. These were collected but under the microscope most of the crystals were twins or clusters, only the very small crystals (dimensions <0.3mm) were untwinned. The crystals were analysed as CuHTM as above. Some of the CuHTM . $2.5H_2O$ crystals were suitable for structural determination, but none of the crystals for the other 2 phases were.

***Structure determination of CuHTM . $2.5H_2O$***
*(J. Kivikoski, University of Durham)*

| Colour Blue | Habit Diamond plate | Size (mm) 0.1 x 0.1 x 0.2 |
|---|---|---|

| | |
|---|---|
| a (Å) | 7.797(2) |
| b (Å) | 11.404(4) |
| c (Å) | 24.100(7) |
| α (°) | 90 |
| β (°) | 97.58(2) |
| γ (°) | 90 |
| Volume (Å$^3$) | 2124(1) |

| | |
|---|---|
| Formula | $C_9H_4CuO_6$ x 2.5 $H_2O$ |
| Formula weight | 316.70 |
| Crystal system | Monoclinic |
| Space group | C 2/C (15) |
| Z | 8 |
| $D_c$ (gcm$^{-3}$) | 1.981 |
| Linear absorption coefficient (cm$^{-1}$) | 21.0 |

**Data collection**

| | |
|---|---|
| Diffractometer | Rigaku AFC6 |
| Radiation | MoKα |
| Temperature (K) | 150 |
| Scan technique | ω |
| Scan width (°) | 0.73 + 0.3tanθ |
| Scan rate (°min$^{-1}$) | 1 - 8 |
| 2θ range (°) | 6 - 56 |
| Absorption correction | Empirical |
| Transmission (%) | 0.853 - 1.000 |

| **Limits:** | min. | max. |
|---|---|---|
| h | 0 | 10 |
| k | 0 | 14 |
| l | -31 | 31 |

| **Data:** | |
|---|---|
| total | 2858 |

| | |
|---|---|
| Decay (%) | None |
| Merging R-factor (%) | 3.3 |

| | |
|---|---|
| unique | 2536 |
| I≥3σ(I) | 1536 |

**Solution and Refinement**

| | | | |
|---|---|---|---|
| Package used | CRYSTALS | Final R (%) | 5.3 |
| Solution | Direct methods (SHELXS86) | Final $R_W$ (%) | 3.9 |
| Refinement method | Full matrix | Goodness-of-fit | 1.27 |
| Weights (Chebychev) | 1.42 -3.60 0.0261 -0.956 -0.656 | Observations/parameters | 9.05 |
| Extinction correction | None | Max. difference peak (eÅ$^{-3}$) | 0.70 |
| Anomalous dispersion correction | None | Min. difference peak (eÅ$^{-3}$) | -0.74 |

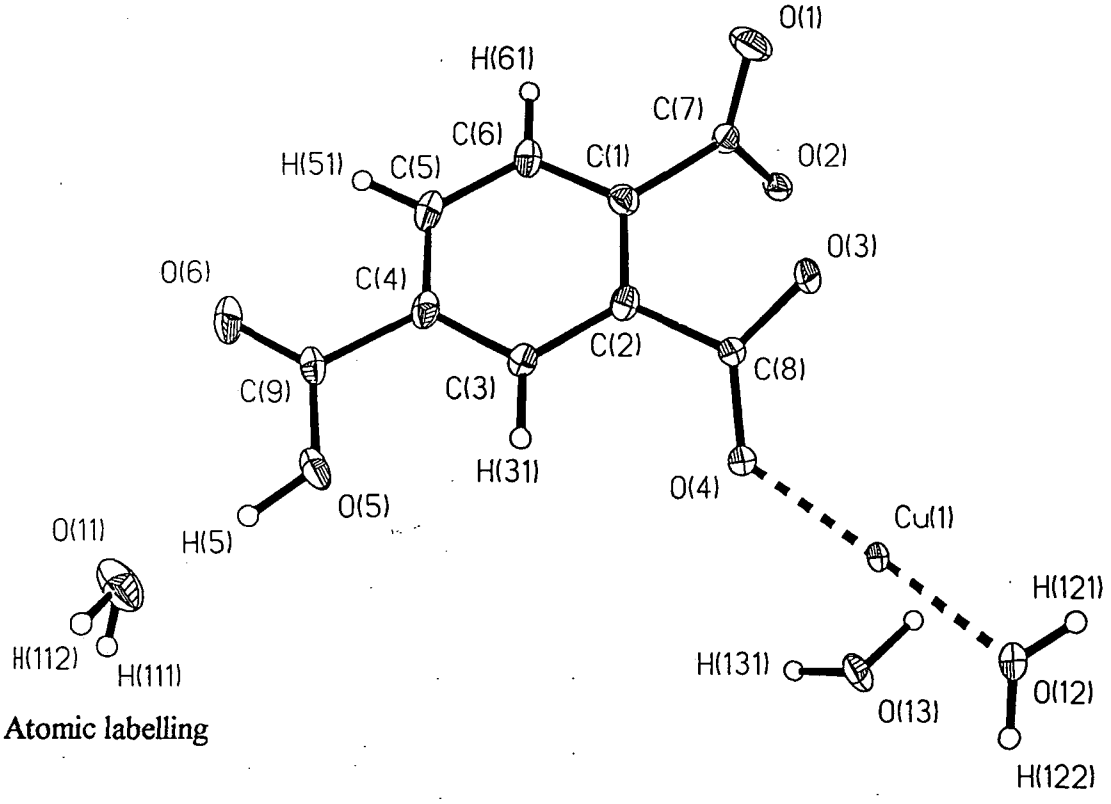


Atomic labelling

Bond lengths (Å) for CuHTM . 2.5$H_2O$.

| | | | |
|---|---|---|---|
| Cu(l)- O(2) | 1.959(4) | O(12)- H(121) | 0.84 |
| Cu(1)- O(3) | 1.946(4) | O(12)- H(122) | 0.93 |
| Cu(1)- O(4) | 1.951(4) | O(13)- H(131) | 1.09 |
| Cu(1)- O(12) | 1.954(4) | C(1)- C~2) | 1.412(8) |
| Cu(1)- O(13) | 2.501(3) | C(1)- C(6) | 1.389(7) |
| O(1)- C(7) | 1.236(6) | C(1)- C(7) | 1.524(7) |
| O(2)- C(7) | 1.281(6) | C(2)- C(3) | 1.397(7) |
| O(3)- C(8) | 1.264(6) | C(2)- C(8) | 1.499(7) |
| O(4)- C(8) | 1.268(6) | C(3)- C(4) | 1.399(7) |
| O(5)- C(9) | 1.321(7) | C(4)- C(5) | 1.391(8) |
| O(6)- C(9) | 1.222(7) | C(4)- C(9) | 1.497(7) |
| O(5)--H(5) | 0.94 | C(5)- C(6) | 1.397(7) |
| O(11)- H(111) | 0.80 | | |
| O(11)- H(112) | 0.98 | | |

Bond angles (in degrees) for CuHTM . 2.5$H_2O$.

| | | | |
|---|---|---|---|
| O(3)-Cu(1)-O(2) | 172.5(2) | C(8)-C(2)-C(1) | 121.3(5) |
| O(4)-Cu(1)-O(2) | 88.0(2) | C(8)-C(2)-C(3) | 119.1(5) |
| O(4)-Cu(1)-O(3) | 94.1(2) | C(4)-C(3)-C(2) | 119.8(5) |
| O(12)-Cu(1)-O(2) | 87.3(2) | C(5)-C(4)-C(3) | 121.0(5) |
| O(12)-Cu(1)-O(3) | 91.3(2) | C(9)-C(4)-C(3) | 120.7(5) |
| O(12)-Cu(1)-O(4) | 173.4(2) | C(9)-C(4)-C(5) | 118.3(5) |
| O(13)-Cu(1)-O(2) | 86.6(1) | C(6)-C(5)-C(4) | 119.0(5) |
| O(13)-Cu(1)-O(3) | 86.1(1) | C(5)-C(6)-C(1) | 120.8(5) |
| O(13)-Cu(1)-O(4) | 94.5(1) | O(2)-C(7)-O(1) | 124.0(5) |
| O(13)-Cu(1)-O(12) | 89.8(1) | C(1)-C(7)-O(1) | 121.3(5) |
| H(112)-O(11)-H(111) | 86.4 | C(1)-C(7)-O(2) | 114.6(5) |
| H(122)-O(12)-H(121) | 117.1 | O(4)-C(8)-O(3) | 126.5(5) |
| H(131)-O(13)-H(132) | 98.9 | C(2)-C(8)-O(3) | 115.7(4) |
| C(6)-C(1)-C(2) | 120.0(5) | C(2)-C(8)-O(4) | 117.7(5) |
| C(7)-C(1)-C(2) | 123.1(5) | O(6)-C(9)-O(5) | 124.9(5) |
| C(7)-C(1)-C(6) | 116.8(5) | C(4)-C(9)-O(5) | 114.0(5) |
| C(3)-C(2)-C(1) | 119.3(5) | C(4)-C(9)-O(6) | 121.0(6) |

Atomic coordinates with standard deviations in parentheses and equivalent isotropic temperature factors U(iso).

| **Atom** | **x** | **y** | **z** | **U(iso)** |
|---|---|---|---|---|
| Cu(1) | -0.22837(9) | 0.05610(6) | 0.24500(3) | 0.0111 |
| O(1) | 0.3728(5) | -0.2617(4) | 0.1711(2) | 0.0226 |
| O(2) | 0.1295(5) | -0.3370(4) | 0.1945(1) | 0.0144 |
| O(3) | 0.1154(4) | -0.0590(4) | 0.2028(1) | 0.0152 |
| O(4) | -0.1706(5) | -0.0260(3) | 0.1789(1) | 0.0151 |
| O(5) | -0.3083(5) | -0.0115(4) | -0.0290(2) | 0.0211 |
| O(6) | -0.1703(6) | -0.1324(4) | -0.0826(2) | 0.0231 |
| O(11) | -0.4913(6) | 0.0776(4) | -0.1165(2) | 0.0291 |
| O(12) | -0.2817(5) | 0.1552(4) | 0.3066(1) | 0.0168 |
| O(13) | -0.50000 | -0.0579(6) | 0.25000 | 0.0181 |
| C(1) | 0.1043(7) | -0.2215(5) | 0.1124(2) | 0.0152 |
| C(2) | -0.0159(7) | -0.1302(5) | 0.1163(2) | 0.0140 |
| C(3) | -0.1167(7) | -0.0904(5) | 0.0678(2) | 0.0139 |
| C(4) | -0.0953(7) | -0.1398(5) | 0.0160(2) | 0.0142 |
| C(5) | 0.0192(7) | -0.2320(5) | 0.0122(2) | 0.0161 |
| C(6) | 0.1185(7) | -0.2726(5) | 0.0609(2) | 0.0167 |
| C(7) | 0.2140(7) | -0.2744(5) | 0.1633(2) | 0.0127 |
| C(8) | -0.0254(6) | -0.0673(5) | 0.1704(2) | 0.0131 |
| C(9) | -0.1949(7) | -0.0939(5) | -0.0369(2) | 0.0144 |
| H(5) | -0.3872(5) | 0.0134(4) | -0.0597(2) | 0.0800 |
| H(31) | -0.2048(7) | -0.0273(5) | 0.0698(2) | 0.0800 |
| H(51) | 0.0295(7) | -0.2689(5) | -0.0248(2) | 0.0800 |
| H(61) | 0.2011(7) | -0.3389(5) | 0.0587(2) | 0.0800 |
| H(111) | -0.5952(6) | 0.0769(4) | -0.1229(2) | 0.0800 |
| H(112) | -0.4989(6) | 0.1610(4) | -0.1255(2) | 0.0800 |
| H(121) | -0.2139(5) | 0.1384(4) | 0.3354(1) | 0.0800 |
| H(122) | -0.3993(5) | 0.1570(4) | 0.3099(1) | 0.0800 |
| H(131) | -0.56417(1) | -0.1198(6) | 0.21988(1) | 0.0800 |

Torsional angles (in degrees) for CuHTM . $2.5H_2O$.

| | | | |
|---|---|---|---|
| C(1 ) - C(2) - C(3) - C(4) | -1.2 | O(1) - C(7) - C(1) - C(2) | -113.1 |
| C(2) - C(3) - C(4) - C(5) | 3.1 | O(1) - C(7) - C(1) - C(6) | 71.1 |
| C(3) - C(4) - C(5) - C(6) | -2.3 | O(2) - C(7) - C(1) - C(2) | 70.7 |
| C(4) - C(5) - C(6) - C(1 ) | -0.4 | O(2) - C(7) - C(1) - C(6) | -105.1 |
| C(5) - C(6) - C(1) - C(2) | 2.2 | O(3) - C(8) - C(2) - C(1 ) | 31.0 |
| C(6) - C( 1 ) - C(2) - C(3) | -1.5 | O(3) - C(8) - C(2) - C(3) | -143.0 |
| C(7) - C(1) - C(2) - C(3) | -177.2 | O(4) - C(8) - C(2) - C(1 ) | -150.4 |
| C(7) - C(1) - C(6) - C(5 | 178.2 | O(4) - C(8) - C(2) - C(3) | 35.6 |
| C(7) - C(1) - C(2) - C(8) | 8.8 | O(5) - C(9) - C(4) - C(3) | -4.4 |
| C(8) - C(2) - C(1) - C(6) | -175.5 | O(5) - C(9) - C(4) - C(5) | 176.0 |
| C(8) - C(2) - C(3) - C(4) | 173.0 | 0~6) - C(9) - C(4) - C(3) | 176.2 |
| C(9) - C(4) - C(3) - C(2) | -176.6 | O(6) - C(9) - C(4) - C(5) | -3.5 |
| C(9) - C(4) - C(5) - C(6) | 177.3 | | |

General displacement parameter expressions - U's (standard deviations in parentheses)

| Atom | U(11) | U(22) | U(33) | U(23) | U(13) | U(12) |
|---|---|---|---|---|---|---|
| Cu(1) | 0.0127(3) | 0.0183(3) | 0.0062(2) | 0.0013(3) | 0.0001(2) | 0.0033(3) |
| O(1) | 0.013(2) | 0.035(3) | 0.028(2) | 0.006(2) | -0.003(2) | -0.001(2) |
| O(2) | 0.012(2) | 0.022(2) | 0.013(2) | 0.007(2) | 0.002(1) | 0.002(2) |
| O(3) | 0.014(2) | 0.025(2) | 0.011(2) | -0.004(2) | -0.002(1) | -0.002(2) |
| O(4) | 0.014(2) | 0.025(2) | 0.011(2) | 0.001(1) | 0.001(1) | 0.004(2) |
| O(5) | 0.025(2) | 0.031(2) | 0.015(2) | 0.003(2) | -0.006(2) | 0.007(2) |
| O(6) | 0.033(2) | 0.035(3) | 0.011(2) | -0.002(2) | -0.001(2) | 0.001(2) |
| O(11) | 0.022(2) | 0.039(3) | 0.035(3) | 0.012(2) | -0.009(2) | -0.005(2) |
| O(12) | 0.019(2) | 0.025(2) | 0.010(2) | -0.003(2) | -0.001(2) | 0.004(2) |
| O(13) | 0.018(3) | 0.025(3) | 0.016(2) | 0.0000 | -0.007(2) | 0.0000 |
| C(1) | 0.013(2) | 0.019(3) | 0.015(2) | 0.001(2) | 0.000(2) | -0.002(2) |
| C(2) | 0.019(3) | 0.013(3) | 0.012(2) | 0.000(2) | 0.003(2) | -0.001(2) |
| C(3) | 0.018(3) | 0.014(3) | 0.012(2) | -0.000(2) | 0.004(2) | 0.000(2) |
| C(4) | 0.017(3) | 0.019(3) | 0.012(2) | 0.002(2) | 0.004(2) | -0.007(2) |
| C(5) | 0.023(3) | 0.018(3) | 0.012(2) | -0.002(2) | 0.005(2) | -0.006(2) |
| C(6) | 0.022(3) | 0.019(3) | 0.012(2) | 0.002(2) | 0.003(2) | -0.002(2) |
| C(7) | 0.017(3) | 0.014(3) | 0.011(2) | 0.003(2) | 0.002(2) | 0.006(2) |
| C(8) | 0.012(2) | 0.019(3) | 0.011(2) | 0.002(2) | 0.002(2) | 0.003(2) |
| C(9) | 0.019(3) | 0.017(3) | 0.010(2) | 0.004(2) | -0.001(2) | -0.004(2) |

Bond lengths and angles for hydrogen bonding

| Hydrogen bond | O···H (Å) | O···O (Å) | O–H···O (°) |
|---|---|---|---|
| O(5)–H(5)···O(11) | 1.67(2) | 2.591(6) | 167(1) |
| O(11)–H(111)···O(4) | 2 20(2) | 2.917(6) | 149(1) |
| O(11)–H(112)···O(1) | 1.94(2) | 2.705(6) | 133(1) |
| O(12)–H(121)···O(6) | 1.96(2) | 2.709(5) | 148(1) |
| O(12)–H(122)···O(2) | 1.79(2) | 2.710(5) | 172(1) |
| O(13)–H(131)···O(1) | 2 02(2) | 3 084(7) | 165(1) |
| O(13)–H(132)···O(1) | 2 02(2) | 3 084(7) | 165(1) |

***b) Zinc nitrate - Gel***

4mls of 0.1M potassium trimellitate were used as the supernatant liquid for a gel impregnated with zinc nitrate. A white residue formed almost immediately at the gel-solution interface, but after a couple of days crystals were observed on the white residue and also on the walls of the test tube. Under a microscope it was observed that only the clear prisms of dimensions <0.4mm were untwinned.

*Elemental analysis (%):* Zn,33.8 C,26.9 H,2.1 Na,0.1 N,0.0
Calculated for $Zn_2(OH)TM \cdot 2H_2O$: Zn,33.4 C,27.6 H,2.0

*IR ($cm^{-1}$):* 3545, 3359(b), 1617(s), 1588(s), 1542(s), 1490, 1397(s), 1362(s), 1258, 1155(w), 1137(w), 1077(w), 861(w), 774, 715, 670, 620, 573, 524, 441(w).
Same as basic zinc trimellitate

*Powder XRD (4θ):* Basic zinc trimellitate.

***Structure determination of $Zn_2(OH)TM \cdot 2H_2O$***

(J. Kivikoski, University of Durham)

| Colour clear | Habit hexagonal | Size (mm) 0.15 x 0.10 x 0.20 |
|---|---|---|

| | |
|---|---|
| a (Å) | 11.365(3) |
| b (Å) | 6.495(2) |
| c (Å) | 15.603(7) |
| α (°) | 90 |
| β (°) | 105.19(3) |
| γ (°) | 90 |
| Volume ($Å^3$) | 1111.4(7) |

| | |
|---|---|
| Formula | $C_9H_4Zn_2O7 \times 2H_2O$ |
| Formula weight | 390.89 |
| Crystal system | monoclinc |
| Space group | $P2_1/c$ (14) |
| Z | 4 |
| $D_c$ ($gcm^{-3}$) | 2.33 |
| Linear absorption coefficient ($cm^{-1}$) | 43.6 |

**Data collection**

| | |
|---|---|
| Diffractometer | Rigaku AFC6 |
| Radiation | Mo Kα |
| Temperature (K) | 150 |
| Scan technique | 2θ/ω |
| Scan width (°) | 1.10 + 0.3tanθ |
| Scan rate ($°min^{-1}$) | 1.3-8 |
| 2θ range (°) | 6-45 |
| Absorption correction | Empirical |
| Transmission (%) | 0.718-1.000 |
| Decay (%) | None |
| Merging R-factor (%) | 2.5 |

| **Limits:** | min. | max. |
|---|---|---|
| h | -1 | 12 |
| k | -1 | 6 |
| l | -16 | 16 |

| **Data:** | |
|---|---|
| total | 2225 |
| unique | 1441 |
| I_3σ(I) | 1119 |

**Solution and Refinement**

| | | | |
|---|---|---|---|
| Package used | CRYSTALS | Final R (%) | 3.7 |
| Solution | Patterson (SHELXS86) | Final $R_W$ (%) | 3.3 |
| Refinement method | Full Matrix | Goodness-of-fit | 1.28 |
| Weights (Chebychev) | 2.34 -1.94 1.36 | Observations/parameters | 1119/181 |
| Extinction correction | None | Max. difference peak ($eÅ^{-3}$) | 0.67 |
| Anomalous dispersion correction | None | Min. difference peak ($eÅ^{-3}$) | -0.58 |

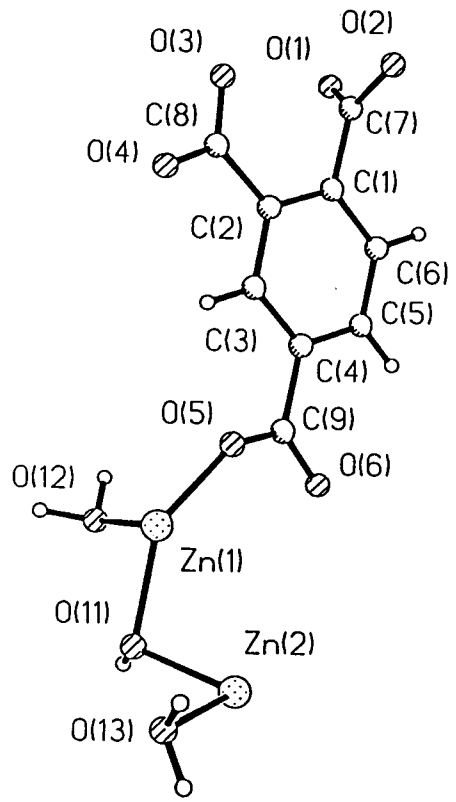


Atomic labelling

Bond lengths (Å) for $Zn_2OH(TM) . 2H_2O$.

| | | | |
|---|---|---|---|
| Zn(1)-Zn(2) | 3.178(1) | O(11)-H(111) | 0.85 |
| Zn(1)-O(2) | 2.126(4) | O(12)-H(121) | 0.96 |
| Zn(1)-O(4) | 1.966(4) | O(12)-H(122) | 0.95 |
| Zn(1)-O(5) | 1.955(4) | O(13)-H(131) | 0.96 |
| Zn(1)-O(11) | 1.999(4) | O(13)-H(132) | 0.91 |
| Zn(1)-O(12) | 2.094(4) | C(1)-C(2) | 1.379(9) |
| Zn(2)-O(2) | 2.065(4) | C(1)-C(6) | 1.406(9) |
| Zn(2)-O(3) | 2.033(4) | C(1)-C(7) | 1.507(8) |
| Zn(2)-O(11) | 2.068(4) | C(2)-C(3) | 1.403(9) |
| Zn(2)-O(11) | 2.039(4) | C(2)-C(8) | 1.490(9) |
| Zn(2)-O(13) | 2.060(4) | C(3)-C(4) | 1.387(9) |
| O(1)-C(7) | 1.236(7) | C(4)-C(5) | 1.388(9) |
| O(2)-C(7) | 1.285(7) | C(4)-C(9) | 1.513(8) |
| O(3)-C(8) | 1.261(8) | C(5)-C(6) | 1.397(9) |
| O(4)-C(8) | 1.265(7) | | |
| O(5)-C(9) | 1.248(7) | | |
| O(6)-C(9) | 1.276(7) | | |

Bond angles (in degrees) for $Zn_2OH(TM) . 2H_2O$.

| | | | |
|---|---|---|---|
| O(4)-Zn(1)-O(2) | 98.6(2) | H(122)-O(12)-H(121) | 92.4 |
| O(5)-Zn(1)-O(2) | 93.8(2) | H(132)-O(13)-H(131) | 93.3 |
| O(5)-Zn(1)-O(4) | 103.3(2) | C(6)-C(1)-C(2) | 119.8(5) |
| O(11)-Zn(1)-O(2) | 77.5(2) | C(7)-C(1)-C(2) | 122.1(6) |
| O(11)-Zn(1)-O(4) | 110.5(2) | C(7)-C(1)-C(6) | 118.1(5) |
| O(11)-Zn(1)-O(5) | 146.0(2) | C(3)-C(2)-C(1) | 119.5(6) |
| O(12)-Zn(1)-O(2) | 164.4(2) | C(8)-C(2)-C(1) | 122.2(5) |
| O(12)-Zn(1)-O(4) | 95.8(2) | C(8)-C(2)-C(3) | 118.3(6) |
| O(12)-Zn(1)-O(5) | 88.8(2) | C(4)-C(3)-C(2) | 120.9(6) |
| O(12)-Zn(1)-O(11) | 91.8(2) | C(5)-C(4)-C(3) | 119.7(6) |
| O(3)-Zn(2)-O(2) | 158.3(2) | C(9)-C(4)-C(3) | 118.2(6) |
| O(11)-Zn(2)-O(2) | 77.4(2) | C(9)-C(4)-C(5) | 122.1(6) |
| O(11)-Zn(2)-O(3) | 86.6(2) | C(6)-C(5)-C(4) | 119.7(6) |
| O(11)-Zn(2)-O(2) | 93.2(2) | C(5)-C(6)-C(1) | 120.3(6) |
| O(11)-Zn(2)-O(3) | 95.0(2) | O(2)-C(7)-O(1) | 122.4(5) |
| O(11)-Zn(2)-O(11) | 154.1(1) | C(1)-C(7)-O(1) | 119.4(5) |
| O(13)-Zn(2)-O(2) | 98.4(2) | C(1)-C(7)-O(2) | 118.1(5) |
| O(13)-Zn(2)-O(3) | 98.0(2) | O(4)-C(8)-O(3) | 125.1(6) |
| O(13)-Zn(2)-O(11 ) | 97.0(2) | C(2)-C(8)-O(3) | 117.3(5) |
| O(13)-Zn(2)-O(11) | 108.3(2) | C(2)-C(8)-O(4) | 117.6(5) |
| Zn(2)-O(2)-Zn(1) | 98.6(2) | O(6)-C(9)-O(5) | 124.1(5) |
| Zn(2)-O(11)-Zn(1) | 102.8(2) | C(4)-C(9)-O(5) | 115.6(6) |
| Zn(2)-O(11)-Zn(1) | 115.2(2) | C(4)-C(9)-O(6) | 120.3(6) |
| Zn(2)-O(11)-Zn(2) | 108.7(2) | | |

Atomic coordinates and isotropic displacement parameters for $Zn_2OH(TM) . 2H_2O$.

| **Atom** | **x** | **y** | **z** | **U(iso)** |
|---|---|---|---|---|
| Zn(1) | 0.31844(6) | 0.0730(1) | 0.09488(5) | 0.0115 |
| Zn(2) | 0.50699(7) | 0.2056(1) | 0.27537(5) | 0.0137 |
| O(1) | -0.2678(4) | 0.6681(8) | -0.3341(3) | 0.0194 |
| O(2) | -0.3228(4) | 0.7682(7) | -0.2148(3) | 0.0111 |
| O(3) | -0.3115(4) | 0.3200(7) | -0.2140(3) | 0.0157 |
| O(4) | -0.1965(4) | 0.1376(7) | -0.1008(3) | 0.0169 |
| O(5) | 0.2220(4) | 0.2862(7) | 0.0196(3) | 0.0151 |
| O(6) | 0.3222(4) | 0.5409(7) | -0.0262(3) | 0.0152 |
| O(11) | 0.4818(4) | -0.0048(6) | 0.1727(3) | 0.0124 |
| O(12) | 0.3613(4) | -0.0477(7) | -0.0176(3) | 0.0163 |
| O(13) | 0.4970(4) | -0.0006(7) | 0.3735(3) | 0.0177 |
| C(1) | -0.1253(5) | 0.616(1) | -0.1946(4) | 0.0087 |
| C(2) | -0.1104(5) | 0.4304(9) | -0.1502(4) | 0.0090 |
| C(3) | 0.0050(6) | 0.376(1) | -0.0967(4) | 0.0103 |
| C(4) | 0.1044(5) | 0.505(1) | -0.0886(4) | 0.0097 |
| C(5) | 0.0905(5) | 0.690(1) | -0.1350(4) | 0.0125 |
| C(6) | -0.0247(6) | 0.747(1) | -0.1868(4) | 0.0129 |
| C(7) | -0.2470(5) | 0.684(1) | -0.2526(4) | 0.0090 |
| C(8) | -0.2139(6) | 0.286(1) | -0.1550(4) | 0.0125 |
| C(9) | 0.2255(6) | 0.439(1) | -0.0279(4) | 0.0069 |
| H(31) | 0.0159(6) | 0.242(1) | -0.0640(4) | 0.0800 |
| H(51) | 0.1622(5) | 0.782(1) | -0.1308(4) | 0.0800 |
| H(61) | -0.0366(6) | 0.882(1) | -0.2192(4) | 0.0800 |
| H(111) | 0.5314(4) | -0.0181(6) | 0.1406(3) | 0.0800 |
| H(121) | 0.3123(4) | -0.0078(7) | -0.0755(3) | 0.0800 |
| H(122) | 0.3434(4) | -0.1898(7) | -0.0292(3) | 0.0800 |
| H(131) | 0.4339(4) | 0.0234(7) | 0.4032(3) | 0.0800 |
| H(132) | 0.5580(4) | 0.0307(7) | 0.4226(3) | 0.0800 |

Torsional angles (in degrees) for $Zn_2OH(TM) . 2H_2O$.

| | | | |
|---|---|---|---|
| C(1)-C(2)-C(3)-C(4) | -0.59 | O(1)-C(7)-C(1)-C(2) | -101.48 |
| C(2)-C(3)-C(4)-C(5) | -1.09 | O(1)-C(7)-C(1)-C(6) | 78.21 |
| C(3)-C(4)-C(5)-C(6) | 2.57 | O(2)-C(7)-C(1)-C(2) | 82.23 |
| C(4)-C(5)-C(6)-C(1) | -2.41 | O(2)-C(7)-C(1)-C(6) | -98.08 |
| C(5)-C(6)-C(1)-C(2) | 0.73 | O(3)-C(8)-C(2)-C(1) | 13.15 |
| C(6)-C(1)-C(2)-C(3) | 0.77 | O(3)-C(8)-C(2)-C(3) | -168.47 |
| C(7)-C(1)-C(2)-C(3) | -179.55 | O(4)-C(8)-C(2)-C(1) | -168.23 |
| C(7)-C(1)-C(6)-C(5) | -178.97 | O(4)-C(8)-C(2)-C(3) | 10.14 |
| C(7)-C(1)-C(2)-C(8) | -1.20 | O(5)-C(9)-C(4)-C(3) | -9.48 |
| C(8)-C(2)-C(1)-C(6) | 179.12 | O(5)-C(9)-C(4)-C(5) | 169.97 |
| C(8)-C(2)-C(3)-C(4) | -179.01 | O(6)-C(9)-C(4)-C(3) | 171.81 |
| C(9)-C(4)-C(3)-C(2) | 178.37 | O(6)-C(9)-C(4)-C(5) | -8.75 |
| C(9)-C(4)-C(5)-C(6) | -176.87 | | |

Anisotropic displacement parameters ($Å^2$) for $Zn_2OH(TM) . 2H_2O$.

| **Atom** | **U(11)** | **U(22)** | **U(33)** | **U(23)** | **U(13)** | **U(12)** |
|---|---|---|---|---|---|---|
| Zn(1) | 0.0100(4) | 0.0116(4) | 0.0132(4) | 0.0028(3) | -0.0012(3) | -0.0005(3) |
| Zn(2) | 0.0108(4) | 0.0122(4) | 0.0200(4) | -0.0039(4) | -0.0021(3) | 0.0011(3) |
| O(1) | 0.018(2) | 0.036(3) | 0.011(2) | -0.001(2) | -0.001(2) | 0.002(2) |
| O(2) | 0.006(2) | 0.016(2) | 0.015(2) | -0.004(2) | -0.002(2) | 0.001(2) |
| O(3) | 0.006(2) | 0.022(3) | 0.030(3) | 0.008(2) | -0.000(2) | 0.001(2) |
| O(4) | 0.013(2) | 0.016(3) | 0.028(3) | 0.004(2) | 0.001(2) | -0.007(2) |
| O(5) | 0.016(2) | 0.015(3) | 0.019(2) | 0.009(2) | 0.003(2) | 0.004(2) |
| O(6) | 0.012(2) | 0.013(2) | 0.023(2) | -0.002(2) | 0.003(2) | 0.000(2) |
| O(11) | 0.012(2) | 0.008(2) | 0.018(2) | -0.000(2) | 0.003(2) | 0.000(2) |
| O(12) | 0.021(2) | 0.014(2) | 0.014(2) | 0.002(2) | 0.001(2) | 0.001(2) |
| O(13) | 0.013(2) | 0.018(3) | 0.022(2) | 0.003(2) | 0.001(2) | 0.001(2) |
| C(1) | 0.008(3) | 0.012(3) | 0.014(3) | 0.001(3) | 0.006(3) | 0.005(3) |
| C(2) | 0.009(3) | 0.009(3) | 0.012(3) | -0.004(3) | 0.002(3) | -0.003(3) |
| C(3) | 0.018(4) | 0.013(3) | 0.011(3) | -0.008(3) | 0.008(3) | -0.005(3) |
| C(4) | 0.007(3) | 0.022(4) | 0.008(3) | -0.006(3) | -0.001(3) | 0.001(3) |
| C(5) | 0.010(3) | 0.014(3) | 0.015(3) | 0.003(3) | 0.001(3) | 0.003(3) |
| C(6) | 0.020(4) | 0.008(3) | 0.016(3) | 0.003(3) | 0.006(3) | -0.001(3) |
| C(7) | 0.005(3) | 0.011(3) | 0.018(4) | -0.005(3) | 0.003(3) | -0.004(3) |
| C(8) | 0.020(4) | 0.011(3) | 0.012(3) | -0.002(3) | 0.006(3) | 0.004(3) |
| C(9) | 0.010(3) | 0.013(4) | 0.009(3) | -0.010(3) | 0.000(3) | -0.000(3) |

Distances from the mean basal plane for the zinc coordination

| **Zn(1) coordination** | | **Zn(2) coordination** | |
|---|---|---|---|
| | **Height from base (Å)** | | **Height from base (Å)** |
| Zn(1) | 0.415 | Zn(2) | 0.383 |
| O(4b) | 2.376 | O(13) | 2.433 |
| O(2a) | 0.163 | O(2a) | 0.070 |
| O(5) | -0.148 | O(3a) | 0.064 |
| O(11) | -0.166 | O(11) | -0.074 |
| O(12) | 0.151 | O(11a) | -0.060 |

### *c) ($Zn_{0.5}Cu_{0.5}$) nitrate - Gel*

After 6 months it was noticed that some green crystals had formed on the surface of the gel and the walls of the test tube. Those on the wall were of a better quality. Under the microscope the crystals were observed to be distorted octahedra; once again the single crystals had dimensions <0.3mm.

*Elemental analysis (%):* Zn,15.1 Cu,18.2 C,26.6 H,2.2 Na,0.0 N,0.0
Calculated for $ZnCu(OH)TM \cdot 2H_2O$: Zn,16.8 Cu,16.3 C,27.8 H,2.1
for $(Zn_{0.45}Cu_{0.55})_2(OH)TM \cdot 2H_2O$: Zn,15.1 Cu,18.0 C,27.8 H,2.1

*IR ($cm^{-1}$):* 3648(sh), 3332(sh), 3169(b), 1617(s), 1592(s), 1541(s), 1489, 1403(s), 1354(s), 1258, 1153(w), 1134(w), 1076(w), 910(w), 860(w), 813, 771, 712, 671, 626, 582, 526, 459(w).

*Powder XRD (4θ):* Basic zinc phase.

### *Structure determination of $ZnCu(OH)TM \cdot 2H_2O$*

*(J. Kivikoski, University of Durham)*

| Colour | Green | Habit | Diamond | Size (mm) | 0.20 x 0.30 x 0.30 |
|---|---|---|---|---|---|

| | |
|---|---|
| a (Å) | 11.372(2) |
| b (Å) | 6.443(3) |
| c (Å) | 15.563(3) |
| α (°) | 90 |
| β (°) | 105.32(1) |
| γ (°) | 90 |
| Volume ($Å^3$) | 1099.9(6) |

| | |
|---|---|
| Formula | $C_9H_4ZnCuO_7 \times 2H_2O$ |
| Formula weight | 389.06 |
| Crystal system | monoclinic |
| Space group | $P2_1/c$ (14) |
| Z | 4 |
| $D_c$ ($gcm^{-3}$) | 2.35 |
| Linear absorption coefficient ($cm^{-1}$) | 41.6 |

**Data collection**

| | |
|---|---|
| Diffractometer | Rigaku AFC6 |
| Radiation | Mo Kα |
| Temperature (K) | 150 |
| Scan technique | 2θ/ω |
| Scan width (°) | 1.68 + 0.3tanθ |
| Scan rate ($°min^{-1}$) | 1-8 |
| 2θ range (°) | 6-50 |
| Absorption correction | Empirical |
| Transmission (%) | 0.866-1.000 |
| Decay (%) | None |
| Merging R-factor (%) | ---- |

| **Limits:** | min. | max. |
|---|---|---|
| h | 0 | 13 |
| k | 0 | 7 |
| l | -18 | 17 |

| **Data:** | |
|---|---|
| total | 2135 |
| unique | 1946 |
| I_3σ(I) | 1263 |

**Solution and Refinement**

| | | | |
|---|---|---|---|
| Package used | CRYSTALS | Final R (%) | 8.2 |
| Solution | Patterson (SHELXS86) | Final $R_W$ (%) | 6.4 |
| Refinement method | Full Matrix | Goodness-of-fit | 1.24 |
| Weights (Chebychev) | 4.31 -3.8 2.18 | Observations/parameters | 1263/169 |
| Extinction correction | None | Max. difference peak ($eÅ^{-3}$) | 1.24 |
| Anomalous dispersion correction | None | Min. difference peak ($eÅ^{-3}$) | -1.57 |

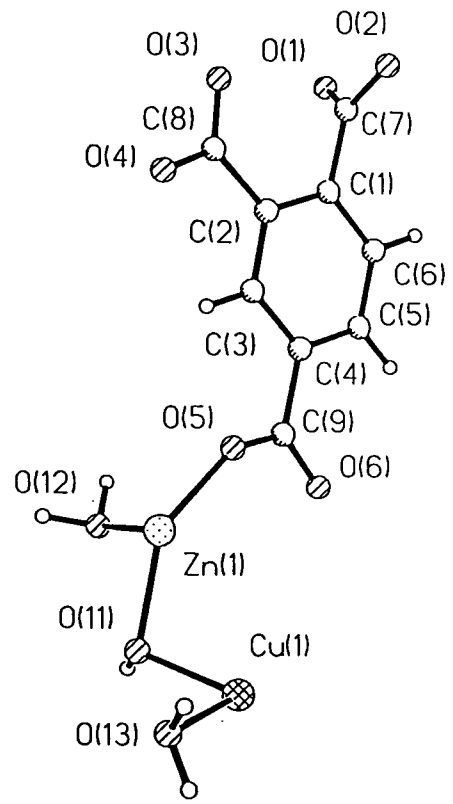


Atomic labelling

Bond lengths (Å) for ZnCuOH(TM) . $2H_2O$.

| | | | |
|---|---|---|---|
| Zn(1)-Cu(1) | 3.069(2) | O(4)-C(8) | 1.262(15) |
| Zn(1)-O(2) | 2.116(8) | O(5)-C(9) | 1.235(15) |
| Zn(1)-O(4) | 1.981(8) | O(6)-C(9) | 1.294(15) |
| Zn(1)-O(5) | 1.928(8) | O(12)-H(121) | 1.01 |
| Zn(1)-O(11) | 2.012(8) | O(13)-H(131) | 0.81 |
| Zn(1)-O(12) | 2.068(9) | C(1)-C(2) | 1.380(17) |
| Cu(1)-Cu(1) | 3.237(3) | C(1)-C(6) | 1.378(17) |
| Cu(1)-Cu(1) | 3.237(3) | C(1)-C(7) | 1.529(16) |
| Cu(1)-O(2) | 1.996(7) | C(2)-C(3) | 1.409(16) |
| Cu(1)-O(3) | 1.945(9) | C(2)-C(8) | 1.488(17) |
| Cu(1)-O(11) | 2.024(8) | C(3)-C(4) | 1.403(17) |
| Cu(1)-O(11) | 1.981(8) | C(4)-C(5) | 1.388(17) |
| Cu(1)-O(13) | 2.362(9) | C(4)-C(9) | 1.512(16) |
| O(1)-C(7) | 1.240(15) | C(5)-C(6) | 1.360(17) |
| O(2)-C(7) | 1.281(14) | | |
| O(3)-C(8) | 1.263(14) | | |

Bond angles (in degrees) for ZnCuOH(TM) . $2H_2O$.

| | | | |
|---|---|---|---|
| O(4)-Zn(1)-O(2) | 98.6(3) | C(6)-C(1)-C(2) | 120.8(11) |
| O(5)-Zn(1)-O(2) | 94.6(3) | C(7)-C(1)-C(2) | 119.3(10) |
| O(5)-Zn(1)-O(4) | 100.5(4) | C(7)-C(1)-C(6) | 119.8(11) |
| O(11)-Zn(1)-O(2) | 76.9(3) | C(3)-C(2)-C(1) | 117.6(11) |
| O(11)-Zn(1)-O(4) | 105.6(3) | C(8)-C(2)-C(1) | 124.1(11) |
| O(11)-Zn(1)-O(5) | 153.5(4) | C(8)-C(2)-C(3) | 118.2(11) |
| O(12)-Zn(1)-O(2) | 164.5(3) | C(4)-C(3)-C(2) | 121.4(12) |
| O(12)-Zn(1)-O(4) | 95.2(4) | C(5)-C(4)-C(3) | 118.5(11) |
| O(12)-Zn(1)-O(5) | 89.7(4) | C(9)-C(4)-C(3) | 117.3(11) |
| O(12)-Zn(1)-O(11) | 92.7(3) | C(9)-C(4)-C(5) | 124.2(11) |
| O(3)-Cu(1)-O(2) | 165.9(4) | C(6)-C(5)-C(4) | 120.1(11) |
| O(11)-Cu(1)-O(2) | 79.4(3) | C(5)-C(6)-C(1) | 121.6(12) |
| O(11)-Cu(1)-O(3) | 88.5(3) | O(2)-C(7)-O(1) | 123.3(11) |
| O(11)-Cu(1)-O(2) | 92.9(3) | C(1)-C(7)-O(1) | 119.3(11) |
| O(11)-Cu(1)-O(3) | 98.3(3) | C(1)-C(7)-O(2) | 117.4(10) |
| O(11)-Cu(1)-O(11) | 170.5(2) | O(4)-C(8)-O(3) | 124.9(12) |
| O(13)-Cu(1)-O(2) | 91.8(3) | C(2)-C(8)-O(3) | 117.4(11) |
| O(13)-Cu(1)-O(3) | 94.9(3) | C(2)-C(8)-O(4) | 117.8(11) |
| O(13)-Cu(1)-O(11) | 87.5(3) | O(6)-C(9)-O(5) | 125.3(11) |
| O(13)-Cu(1)-O(11) | 98.5(3) | C(4)-C(9)-O(5) | 115.6(11) |
| Cu(1)-O(2)-Zn(1) | 96.5(3) | C(4)-C(9)-O(6) | 119.1(11) |
| Cu(1)-O(11)-Zn(1) | 99.0(4) | | |
| Cu(1)-O(11)-Zn(1) | 118.2(4) | | |
| Cu(1)-O(11)-Cu(1) | 107.9(4) | | |

Atomic coordinates and isotropic displacement parameters for ZnCuOH(TM) . $2H_2O$.

| **Atom** | **x** | **y** | **z** | **U(iso)** |
|---|---|---|---|---|
| Zn(l) | 0.3224(1) | 0.0812(2) | 0.0909(1) | 0.0159 |
| Cu(1) | 0.5112(1) | 0.2341(2) | 0.2584(1) | 0.0126 |
| O(1) | -0.2768(9) | 0.685(1) | -0.3339(6) | 0.0264 |
| O(2) | -0.3305(7) | 0.753(1) | -0.2096(5) | 0.0128 |
| O(3) | -0.3142(8) | 0.305(1) | -0.2232(6) | 0.0171 |
| O(4) | -0.2044(8) | 0.136(1) | -0.1029(6) | 0.0195 |
| O(5) | 0.2148(7) | 0.276(2) | 0.0147(6) | 0.0198 |
| O(6) | 0.3163(7) | 0.544(1) | -0.0243(7) | 0.0153 |
| O(11) | 0.4834(7) | -0.007(1) | 0.1720(6) | 0.0127 |
| O(12) | 0.3616(8) | -0.050(1) | -0.0196(6) | 0.0213 |
| O(13) | 0.4943(8) | -0.005(1) | 0.3694(6) | 0.0226 |
| C(1) | -0.129(1) | 0.618(2) | -0.1957(8) | 0.0106 |
| C(2) | -0.117(1) | 0.427(2) | -0.1540(8) | 0.0140 |
| C(3) | -0.001(1) | 0.373(2) | -0.0998(8) | 0.0168 |
| C(4) | 0.099(1) | 0.508(2) | -0.0885(8) | 0.0149 |
| C(5) | 0.082(1) | 0.696(2) | -0.1338(8) | 0.0117 |
| C(6) | -0.031(1) | 0.750(2) | -0.1838(8) | 0.0162 |
| C(7) | -0.255(1) | 0.687(2) | -0.2515(8) | 0.0172 |
| C(8) | -0.219(1) | 0.279(2) | -0.1602(8) | 0.0189 |
| C(9) | 0.219(1) | 0.438(2) | -0.0271(8) | 0.0123 |
| H(31) | 0.010(1) | 0.239(2) | -0.0668(8) | 0.0800 |
| H(51) | 0.153(1) | 0.788(2) | -0.1305(8) | 0.0800 |
| H(61) | -0.043(1) | 0.890(2) | -0.2125(8) | 0.0800 |
| H(121) | 0.3237(8) | -0.187(1) | -0.0442(6) | 0.0800 |
| H(131) | 0.5264(8) | 0.082(1) | 0.3461(6) | 0.0800 |

Anisotropic displacement parameters ($Å^2$) for ZnCuOH(TM) . $2H_2O$.

| Atom | U(11) | U(22) | U(33) | U(23) | U(13) | U(12) |
|---|---|---|---|---|---|---|
| Zn(1) | 0.0173(7) | 0.0165(8) | 0.0156(7) | 0.0052(7) | 0.0016(6) | 0.0043(7) |
| Cu(1) | 0.0105(7) | 0.0099(8) | 0.0196(8) | -0.0036(7) | -0.0018(6) | 0.0009(7) |
| O(1) | 0.023(5) | 0.033(6) | 0.022(5) | 0.004(4) | -0.001(4) | -0.000(4) |
| O(2) | 0.007(4) | 0.015(5) | 0.020(4) | -0.003(4) | -0.002(3) | 0.001(4) |
| O(3) | 0.016(4) | 0.012(5) | 0.025(5) | -0.000(4) | -0.003(4) | 0.002(4) |
| O(4) | 0.022(5) | 0.017(5) | 0.025(5) | 0.006(4) | -0.005(4) | -0.007(4) |
| O(5) | 0.020(4) | 0.024(5) | 0.023(5) | 0.004(5) | 0.009(4) | 0.010(4) |
| O(6) | 0.007(4) | 0.011(5) | 0.048(6) | -0.003(4) | 0.004(4) | -0.002(4) |
| O(11) | 0.010(4) | 0.013(4) | 0.020(5) | 0.000(4) | -0.001(4) | 0.005(3) |
| O(12) | 0.032(5) | 0.012(5) | 0.027(5) | 0.003(4) | 0.010(4) | 0.003(4) |
| O(13) | 0.024(5) | 0.019(5) | 0.025(5) | -0.003(4) | 0.003(4) | 0.002(4) |
| C(1) | 0.008(6) | 0.020(7) | 0.013(6) | -0.001(5) | 0.007(5) | 0.004(5) |
| C(2) | 0.0140 | 0.0140 | 0.0140 | 0.0000 | 0.0038 | 0.0000 |
| C(3) | 0.027(7) | 0.018(7) | 0.014(6) | -0.006(6) | 0.009(5) | -0.003(6) |
| C(4) | 0.016(6) | 0.018(6) | 0.013(6) | 0.001(5) | 0.005(5) | -0.002(5) |
| C(5) | 0.020(6) | 0.017(7) | 0.011(6) | -0.005(5) | -0.005(5) | -0.010(5) |
| C(6) | 0.026(6) | 0.009(6) | 0.021(6) | -0.006(6) | 0.003(5) | -0.001(6) |
| C(7) | 0.0172 | 0.0172 | 0.0172 | 0.0000 | 0.0046 | 0.0000 |
| C(8) | 0.023(6) | 0.030(8) | 0.012(6) | 0.001(6) | 0.007(5) | 0.005(6) |
| C(9) | 0.020(6) | 0.027(8) | 0.015(6) | 0.012(6) | 0.013(5) | 0.016(6) |

Torsional angles (in degrees) for ZnCuOH(TM) . $2H_2O$.

| | | | |
|---|---|---|---|
| C(1)-C(2)-C(3)-C(4) | -0.20 | O(1)-C(7)-C(1)-C(2) | -105.83 |
| C(2)-C(3)-C(4)-C(5) | -1.43 | O(1)-C(7)-C(1)-C(6) | 77.43 |
| C(3)-C(4)-C(5)-C(6) | 3.64 | O(2)-C(7)-C(1)-C(2) | 77.24 |
| C(4)-C(5)-C(6)-C(1) | -4.31 | O(2)-C(7)-C(1)-C(6) | -99.50 |
| C(5)-C(6)-C(1)-C(2) | 2.63 | O(3)-C(8)-C(2)-C(1) | 18.18 |
| C(6)-C(1)-C(2)-C(3) | -0.35 | O(3)-C(8)-C(2)-C(3) | -164.28 |
| C(7)-C(1)-C(2)-C(3) | -177.06 | O(4)-C(8)-C(2)-C(1) | -162.64 |
| C(7)-C(1)-C(6)-C(5) | 179.32 | O(4)-C(8)-C(2)-C(3) | 14.90 |
| C(7)-C(1)-C(2)-C(8) | 0.49 | O(5)-C(9)-C(4)-C(3) | -6.93 |
| C(8)-C(2)-C(1)-C(6) | 177.20 | O(5)-C(9)-C(4)-C(5) | 172.98 |
| C(8)-C(2)-C(3)-C(4) | -177.89 | O(6)-C(9)-C(4)-C(3) | 170.66 |
| C(9)-C(4)-C(3)-C(2) | 178.49 | O(6)-C(9)-C(4)-C(5) | -9.42 |
| C(9)-C(4)-C(5)-C(6) | -176.28 | | |

Distances from the mean basal plane for the metal coordination

| Zn(1) coordination | | Cu coordination | |
|---|---|---|---|
| | Height from base (Å) | | Height from base (Å) |
| Zn(1) | 0.345 | Cu | 0.123 |
| O(4b) | 2.330 | O(13) | 2.481 |
| O(2a) | 0.104 | O(2a) | -0.014 |
| O(5) | -0.094 | O(3a) | -0.013 |
| O(11) | -0.105 | O(11) | 0.015 |
| O(12) | 0.095 | O(11a) | 0.012 |

# 5. PREPARATION OF ZINC/COPPER MIXED METAL PYROMELLITATES

## 5.1 Introduction

This chapter describes the preparation and characterisation of zinc/copper pyromellitates. To put the work reported in this chapter into context, a brief introduction to pyromellitate chemistry (including previous work by this research group) is given first. This is followed by a discussion of the results and the conclusions drawn from the study. Finally the experimental details are given at the end of the chapter.

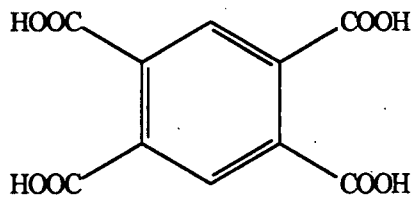


Figure 5.1 Pyromellitic acid

There has recently been growing interest in the salts of pyromellitic acid (1,2,4,5-benzenetetracarboxylic acid, figure 5.1)[2,3,8-10,13,65,95,101-3]. The areas of research include fire retardants[10], one-dimensional conductors[65], magnetic exchange interactions between cations[8,9], and catalysis[13,101]. Several crystal structures have been determined, including those of many f-block metals[118-23], but we shall only concern ourselves with the salts of divalent group IIa and d-block metals (the structures discussed here have been dealt with more rigorously in chapter 2, Preparation, Properties and Uses of Metal Carboxylates).

The pyromellitate salts have a varied structural chemistry owing to the pyromellitate group possessing eight potential donor sites (from the four carboxyl groups). Depending on the number of protons displaced the pyromellitate group can be a mono-, di-, tri-, or tetra-anion. The structures reported include ionic (no coordination between the anion and cation), one-, two- and three-dimensional networks. For example, $[Co(H_2O)_6]^{2+}$ $[H_2PM]^{2-}$ (where $H_4PM$ is pyromellitic acid) has an ionic structure, in which layers of octahedral $[Co(H_2O)_6]^{2+}$ are separated by $H_2PM^{2-}$ ions. The structure is held together by H-bonding between pyromellitate and water[65]. The acidic protons of the pyromellitate group are involved in very strong internal H-bonding between adjacent carboxyl groups (figure 5.2).

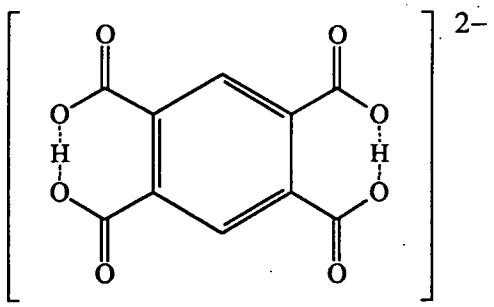

Figure 5.2 Pyromellitate dianion in $[Co(H_2O)_6]^{2+}$ $[H_2PM]^{2-}$.

A one-dimensional structure was found[25] for $Co_2PM.18H_2O$. The pyromellitate anion acts as a bismonodentate ligand, bridging between the cations and forming polymeric chains. However, layers are the most commonly reported structures[31,32,64]. This is perhaps not too surprising considering the anion consists of four carboxyl groups situated around a planar ring. Two salts of interest to this project have layer structures; $Cu_2PM$ . $10H_2O$ has a planar structure[64] and the crystal structure for $Zn_2PM$ . $7H_2O$ was reported[31] to consist of corrugated layers. In both examples the pyromellitate coordinates through all four carboxylate groups to metal centres.

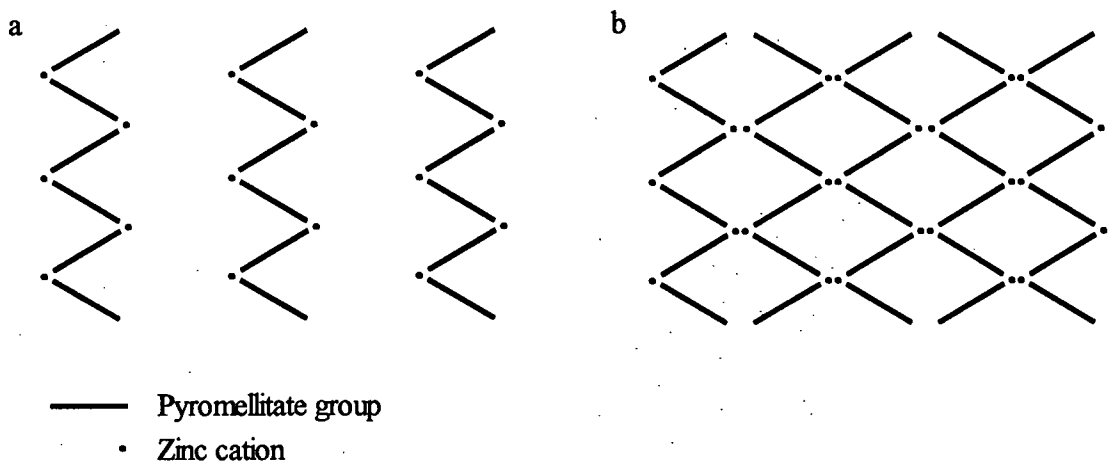


Figure 5.3. Schematic of the cross section through a) corrugated layers of $Zn_2PM.7H_2O$ and b) channel structure of $Na_2ZnPM.9H_2O$.

Only one three-dimensional structure was reported[63], that for $Na_2ZnPM$ . $9H_2O$, which had a zeolite-like channel structure. Figure 5.3 illustrates the similarities between the zinc and the sodium/zinc pyromellitate structures. For $Zn_2PM$ . $7H_2O$, tetrahedral zinc ions coordinated pyromellitate groups together, forming corrugated layers. One can see from figure 5.3 that superimposing another layer structure (180° out of phase) would produce a channel structure similar to that found for $Na_2ZnPM.9H_2O$. In both structures the stoichiometry of the framework was $(ZnPM^{2-})_n$ and the counter cations were located between the layers in the zinc salt and in the channels for the mixed metal salt.

Luehrs *et al* have used IR to identify structural features in a number of pyromellitate salts[24]. They found that, as with acetates, the carboxylate coordination can be deduced from $\Delta\nu_{(asym\text{-}sym)}$, the separation between asymmetric (1620-1550cm$^{-1}$) and symmetric (1440-1350cm$^{-1}$) carboxylate $\nu(CO_2)$ stretching bands, i.e.

| $\Delta\nu_{(asym\text{-}sym)}$ / cm$^{-1}$ | **Carboxylate Coordination** |
|---|---|
| >200 | – monodentate |
| 180-170 | – ionic (no coordination to metal centre) |
| 150-90 | – chelating or bridging |

However, acidic salts like $[Co(H_2O)_6]^{2+}$ $[H_2PM]^{2-}$ had much larger values of $\Delta\nu_{(asym\text{-}sym)}$ than expected. As previously mentioned, the cobalt salt had an ionic structure, but the separation between the $\nu(CO_2)$ bands was 240cm$^{-1}$, much larger than expected. It was suggested by the authors that the large value of $\Delta\nu_{(asym\text{-}sym)}$ was due to extensive H-bonding between water and the carboxyl groups. Surprisingly, no consideration was given to the very strong intra-molecular H-bond between adjacent carboxylate groups found for the cobalt salt[65] (see figure 5.2). The hydrogen can be considered as a pseudo-metal, bridging between the carboxylates. Thus each carboxylate group is monodentate rather than non-coordinated. Likewise, $NaH(O_2CMe)_2$ has an ionic structure, but a $\Delta\nu_{(asym\text{-}sym)}$ value of 310 cm$^{-1}$. The hydrogen bridges between two acetate groups, making them monodentate[70].

Several compounds were found to have broad intense envelopes from 1800 to 900cm$^{-1}$, indicative of very strong H-bonding. Luehrs *et al* neglected to point out that the compounds with such bands in their spectra all had acidic protons associated with the pyromellitate groups. One would conclude from these results that all the salts had very strong intra-molecular H-bonding similar to that for the cobalt salt. This hypothesis was further supported by the values of $\Delta\nu_{(asym\text{-}sym)}$ determined for the compounds, which were all >200cm$^{-1}$. Large separations like these are indicative of monodentate carboxylate coordination, presumably owing to the protons acting as pseudo-metals, bridging between adjacent carboxylates (cf. cobalt dihydrogen pyromellitate, figure 5.2).

Previous work carried out at Durham centred on the synthesis of zinc/copper pyromellitates and the structural determination of the products[2,3]. It was found that precipitates formed by the addition of potassium pyromellitate solution to aqueous copper sulphate solution were dependent on pH, and that single phases were only obtained if the pH of the reaction was carefully controlled. The reactions below show the products obtained at different pH levels.

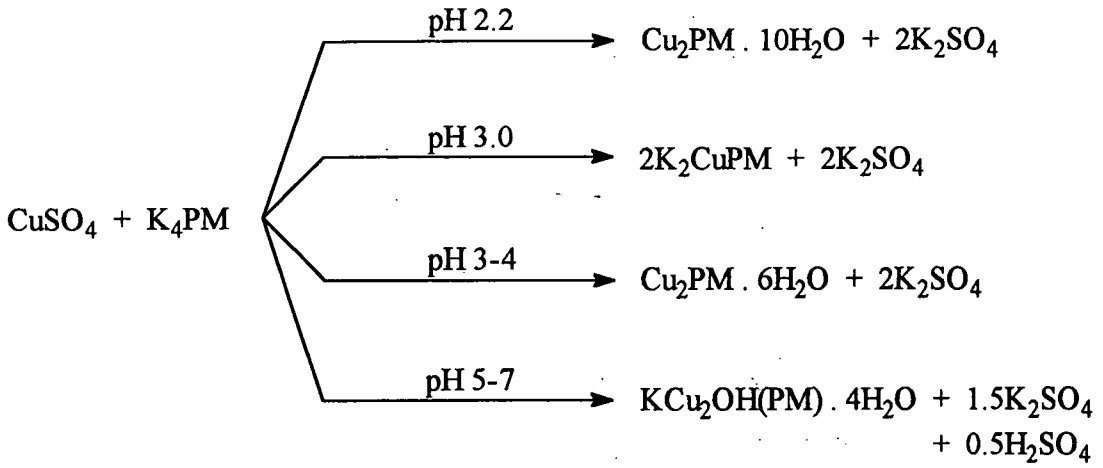


The precipitations from zinc sulphate solutions yielded similar results ($Zn_2PM$ . $3H_2O$ for pH ~4 and $K_2ZnPM$ . $3H_2O$ for pH 5-6). Little success was achieved in preparing mixed metal zinc/copper pyromellitates as all the products contained potassium, e.g. $KZnCuOH(PM)$ . $7H_2O$ (such salts are less than desirable for use as catalyst precursors because their thermolysis products will be contaminated with alkali metal). Some of the above reactions were repeated using copper nitrate solutions (the change was made because sulphur poisons Cu/ZnO catalysts). Surprisingly, different products were formed under otherwise analogous conditions, e.g.

$$2Cu(NO_3)_2 + K_4PM \xrightarrow{pH,\ 2\text{-}3} K_2CuPM . 4H_2O + Cu_2PM . 4H_2O$$

It was found that the alkali metal also affected the reaction. When sodium pyromellitate was used instead of the potassium salt, the product was a mixed sodium/copper pyromellitate.

$$2Cu(NO_3)_2 + 3Na_4PM \xrightarrow{pH,\ 3.0} Na_2Cu_3H_4PM_3 . 10H_2O$$

Because of the complexity of the precipitation route some experiments were carried out reacting solid zinc/copper hydroxycarbonates with the free acid dissolved in water. As mentioned in the previous chapter this route offered several advantages:

i) exclusion of the alkali metals;
ii) buffer effect, the solid hydroxycarbonate controlled the pH; and
iii) zinc/copper templates for the formation of mixed metal pyromellitates.

$Cu_2PM$ . $6H_2O$ was prepared by reacting solid copper hydroxycarbonate with a boiling solution of pyromellitic acid. As with the trimellitate preparations, the reaction involved the conversion of one solid into another, and gave near quantitative yields.

$$Cu_2CO_3(OH)_2 + H_4PM \xrightarrow{\Delta} Cu_2PM . 6H_2O + CO_2$$

The pyromellitate salts, although more soluble than the trimellitates (ca. x20 more soluble), had low solubilities and attempts to recrystallise the products were unsuccessful in producing suitable crystals for structure determination. The gel method was found to be the most satisfactory route for growing crystals (described in section 2.1a), and structures were determined for $Cu_2PM \cdot 6H_2O$, $K_2CuPM \cdot 4H_2O$ (two of the phases from the nitrate precipitations) and a basic mixed metal salt, $(Zn_{0.75}Cu_{0.25})_{2.5}OH(PM) \cdot 7H_2O$.

In figure 5.4 the structures of copper pyromellitate decahydrate and hexahydrate are shown. The structure for the decahydrate salt was previously reported by Usubaliev *et al*[64], and in comparison with the hexahydrate one can see that the structures were very different even though the compounds had similar stoichiometries. The copper for the decahydrate salt is coordinated to three waters and two carboxyl oxygens, forming a square based pyramid. The carboxyl oxygens are positioned trans in the base. The pyromellitate group is coordinated to four metal sites, bridging between them, forming a polymeric layer.

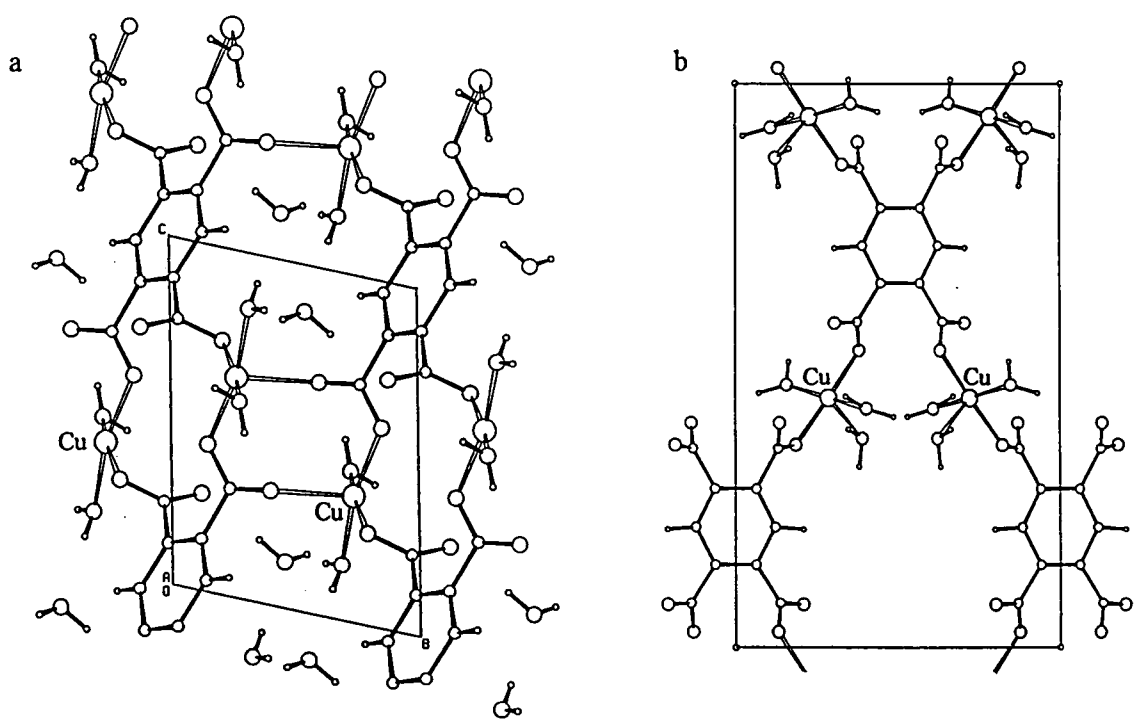


Figure 5.4 Structure of a) $Cu_2PM \cdot 6H_2O$ and b) $Cu_2PM \cdot 10H_2O$

The copper atom for the hexahydrate salt is also square based pyramidal but coordinated to three carboxyl oxygens, fac. The pyromellitate group is coordinated to five copper sites and the greater number of bonding contacts produces a more complicated layer structure. In both structures water is situated between the layers and is involved in H-bonding to the layers.

For $K_2CuPM \cdot 4H_2O$ (figure 5.5a) copper is coordinated to four carboxyl oxygens in a square planar arrangement. The pyromellitate bridges between four copper sites to form planar layers. There are two potassium sites (one was 7 coordinate, the other 8) and both are located between the layers.

It is interesting to note that this structure is analogous to that found for the ortho phthalate salt $K_2Cu(pht) \cdot 2H_2O$ (pht = $C_8H_4O_2$, figure 5.5b). The phthalate salt[53] has square planar copper sites bridged by the anions, forming chains. For the pyromellitate salt, the anion can be thought of as two superimposed phthalate groups, bridging between the chains, forming layers.

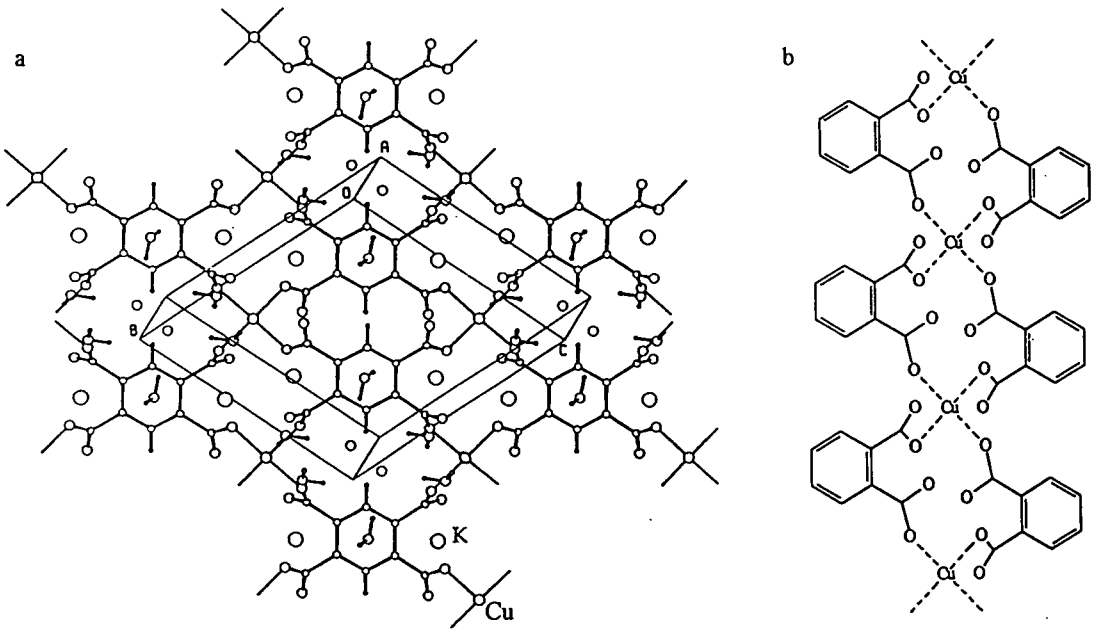


Figure 5.5 Structure of a) $K_2CuPM \cdot 4H_2O$, b) $K_2Cu(pht) \cdot 4H_2O$.

Crystals of $(Zn_{0.75}Cu_{0.25})_{2.5}OH(PM) \cdot 7H_2O$ were also obtained, however the structure has not been satisfactorily resolved. The basic structure of the salt was deduced and consisted of a layer network with quadrangular vacancies (figure 5.6). The sides of the vacancies are pyromellitate groups which are held together by metals situated at the intersects. The metal coordination at the lattice intersects (figure 5.7) consists of four metals coordinated together by two hydroxyl oxygens and four carboxyl groups (from different pyromellitate groups). Unfortunately, it has not been possible to determine the precise metal coordination.

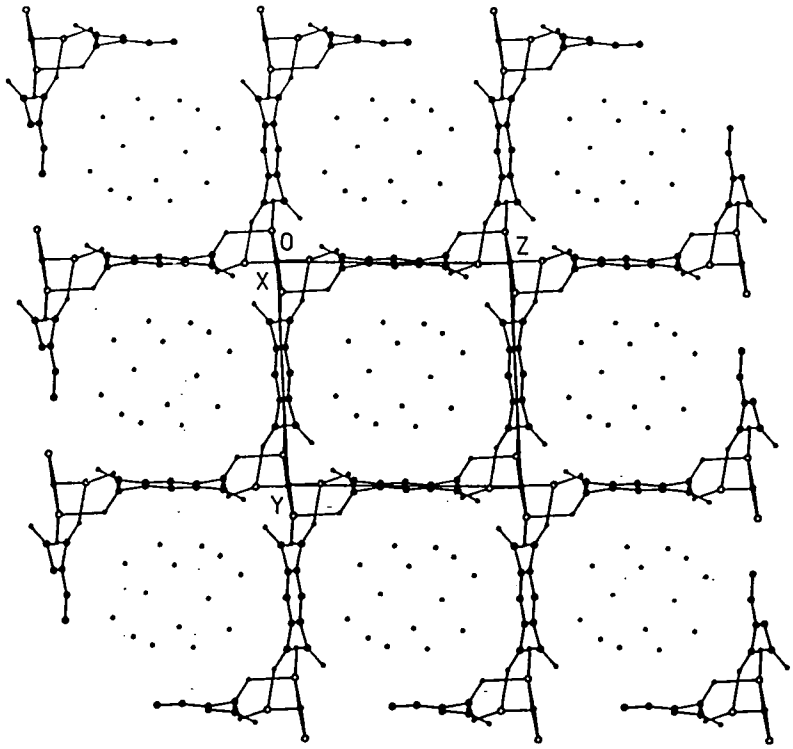


Figure 5.6 Two-dimensional network of $(Zn_{0.75}Cu_{0.25})_{2.5}OH(PM) \cdot 7H_2O$.

The stoichiometry of the layers is $M_2OH(PM)^-$ and the layers stack, forming channels through the structure. Located in the channels are 14 waters and 1 cation per lattice vacancy. The random distribution of water molecules and cations in the channels has hampered efforts to fully solve the structure.

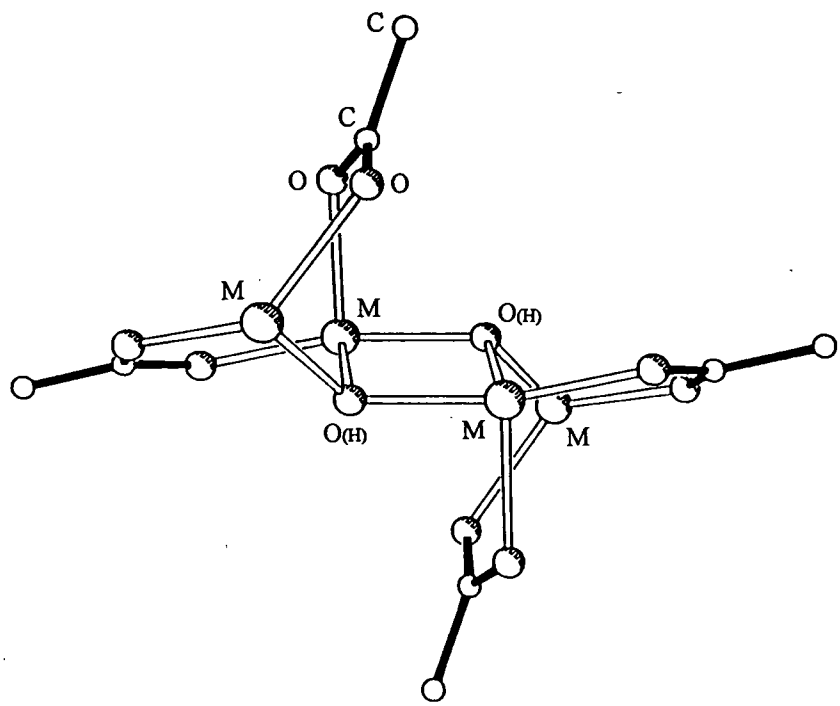


Figure 5.7 Metal coordination within the layer in $(Zn_{0.75}Cu_{0.25})_{2.5}OH(PM) \cdot 7H_2O$.

The aim of the work reported here was to investigate the preparation of zinc/copper pyromellitates by the hydroxycarbonate route. A discussion of the results and conclusions from this work now follow. The experimental details are given at the end of the chapter.

## 5.2 Discussion of Results

A series of experiments was undertaken reacting aqueous solutions of pyromellitic acid with a number of hydroxycarbonates covering a range of zinc/copper ratios (x=0.0, 0.1, 0.2, . . . 0.9, 1.0, where x = Zn/(Zn+Cu)). First the preparations will be discussed, followed by the characterisation of the phases obtained, and finally the conclusions.

### *5.2a Preparation*

Micro-crystalline powders of $Cu_2PM \cdot 6H_2O$ (the same phase as reported earlier) and $Zn_2PM \cdot 4H_2O$ (a different phase to the heptahydrate reported in the literature, deduced by XRD) were prepared by adding solid hydroxycarbonate to an aqueous solution of pyromellitic acid, producing a suspension, and refluxing the mixture for at least 1 hour. Substitution of one cation into the salt of the other occurred to a limited extent, 2% zinc substitution into the copper salt and 10% for copper into the zinc salt.

$$2Zn_5(CO_3)_2(OH)_6 + 5H_4PM \xrightarrow{\Delta} 5Zn_2PM \cdot 4H_2O + 4CO_2$$

(up to 10% copper substitution)

$$Cu_2CO_3(OH)_2 + H_4PM \xrightarrow{\Delta} Cu_2PM \cdot 6H_2O + CO_2$$

(up to 2% zinc substitution)

During experiments to prepare mixed metal salts with x=0.2-0.4 (metal to pyromellitate ratio of the reactants was 2:1), it was observed that a light blue solid was formed, but after 10 to 15 minutes its colour started to darken and went turquoise. The products collected after <10 minutes reaction were found to be basic mixed metal salts with the general formula $(Zn_xCu_{1-x})_{2.5}OH(PM) \cdot 7H_2O$. It was deduced from the XRD's that these samples were the same phase as the crystals obtained from the previous work. Further reaction of the basic salt with the mother liquor (refluxing for several hours) produced another mixed metal phase, this time the neutral salt $(Zn_xCu_{1-x})_2PM \cdot 1\text{-}2H_2O$.

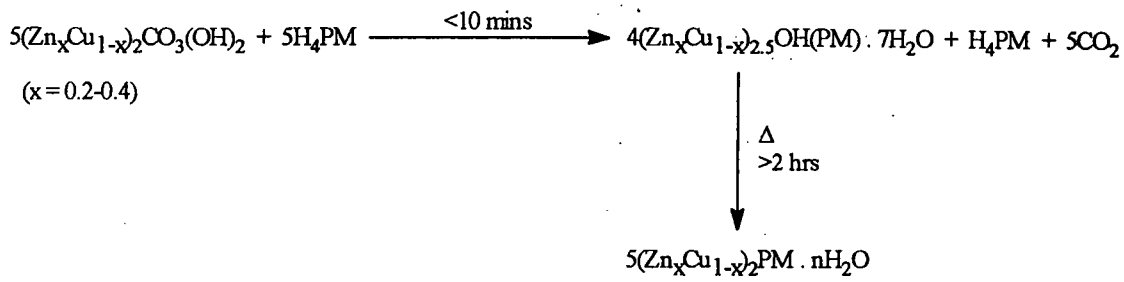


The zinc/copper pyromellitates produced had lower zinc contents than expected. The solvated zinc later crystallised out as clear thin quadrangular prisms which were characterised as the acidic salt $ZnH_2PM \cdot 6H_2O$ (the crystal structure will be discussed later, section 5.2c). Blue hexagonal plate crystals of $Cu_2PM \cdot 6H_2O$ also developed in the mother liquor for some of the experiments.

Adding zinc/copper hydroxycarbonates with cation ratios of x=0.5-0.8 to boiling solutions of pyromellitic acid quickly produced the respective basic mixed metal salts (no $ZnH_2PM \cdot 6H_2O$ crystallised from the mother liquors of the zinc-rich preparations). Further refluxing of the reaction mixture produced a small amount of $Zn_2PM \cdot 4H_2O$ impurity (<5%). Under a microscope tiny (<0.2mm) colourless rod-like crystals were observed scattered through the product. The crystals were found to be zinc pyromellitate tetrahydrate.

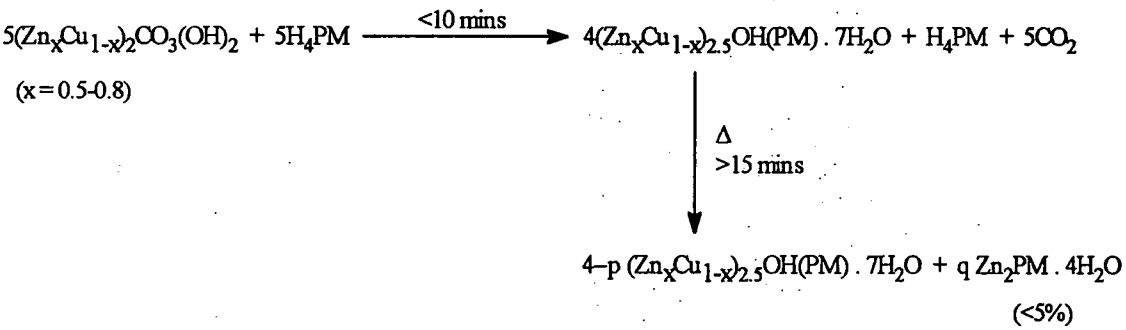


In these experiments the basic mixed metal salt appeared to be slowly reacting with excess acid, forming crystallites of zinc pyromellitate. This further reaction would not only produce an impurity but would also reduce the zinc content for the mixed metal phase.

These experiments have demonstrated that the basic mixed metal phase had a large zinc/copper solid solution series (x=0.1-0.8). However, the products were unstable in the presence of excess pyromellitic acid. To successfully scale-up the preparation of the basic mixed metal salt, the following conditions were imposed.

i) Metal:pyromellitic acid ratio of the reactants = 5:2, i.e. no excess acid was used. This prevented the formation of the neutral mixed metal salt, and hindered the formation of zinc pyromellitate crystal, e.g.

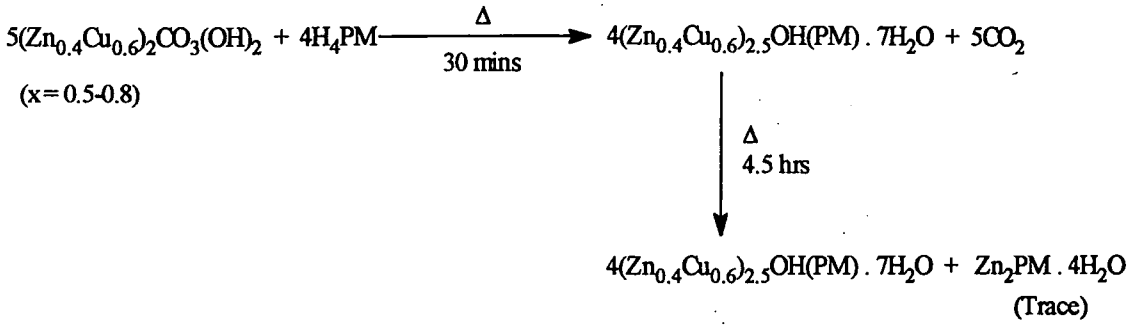


ii) Reaction at room temperature. Lowering the reaction temperature further hindered the formation of zinc pyromellitate. The above reaction was repeated at room temperature and after 4.5 hours no zinc pyromellitate was detected.

iii) Adding the hydroxycarbonate solid as a slurry. Under such mild conditions, incomplete reaction of the larger grains of zinc/copper hydroxycarbonate became a problem. It was found that a slurry of hydroxycarbonate powder in water, stirred for several hours, afforded a fine suspension (more efficient than grinding in a mortar and pestle) which enabled a fast and complete reaction with pyromellitic acid.

### *5.2b Characterisation*

Powder XRD was very important in the identification of the phases. The experimental data (4θ and d spacings) for the salts prepared by the hydroxycarbonate route are given in table 5.1.

| $Cu_2PM \cdot 6H_2O$ | | $Zn_2PM \cdot 4H_2O$ | | $(Zn,Cu)_2PM \cdot nH_2O$ | | $(Zn,Cu)_{2.5}OH(PM) \cdot 7H_2O$ | | $ZnH_2PM \cdot 6H_2O$ | |
|---|---|---|---|---|---|---|---|---|---|
| 4θ | d(Å) | 4θ | d(Å) | 4θ | d(Å) | 4θ | d(Å) | 4θ | d(Å) |
| 20.75 | 8.56(4) | 30.05 | 5.92(2) | 21.75 | 8.16(4) | 15.95 | 11.12(7) | 20.05 | 8.85(4) |
| 30.45 | 5.84(2) | 38.10 | 4.67(1) | 30.90 | 5.76(2) | 16.75 | 10.59(6) | 30.45 | 5.84(2) |
| 31.05 | 5.73(2) | 39.55 | 4.51(1) | 35.15 | 5.06(1) | 23.10 | 7.69(3) | 31.15 | 5.71(2) |
| 33.45 | 5.32(2) | 40.60 | 4.39(1) | 40.15 | 4.44(1) | 28.10 | 6.33(2) | 33.60 | 5.30(2) |
| 36.25 | 4.91(1) | 43.30 | 4.12(1) | 49.85 | 3.58(1) | 29.25 | 6.08(2) | 34.05 | 5.23(2) |
| 38.05 | 4.68(1) | 44.00 | 4.05(1) | 53.40 | 3.35(1) | 31.75 | 5.60(2) | 35.65 | 4.99(2) |
| 41.50 | 4.30(1) | 44.70 | 3.99(1) | 67.25 | 2.67(1) | 33.60 | 5.30(2) | 40.20 | 4.43(2) |
| 42.10 | 4.24(1) | 45.55 | 3.92(1) | 71.10 | 2.53(1) | 36.00 | 4.95(1) | 44.30 | 4.03(1) |
| 43.25 | 4.12(1) | 48.50 | 3.68(1) | 84.80 | 2.14(1) | 36.90 | 4.83(1) | 46.00 | 3.88(1) |
| 53.20 | 3.36(1) | 49.00 | 3.65(1) | | | 42.70 | 4.18(1) | 46.80 | 3.81(1) |
| 55.35 | 3.23(1) | 59.90 | 2.99(1) | | | 45.75 | 3.90(1) | 49.15 | 3.64(1) |
| 55.95 | 3.20(1) | 61.10 | 2.94(1) | | | 50.75 | 3.52(1) | 49.85 | 3.58(1) |
| 58.05 | 3.09(1) | 61.95 | 2.90(1) | | | 53.15 | 3.37(1) | 50.75 | 3.52(1) |
| 69.85 | 2.58(1) | 68.65 | 2.62(1) | | | 55.75 | 3.21(1) | 53.75 | 3.33(1) |
| 73.00 | 2.47(1) | 76.85 | 2.35(1) | | | 58.90 | 3.04(1) | 55.70 | 3.21(1) |
| 79.65 | 2.27(1) | 77.35 | 2.34(1) | | | 60.45 | 2.97(1) | 57.95 | 3.09(1) |
| 80.25 | 2.26(1) | 78.10 | 2.31(1) | | | 68.55 | 2.63(1) | 59.90 | 2.99(1) |
| 84.70 | 2.14(1) | 80.00 | 2.26(1) | | | 70.65 | 2.55(1) | 61.80 | 2.90(1) |
| 90.70 | 2.01(1) | 80.60 | 2.25(1) | | | 76.05 | 2.37(1) | 68.75 | 2.62(1) |
| 93.00 | 1.96(1) | 83.10 | 2.18(1) | | | 81.15 | 2.23(1) | 81.85 | 2.21(1) |
| | | 85.20 | 2.13(1) | | | 82.55 | 2.19(1) | 88.75 | 2.05(1) |
| | | 91.20 | 2.00(1) | | | 84.30 | 2.15(1) | 90.95 | 2.00(1) |
| | | 93.30 | 1.95(1) | | | | | 93.80 | 1.94(1) |
| | | 96.65 | 1.89(1) | | | | | 97.05 | 1.88(1) |

Table 5.1 Powder XRD data for pyromellitate compounds prepared via zinc/copper hydroxycarbonates. Only medium to strong lines are reported, the error for 4θ values was ± 0.1; estimated standard deviations are given in parentheses.

The IR spectra for the compounds are shown in figure 5.8. The spectra had broad intense bands above 2500$cm^{-1}$ due to ν(O-H) and ν(C-H). The 1700-1300$cm^{-1}$ region was dominated by carboxylate ν($CO_2$) absorptions (asymmetric stretch 1620-1550$cm^{-1}$ and symmetric stretch 1440-1350$cm^{-1}$). There were also absorptions from the aromatic ring (ν(C=C) ~1610 and ~1500$cm^{-1}$) complicating this part of the spectrum. Below 1300$cm^{-1}$ there were ν(C-H) in plane (1295, 1145-1138$cm^{-1}$) and out of plane (830-815$cm^{-1}$) bending vibrations, and ν($CO_2$) carboxylate symmetrical bend (690-675$cm^{-1}$).

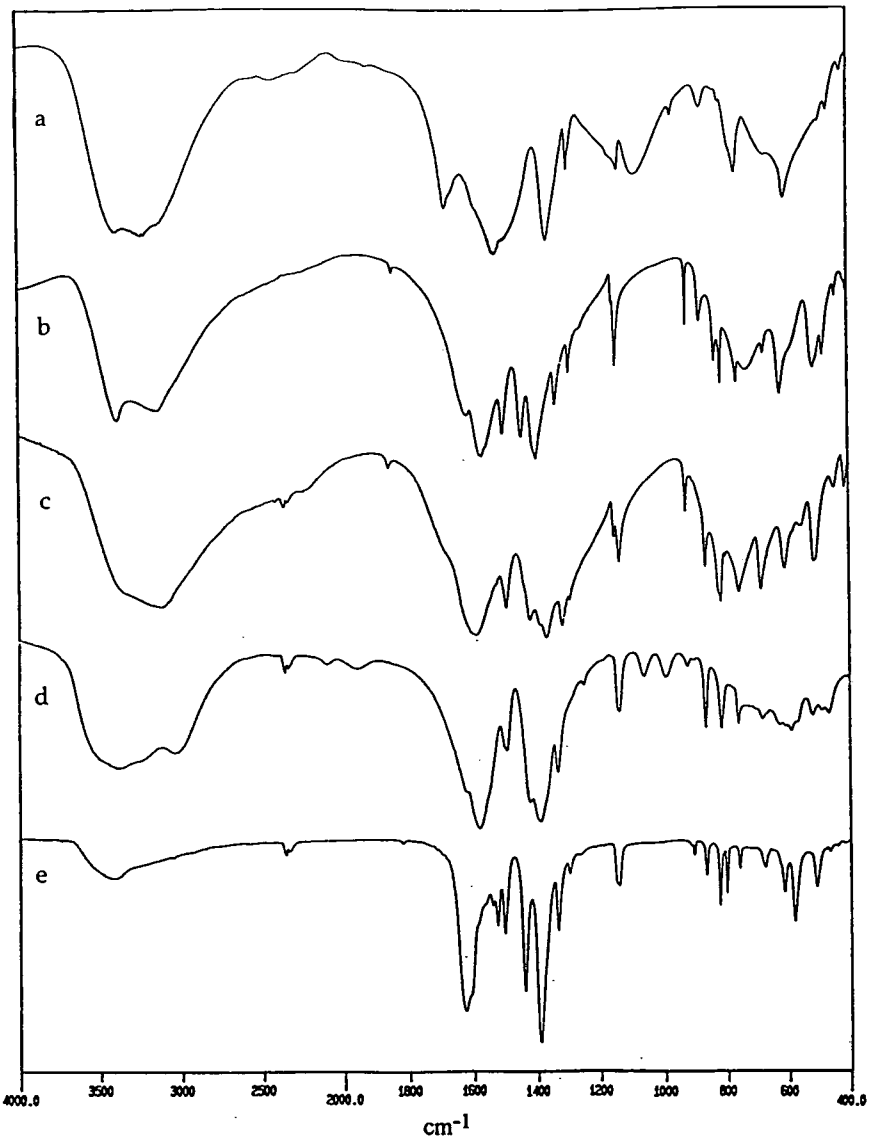


Figure 5.8 IR spectra of a) $ZnH_2PM \cdot 6H_2O$, b) $Zn_2PM \cdot 4H_2O$, c) $Cu_2PM \cdot 6H_2O$, d) $(Zn,Cu)_{2.5}OH(PM) \cdot 7H_2O$, e) $(Zn,Cu)_2PM \cdot nH_2O$.

Distinguishing features of the basic mixed metal spectra were four broad absorptions at 2100, 1955, 1065 and 995$cm^{-1}$. These bands have not been positively assigned. An obvious difference of the spectrum for $ZnH_2PM \cdot 6H_2O$ was the $\nu(C{=}O)$ absorption at 1679$cm^{-1}$. This corresponded to a carbonyl group from an intramolecular H-bonded acid group. The symmetric and asymmetric $\nu(CO_2)$ frequencies are at much lower wavenumbers, 1523 and 1361$cm^{-1}$.

It was previously mentioned that the separation between the asymmetric and symmetric $\nu(CO_2)$ stretching frequencies, $\Delta\nu_{(asym\text{-}sym)}$, can give structural information about the coordination of the carboxyl groups. For pyromellitate salts it was found that:

| $\Delta\nu_{(asym\text{-}sym)}$ / $cm^{-1}$ | **Carboxylate Coordination** |
|---|---|
| >200 | - monodentate |
| 180-170 | - ionic (no coordination to metal centre) |
| 150-90 | - chelating or bridging |

Table 5.2 gives values of $\Delta\nu_{(asym\text{-}sym)}$ for some of the pyromellitates described in this chapter, and crystal structure data for the pyromellitate anion where known.

| Compound | $\Delta\nu_{(asym\text{-}sym)}$ / $cm^{-1}$ | Carboxylate coordination [a] |
|---|---|---|
| $Zn_2PM \cdot 7H_2O$ | 230<br>142 | 3 x monodentate<br>bridging [b] |
| $Zn_2PM \cdot 4H_2O$ | 170<br>123 | —— |
| $ZnH_2PM \cdot 6H_2O$ | 162 | ionic [c] |
| $Cu_2PM \cdot 6H_2O$ | 220<br>168 | 2 x monodentate<br>2 x bridging |
| $(Zn_xCu_{1-x})_2PM \cdot nH_2O$ | 235<br>86 | —— |
| $(Zn_xCu_{1-x})_{2.5}OH(PM) \cdot 7H_2O$ | 190<br>157 | 2 x non coordinate<br>2 x bridging |
| $K_2CuPM \cdot 4H_2O$ | 255<br>162<br>139 | 2 x monatomic + anti<br>2 x bis-monatomic [d] |

Table 5.2 IR and crystal structure data concerning the carboxylate coordination of various zinc and copper pyromellitates.
[a] Deduced from crystal structure determination.
[b] Structure reported by C. Robl[31].
[c] Very strong O-H-O bond exists in this structure.
[d] Coordinations illustrated in figure 5.9.

Comparing the carboxylate coordinations with the values of $\Delta\nu_{(asym\text{-}sym)}$ shows that the values for certain types of coordination were significantly greater than those previously reported. For example, the bridging carboxylates in $Cu_2PM \cdot 6H_2O$ and $(Zn_xCu_{1-x})_{2.5}OH(PM). 7H_2O$ had $\Delta\nu_{(asym\text{-}sym)}$ values of 168 and 157$cm^{-1}$, and the non coordinated carboxylate groups of the basic mixed metal salt had a $\Delta\nu_{(asym\text{-}sym)}$ value of 190$cm^{-1}$. Therefore, the following $\Delta\nu_{(asym\text{-}sym)}$ values are proposed for the different carboxylate coordinations.

| $\Delta\nu_{(asym\text{-}sym)}$ / $cm^{-1}$ | Carboxylate Coordination |
|---|---|
| >210 | – monodentate |
| 195-175 | – ionic (no coordination to metal centre) |
| <170 | – chelating or bridging |

The lower limit for monodentate coordination has been increased because of the ambiguity existing for $\Delta\nu_{(asym\text{-}sym)}$=200$cm^{-1}$. The monodentate carboxylate coordination for $Cu_2PM \cdot 6H_2O$ had one of the lowest reported $\Delta\nu_{(asym\text{-}sym)}$ values at 220$cm^{-1}$, and the largest reported value for a non-coordinated carboxyl group was 190$cm^{-1}$. Without further examples, $\Delta\nu_{(asym\text{-}sym)}$ values of 200$cm^{-1}$ cannot be unambiguously assigned to either monodentate or non coordinated.

$\Delta\nu_{(asym\text{-}sym)}$ for $ZnH_2PM$ . $6H_2O$ was lower than expected for ionic or monodentate coordination. As will be shown from the crystal structure, the zinc salt has a very strong intra-molecular H-bond similar to $CoH_2PM$ . $6H_2O$ (figure 5.2), and one would expect the separation between the $\nu(CO_2)$ absorptions to be similar ($240cm^{-1}$). This will be discussed further along with the crystal structure below.

The carboxylate coordination for $K_2CuPM$ . $4H_2O$ does not correspond entirely to any of the above categories for $\Delta\nu_{(asym\text{-}sym)}$. The pyromellitate anion has two bis-monatomic and two monatomic + anti carboxyl groups (figure 5.9). Although both carboxylate groups were bridging, one of the $\Delta\nu_{(asym\text{-}sym)}$ values was much larger than expected for such a coordination ($255cm^{-1}$). It is possible that the uneven distribution of metal centres for the monatomic + anti carboxyl group (an extra copper on one of the oxygens) had a similar $\Delta\nu_{(asym\text{-}sym)}$ to monodentate coordination. This implies that the even distribution for the bis-bidentate carboxyl groups produced similar values of $\Delta\nu_{(asym\text{-}sym)}$ to those found for normal bridging carboxylates. Further examples are needed to clarify the situation for such carboxylates.

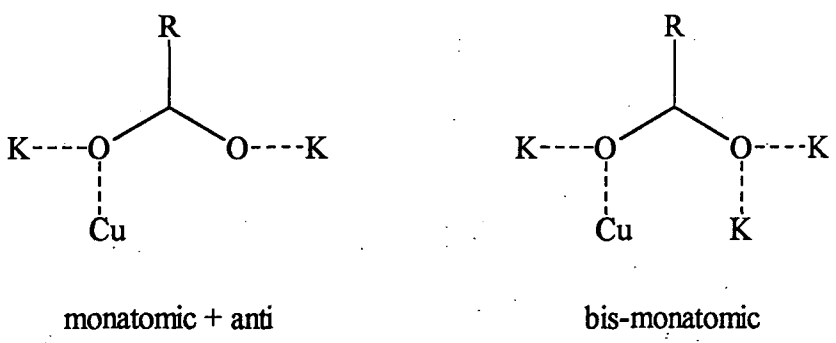


monatomic + anti bis-monatomic

Figure 5.9 Coordination of the carboxylate groups in $K_2CuPM$ . $4H_2O$.

From the above information one can deduce the carboxylate coordination of the two salts for which crystal structures have not been determined. $Zn_2PM$ . $4H_2O$ had $\Delta\nu_{(asym\text{-}sym)}$ values of 170 and $123cm^{-1}$, both indicative of bridging or chelating carboxylate coordination. Therefore, as all four carboxylates were coordinated to metal centres, the crystal structure for the salt must be either a two- or three-dimensional network. The $\nu(CO_2)$ carboxylate absorptions for the neutral mixed metal pyromellitate, $(Zn_xCu_{1-x})_2PM$ . $nH_2O$, have been more difficult to assign. It was assumed that the asymmetric $\nu(CO_2)$ bands were 1625 and $1526cm^{-1}$ and that the corresponding symmetric bands were 1391 and $1440cm^{-1}$. This gives $\Delta\nu_{(asym\text{-}sym)}$ values of 235 and $86cm^{-1}$ which correspond to monodentate and bridging/chelating carboxylate groups. Once again the structure must be a two- or three-dimensional network as all the carboxyl groups are coordinated to metal centres.

### *5.2c Structure of $ZnH_2PM . 6H_2O$*

The crystal structure, shown in figure 5.10, is an ionic lattice consisting of layers of $[Zn(H_2O)_6]^{2+}$ octahedra and $H_2PM^{2-}$ ions H-bonded together. The coordination around the zinc cation consists of two oxygen atoms lying on a two fold axis parallel to the b axis (these will be considered as the axial positions) and four oxygen atoms in the equatorial plane, slightly distorted towards a tetrahedron. The bond lengths for the axial oxygens are 2.108(1) and 2.050(1)Å and the O-Zn-O bond angle is 180° (all three atoms are on the b axis or parallel to it). Because of the $C_2$ symmetry of the octahedron there are two non equivalent oxygen sites in the equatorial plane. The bond lengths are 2.0761(7) and 2.1200(7)Å, the bond angles with the axial oxygens are 92.90(2), 86.24(2)° and the reciprocal angles are 87.10(2) and 93.76(2)°.

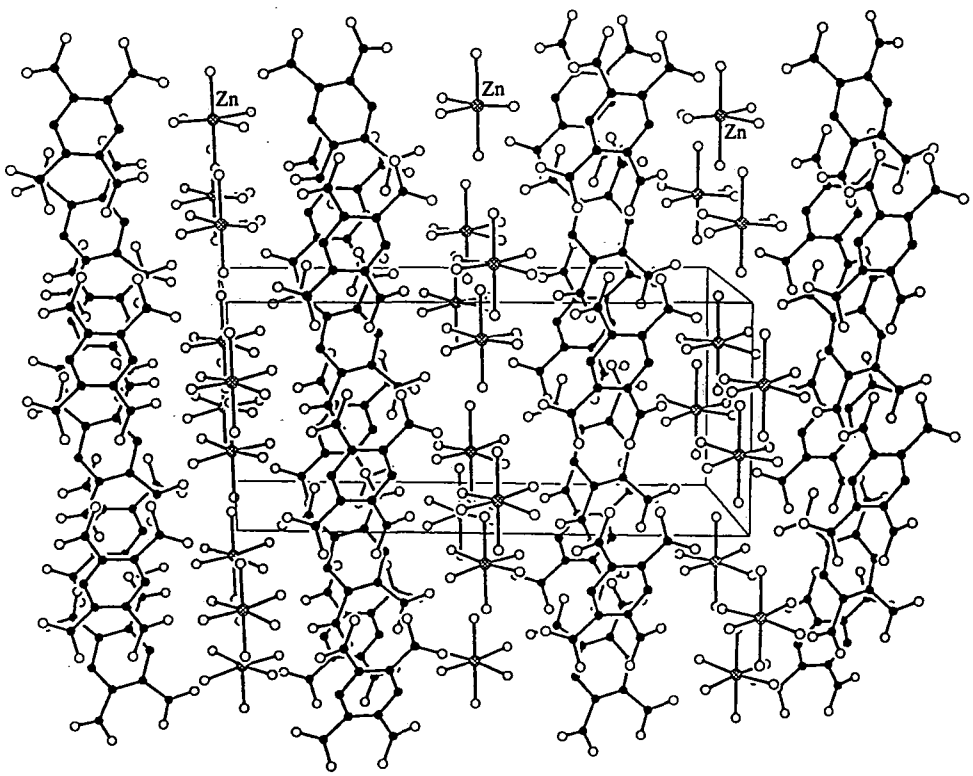


Figure 5.10 Crystal structure for $ZnH_2PM . 6H_2O$.

The acidic protons of the pyromellitate dianion (figure 5.11) are involved in very strong H-bonding between adjacent carboxyl groups (O···O, 2.420(1)Å), similar to that found[65] for $CoH_2PM . 6H_2O$ (O···O, 2.381(2)Å). However, the proton in the cobalt compound is equidistant from the two oxygens (1.211(7)Å), whereas in the zinc salt the proton is 1.11(2)Å from O(21) and 1.31(3)Å from O(31). The anion can be thought of

as consisting of three rings, the two outer rings are slightly out of the plane of the phenyl ring producing a chair conformation.

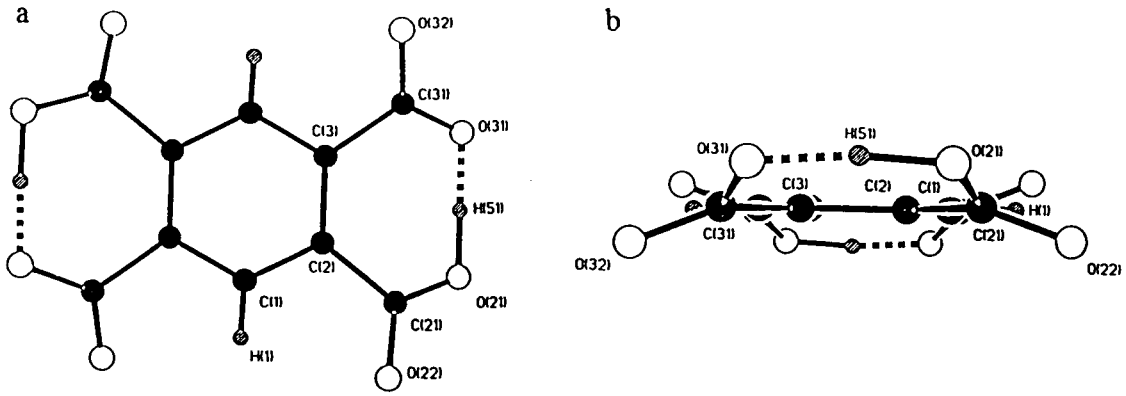


Figure 5.11 Two views of the pyromellitate dianion in $ZnH_2PM \cdot 6H_2O$.

This zinc salt and cobalt dihydrogen pyromellitate hexahydrate have very similar structures and carboxylate coordination. However, the value of $\Delta\nu_{(asym\text{-}sym)}$ for the cobalt salt ($240cm^{-1}$) is much larger than that for the zinc salt ($162cm^{-1}$). Luehrs *et al*[24] suggested that H-bonding with the water was the cause of the large $\Delta\nu_{(asym\text{-}sym)}$ found for the cobalt salt, but there is extensive H-bonding in both compounds. A more plausible explanation is that the hydrogen acts as a pseudo-metal and therefore the carboxylate coordination is monodentate. This explains the large $\Delta\nu_{(asym\text{-}sym)}$ for the cobalt compound and other acidic salts reported by Luehrs *et al* but does not explain the low value found for our zinc salt. A minor difference in the coordination of the two salts is that the acidic proton is equidistant from both oxygens in the cobalt compound but is closer to one of the oxygens in the zinc salt. It is possible that in the zinc salt the H-bond is not strong enough for the proton to act as a pseudo-metal and therefore the carboxylate coordination is best described as non-coordinated. It is also feasible that the compound underwent a transformation when pressed into a KBr disc for IR analysis. Cation exchange and pressure-induced changes (hydrolysis or disruption of the coordination) have been reported for some metal acetates and have produced erroneous IR spectra[70]. Further work needs to be undertaken to verify the factors influencing $\Delta\nu_{(asym\text{-}sym)}$.

## 5.3 Conclusions

It has been shown that the reaction of pyromellitic acid with zinc/copper hydroxycarbonate is a successful route to zinc, copper and mixed metal pyromellitates. The advantages of this route over precipitations from zinc/copper nitrate solution are:

–no control of pH required;
–excludes alkali metals from the products;
–formation of mixed metal zinc/copper pyromellitates of predetermined metal ratios.

Two zinc/copper pyromellitate solid solution series were produced. The neutral mixed metal salt, $(Zn_xCu_{1-x})_2PM \cdot nH_2O$, had a limited zinc/copper substitution (x=0.1-0.35) but the basic salt, $(Zn_xCu_{1-x})_{2.5}OH(PM) \cdot 7H_2O$, could accommodate almost the complete range of cation ratios (x=0.1-0.8). Care had to be taken when preparing the basic salt as it could react further to form either the neutral mixed metal salt or $Zn_2PM \cdot 4H_2O$ crystallites if an excess of acid or elevated temperatures were used.

The crystal structure for the basic mixed metal salt was discussed in the introduction to this chapter. The lattice consists of pyromellitate groups coordinated together via metal-oxygen clusters, forming a layer of quadrangular vacancies (figures 5.6 and 5.7). The layers are stacked such that the vacancies are aligned, forming channels through the structure. Water molecules and hydrated cations are randomly distributed through these channels.

It is possible that the $Zn_2PM \cdot 4H_2O$ crystallites were formed by zinc leaching out of the channels and reacting with pyromellitic acid. This suggests that only hydrated zinc cations were present in the channels, otherwise one would expect copper pyromellitate crystals to be formed as well.

This research has also added to previous work on the structural characterisation of pyromellitate compounds by IR. The carboxylate coordination can be deduced from $\Delta\nu_{(asym-sym)}$, and similar results were found to those for acetates[70], although values of $\Delta\nu_{(asym-sym)}$ were slightly larger.

| **Pyromellitate** $\Delta\nu_{(asym-sym)}$ / **cm$^{-1}$** | **Carboxylate Coordination** | **Acetate** $\Delta\nu_{(asym-sym)}$ / **cm$^{-1}$** |
|---|---|---|
| >210 | monodentate | >200 |
| 195-175 | non-coordinated/ bridging/chelating | 170-150 |
| <170 | bridging/chelating | <150 |
| as yet unknown | chelating/syn-syn | <105 |

Further work is required to deduce $\Delta\nu_{(asym-sym)}$ values for highly coordinated carboxylate groups like those for $K_2CuPM \cdot 4H_2O$. Further clarification is also required to determine the factors influencing $\Delta\nu_{(asym-sym)}$ for $ZnH_2PM \cdot 6H_2O$ and $CoH_2PM \cdot 6H_2O$. The carboxyl groups in these compounds are not coordinated to any metal centres, but do have a very strong H-bond between adjacent carboxylates. Despite the similarities in structure and carboxylate coordination, the zinc salt has a $\Delta\nu_{(asym-sym)}$

value of 162cm$^{-1}$ compared to 240cm$^{-1}$ for the cobalt salt. With only these results it was not possible to determine the reasons for the difference.

As a successful route to zinc/copper pyromellitates was achieved, the main area for future work lies in the structural characterisation of pyromellitate salts, such as $Zn_2PM \cdot 4H_2O$. Unfortunately, attempts to grow crystals of $Zn_2PM \cdot 4H_2O$ produced twinned or clusters of crystals and the gel method only produced crystals of the previously reported $Zn_2PM \cdot 7H_2O$. It therefore appears that this goal may be more difficult to achieve than was previously thought.

It would also be interesting to ascertain whether the structural similarity between $K_2CuPM \cdot 4H_2O$ and $K_2Cu(pht) \cdot 4H_2O$ (discussed in the introduction) also exists for other alkali metal/copper salts. The phthalate salts $M_2Cu(pht)$ (M = Li, K, Rb, or Cs) all have similar chain structures[52,53], and one could speculate that the analogous pyromellitate salts will have similar layer structures to $K_2CuPM \cdot 4H_2O$.

In contrast, the sodium copper salt $Na_2Cu(pht) \cdot 4H_2O$ has a layer structure. It will be interesting to see if the analogous pyromellitate salt has a three-dimensional structure based on the phthalate compound, or if the tendency for pyromellitate salts to form two-dimensional networks prevails.

## 5.4 Experimental

Details of the hydroxycarbonates reported here can be found in the experimental section of chapter 3, Preparation of Zinc/Copper Hydroxycarbonates (there is an experiment index at the end of the chapter). The hydroxycarbonates have been given a reference (e.g. IB(0.0/1.0) and A112), and their experimental details can be found using the index at the end of chapter 3 (p. 76).

Pyromellitic acid dihydrate was prepared by refluxing a solution of the anhydride (solid anhydride purchased from Aldrich, 97% purity, the remainder was free acid) for an hour, ensuring that all the solid had dissolved. This was sufficient to hydrolyse the anhydride and pyromellitic acid crystallised from the solution when it was cooled.

It should be pointed out that the percentage yields calculated for the experiments below have been deduced from the elemental analyses for both the hydroxycarbonate starting material and the trimellitate end product. Hence, there may be greater errors associated with the yields than would normally be expected, because both compounds were non-stoichiometric and the actual elemental compositions were not known.

### *5.4a Investigation of zinc/copper pyromellitates*

#### *a) Preparation of copper pyromellitate*

Hydroxycarbonate powder, IB(0.0/1.0) (0.649g, 2.6mmol), was added to a hot aqueous solution of pyromellitic acid (0.792g, 2.7mmol, in 45mls of water). Upon addition a gas was evolved (assumed to be $CO_2$) and the colour of the solid changed from light green to turquoise. The suspension was stirred under reflux conditions for 1 hour, after which 1.128g (89.4%) of blue micro-crystalline solid was collected. Under a microscope it was observed that the solid consisted of small rhombohedral plates. The product was characterised as follows.

*Elemental analysis (%):* Cu,25.5 C,25.1 H,2.8
Calculated for $Cu_2PM \cdot 6H_2O$: Cu,26.2 C,24.7 H,2.9

*IR ($cm^{-1}$):* 3121(b), 1856(w), 1588(s), 1495(s), 1420(s), 1368(s), 1318(s), 1293, 1154(w), 1138, 932, 871, 820, 761, 689, 612, 560(w), 518, 451(w), 415(w).

*Powder XRD (4θ):* 20.75; 21.75; 30.45; 31.05; 33.45; 36.25; 38.05; 40.25; 41.50; 42.10; 43.25; 44.80; 48.85.

#### *b) Attempted preparation of ($Zn_{0.1}Cu_{0.9}$) pyromellitate*

The same procedure as before was used reacting the hydroxycarbonate BP(0.15/0.85) (0.609g, 2.7mmol) with pyromellitic acid (0.741g, 2.5mmol) dissolved in 35mls of water. The reaction mixture was refluxed for 1.5 hours. On addition, a turquoise solid was formed but after refluxing it had become a rich blue colour. Suction filtration yielded 1.034g (91.0%) of blue micro-crystalline solid (the product looked homogeneous under a microscope) and was characterised as follows.

*Elemental analysis (%):* Zn,0.4 Cu,25.9 C,24.9 H,2.8
Calculated for $(Zn_{0.02}Cu_{0.98})_2PM \cdot 6H_2O$: Zn,0.5 Cu,25.7 C,24.7 H,2.9

*IR ($cm^{-1}$):* 3200(b), 1857(w), 1587(s), 1494(s), 1421(s), 1370(s), 1319(s), 1294, 1154(w), 1138, 932(w), 871, 821, 761, 689, 613, 561(w), 520, 453(w), 417(w).

*Powder XRD (4θ):* 20.70; 30.30; 31.00; 33.45; 36.25; 38.00; 41.40; 42.10; 43.30; 44.65; 48.70.
Same phase as copper pyromellitate.

***c) Attempted preparation of ($Zn_{0.2}Cu_{0.8}$) pyromellitate***

**i)**

The same procedure as before was used reacting the hydroxycarbonate RT(0.21/0.79) (0.317g, 1.3mmol) with a hot pyromellitic acid solution (0.371g, 1.3mmol, in 30mls of water) for 5 minutes. Suction filtration yielded 0.365g (64.6%) of light greenish blue powder with a few darker (turquoise in colour) granules. The solid was characterised as follows.

*Elemental analysis (%):* Zn,3.9 Cu,25.4 C,19.5 H,3.1 N,0.3

It was deduced from the presence of nitrogen that the hydroxycarbonate had not fully reacted. It was assumed that the nitrogen content was proportional to the amount of hydroxycarbonate present (the hydroxycarbonate composition was: Zn,11,6; Cu,41.6; C,2.7; H,1.4; N,2.7%). Subtraction of the assumed impurity from the elemental analysis gave the following results.

*Elemental analysis (%):* Zn,3.0 Cu,23.2 C,21.2 H,3.2
Calculated for
$(Zn_{0.11}Cu_{0.89})_{2.34}(OH)_{0.68}PM \cdot 9H_2O$: Zn,2.9 Cu,23.1 C,21.0 H,3.6

*IR ($cm^{-1}$):* 3117(b), 1857(w), 1603(s), 1495(s), 1420(s), 1390(s), 1370, 1319(s), 1294, 1153, 1139, 932, 871, 826, 761, 688, 612, 585(w), 516, 454(w), 417(w).

*Powder XRD (4θ):* 16.00; 16.85; 23.10; 31.85; 33.60; 36.95.
Faint pattern corresponding to basic mixed metal salt, no hydroxycarbonate observed.

**ii)**

The same procedure as before was used reacting the hydroxycarbonate RT(0.21/0.79) (0.633g, 2.6mmol) with pyromellitic acid (0.741g, 2.6mmol) dissolved in 30mls of water. The mixture was refluxed for 2 hours. Suction filtration yielded 1.059g (99.2%) of a heterogeneous green and blue powder. Under a microscope it was observed that the blue phase was micro-crystalline. The solid was characterised as follows.

*Elemental analysis (%):* Zn,2.8 Cu,23.8 C,25.6 H,2.7
Calculated for $(Zn_{0.10}Cu_{0.90})_2PM \cdot 5H_2O$: Zn,2.8 Cu,24.5 C,25.7 H,2.6

*IR ($cm^{-1}$):* 3200(b), 1857(w), 1603(s), 1495(s), 1420(s), 1390(s), 1370(w), 1319(s), 1294, 1153(w), 1139, 932, 871, 826, 762, 688, 612, 585(w), 516, 454(w), 417(w).

*Powder XRD (4θ):* 20.65; **21.75**; 30.25; **31.00**; 33.35; 34.10; **35.25**; 36.25: **38.10**; **40.25**; 41.45; 42.00; 43.20; 44.60; 48.80; **49.85**.
Copper salt plus neutral mixed metal phase (**bold**).

***d) Attempted preparation of $(Zn_{0.3}Cu_{0.7})$ pyromellitate***

**i)**

The same procedure as before was used reacting the hydroxycarbonate RT(0.30/0.70) (0.642g, 2.6mmol) with a hot pyromellitic acid solution (0.741g, 2.6mmol, in 30mls of water) for 8 minutes. Suction filtration yielded 0.875g (87.7%) of light blue powder which looked homogeneous under a microscope. The product was characterised as follows.

*Elemental analysis (%):* Zn,6.7 Cu,23.0 C,21.0 H,3.0
Calculated for
$(Zn_{0.22}Cu_{0.78})_{2.66}(OH)_{1.32}PM \cdot 7H_2O$: Zn,6.7 Cu,23.2 C,21.1 H,3.1

*IR ($cm^{-1}$):* 3392(b), 3040(b), 2101(w), 1955(s), 1582(s), 1494, 1425, 1392(s), 1336, 1251, 1139, 1064, 997, 929, 872, 820, 765, 686, 593, 525(w), 494(w), 472(w).

*Powder XRD (4θ):* 15.95; 16.75; 23.10; 28.10; 29.25; 31.75; 33.60; 36.00; 36.95; 42.70; 45.75; 50.75; 53.15; 55.75; 58.90.
Basic mixed metal phase.

Some of the product (0.402g, 0.7mmol) was added to the mother liquor and refluxed for a further 2.5 hours. Prior to the experiment clear and blue crystals had formed in the mother liquor, but these were readily dissolved on heating. Suction filtration yielded 0.381g (83.4%) of light turquoise powder which was characterised as follows.

*Elemental analysis (%):* Zn,6.4 Cu,23.6 C,22.8 H,2.9
Calculated for
$(Zn_{0.21}Cu_{0.79})_{2.47}(OH)_{0.94}PM \cdot 6H_2O$: Zn,6.4 Cu,23.3 C,22.6 H,2.8

*IR ($cm^{-1}$):* 3368(b), 3040(b), 2102(w), 1955(s), 1624, 1582(s), 1504, 1425, 1392(s), 1336, 1251, 1146, 1139, 1064(w), 998(w), 929(w), 911(w), 872, 821, 764, 687, 614, 593, 524(w), 496(w), 473(w).

*Powder XRD (4θ):* 15.95; 16.90; **21.80**; 23.10; 23.95; 28.20; 29.25; 30.25; **31.00**; 31.80; 32.35; 33.75; **35.25**; 36.10; 36.95; **40.25**; 42.60; 45.80; 46.45; 47.10; **49.75**.
Basic and neutral (**bold**) mixed metal phases.

Blue and clear crystals once again formed in the mother liquor a few days after filtration, these were collected (~0.153g of clear and ~0.012g of blue crystals) and characterised as follows.

Clear crystals:
*Elemental analysis (%):* Zn,15.1 C,28.3 H,3.8
Calculated for $ZnH_2PM \cdot 6H_2O$: Zn,15.4 C,28.2 H,3.8

*Powder XRD (4θ):* 20.40; 30.75; 31.35; 33.95; 34.35; 35.90; 40.45; 44.55; 45.40; 46.20; 47.05; 49.40; 50.10.

Blue crystals:

Unfortunately there was insufficient sample for a C, H, N elemental analysis; also the sample was contaminated with clear crystals.
*Elemental analysis (%):* Cu,25.1 Zn,0.8
Calculated for $Cu_2PM \cdot 6H_2O$: Cu,26.2

*Powder XRD (4θ):* 20.70; 30.40; 31.00; 43.35; 53.35.
The pattern was very weak but corresponded to $Cu_2PM \cdot 6H_2O$.

**ii)**

The above reaction was repeated in an attempt to prepare only the neutral mixed metal phase. Pyromellitic acid (0.264g, 0.91mmol), dissolved in 20mls of water, was reacted with the hydroxycarbonate RT(0.30/0.70) (0.220g, 0.9mmol). The suspension that formed was stirred under reflux conditions for 6 hours. Suction filtration yielded 0.309g (90.8%) of turquoise powder similar in appearance to the previous product. When observed under a microscope the bulk of the solid appeared to be a homogeneous powder, but there were some small rod-like crystallites which appeared to be pale turquoise in colour. The product was characterised as follows.

*Elemental analysis (%):* Zn,5.2 Cu,25.0 C,25.9 H,1.8
Calculated for
$(Zn_{0.17}Cu_{0.83})_{2.2}(OH)_{0.4}PM \cdot 4H_2O$: Zn,5.2 Cu,24.7 C,25.6 H,2.2

*Powder XRD (4θ):* **15.85**; **16.90**; 21.65; **23.15**; 35.15; **36.95**; 40.20; **42.60**; **45.90**; 49.80.
Neutral and basic (**bold**) mixed metal phases.

Because a single phase had not been obtained the product (0.150g) was refluxed in the mother liquor for a further 28 hours. Suction filtration yielded 0.132g (100%) of light turquoise solid. When observed under a microscope the powder looked the same as before but there was an abundance of crystallites. The product was characterised as follows.

*Elemental analysis (%):* Zn,4.7 Cu,27.0 C,30.6 H,0.8
Calculated for $(Zn_{0.15}Cu_{0.85})_{2.0}PM \cdot H_2O$: Zn,4.9 Cu,27.3 C,30.3 H,1.0

*IR ($cm^{-1}$):* 3430(w, b), 1819(w), 1625(s), 1541, 1526, 1504, 1440(s), 1391(s), 1336, 1299(w), 1142, 920(w), 911, 872, 827, 805, 763(w), 679(w), 618, 584, 513, 472(w).

*Powder XRD (4θ):* 21.75; 30.90; 35.15; 40.15; 49.85.
Neutral mixed metal phase only.

Enough crystals were picked to take an IR spectrum:
*IR ($cm^{-1}$):* 3380(s), 3132(b), 1843(w), 1616, 1569(s), 1501(s), 1442(s), 1396(s), 1335, 1292, 1142, 928, 885, 836, 816, 763, 731, 676(w), 622, 515, 483, 442(w).
Same as zinc pyromellitate spectrum.

***e) Attempted preparation of $(Zn_{0.4}Cu_{0.6})$ pyromellitate***

**i)**

The same procedure as before was used reacting the hydroxycarbonate IB(0.41/0.59) (0.624g, 2.6mmol) with a hot solution of pyromellitic acid (0.795g, 2.7mmol, in 30mls of water) for 5 minutes. Suction filtration yielded 0.890g (95.9%) of light blue powder which looked homogeneous under a microscope. The product was characterised as follows.

*Elemental analysis (%):* Zn,8.1 Cu,21.0 C,21.6 H,3.1
Calculated for
$(Zn_{0.27}Cu_{0.73})_{2.51}(OH)_{1.02}PM \cdot 7H_2O$: Zn,8.0 Cu,21.0 C,21.6 H,3.1

*IR ($cm^{-1}$):* 3436(b), 3050(b), 2101(w), 1955(w), 1587(s), 1494, 1387(s), 1336, 1140, 1064(w), 996(w), 929(w), 871, 819, 765, 685(w), 591, 522(w), 471(w).

*Powder XRD (4θ):* 15.95; 16.90; 23.15; 31.75; 33.75; 37.00; 45.80.
Basic mixed metal phase.

The product (0.389g, 0.7mmol) was added to the mother liquor and refluxed for a further 3 hours, during which time the colour of the solid darkened. Suction filtration yielded 0.427g (99.5%) of blue powder. Under a microscope it was observed that the product consisted of a blue powder and some crystals (hexagonal rod-like prisms, <0.2mm in length) which appeared to have a slight blue-ish colouration. The solid was characterised as follows.

*Elemental analysis (%):* Zn,10.0 Cu,21.7 C,29.1 H,1.3
Calculated for $(Zn_{0.31}Cu_{0.69})_2PM \cdot 2H_2O$: Zn,9.6 Cu,21.2 C,29.0 H,1.5

*IR ($cm^{-1}$):* 3388(b), 1819(w), 1631(s), 1582, 1526, 1504, 1440(s), 1391(s), 1335, 1298, 1143, 911(w), 872, 828, 802, 763, 679(w), 618, 583, 513.

*Powder XRD (4θ):* 20.60; 21.75; 31.05; 35.25; 38.10; 40.10; 44.05; 44.85; 49.80.
Neutral mixed metal phase.

Clear crystals (thin quadrangular prisms) later developed in the mother liquor, the crystals (0.117g) were collected and characterised as follows.

*Elemental analysis (%):* Zn,15.5 C,28.2 H,3.9
Calculated for $ZnH_2PM \cdot 6H_2O$: Zn,15.4 C,28.2 H,3.8

*Powder XRD (4θ):* 20.05; 30.45; 31.15; 33.60; 34.05; 35.65; 40.20; 44.30; 45.15; 46.00; 46.80; 49.15; 49.85.
Same as $ZnH_2PM$ salt.

**ii)**

In an attempt to produce a basic mixed metal salt and inhibit the conversion to a neutral phase, the above reaction was repeated using a metal to pyromellitate ratio of 2.5:1. Pyromellitic acid (0.261g, 0.9mmol) was dissolved in 25mls of water and reacted with the hydroxycarbonate IB(0.41/0.59) (0.263g, 1.1mmol), refluxing for 0.5 hours. Suction filtration yielded 0.440g (97.4%) of light blue powder which, under a microscope, was observed to consist of a light blue solid (mostly small lumps) and a fine powder (more grey in colour). The product was characterised as follows.

*Elemental analysis (%):* Zn,10.4 Cu,18.9 C,21.2 H,3.0
Calculated for
$(Zn_{0.35}Cu_{0.65})_{2.6}(OH)_{1.2}PM \cdot 7H_2O$: Zn,10.6 Cu,19.1 C,21.3 H,3.1
$(Zn_{0.35}Cu_{0.65})_{2.5}(OH)_{1.0}PM \cdot 7H_2O$: Zn,10.3 Cu,18.6 C,21.7 H,3.1

*IR ($cm^{-1}$):* 3392(b), 3068(b), 2101(w), 1955(w), 1582(s), 1500, 1420(sh), 1392(s), 1336, 1251, 1144, 1064(w), 996(w), 929(w), 871, 819, 765, 686(w), 593, 520(w), 467(w).

*Powder XRD (4θ):* 15.95; 16.90; 23.10; 31.80; 33.65; 37.00; 45.85.
Basic mixed metal phase.

The product (0.228g) was added to the mother liquor and the suspension refluxed for a further 4.5 hours to see if the product would react with it. Suction filtration yielded 0.216g of light blue powder, the product did not appear to have changed, but under a microscope some very small rod-like crystals were observed. The product was characterised as follows.

| | |
|---|---|
| *Elemental analysis (%):* | Zn,10.2 Cu,18.1 C,21.8 H,3.0 |
| Calculated for | |
| $(Zn_{0.35}Cu_{0.65})_{2.4}(OH)_{0.8}PM \cdot 7H_2O$: | Zn,10.1 Cu,18.2 C,22.1 H,3.1 |
| $(Zn_{0.35}Cu_{0.65})_{2.5}(OH)_{1.0}PM \cdot 7H_2O$: | Zn,10.3 Cu,18.6 C,21.7 H,3.1 |

*IR ($cm^{-1}$):* 3370(b), 2099(w), 1951(w), 1622, 1580(s), 1501, 1425, 1391(s), 1375, 1250, 1146, 1138, 1063(w), 997(w), 928(w), 872, 819, 765, 686(w), 610, 520(w), 473(w).

*Powder XRD (4θ):* 15.90; 16.85; 23.10; 23.85; 28.10; **31.05**; 31.65; 32.20; 33.60; 35.95; 36.90; **38.00**; 42.40; **43.95**; 44.80.
Basic mixed metal phase and zinc pyromellitate (**bold**).

**iii)**

The above reaction was repeated at room temperature to see if this would hinder further reaction of the basic phase with the acid. Pyromellitic acid (1.325g, 4.56mmol) was dissolved in 100.0mls of water, 20mls of this solution (0.913mmol of acid) was added to IB(0.41/0.59) hydroxycarbonate (0.267g, 1.12mmol). $CO_2$ was given off, and the suspension was stirred for 4 hours. Suction filtration yielded 0.441g (97.7%) of light blue powder, which under a microscope looked homogeneous. The product was characterised as follows.

| | |
|---|---|
| *Elemental analysis (%):* | Zn,10.2 Cu,18.9 C,21.1 H,3.1 |
| Calculated for | |
| $(Zn_{0.34}Cu_{0.66})_{2.5}(OH)PM \cdot 7H_2O$: | Zn,10.0 Cu,18.9 C,21.7 H,3.1 |
| $(Zn_{0.34}Cu_{0.66})_{2.6}(OH)_{1.2}PM \cdot 7H_2O$: | Zn,10.2 Cu,18.7 C,21.4 H,3.1 |

*IR ($cm^{-1}$):* 3392(b), 2099(w), 1952(w), 1583(s), 1495, 1424, 1391(s), 1336, 1251, 1139, 1063(w), 995(w), 929(w), 871, 819, 765, 686(w), 592, 520(w), 472(w).

*Powder XRD (4θ):* 15.90; 16.80; 23.15; 37.00; 45.75.
Basic mixed metal phase.

***f) Attempted preparation of ($Zn_{0.5}Cu_{0.5}$) pyromellitate***

The same procedure as before was used reacting the hydroxycarbonate IB(0.47/0.53) (0.599g, 2.7mmol) with a hot solution of pyromellitic acid (0.741g, 2.6mmol, in 30mls of water). Initially a dark turquoise solid formed but after refluxing for 1hr the colour of the solid had changed to light blue. Suction filtration yielded 0.875g (91.7%) of light blue powder, which was observed under a microscope to consist of a fine powder and rod-like micro-crystals. It was difficult to distinguish the colour, if any, of the crystals as they were coated in powder. The solid was characterised as follows.

*Elemental analysis (%):* Zn,11.7 Cu,17.5 C,22.9 H,2.8
Calculated for
$(Zn_{0.39}Cu_{0.61})_{2.4}(OH)_{0.8}PM \cdot 6H_2O$: Zn,11.6 Cu,17.7 C,22.8 H,2.8

*IR ($cm^{-1}$):* 3377(b), 2102(w), 1955(w), 1623(sh), 1582(s), 1501, 1392(s), 1335, 1145, 1065(w), 998(w), 928(w), 872, 819, 765, 686(w), 621, 593, 516, 474(w).

*Powder XRD (4θ):* 15.85; 16.80; 23.05; **31.00**; 36.90; **38.10**; **44.00**; 45.70.
Basic mixed metal and neutral zinc (**bold**) phase.

Clear crystals later appeared in the mother liquor, these were collected (0.161g) and analysed as follows.

*Elemental analysis (%):* Zn,14.5 C,28.3 H,3.8
Calculated for $ZnH_2PM \cdot 6H_2O$: Zn,15.4 C,28.2 H,3.8

*IR ($cm^{-1}$):* 3387(b), 3230(b), 1679, 1528(s), 1500(sh), 1366(s), 1294, 1135, 1085(b), 970(w), 879(w), 766, 606, 468(w), 423(w).

*Powder XRD (4θ):* 20.15; 30.70; 31.20; 33.75; 34.15; 35.75; 40.30; 44.35; 45.25; 46.10; 46.85; 49.20; 49.95.
Acidic zinc pyromellitate.

***g) Attempted preparation of $(Zn_{0.6}Cu_{0.4})$ pyromellitate***

The same procedure as before was used reacting the hydroxycarbonate IB(0.59/0.41) (0.604g, 2.7mmol) with a hot solution of pyromellitic acid (0.741g, 2.6mmol, in 30mls of water) and refluxing for 3 hours. Suction filtration yielded 0.779g (84.3%) of blue powder. Under a microscope the product was observed to consist of a fine powder and a micro-crystalline phase. The crystallites were hexagonal rod-like prisms, similar to previous examples, and were abundant in the sample. The product was characterised as follows.

*Elemental analysis (%):* Zn,17.9 Cu,15.6 C,23.7 H,2.6
Calculated for
$(Zn_{0.53}Cu_{0.47})_{2.62}(OH)_{1.24}PM \cdot 4H_2O$: Zn,17.7 Cu,15.2 C,23.5 H,2.2

*IR ($cm^{-1}$):* 3377(b), 2101(w), 1955(w), 1622(sh), 1577(s), 1500, 1392(s), 1335, 1292(w), 1145, 1063(w), 999(w), 928(w), 872, 819, 764, 687(w), 622, 516(w), 481(w).

*Powder XRD (4θ):* **15.85**; **16.80**; **23.15**; 31.10; **36.95**; 38.15; 39.55; 40.65; 43.40; 44.10; 44.85; **45.75**.
Basic mixed metal phase (**bold**) and neutral zinc salt.

In an attempt to increase the yield of crystallites (in order to characterise the crystalline phase), 0.343g of the product was added to half the mother liquor. The suspension was stirred under reflux conditions for 4 hours and 0.338g of light turquoise powder was collected. It was observed under a microscope that the crystalline phase was present in a larger yield. The crystals, hexagonal rod-like prisms, were <0.2mm long and appeared to vary in colour from colourless to light turquoise. The apparent colour was probably due to powder adhering to the crystals. A sample of the crystalline phase was crudely separated from the powder and the products were analysed as follows.

Turquoise powder:
*Elemental analysis (%):* Zn,11.4 Cu,17.8 C,23.9 H,2.4
Calculated for
$(Zn_{0.38}Cu_{0.62})_{2.3}(OH)_{0.6}PM \cdot 5H_2O$: Zn,11.4 Cu,18.2 C,24.1 H,2.5

*Powder XRD (4θ):* 15.80; 16.85; 23.10; **31.10**; 36.85; **38.25**; **43.95**; 45.80.
Basic mixed metal and neutral zinc (**bold**) phases.

Crystalline phase:
*Elemental analysis (%):* Zn,26.9 Cu,2.7 C,26.3 H,2.1

It was assumed that the copper present was due to powder mixed in with the crystals. Subtraction of the assumed impurity from the elemental analysis gave the following results.

*Elemental analysis (%):* Zn,29.6 C,26.7 H,2.1
Calculated for $Zn_2PM \cdot 4H_2O$: Zn,28.9 C,26.5 H,2.2

*Powder XRD (4θ):* 31.05; 38.25; 39.60; 40.85; 44.20; 44.80; 45.75; 48.60; 49.00.
Neutral zinc salt.

***h) Preparation of $(Zn_{0.7}Cu_{0.3})$ pyromellitate***

**i)**

The same procedure as before was used reacting the hydroxycarbonate IB(0.68/0.32) (0.607g, 2.7mmol) with a solution of pyromellitic acid (0.741g, 2.6mmol, in 30mls of water) and refluxing for 2 hours. Suction filtration yielded 1.099g (97.4%) of blue-ish green powder. Under a microscope the product was observed to consist of a turquoise powder and rod-like crystallites. The product was characterised as follows.

*Elemental analysis (%):* Zn,24.0 Cu,9.6 C,24.3 H,2.5
Calculated for
$(Zn_{0.71}Cu_{0.29})_{2.56}(OH)_{1.12}PM \cdot 3H_2O$: Zn,24.3 Cu,9.6 C,24.5 H,1.9

*IR ($cm^{-1}$):* 3377(b), 2101(w), 1955(w), 1843(w), 1623(sh), 1577(s), 1500, 1424(w), 1392(s), 1335, 1291, 1145, 1065(w), 998(w), 928(w), 872, 819, 764, 687(w), 622, 515, 481(w).

*Powder XRD (4θ):* **15.85**; **16.80**; **23.15**; 31.10; 35.90; **36.95**; 38.15; 39.55; 40.65; 43.40; 44.10; 44.85; 45.75; 47.65; 48.65; 49.15.
Mixture of basic mixed metal (**bold**) and neutral zinc phases.

**ii)**

The experiment was repeated using a slurry of the hydroxycarbonate P75 (0.30g, 0.54mmol) which had been left stirring overnight to produce a fine suspension. A hot solution of pyromellitic acid dihydrate (0.332g, 1.15mmol, in 15mls of water) was added, and the suspension was stirred for 0.5 hours until the mixture looked homogeneous. Suction filtration yielded 0.476g (80%) of blue powder which was observed to be micro-crystalline under the microscope. The product was characterised as follows.

*Elemental analysis (%):* Zn,20.3 Cu,11.2 C,21.6 H,3.0
Calculated for
$(Zn_{0.67}Cu_{0.33})_{2.5}OH(PM) \cdot 7H_2O$: Zn,19.7 Cu,9.4 C,21.6 H,3.1

*IR ($cm^{-1}$):* 3444(b), 1577(s), 1496, 1417(w), 1380(s), 1335, 1138(w), 933(w), 870(w), 815(w), 761(w), 568(w).

*Powder XRD (4θ):* Basic mixed metal phase.

***i) Preparation of $(Zn_{0.8}Cu_{0.2})$ pyromellitate***

The same procedure as before was used reacting the hydroxycarbonate RT(0.73/0.27) (0.591g, 2.7mmol) with a solution of pyromellitic acid (0.741g, 2.6mmol, in 30mls of water) and refluxing for 2 hours. Suction filtration yielded 0.936g (90.3%) of greenish blue powder, observation under a microscope revealed that clear rod-like crystals were present. The product was characterised as follows.

*Elemental analysis (%):* Zn,28.8 Cu,5.6 C,25.5 H,2.4
Calculated for
$(Zn_{0.83}Cu_{0.17})_{2.49}(OH)_{0.98}PM \cdot 3H_2O$: Zn,28.0 Cu,5.6 C,24.9 H,1.9

*IR ($cm^{-1}$):* 3377(b), 1843(w), 1577(s), 1500, 1392(s), 1335, 1291(w), 1145, 1066(w), 998(w), 928(w), 872, 818, 764, 732(w, b), 676(w), 621, 510, 482.

*Powder XRD (4θ):* **15.85**; **16.75**; **23.05**; 31.05; 35.90; **36.95**; 38.10; 39.50; 40.65; 43.40; 44.00; 44.80; 45.75; 48.65; 49.05.
Two phases present, basic mixed metal (**bold**) and neutral zinc pyromellitate.

***j) Preparation of ($Zn_{0.9}Cu_{0.1}$) pyromellitate***

The same procedure as before was used reacting the hydroxycarbonate RT(0.91/0.09) (0.585g, 2.6mmol) with a solution of pyromellitic acid (0.741g, 2.6mmol, in 30mls of water) and refluxing for 2 hours. Suction filtration yielded 1.079g (90.1%) of light blue powder. Under a microscope the product was observed to be a light blue micro-crystalline powder. The product was characterised as follows.

*Elemental analysis (%):* Zn,25.4 Cu,2.9 C,26.1 H,2.2
Calculated for $(Zn_{0.89}Cu_{0.11})_{2.0}PM \cdot 4H_2O$: Zn,25.7 Cu,3.1 C,26.5 H,2.2

*IR ($cm^{-1}$):* 3377(s), 3148(b), 1843(w), 1613(w), 1571(s), 1500, 1440(s), 1397(s), 1335, 1292, 1146, 928, 885, 837, 816, 764, 722(b), 676(w), 623, 515, 484.

*Powder XRD (4θ):* 31.00; 38.10; 39.50; 40.65; 43.35; 44.00; 44.75; 45.70; 48.60; 49.10.
Neutral zinc phase.

***k) Preparation of Zn pyromellitate***

The same procedure as before was used reacting the hydroxycarbonate BP(1.0/0.0) (0.582g, 1.1mmol) with pyromellitic acid solution (0.741g, 2.6mmol, in 30mls of water) and refluxing for 2 hours. Suction filtration yielded 1.063g (85.3%) of white micro-crystalline powder which was characterised as follows.

*Elemental analysis (%):* Zn,29.6 C,26.2 H,2.2
Calculated for $Zn_2PM \cdot 4H_2O$: Zn,28.9 C,26.5 H,2.2

*IR ($cm^{-1}$):* 3381(s), 3138(b), 1843(w), 1613(w), 1570(s), 1500, 1443, 1397(s), 1336, 1292, 1145, 928, 885, 836, 817, 764, 731(b), 676(w), 623, 515, 484.

*Powder XRD (4θ):* 31.05; 38.10; 39.55; 40.60; 43.30; 44.00; 44.70; 45.55; 48.50; 49.00.
Zinc pyromellitate

***5.4b Scaled up pyromellitate preparations***

***a) Zinc pyromellitate***

Hydrozincite (P52; 29.51g, 52.0mmol) was added to a hot solution of pyromellitic acid (42.30g, 146mmol, in 200mls of water). A gas was evolved ($CO_2$) and the suspension was refluxed for 24 hours. Suction filtration yielded 47.67g (81%) of white micro-crystalline solid. Clear rhombohedral crystals (~6g) later developed in the filtrate. The products were characterised as follows.

White powder:
Elemental analysis (%): Zn,28.5 C,26.7 H,2.2
Calculated for $Zn_2PM \cdot 4H_2O$: Zn,28.9 C,26.5 H,2.2

*IR ($cm^{-1}$):* 3375(b), 3152(b), 1843(w), 1612, 1566(s), 1501(s), 1443(s), 1396(s), 1336, 1292, 1146, 928, 885, 836, 816, 764, 734(w, b), 676(w), 622, 515, 483.

*Powder XRD (4θ):* 21.75; 24.60; 31.00; 38.00; 39.45; 40.60; 43.35; 43.90; 44.65; 45.65; 48.95.
Same as previous zinc salt.

Clear crystals:
*Elemental analysis (%):* Zn,14.8 C,28.4 H,3.9
Calculated for $ZnH_2PM \cdot 6H_2O$: Zn,15.4 C,28.2 H,3.8

*Powder XRD (4θ):* Same pattern as the zinc dihydrogen salt.

***b) ($Zn_{0.5}Cu_{0.5}$) pyromellitate***

A slurry of georgite (P70; 20.17g, 83.7mmol) was added to a hot solution of pyromellitic acid (19.46g, 67.1mmol, in 100mls of water). A gas was evolved ($CO_2$) and a turquoise solid immediately formed. The solid slowly became lighter in colour and the suspension was refluxed for 20 hours. Suction filtration yielded 36.36g (97.9%) of light blue powder which was characterised as follows.

*Elemental analysis (%):* Zn,13.8 Cu,15.1 C,21.3 H,2.7
Calculated for
$(Zn_{0.5}Cu_{0.5})_{2.5}OH(PM) \cdot 7H_2O$: Zn,14.7 Cu,14.3 C,21.6 H,3.1

*IR ($cm^{-1}$):* 3400(b), 2099(w), 1952(w), 1581(s), 1497, 1390(s), 1335, 1140, 1063(w), 997(w), 931(w), 871, 818, 765, 685(w), 590, 519(w), 470.

*Powder XRD (4θ):* Basic mixed metal phase.

***c) ($Zn_{0.3}Cu_{0.7}$) pyromellitate***

A slurry of georgite (P62; 10.00g, 41.6mmol) was added to a hot solution of pyromellitic acid (10.19g, 35.1mmol, in 190mls of water). A gas was evolved ($CO_2$) and a turquoise solid formed immediately. The suspension was stirred, without heating, for 3 hours. Suction filtration yielded 17.72g (96.0%) of light turquoise powder which was characterised as follows.

*Elemental analysis (%):* Zn,9.7 Cu,19.1 C,21.7 H,3.1
Calculated for
$(Zn_{0.33}Cu_{0.67})_{2.5}OH(PM) . 7H_2O$: Zn,9.5 Cu,19.2 C,21.7 H,3.1

*IR ($cm^{-1}$):* 3374(b), 3057, 2100(w), 1949(w), 1622, 1579(s), 1500, 1425, 1391(s), 1335, 1250(w), 1146, 1064(w), 996(w), 931(w), 872, 820, 764, 686, 593, 521(w), 496(w), 472(w).
Spectrum of basic mixed metal phase.

*Powder XRD (4θ):* Basic mixed metal phase plus two very faint lines which correspond to neutral zinc pyromellitate.

## *Structure determination of $ZnH_2TM . 6H_2O$*

*(R.C.B. Copley, University of Durham)*

**Crystal data**

| Colour: Colourless | Habit: Prism | Size (mm): 0.25 x 0.50 x 0.50 |
|---|---|---|

| | |
|---|---|
| a (Å) | 21.931(2) |
| b (Å) | 9.773(1) |
| c (Å) | 7.2059(9) |
| α (°) | 90 |
| β (°) | 105.017(9) |
| γ (°) | 90 |
| Volume ($Å^3$) | 1491.8(3) |

| | |
|---|---|
| Formula | $C_{10}H_{16}O_{14}Zn$ |
| Formula weight | 425.60 |
| Crystal system | Monoclinic |
| Space group | C2/c (15) |
| Z | 2 |
| $D_c$ ($gcm^{-3}$) | 0.947 |
| Linear absorption coefficient ($cm^{-1}$) | 8.6 |

**Data collection**

| | |
|---|---|
| Diffractometer | Rigaku AFC6S |
| Radiation | Mo-Kα (λ = 0.71073Å) |
| Temperature (K) | 120 |
| Scan technique | ω scans |
| Scan width (°) | 1.10 + 0.3tanθ |
| Scan rate ($°min^{-1}$) | 1-8 |
| 2θ range (°) | 5-60 |
| Absorption correction | Empirical |
| Transmission (%) | 0.719-1.000 (av. 0.886) |
| Decay (%) | 0 |
| Merging R-factor (%) | 1.8 |

| **Limits:** | min. | max. |
|---|---|---|
| h | 0 | 30 |
| k | 0 | 13 |
| l | -10 | 9 |

| **Data:** | |
|---|---|
| total | 2346 |
| unique | 2174 |
| I≥3σ(I) | 2012 |

**Solution and Refinement**

| | | | |
|---|---|---|---|
| Package used | CRYSTALS | Final R (%) | 2.16 |
| Solution | SHELXS | Final $R_w$ (%) | 2.14 |
| Refinement method | Full matrix | Goodness-of-fit | 1.21 |
| Weights | Chebychev (0.956, 0.577, 1.00, 0.186, 0.285) | Observations/parameters | 2012/148 (13.6) |

| | | | |
|---|---|---|---|
| Extinction correction | Yes | Largest difference peak ($eÅ^{-3}$) | 0.52 |
| Anomalous dispersion correction | No | Largest difference trough ($eÅ^{-3}$) | -0.35 |

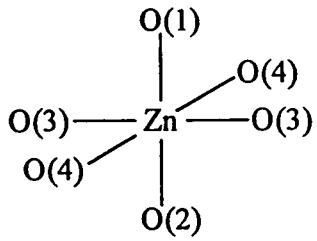


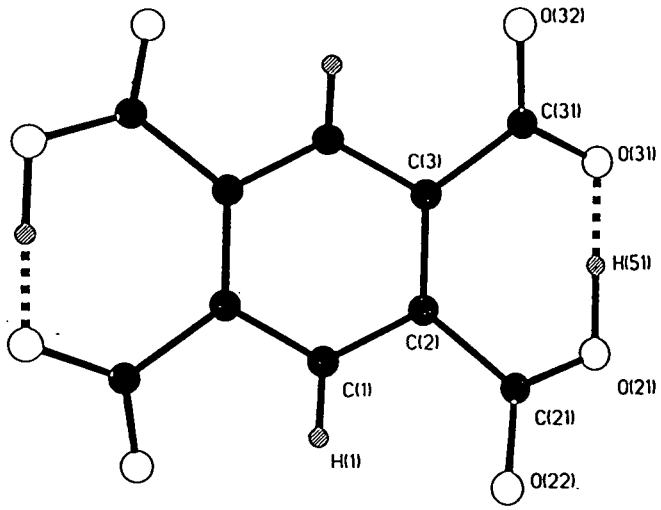


Atomic labelling

Atomic coordinates and isotropic displacement parameters for $ZnH_2TM \cdot 6H_2O$.

| | x | y | z | U(eq)/Å$^2$ |
|---|---|---|---|---|
| Zn(1) | 0 | 0.29940(2) | 1/4 | 0.0109 |
| O(1) | 0 | 0.5150(1) | 1/4 | 0.0169 |
| O(2) | 0 | 0.0896(1) | 1/4 | 0.0170 |
| O(3) | 0.08046(3) | 0.28867(8) | 0.4773(1) | 0.0155 |
| O(4) | 0.05741(3) | 0.31362(7) | 0.0551(1) | 0.0138 |
| C(1) | 0.31204(4) | -0.23168(9) | 0.5929(1) | 0.0115 |
| C(2) | 0.27093(4) | -0.12123(9) | 0.5832(1) | 0.0110 |
| C(3) | 0.20661(4) | -0.14022(9) | 0.4874(1) | 0.0112 |
| C(21) | 0.30253(4) | 0.00871(9) | 0.6748(1) | 0.0120 |
| C(31) | 0.15391(4) | -0.03503(9) | 0.4585(1) | 0.0131 |
| O(21) | 0.27789(3) | 0.12616(7) | 0.6168(1) | 0.0153 |
| O(22) | 0.35317(3) | 0.00005(7) | 0.7997(1) | 0.0152 |
| O(31) | 0.16790(3) | 0.09177(7) | 0.4521(1) | 0.0173 |
| O(32) | 0.09877(3) | -0.07604(7) | 0.4342(1) | 0.0160 |

| | x | y | z | U(iso)/Å$^2$ |
|---|---|---|---|---|
| H(1) | 0.3549(8) | -0.221(2) | 0.652(2) | 0.020(3) |
| H(11) | 0.0172(8) | 0.566(2) | 0.337(2) | 0.026(4) |
| H(21) | 0.0297(8) | 0.041(2) | 0.305(2) | 0.027(4) |
| H(31) | 0.1085(9) | 0.229(2) | 0.467(3) | 0.031(4) |
| H(32) | 0.1001(9) | 0.355(2) | 0.534(3) | 0.035(5) |
| H(41) | 0.0702(9) | 0.240(2) | 0.021(2) | 0.029(4) |
| H(42) | 0.0894(8) | 0.362(2) | 0.108(2) | 0.024(4) |
| H(51) | 0.228(1) | 0.114(2) | 0.533(3) | 0.067(7) |

Anisotropic displacement parameters ($Å^2$) for $ZnH_2TM \cdot 6H_2O$.

| | $U_{11}$ | $U_{22}$ | $U_{33}$ | $U_{12}$ | $U_{13}$ | $U_{23}$ |
|---|---|---|---|---|---|---|
| Zn(1) | 0.00889(8) | 0.01089(8) | 0.01268(8) | 0 | 0.00153(5) | 0 |
| O(1) | 0.0212(5) | 0.0119(4) | 0.0178(5) | 0 | 0.0001(4) | 0 |
| O(2) | 0.0131(4) | 0.0119(4) | 0.0314(6) | 0 | -0.0049(4) | 0 |
| O(3) | 0.0123(3) | 0.0156(3) | 0.0191(3) | 0.0014(3) | -0.0018(3) | -0.0026(3) |
| O(4) | 0.0117(3) | 0.0131(3) | 0.0177(3) | -0.0016(2) | 0.0034(2) | -0.0023(2) |
| O(21) | 0.0132(3) | 0.0107(3) | 0.0240(3) | -0.0001(2) | 0.0014(2) | -0.0001(2) |
| O(22) | 0.0129(3) | 0.0141(3) | 0.0184(3) | -0.0012(2) | -0.0004(2) | -0.0011(2) |
| O(31) | 0.0123(3) | 0.0110(3) | 0.0364(4) | 0.0010(2) | 0.0015(3) | 0.0014(3) |
| O(32) | 0.0104(3) | 0.0145(3) | 0.0273(4) | 0.0015(2) | 0.0034(3) | 0.0027(3) |
| C(1) | 0.0097(4) | 0.0115(4) | 0.0133(4) | 0.0004(3) | 0.0021(3) | -0.0004(3) |
| C(2) | 0.0103(3) | 0.0102(4) | 0.0126(4) | -0.0003(3) | 0.0026(3) | -0.0004(3) |
| C(3) | 0.0098(3) | 0.0108(4) | 0.0129(4) | 0.0007(3) | 0.0026(3) | 0.0004(3) |
| C(21) | 0.0113(4) | 0.0116(4) | 0.0140(4) | -0.0010(3) | 0.0041(3) | -0.0012(3) |
| C(31) | 0.0114(4) | 0.0122(4) | 0.0158(4) | 0.0015(3) | 0.0021(3) | 0.0004(3) |

Selected bond lengths and angles for $ZnH_2TM \cdot 6H_2O$.

**Bond lengths (Å)**

| | |
|---|---|
| Zn(1)-O(1) | 2.108(1) |
| Zn(1)-O(2) | 2.050(1) |
| Zn(1)-O(3) | 2.0761(7) |
| Zn(1)-O(4) | 2.1200(7) |
| C(1)-C(2) | 1.397(1) |
| C(1)-C(3A) | 1.395(1) |
| C(2)-C(3) | 1.413(1) |
| C(2)-C(21) | 1.514(1) |
| C(3)-C(31) | 1.520(1) |
| C(21)-O(21) | 1.291(1) |
| C(21)-O(22) | 1.238(1) |
| C(31)-O(31) | 1.280(1) |
| C(31)-O(32) | 1.243(1) |
| C(1)-H(1) | 0.93(2) |
| O(1)-H(11) | 0.81(2) |
| O(2)-H(21) | 0.82(2) |
| O(3)-H(31) | 0.87(2) |
| O(3)-H(32) | 0.83(2) |
| O(4)-H(41) | 0.83(2) |
| O(4)-H(42) | 0.85(2) |
| O(21)-H(51) | 1.11(2) |
| O(31)-H(51) | 1.31(3) |

**Bond angles (°)**

| | |
|---|---|
| O(1)-Zn(1)-O(2) | 180.00 |
| O(1)-Zn(1)-O(3) | 92.90(2) |
| O(1)-Zn(1)-O(4) | 86.24(2) |
| O(2)-Zn(1)-O(3) | 87.10(2) |
| O(2)-Zn(1)-O(4) | 93.76(2) |
| O(3)-Zn(1)-O(3A) | 174.21(4) |
| O(3)-Zn(1)-O(4) | 89.81(3) |
| O(3)-Zn(1)-O(4A) | 90.56(3) |
| O(4)-Zn(1)-O(4A) | 172.48(4) |
| C(2)-C(1)-C(3A) | 123.82(8) |
| C(1)-C(2)-C(3) | 118.21(8) |
| C(1)-C(2)-C(21) | 114.19(8) |
| C(3)-C(2)-C(21) | 127.56(8) |
| C(1A)-C(3)-C(2) | 117.97(8) |
| C(1A)-C(3)-C(31) | 114.78(8) |
| C(2)-C(3)-C(31) | 127.25(8) |
| C(2)-C(21)-O(21) | 119.92(8) |
| C(2)-C(21)-O(22) | 118.86(8) |
| O(21)-C(21)-O(22) | 121.16(8) |
| C(3)-C(31)-O(31) | 118.61(8) |
| C(3)-C(31)-O(32) | 118.60(8) |
| O(31)-C(31)-O(32) | 122.72(9) |
| C(21)-O(21)-H(51) | 110.4(13) |
| C(31)-O(31)-H(51) | 111.3(11) |
| O(21)-H(51)-O(31) | 173.1(24) |

Hydrogen bonding

| | O···H (Å) | O···O (Å) | O–H···O (Å) |
|---|---|---|---|
| O(1)–H(11)···0(4) | 1.98(2) | 2.7906(9) | 178.0(17) |
| O(2)–H(21)···0(32) | 1.93(2) | 2.7543(9) | 179.2(17) |
| O(3)–H(31)···0(31) | 1.89(2) | 2.756(1) | 176.8(17) |
| O(3)–H(32)···0(22) | 1.96(2) | 2.785(1) | 172.4(18) |
| O(4)–H(41)···0(32) | 1.88(2) | 2.717(1) | 177.6(17) |
| O(4)–H(42)···0(22) | 1.84(2) | 2.682(1) | 167.3(16) |
| O(21)–H(51)···0(31) | 1.31(3) | 2.420(1) | 173.1(24) |

# 6. THERMAL DECOMPOSITION OF ZINC/COPPER TRIMELLITATES AND PYROMELLITATES

## 6.1 Introduction

This chapter describes work undertaken to study the thermal decomposition of zinc/copper salts discussed in chapters 4 and 5. Thermal decomposition is a standard technique for the formation of metals and metal oxides from their respective salts, and many areas of chemistry (including catalysis[73,74], metal oxide supports[76], ceramics[75,77] and thin film deposition[75]) use this method of preparation. The type of salt used as the precursor can alter the physical and chemical properties of the decomposition product, e.g. surface area, porosity[76,77], catalytic activity[73,74]. Thus, to enable a better understanding of the effect of the precursor on the final product, the decomposition must be properly characterised.

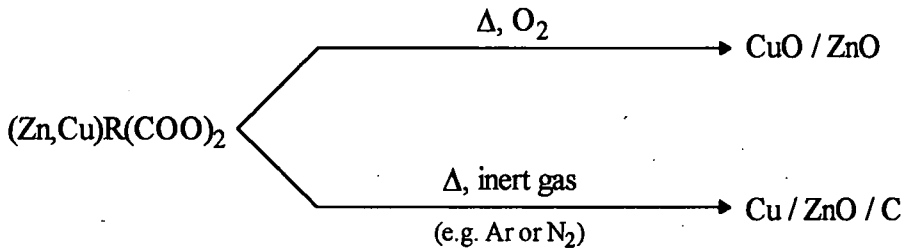


Zinc/copper carboxylates thermally decompose under oxygen forming the respective metal oxides and under an inert atmosphere, zinc oxide, copper and carbon are produced[23]. As mentioned in chapter 2, some DTA-TG studies of the decomposition of aromatic polycarboxylates have been published[90-92,124-27]. Brzyska *et al* have prepared and studied the decompositions of a variety of transition metal carboxylates, including copper[90,92] and zinc[91]. They identified two events when samples were heated under air: dehydration (an endothermic event), followed by decomposition (an exothermic event). Some samples lost water in two stages, but all the decompositions were assumed to be one step, producing the metal oxide. For some copper salts, it was deduced that copper(I) oxide was formed during decompositions at slower heating rates (5°C $min^{-1}$, cf. 10°C $min^{-1}$). The copper(I) oxide was subsequently oxidised to copper(II) oxide.

Brzyska *et al* appear to have overlooked the fact that, for the zinc and copper salts at least, most of the weight loss detected during the decomposition occurred at the beginning of the broad exotherm. For example, the weight loss of a zinc phthalate sample was ~40% during the first quarter of the decomposition exotherm and only ~15% during the rest of the exotherm. This suggests that at least two processes occurred

during the decomposition, one involved a large loss of weight, and the other (a more exothermic event) a smaller weight loss.

This chapter discusses work undertaken to study the decomposition of zinc/copper trimellitates and pyromellitates. The decomposition of the salts under both oxidising and inert atmospheres was studied using DSC, XRD, IR and TPDec (Temperature Programmed Decomposition). The aims were to deduce the mechanism of decomposition, to see how cation substitution affected it, and to deduce the factors determining the decomposition temperature. The apparatus and experiments are described in the experimental section which precedes the results and discussion. Finally the summary and conclusions are given.

## 6.2 Experimental

The thermal decomposition of zinc/copper trimellitates and pyromellitates (reported in previous chapters) were studied by DSC and TPDec (the specifications of the equipment used are given in the appendix). The samples studied were:

$(Zn_xCu_{1-x})_{2.5}(OH)_2TM \cdot 2\text{-}3H_2O$ (x=1.0, 0.90 and 0.75)

$(Zn_xCu_{1-x})_{1.5}TM \cdot 2H_2O$ (x=0.0 and 0.20)

$Zn_2PM \cdot 4H_2O$

$Cu_2PM \cdot 6H_2O$

$(Zn_xCu_{1-x})_{2.5}OH(PM) \cdot 7H_2O$ (x=0.50 and 0.33)

The DSC experiments were carried out in air, the heating rate was 5°C $min^{-1}$ and the samples (~5mg) were heated up to 600°C. For some salts subsequent experiments were undertaken in which fresh samples were heated past specific thermodynamic events, as identified by DSC, and the products were analysed by XRD and IR.

The TPDec experiments involved the use of a quadrupole mass spectrometer to identify the volatile products of decomposition. 1.0g samples were heated under either an inert (argon) or an oxidising (oxygen) atmosphere at a rate of 1°C $min^{-1}$. The carrier gas, argon or oxygen, was passed over the sample at a flow rate of 25$cm^3min^{-1}$. The mass spectrometer was connected to the gas outlet from the furnace via a heated capillary tube.

The experiment was undertaken in two stages, first a TPDec experiment with the mass spectrometer recording spectra (0-200m/e) every 5 minutes. From these mass spectra the decomposition volatiles were deduced. (Table 6.1 gives the mass fragmentation for the compounds of interest). Then the experiment was repeated using a fresh sample, and this time only the intensities of selected values of m/e were recorded (every two minutes), producing a decomposition profile of the volatile products. Each experiment was repeated to ensure reproducibility.

In order to make a semi-quantitative analysis of the results, the peak areas for the profiles were determined. Although the absolute peak areas vary between experiments (because the m/e intensities are relative to the total gas present) the ratio of the peak areas for similar experiments was in reasonable agreement. An experimental error of 5% was estimated for the peak areas and ±2°C for the peak temperatures. The very broad peaks have a larger error associated with the peak temperature, ±4°C. The calculated peak areas are given to three significant figures, to a maximum of one decimal place. To resolve overlapping peaks a Gaussian peak fitting programme was used. It has been reported that a Gaussian peak is a good approximation for desorption profiles[128] but for reaction profiles this is rarely the case. Only the peaks that could be easily resolved had separate areas calculated and the peaks that were more ambiguous (e.g. a peak with a shoulder) have had the sum of the areas quoted.

| Compound | Sensitivity correction | m/e fragmentation (percentage intensity) |
|---|---|---|
| $C_6H_6$ | — | **78** (100), 52 (43), 51 (42), 39 (39), 50 (36), 77 (25), 38 (13), 27 (10), 26 (10) |
| $CO_2$ | 1.00 | **44** (100), 28 (15), 16 (12), 12 (7) |
| Ar | — | **40** (100), 20 (16), 36 (0.4) |
| $^aO_2$ | — | **32** (100), 16 (4), 28 (0.4) |
| CO | 0.70 | **28** (100), 12 (3), 16 (0.7) |
| $H_2O$ | — | **18** (100), 17 (21), 16 (1) |
| $CH_4$ | 0.89[b] | 16 (100), **15** (88), 14 (14), 13 (6) |
| $^aH_2$ | — | **2** (100), 1 (2) |

Table 6.1 Mass spectral data including sensitivity correction factors calculated for $CO_2$, CO and $CH_4$. The m/e values in bold were used for the decomposition profiles. Only the strongest m/e signals are shown.
[a] intensities from literature[129]
[b] correction factor calculated for m/e 15

As is evident from the fragmentation patterns in table 6.1, carbon dioxide also contributes to m/e 28 (carbon monoxide) and m/e 16 (methane) profiles. To obtain the carbon monoxide profile, the intensity due to carbon dioxide was subtracted from the m/e 28 signal. Methane profiles were obtained using m/e 15.

Also given in the table are the sensitivity correction factors for carbon dioxide, carbon monoxide and methane (m/e 15). The sensitivities have been calculated with respect to carbon dioxide, for instance the quadrupole mass spectrometer was more sensitive to carbon monoxide than carbon dioxide, and the carbon monoxide m/e 28 intensity must be multiplied by 0.70 to give a comparable signal. The water and benzene sensitivities were not calculated as these proved to be technically difficult (see appendix).

## 6.3 Results and Discussion

In this section the decomposition of each compound will be discussed separately. First the decompositions of zinc and copper trimellitate under inert and oxidising conditions are discussed in some detail. The results for the mixed metal trimellitates will then be described, comparing the decompositions with those of the single metal trimellitates, highlighting the effect of zinc and copper substitution on the decompositions. The decompositions of the pyromellitates will then be compared with the trimellitates. This section is followed by the summary and conclusions.

### *6.3a Decomposition of zinc trimellitate*

*$Zn_{2.5}(OH)_2TM \cdot 2H_2O$, decomposition under inert atmosphere.*

Decomposing zinc trimellitate under an inert atmosphere yielded a zinc oxide/carbon product. The product was a charcoal grey powder. Elemental analysis of the product gave a zinc/carbon ratio of 1:1.3 (≡ 2.5ZnO + 3.25C). The solid was characterised by XRD and IR, the XRD pattern was of zinc oxide and the IR spectrum had one absorption at 423$cm^{-1}$, indicative of zinc oxide.

After the TPDec experiment, some metallic zinc (~10mg) and some brown solid were found to have deposited at the end of the reactor tube, just outside the furnace. The zinc was identified by atomic absorption spectroscopy (AAS). The IR spectra of the brown solid was characteristic of benzoic acid (b.pt.=249°C), the strongest absorptions were 3070-2533; 1686; 1453; 1424; 1326; 1292; 934; 707; 667$cm^{-1}$.

| Product | Temperature (°C) | | | | | | |
|---|---|---|---|---|---|---|---|
| | 135-260 | 329 | 381 | 462 | 500 | 550 | 700 |
| $CO_2$ | — | — | 165 | 551 | — | — | — |
| CO | — | — | 1.5 | 46.7 | 192 | — | — |
| $H_2O$ | 243 | 104 | — | 26.0 | — | — | — |
| $C_6H_6$ | — | — | — | 139 | — | — | — |
| $H_2$ | — | — | — | 5.0 | — | 8.6 | 87.1 |

Table 6.2 Peak areas for the TPDec under argon of $Zn_{2.5}(OH)_2TM \cdot 2H_2O$.

The TPDec profile is shown in figure 6.1 and the peak areas are given in table 6.2. From the profile it can be seen that dehydration occurred up to 400°C. The water evolution reached a maximum rate, producing a plateau in the profile. This could be due to the water condensing just outside the furnace (before the heated tubing) and then slowly evaporating.

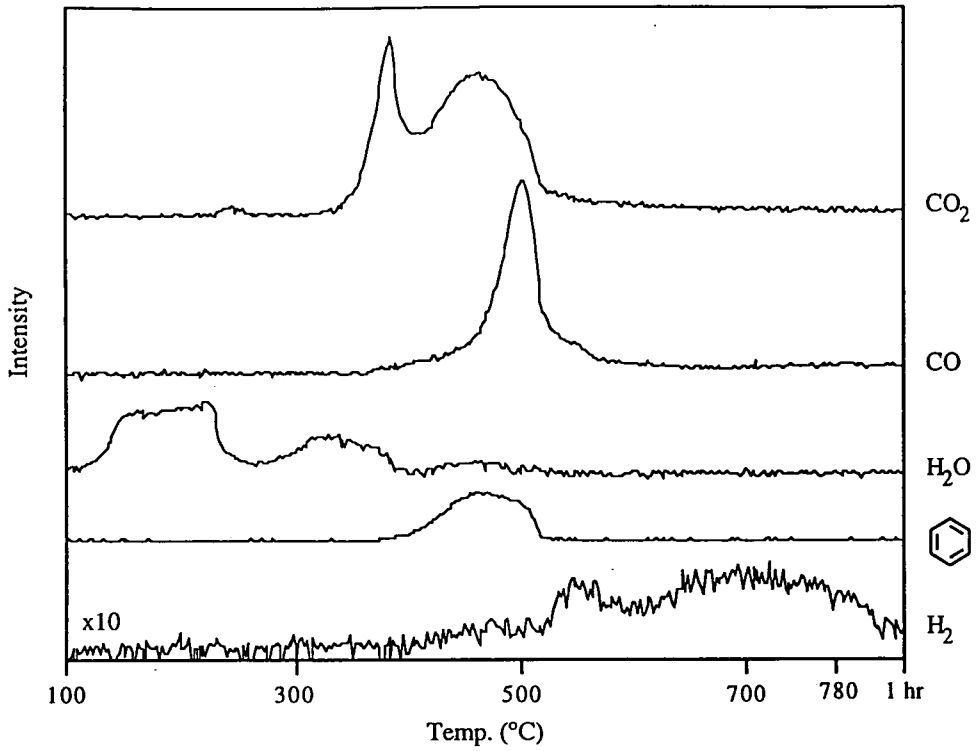


Figure 6.1 TPDec profile of $Zn_{2.5}(OH)_2TM \cdot 2H_2O$ under argon.

After dehydration the salt decomposes in three stages, carbon dioxide was produced in the first two (381, 463°C) and carbon monoxide in the final stage (500°C). The ratio of the carbon oxide peak areas was 1:3.8:1.2 respectively. Benzene, water and hydrogen were also evolved with the final two stages. An IR spectra of a sample heated to 600°C had only zinc oxide absorptions proving that by 600°C the salt had decomposed. After decomposition, hydrogen was desorbed at 550°C, and a ten-fold amount at 700°C. A trace of methane was also detected.

The carbon monoxide and dioxide profiles suggest that after dehydration, zinc trimellitate decomposes by the successive loss of carboxylate groups, first as carbon dioxide, and finally as carbon monoxide. The decarboxylation (loss of carbon dioxide) is most likely to be a Henkel type reaction[15]. It is believed that metal ions catalyse a Henkel decarboxylation by conjugation of the carboxylate group. The carboxylate group is lost as carbon dioxide, forming a carbanion transition state which can then react with an electrophile, figure 6.2. For zinc trimellitate the most probable source of electrophile is a proton from an hydroxyl group, forming a dicarboxylate and zinc oxide.

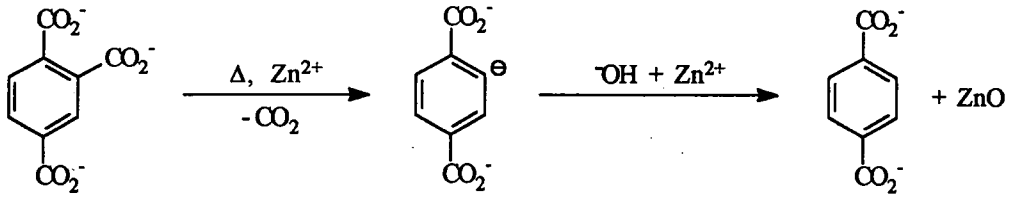


Figure 6.2 Decarboxylation of trimellitate anion.

Using the simple principle of electron donation from a carboxylate group to an aromatic ring, one would expect the 2 position to be the most favourable site for decarboxylation, producing terephthalate (1,4-benzenedicarboxylate). This is owing to electron donating groups (like carboxylates) pushing electron density into the para position, making it less stable for a carbanion transition state. For the trimellitate ion, the carboxylate in the 2 position was the only one to have no carboxylate groups para to it. Therefore, it was the most favourable site for the formation of a carbanion intermediate during decarboxylation.

Figure 6.3 illustrates how the trimellitate salt decomposes in three stages. The first two stages involve Henkel type decarboxylations producing zinc benzoate. After these decarboxylations there are no hydroxyl groups left. This has two consequences: i) no available electrophile for further Henkel reactions, and ii) oxygen for the zinc oxide product must now come from a carboxylate group. Zinc benzoate will initially undergo loss of carboxylate groups, evolving carbon dioxide and carbon monoxide (because of zinc oxide formation), with the aromatic rings dissociating to carbon and hydrogen. It appears from the TPDec profile that hydrogen was retained by the substrate and desorbed at higher temperatures. The initial ring degradation makes several decomposition routes possible (see figure 6.3). The adsorbed hydrogen could act as an electrophile allowing decarboxylation of benzoate producing benzene, or protonate benzoate to benzoic acid (both were products of decomposition). It is also possible that carboxylate groups oxidised some of the carbon and hydrogen from ring degradation, producing carbon monoxide and water.

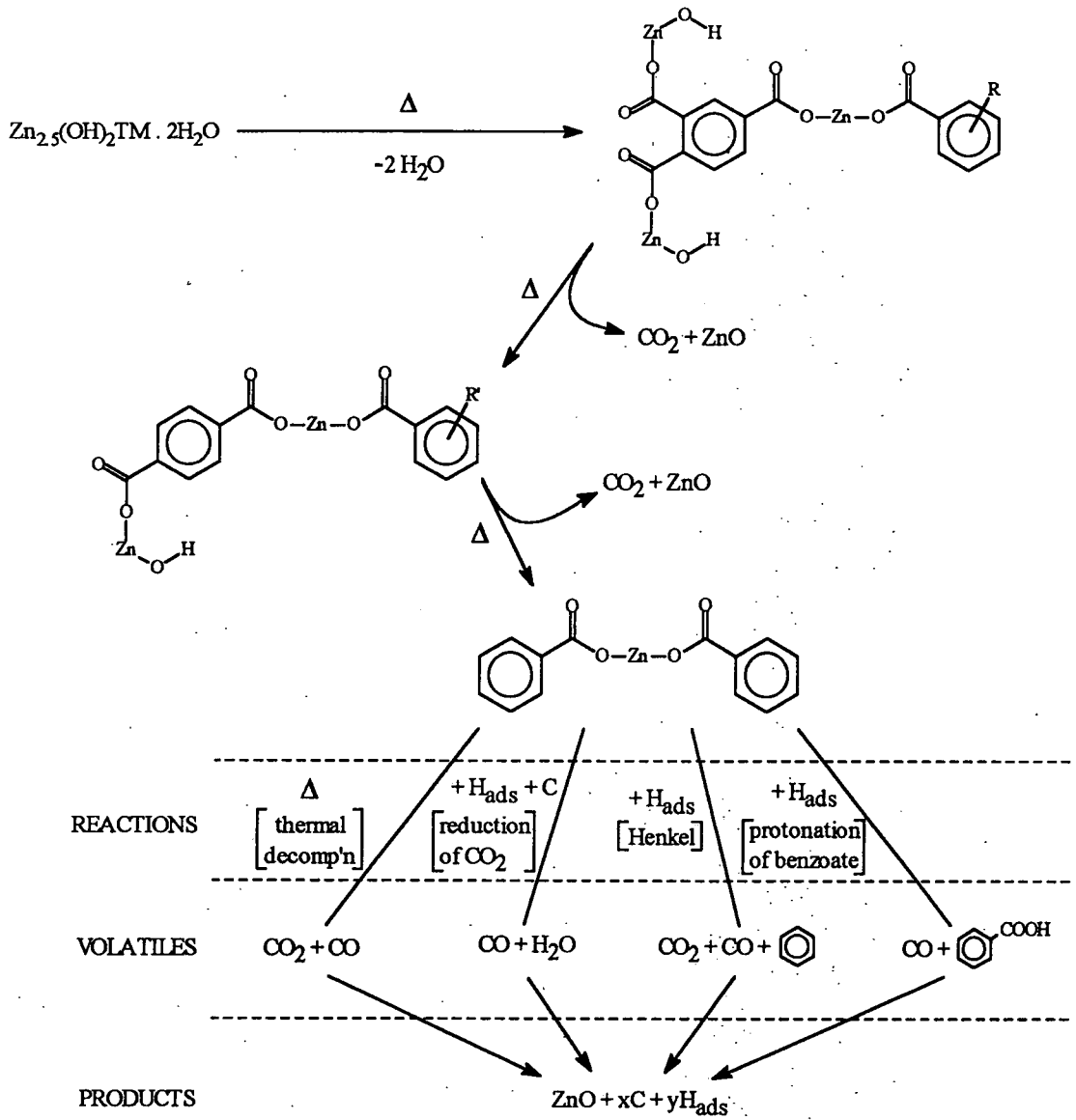


Figure 6.3 Decomposition scheme for $Zn_{2.5}(OH)_2TM$ . $2H_2O$ under an inert atmosphere.

*$Zn_{2.5}(OH)_2TM$ . $2H_2O$, decomposition under oxidising atmosphere.*

The decomposition under oxygen produced a cream coloured powder which was characterised (by XRD, IR and AAS) as zinc oxide, no carbon remained. Benzoic acid crystallised at the end of the reactor tube, but no zinc or its oxide were observed there. Enough of the acid was collected for IR and MS analysis to confirm the identity of the organic phase: m/e fragmentation 105 (100%), 122 (97.6%), 77 (68.3%), 57 (37.0%).

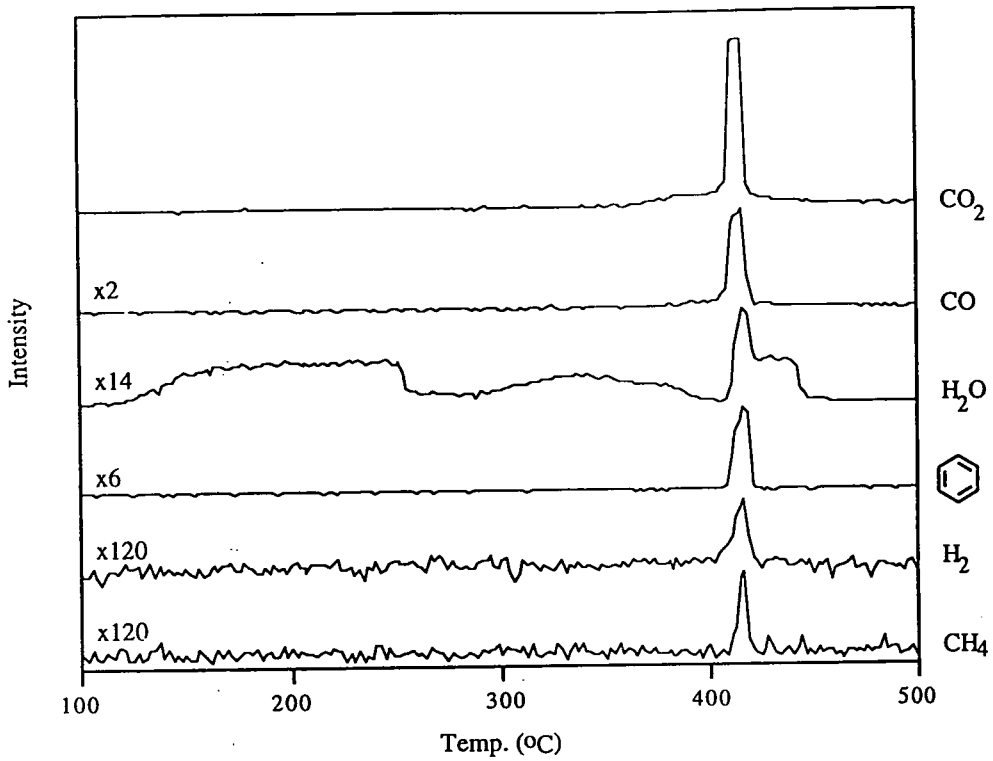


Figure 6.4 TPDec profile of $Zn_{2.5}(OH)_2TM$ . $2H_2O$ under oxygen.

Comparing the TPDec data, figure 6.4 and table 6.3, with the previous experiment, one can see that there was no change in the loss of water up to 400°C. In contrast, the majority of the decomposition occurred over a small temperature range, 408-416°C. The profile of the carrier gas, oxygen, was the inverse of that for carbon dioxide, i.e. the intensity falling to approximately zero at 408-416°C. A closer study of the carbon dioxide profile reveals a small evolution at 387°C prior to the large carbon dioxide peak.

| Product | Temperature (°C) | | | | | | |
|---|---|---|---|---|---|---|---|
| | 115-275 | 338 | 387 | 408-416 | 415 | 416 | 416-450 |
| $CO_2$ | — | — | 146 | 1593 | — | — | — |
| CO | — | — | — | 169 | — | — | — |
| $H_2O$ | 242 | 108 | — | — | — | 51.2 | 89.5 |
| $C_6H_6$ | — | — | — | — | — | 89.0 | — |
| $H_2$ | — | — | — | — | 6.3 | — | — |
| $CH_4$ | — | — | — | — | 2.1 | — | — |

Table 6.3 Peak areas for the TPDec under oxygen of $Zn_{2.5}(OH)_2TM$ .$2H_2O$.

The amount of carbon dioxide produced by decomposition under oxygen was much larger than under argon, but there were comparable amounts of carbon monoxide

and benzene produced. Water, hydrogen and methane were also detected during the decomposition.

The DSC data for zinc trimellitate are given in table 6.4, along with the XRD results of the intermediate thermolysis products. It should be remembered that because of the different heating rates used there are discrepancies between the temperatures quoted for TPDec and DSC. There were three thermodynamic events detected: two endotherms, followed by an exotherm. No change was observed by XRD after the first endotherm (loss of water, cf. TPDec profile, figure 6.4), but after the second endotherm only a weak zinc oxide pattern was obtained by XRD. Finally, there was a large exotherm, signifying oxidative decomposition of the substrate to zinc oxide. This exotherm terminated at 485°C.

| Temp. (°C) | ΔH (kJ $mol^{-1}$) | % weight loss | Molar weight loss | XRD | Comments |
|---|---|---|---|---|---|
| 158 | 56 | 4.0 | 18 | same as precursor | loss of $H_2O$ |
| 389 | 21 | 18.2 | 80 | faint ZnO pattern | further loss of $H_2O$ and $CO_2$ |
| 475 (445 sh) | -706 | 52.0 | 229 | strong ZnO pattern | Calculated weight loss = 53.8% |

Table 6.4 DSC results for $Zn_{2.5}(OH)_2TM \cdot 2H_2O$.

IR spectra of the thermolysis products are shown in figure 6.5. The decrease in intensity of the ν(O-H) band, 3700-2500$cm^{-1}$, with heating to 400°C indicates loss of water. The progressive formation of zinc oxide was detected by the increasing intensity of the broad band at 440$cm^{-1}$, first observed at 400°C.

The spectra below 1300$cm^{-1}$ can give information about the degree of substitution of the aromatic ring during decomposition. The spectrum of the sample heated to 180°C had peaks at the same wavenumbers as zinc trimellitate, but with different intensities, indicative of the trimellitate anion being in a modified environment. By 400°C the absorptions had changed and were much weaker. This spectrum was compared with the spectra of zinc benzoate and basic benzene dicarboxylates (1:2, 1:3 and 1:4 substituted) and it was found that benzoate and terephthalate (1:4 disubstituted) salts accounted for all the absorptions. In particular, the absorptions at 745 and 719$cm^{-1}$ corresponded to terephthalate and benzoate ν(C-H) out of plane vibrations respectively. At 400°C the 745$cm^{-1}$ peak was larger than 719$cm^{-1}$ but as the decomposition proceeded the ratio between the two peaks (745:719$cm^{-1}$) became smaller. By 480°C the terephthalate peak was very small. One can therefore deduce that terephthalate was the predominant product at 400°C, but as the decomposition progressed, so the benzoate became the predominant salt. By 600°C only zinc oxide remained.

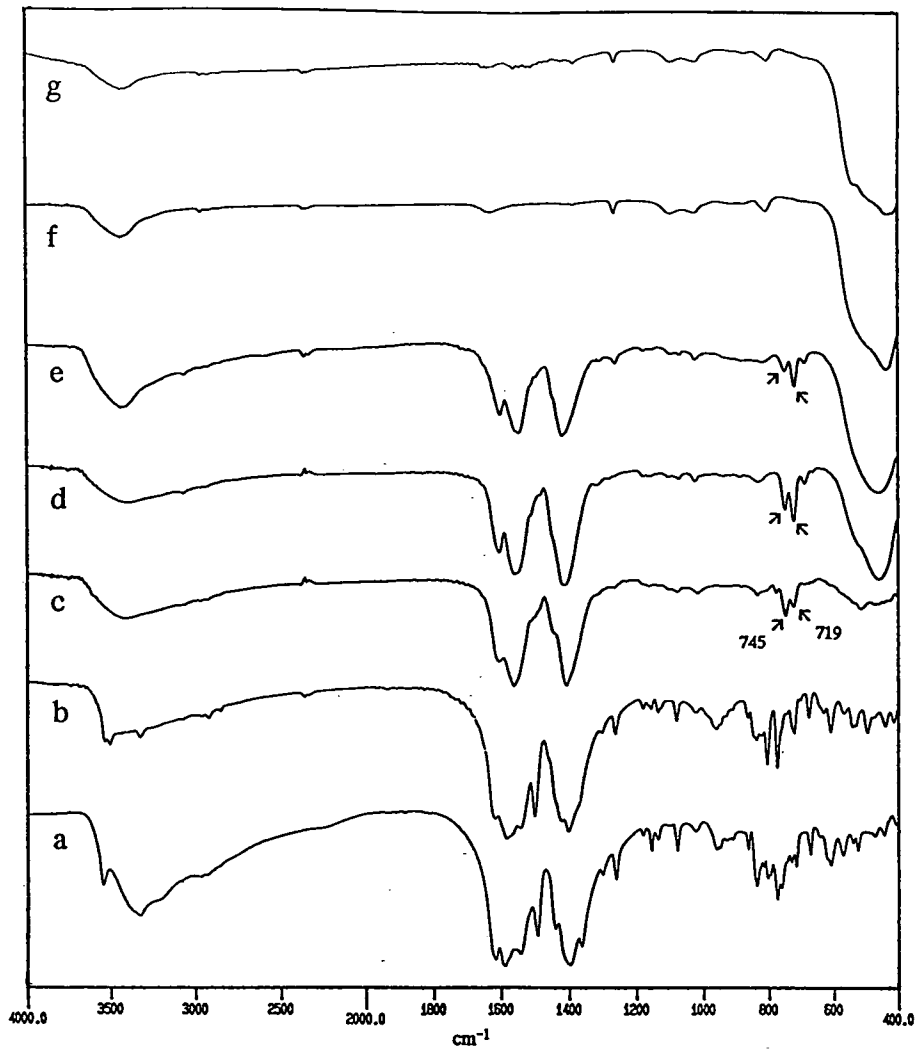


Figure 6.5 IR spectra of $Zn_{2.5}(OH)_2TM \cdot 2H_2O$, a, and of samples heated under air to b, 180; c, 400; d, 420; e,480; f, 600°C; and, g, a spectrum of ZnO (Aldrich).

The TPDec results suggest that decarboxylation similar to that observed under argon occurred at 387°C prior to the main decomposition, 408-416°C. This is supported by the DSC, XRD and IR results, which showed the presence of zinc oxide, terephthalate, and to a lesser extent benzoate, at 400°C. Referring back to the argon profile, figure 6.1, benzene was evolved with the second stage of decarboxylation. It was also postulated that ring degradation occurred with the evolution of benzene, i.e. after the initial decarboxylation some aromatic rings dissociated to carbon and hydrogen. Under oxygen these products (carbon and hydrogen) will be oxidised (a very exothermic reaction, cf. DSC) leading to localised heating of the substrate. The localised heating will force the rest of the material to decompose.

From the results, it would appear that oxygen did not hinder or prevent the sequential loss of carboxylate groups. This was deduced from the IR spectra of the partially decomposed samples in which both terephthalate and benzoate (both products of decarboxylation) were detected, the relative amount of terephthlalate decreasing as

the decomposition progressed. Comparable amounts of benzene and benzoic acid (also products of decarboxylation) were produced under both oxygen and argon atmospheres, indicating that a similar amount of decarboxylation occurred under both conditions. It therefore appears that the mechanism of decomposition under oxygen was similar to that under argon, except that under oxygen the products of ring dissociation were oxidised. This oxidation was exothermic, leading to localised heating of the substrate, which in turn forced the rest of the material to quickly decompose or decarboxylate.

### *6.3b Decomposition of copper trimellitate*

*$Cu_{1.5}TM \cdot 2H_2O$, decomposition under inert atmosphere.*

Thermal decomposition of copper trimellitate under an inert atmosphere produced copper dispersed on a carbonaceous bed (determined by XRD and elemental analysis). Benzoic acid was produced during the decomposition (characterised by IR), and crystallised on the reactor walls just outside the furnace. Elemental analysis of the copper/carbon product gave an elemental ratio of 1:3.7 (≡ 1.5Cu + 5.5C).

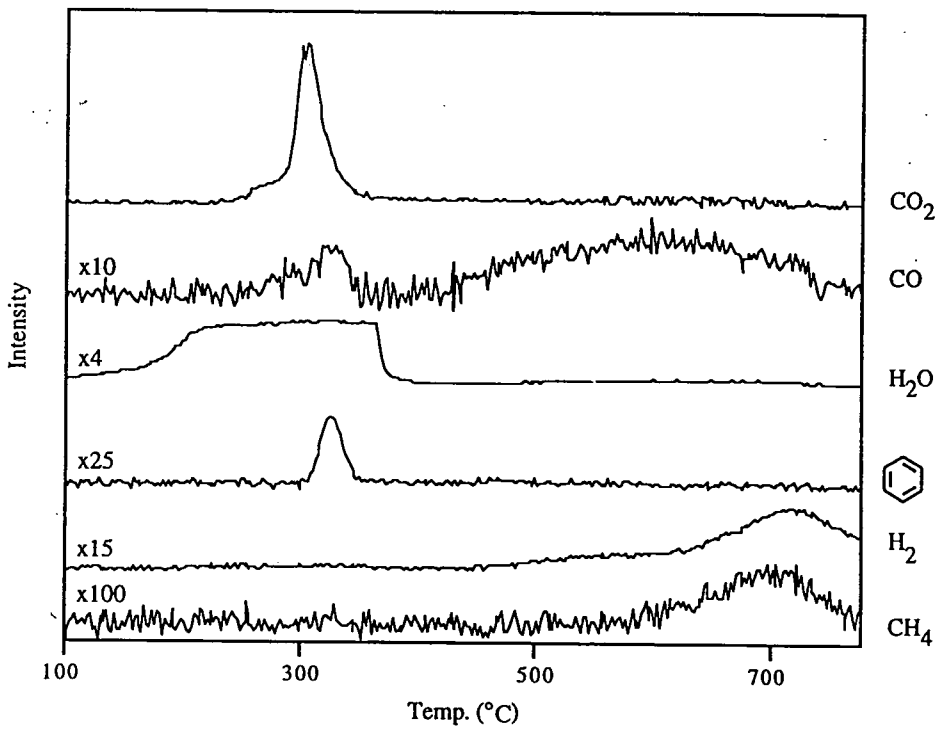


Figure 6.6 TPDec profile of $Cu_{1.5}TM \cdot 2H_2O$ under argon.

The TPDec profile, figure 6.6, can be divided into three processes: i) dehydration, ii) decomposition, and iii) desorption (after decomposition). Water was detected from 140°C, reaching a maximum rate at ~200°C and ending at 375°C. Water was still detected during the decomposition but the water profile appears unperturbed by it. The long water profile, coupled with the water evolution being uninfluenced by the

sample decomposing, suggests that water from dehydration was condensed somewhere in the system and slowly evaporated off.

| Product | Temperature (°C) | | | | |
|---|---|---|---|---|---|
| | 170-375 | 278 | 301,309 | 327 | 455-780 |
| $CO_2$ | — | 40.2 | 474 | 54.8 | — |
| CO | — | — | 10.4 | 12.3 | 88.2 (492 sh, 633°C) |
| $H_2O$ | 312 | — | — | — | 60.2 (508 sh, 662°C) |
| $C_6H_6$ | — | — | — | 7.0 | — |
| $H_2$ | — | — | — | — | 77.2 (568 sh ,720°C) |
| $CH_4$ | — | — | — | — | 6.3 (616 sh, 720°C) |
| $O_2$ | — | — | 1.7 | — | — |

Table 6.5 Peak areas for the TPDec under argon of $Cu_{1.5}TM \cdot 2H_2O$.

Figure 6.7 shows a more detailed profile of the decomposition (intensity measured every 0.4°C). The carbon dioxide peak was quite narrow, had two maxima (301 and 309°C) and a shoulder on either side (278 and 327°C). A small amount of oxygen was evolved with the carbon dioxide.

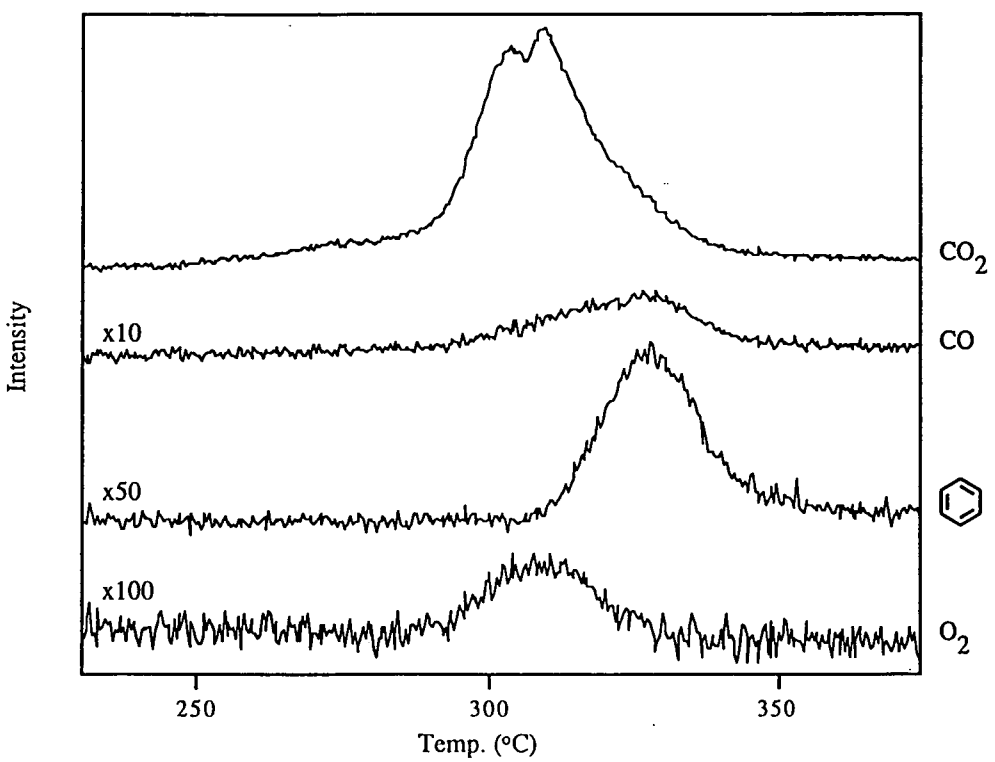


Figure 6.7 Detailed TPDec profile of $Cu_{1.5}TM \cdot 2H_2O$ under argon (measurement every 0.4°C).

Carbon monoxide and benzene were also produced towards the end of the carbon dioxide peak, occurring with the shoulder in the carbon dioxide peak at 327°C.

Carbon, hydrogen and oxygen species were desorbed after the decomposition. Below 600°C the predominant species were carbon monoxide and water. Above 600°C hydrogen became the predominant desorption product and the carbon monoxide and water evolutions tailed off. Methane was also detected along with the hydrogen peak. The results suggest that while oxygen was present on the surface, the main products were carbon monoxide and water. With the depletion of adsorbed oxygen, hydrogen becomes the predominant product. The lack of oxygen also allows hydrogen to react with carbon, forming methane.

From the TPDec results we see that there were three major differences between the decompositions of copper and zinc trimellitates. Firstly, the initial decarboxylation temperature was much lower for the copper salt (278°C, cf. 380°C), due to the Cu-O bond being weaker than Zn-O[131]. Also the copper salt decarboxylates over a short temperature range in contrast with the zinc sample which lost carboxylate groups over three stages. This can be explained by the suitability of the copper salt for a Henkel decarboxylation. The copper salt had no hydroxyl groups, and therefore no readily available hydrogen for a Henkel reaction. This meant that decarboxylation of the trimellitate anion occurred with the dissociation of the aromatic ring (similar to the final stage of the zinc decomposition). The decarboxylations occurred together because the trimellitate ion was breaking up, and the other carboxylate groups for the ion were lost almost simultaneously.

A small amount of benzene and benzoic acid were produced, evidence that some non-destructive decarboxylation occurred. This could have been achieved by the hydrogen produced by ring degradation, protonating the aromatic ring during decarboxylation.

The final difference between the profiles of zinc and copper salts was that very little carbon monoxide was produced during the decarboxylation of copper trimellitate. This was because the copper was reduced from +2 to 0 oxidation state, and did not require oxygen from the carboxylate groups to keep the copper oxidised.

*$Cu_{1.5}TM.\ 2H_2O$, decomposition under oxidising atmosphere.*

Copper trimellitate thermally decomposes to copper(II) oxide when under an oxidising atmosphere. A small amount of benzoic acid was produced during the decomposition and crystallised at the end of the reactor tube. The profile of the decomposition volatiles, figure 6.8, shows loss of water from 170-445°C and the decomposition at 270°C. Compared with the decomposition under argon, the loss of water continued for an extra 70°C. The extra water evolved has come from the oxidation of hydrogen produced during the decomposition.

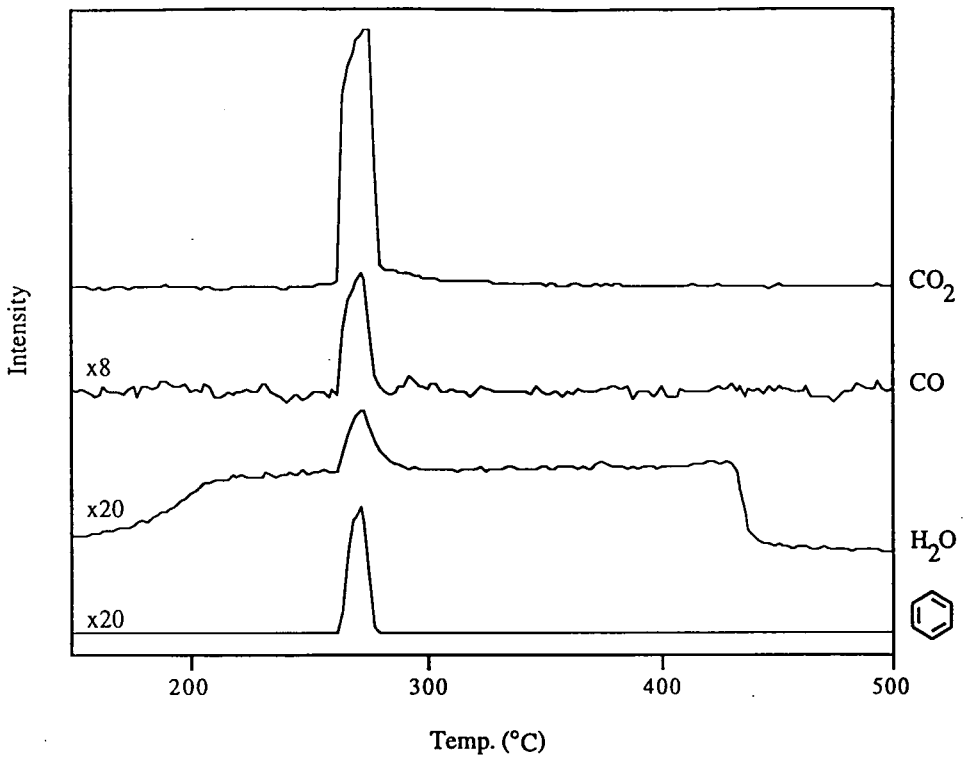


Figure 6.8 TPDec profile of $Cu_{1.5}TM$ . $2H_2O$ under oxygen.

Comparing the oxygen and argon TPDec profiles, it was observed that the decomposition under oxygen coincided with the onset of decarboxylation under argon. As discussed earlier, decarboxylation of the copper salt involved the dissociation of the aromatic ring. Under oxygen the carbon and hydrogen produced by this will be oxidised and the heat produced will force the surrounding material to thermally decarboxylate or decompose.

| Product | Temperature (°C) | | | |
|---|---|---|---|---|
| | 170-445 | 262-275 | 267 (272 sh) | 272 (267 sh) |
| $CO_2$ | — | 1094 | — | — |
| CO | — | 23.5 | — | — |
| $H_2O$ | 292 | — | 7.6 | — |
| $C_6H_6$ | — | — | 16.4 | — |
| $H_2$ | — | — | — | 0.6 |
| $CH_4$ | — | — | — | 0.8 |

Table 6.6 Peak areas for the TPDec under oxygen of $Cu_{1.5}TM$ . $2H_2O$.

A more detailed profile is shown in figure 6.9, where the intensity was measured every 0.2°C. This profile shows that very small amounts of hydrogen and methane were also liberated during the decomposition. The profile also shows in greater detail the

peak shapes for the volatiles. The levelling off of the carbon dioxide profile was due to the depletion of oxygen during decomposition. The profile for oxygen was the inverse of that obtained for carbon dioxide, as found during the oxidative decomposition of zinc trimellitate. It is interesting to note that the benzene profile peaked at the beginning of the decomposition and slowly decreased. In contrast, little methane was produced to begin with but suddenly increases towards the end of the decomposition. The methane profile can be explained by the availability of hydrogen. Towards the end of the decomposition, less hydrogen will be required for decarboxylation (indicated by the decrease in the benzene intensity) so there will be more hydrogen available to react with carbon, producing methane.

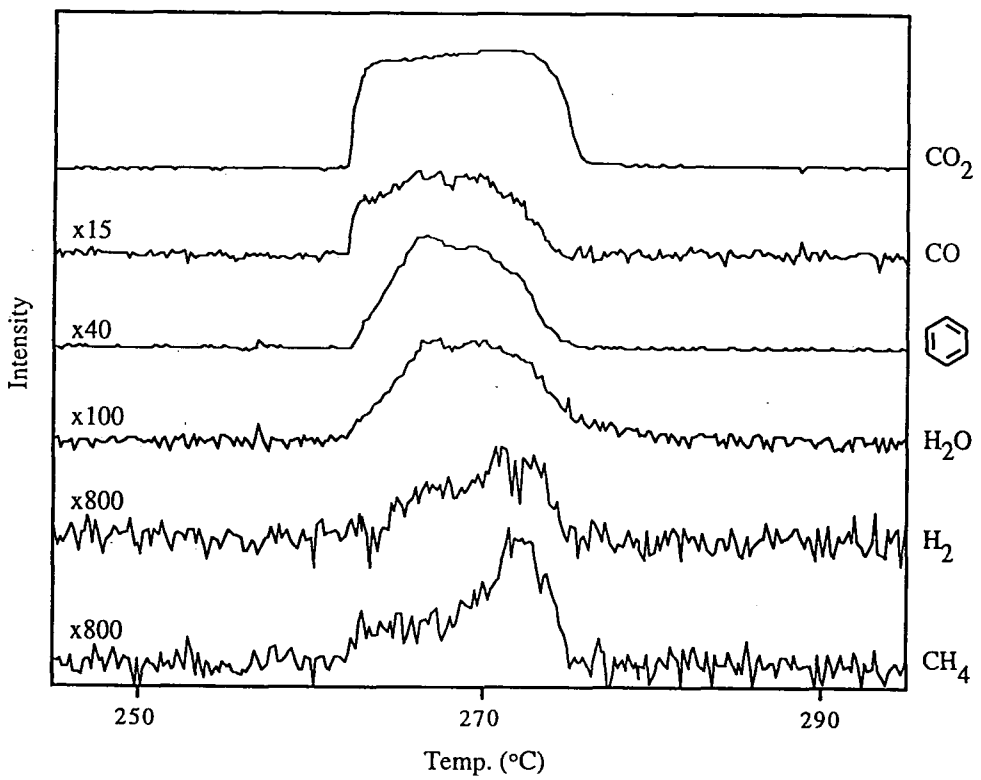


Figure 6.9 Detailed TPDec profile of $Cu_{1.5}TM \cdot 2H_2O$ under oxygen (measurement every 0.2°C).

An endotherm (248°C) and a large exotherm (301°C) were detected by DSC, table 6.7. The endotherm was due to loss of water and the exotherm to oxidative decomposition. The value of ΔH for the exotherm was approximately three times that found for zinc trimellitate.

| Temp. (°C) | ΔH (kJ $mol^{-1}$) | % weight loss found | % weight loss calculated |
|---|---|---|---|
| 248 | 94 | — | — |
| 301 | -2250 | 65.8 | 64.7 |

Table 6.7 DSC results for $Cu_{1.5}TM \cdot 2H_2O$.

XRD and IR studies were made of the intermediate thermolysis products of copper trimellitate (heating rate, 10°C $min^{-1}$). The XRD results, table 6.8, show that at 190°C there was no change in the phase of the sample. There was, however, a loss in mass, probably from the loss of loosely bound water. Further dehydration up to 220°C produced an anhydrous phase. At 310°C, halfway through the decomposition (with respect to weight loss), the substrate was mostly amorphous; only a faint line corresponding to the anhydrous phase was detected. The solid was mostly amorphous at 365°C (almost at the end of the decomposition), but a faint line corresponding to copper(I) oxide was detected. Copper in low oxidation states was also detected in the final product.

With only these results, it is impossible to deduce whether the copper during the decomposition was initially reduced and then oxidised, or if a lack of oxygen during the decomposition led to some of the solid decomposing under an inert atmosphere, producing copper. In either case, copper in reduced oxidation states were encapsulated in copper(II) oxide, preventing complete oxidation.

| Temp. (°C) | % weight loss | Molar weight loss | XRD |
|---|---|---|---|
| 190 (1hr) | 4.8 | 16.2 | $Cu_{1.5}TM . 2H_2O$ |
| 220 (0.5hrs) | 9.1 | 30.8 | $Cu_{1.5}TM$, hydrated + anhydrous phases |
| 310 | 32.4 | 109.7 | first line of anhydrous phase |
| 365 | 64.2 | 217.3 | faint line of $Cu_2O$ |
| 600 | 65.8 | 222.7 | CuO plus faint $Cu_2O$ and Cu° |

Table 6.8 XRD results of $Cu_{1.5}TM . 2H_2O$ samples heated under air. The first two samples were kept at the end temperature for 1 and 0.5 hours respectively.

The dehydration of the copper trimellitate was also evident from the IR spectra of the thermolysis products, figure 6.10. At 190°C there was a loss in intensity of the broad ν(O-H) absorptions (3700-2800$cm^{-1}$) but the bands at 3670 and 3210$cm^{-1}$ were still prominent. On heating to 220°C only the 3670$cm^{-1}$ band remained. This agrees with the XRD results, which showed the incomplete formation of an anhydrous phase at 220°C. Further evidence for the formation of a new phase at 220°C comes from the change in the spectra below 1300$cm^{-1}$. The intensity of the peaks below 1300$cm^{-1}$ (these absorptions are associated with the vibrations of the aromatic anion) was different to those of the starting material, suggesting that the trimellitate anion was in a modified chemical environment. It was deduced that the anion was still trimellitate because the peaks had the same wavenumbers as those for copper trimellitate. Halfway through the decomposition (310°C) the spectrum of the substrate was still of the anhydrous phase.

After complete decomposition only one absorption remained, that for copper(II) oxide, 534cm$^{-1}$.

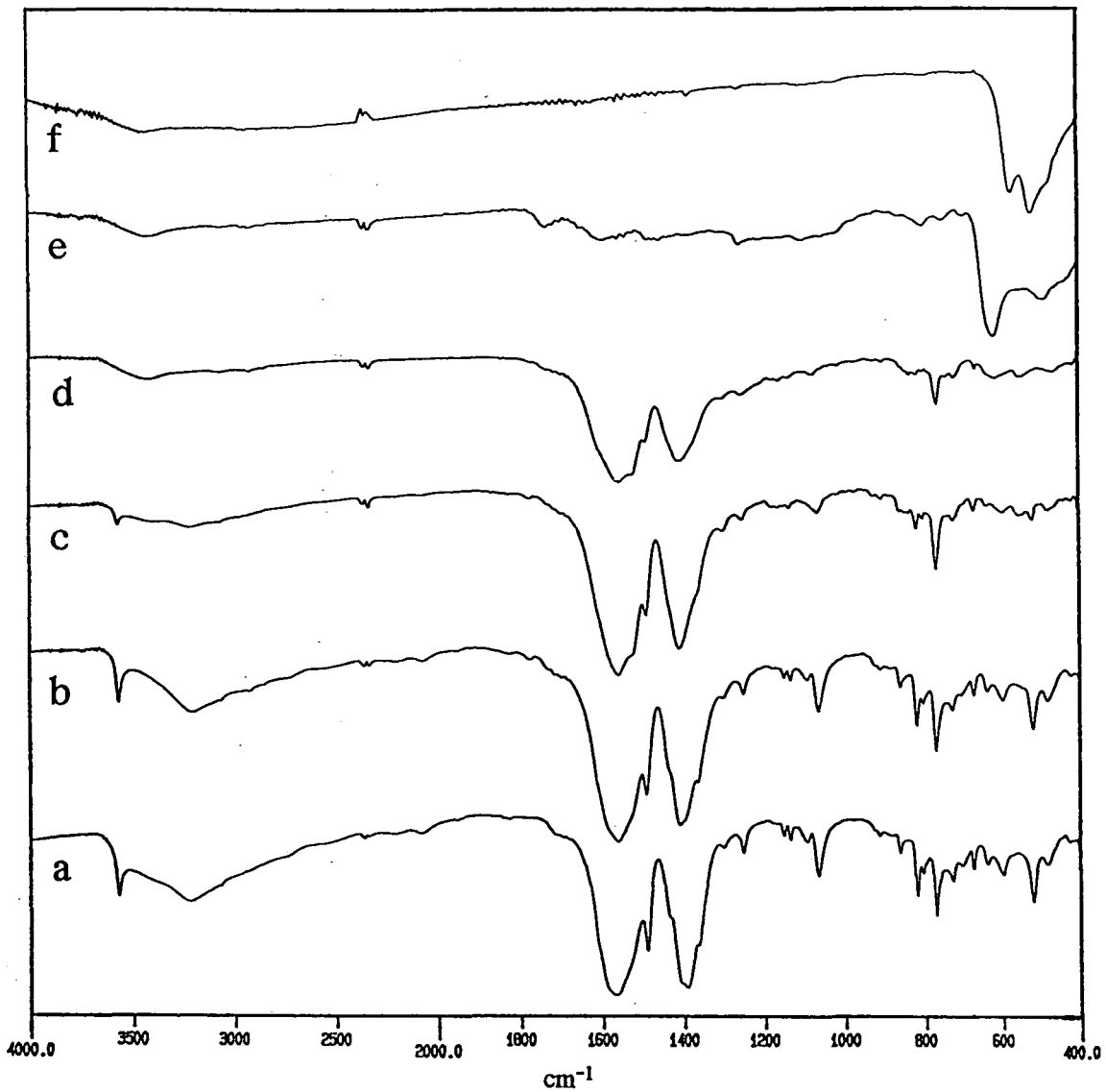


Figure 6.10 IR spectra of, a, $Cu_{1.5}TM$ . $2H_2O$ and of samples heated under air to b, 190; c, 220; d, 310; e, 365; f, 600°C.

It was deduced from the TPDec experiment that decarboxylation occurred during decomposition (by the detection of benzoic acid and benzene). However, no decarboxylation products (dicarboxylate or benzoate) were identified in the IR spectra. Possible explanations are that decarboxylation was concerted and did not form these intermediates, or that the intermediates were short lived and quickly decarboxylated/decomposed, or that too few organic groups decarboxylated non-destructively to be detected by IR. In whichever case, no build up of dicarboxylate or benzoate was detected by IR.

### *6.3c Decomposition of ($Zn_{0.9}Cu_{0.1}$) trimellitate*

*$(Zn_{0.9}Cu_{0.1})_{2.5}(OH)_2TM \cdot 2H_2O$, decomposition under inert atmosphere.*

Having dealt with the single metal trimellitates, we now move on to the mixed metal salts. Under an inert atmosphere the mixed metal salts were thermally decomposed to copper, zinc oxide and carbon. The decomposition product (heated to 780°C) was a black powder. Elemental analysis of the product gave a copper, zinc, carbon ratio of 0.1:0.9:1.8 (≡ 0.25 Cu + 2.25 ZnO + 4.5 C). At the end of the reactor tube a small amount of benzoic acid had crystallised out, as well as some zinc metal.

The profile of the volatile products is shown in figure 6.11 and the peak areas are given in table 6.9. Water was evolved from 125-330°C. A quantitative comparison of the decomposition with that for the zinc salt (figure 6.1 and table 6.2) can be made based on the assumption that the dehydration of both samples corresponded to two equivalents of water.

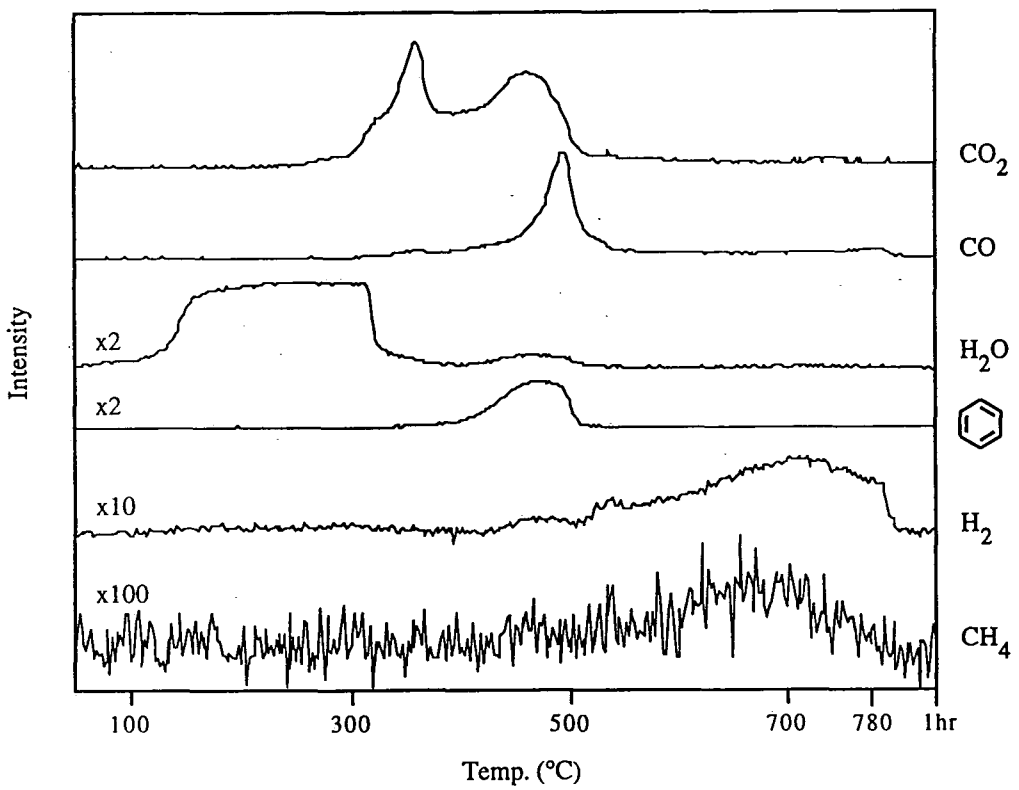


Figure 6.11 TPDec profile of $(Zn_{0.9}Cu_{0.1})_{2.5}(OH)_2TM \cdot 2H_2O$ under argon.

The decomposition profile looks similar to that of zinc trimellitate, but the incorporation of copper has produced a few changes. The first decarboxylation started at lower temperatures, a shoulder was observed at 330°C, and the decarboxylation peaked at 359°C (cf. 381°C for zinc trimellitate). The second carbon dioxide peak and decarbonylation occurred at the same temperatures as those for zinc trimellitate.

Comparing peak areas, the decarbonylation was of a similar magnitude to that for the zinc sample, but there appeared to be more gas evolved with the first decarboxylation and less with the second. The overall peak area for decarboxylation was slightly less (85% of the zinc salts).

| Product | Temperature (°C) | | | | | | | |
|---|---|---|---|---|---|---|---|---|
| | 125-330 | 359 | 460 | 495 | 535 | 656 | 716 | 780 |
| $CO_2$ | — | 265 (328°C sh) | 357 (495°C sh) | — | — | — | — | — |
| CO | — | 3.4 | — | 151 | — | — | — | 30.0 |
| $H_2O$ | 347 | — | 23 | — | — | — | — | — |
| $C_6H_6$ | — | — | 74.5 (495°C sh) | — | — | — | — | — |
| $H_2$ | — | — | 3.4 | — | 3.2 | — | 58.5 | — |
| $CH_4$ | — | — | — | — | — | 4.7 | — | — |

Table 6.9 Peak areas for the TPDec under argon of $(Zn_{0.9}Cu_{0.1})_{2.5}(OH)_2TM \cdot 2H_2O$.

As with the zinc salt, benzene was evolved with the second decarboxylation and the decarbonylation stages, but the amount of benzene produced was approximately half. The amount of benzene evolved is an indication of the level of non-destructive decarboxylation, i.e. the more benzene evolved the greater the level of non-destructive decarboxylation. The substitution of a small amount of copper has halved the amount of benzene produced, indicating greater ring degradation during the decomposition.

The amount of hydrogen desorbed was significantly less and a small amount of methane was also detected. At 780°C a small amount of carbon monoxide was evolved. It was suspected that this was from the reduction of zinc oxide by carbon, producing the gas and metallic zinc. The metal was deposited at the end of the reactor. It is not known whether the zinc deposited was evaporated to the end of the reactor tube as the metal (m.pt. 420°C, b.pt. 907°C) or a more volatile species.

The reduction of zinc oxide by carbon at 780°C has a $\Delta G$ value of[131] $+37.9 kJmol^{-1}$. However, zinc oxide is a non stoichiometric compound and can be partially reduced, forming defects, at lower temperatures than that needed to completely reduce the solid[132].

*$(Zn_{0.9}Cu_{0.1})_{2.5}(OH)_2TM \cdot 2H_2O$, decomposition under oxidising atmosphere.*

Calcination of the salt produced the metal oxides, the product was a grey powder. A small amount of benzoic acid had condensed at the end of the reactor tube. It can be seen from the decomposition profile of the volatile products, figure 6.12, that the salt decomposed at 330°C, and evolved similar volatiles to the zinc salt. However,

the peak areas for the mixed salt were significantly less than those for zinc trimellitate except for carbon dioxide and water.

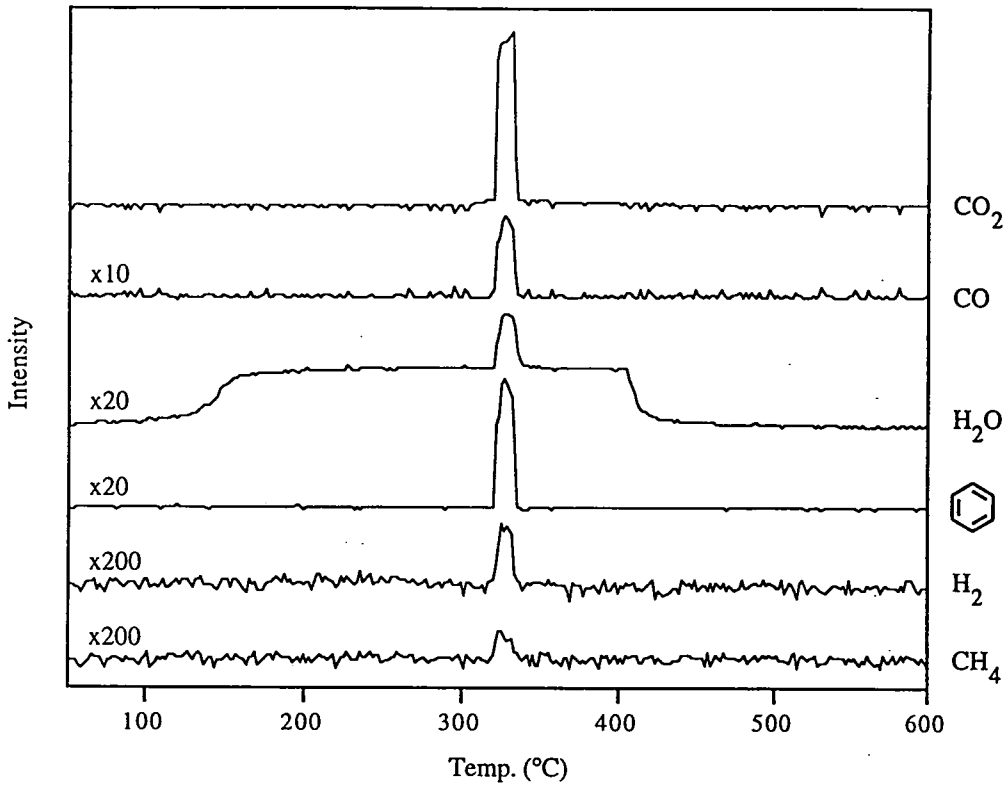


Figure 6.12 TPDec profile of $(Zn_{0.9}Cu_{0.1})_{2.5}(OH)_2TM \cdot 2H_2O$ under oxygen.

| Product | Temperature (°C) | |
|---|---|---|
| | 130-428 | 320-334 |
| $CO_2$ | — | 1690 |
| CO | — | 79.7 |
| $H_2O$ | 568 | 24.8 |
| $C_6H_6$ | — | 50.8 |
| $H_2$ | — | 2.2 |
| $CH_4$ | — | 0.8 |

Table 6.10 Peak areas for the TPDec of $(Zn_{0.9}Cu_{0.1})_{2.5}(OH)_2TM \cdot 2H_2O$ under oxygen.

An endotherm (171°C) and exotherm (427°C) were detected by DSC, table 6.11. The endotherm was due to loss of water and the exotherm to oxidative decomposition. There was a shoulder in the exotherm at 386°C. The endotherm was comparable to that for the zinc salt, but the exotherm was much larger (ca. x 4), indicating a substantial change in the thermodynamics of the decomposition.

| Temp. (°C) | ΔH (kJ mol$^{-1}$) | % weight loss found | % weight loss calculated |
|---|---|---|---|
| 171 | 161 | — | — |
| 427 (386 sh) | -2970 | 57.5 | 53.6 |

Table 6.11 DSC results for $(Zn_{0.9}Cu_{0.1})_{2.5}(OH)_2TM \cdot 2H_2O$.

The decrease in benzene and increase in carbon dioxide and water evolved (with respect to zinc trimellitate) indicate more ring degradation during decomposition. Comparing the argon and oxygen TPDec profiles we see that oxidative decomposition coincided with initial decarboxylation, suggesting that ring dissociation accompanied the initial decarboxylation. In contrast, zinc trimellitate underwent decarboxylation prior to oxidative decomposition because ring dissociation did not occur until the second decarboxylation stage.

The incorporation of copper into zinc trimellitate has altered the decomposition of the salt under both oxidising and inert atmospheres. It was demonstrated earlier that copper trimellitate decarboxylates at a lower temperature than zinc, and that ring degradation accompanies decarboxylation. It follows that in the mixed metal salt the copper was responsible for the lower decarboxylation temperature and the ring degradation occurring with it. This has led to the temperature of decomposition under oxygen being much lower than that for zinc trimellitate (by ~90°C) because the substitution of copper for zinc has enabled oxidative decomposition to take place with the initial decarboxylation.

### *6.3d Decomposition of $(Zn_{0.75}Cu_{0.25})$ trimellitate*

*$(Zn_{0.75}Cu_{0.25})_{2.5}(OH)_2TM \cdot 2H_2O$, decomposition under inert atmosphere.*

The mixed metal salt decomposed under argon to a black powder. XRD of the product gave a strong zinc oxide and faint copper pattern. Elemental analysis gave a copper, zinc, carbon ratio of 0.25:0.75:1.7 (≡ 0.63 Cu + 1.88 ZnO + 4.3 C). At the end of the reactor tube there was a small deposit of zinc metal, but no organic material.

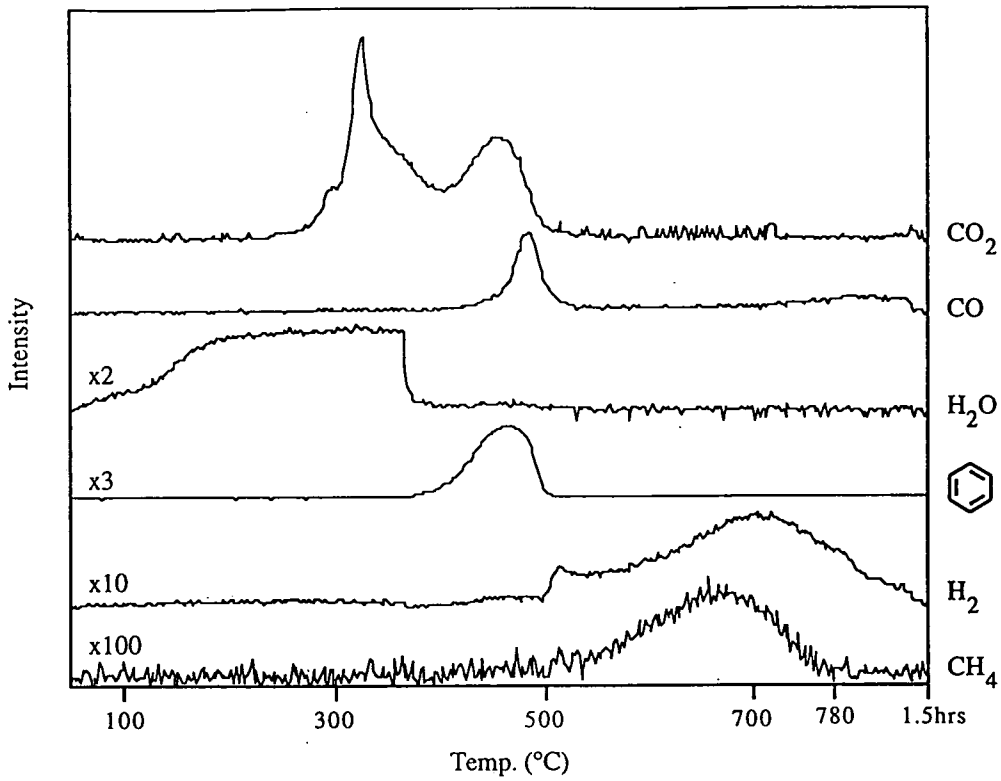


Figure 6.13 TPDec profile of $(Zn_{0.75}Cu_{0.25})_{2.5}(OH)_2TM \cdot 2H_2O$ under argon.

The decomposition profile, figure 6.13, is similar to that of the previous mixed metal salt. However, a comparison of the profiles shows that the first decarboxylation peak at 330°C and the decarbonylation at 491°C occurred at slightly lower temperatures. With respect to the TPDec peak areas for zinc trimellitate, the first decarboxylation was approximately double the area but the other decarboxylation and decarbonylation peaks were approximately half. The area of the benzene peak was about a third of that for the zinc example.

| **Product** | **Temperature (°C)** | | | | | | | |
|---|---|---|---|---|---|---|---|---|
| | 105-380 | 330 | 464 | 491 | 525 | 674 | 735 | 780 |
| $CO_2$ | — | 400 (352°C sh) | 309 (525°C sh) | — | — | — | — | — |
| CO | — | — | — | 82.7 | — | — | — | 81.1 |
| $H_2O$ | 373 | — | 17.6 | — | — | — | 11.8 | — |
| $C_6H_6$ | — | — | 49.1 | — | — | — | — | — |
| $H_2$ | — | — | — | — | 2.3 | — | 97.7 | — |
| $CH_4$ | — | — | — | — | — | 4.7 | — | — |

Table 6.12 Peak areas for the TPDec of $(Zn_{0.75}Cu_{0.25})_{2.5}(OH)_2TM \cdot 2H_2O$ under argon.

It would appear that extra copper in the basic trimellitate increased the amount of material decarboxylating at 330°C, and greatly reduced the amount at 464°C. The amount of decarbonylation at 491°C had also decreased. Two factors involved in the decrease in decarbonylation were:

i) lower zinc content (this meant there was less zinc to be kept oxidised by the remaining carboxylate groups); and

ii) greater ring degradation (deduced from the decrease in benzene evolved; this meant less material decarboxylated to benzoate).

*$(Zn_{0.75}Cu_{0.25})_{2.5}(OH)_2TM \cdot 2H_2O$, decomposition under oxidising atmosphere.*

The calcination was very similar to the previous mixed metal salt. XRD of the product, a black powder, gave strong zinc oxide and faint copper(II) oxide patterns. Benzoic acid crystallised at the end of the reactor tube.

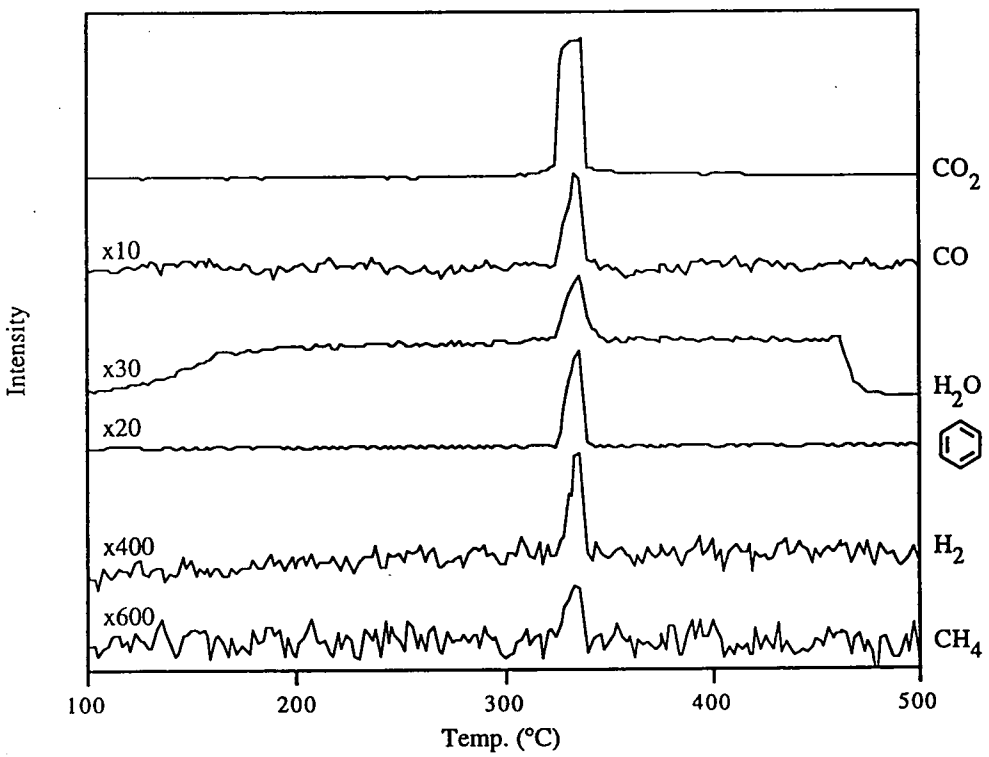


Figure 6.14 TPDec profile of $(Zn_{0.75}Cu_{0.25})_{2.5}(OH)_2TM \cdot 2H_2O$ under oxygen.

The TPDec profile, figure 6.14, was analogous to the previous salt. The decomposition occurred at the same temperature, 330°C, coinciding with initial decarboxylation. One minor difference was that there appeared to be slightly less benzene evolved. This was because the greater copper content led to more ring degradation, as seen in the argon TPDec.

| Product | Temperature (°C) | | |
|---|---|---|---|
| | 105-425 | 327-339 | 335 |
| $CO_2$ | — | 1580 | — |
| CO | — | 24.2 | — |
| $H_2O$ | 587 | — | 22.1 |
| $C_6H_6$ | — | — | 34.4 |
| $H_2$ | — | — | 1.6 |
| $CH_4$ | — | — | 0.7 |

Table 6.13 Peak areas for the TPDec of $(Zn_{0.75}Cu_{0.25})_{2.5}(OH)_2TM \cdot 2H_2O$ under oxygen.

Two thermodynamic events were detected by DSC, table 6.14, i.e. an endotherm at 188°C (loss of water) and an exotherm at 383°C (decomposition). Compared with the previous mixed metal salt, the exotherm occurs at a slightly lower temperature (cf. 427°C) but has a similar value for ΔH (cf. 2970kJ $mol^{-1}$).

| Temp. (°C) | ΔH (kJ $mol^{-1}$) | % weight loss found | % weight loss calculated | XRD |
|---|---|---|---|---|
| 188 | 147 | — | — | — |
| 383 (400 sh) | -2905 | 54.0 | 54.0 | ZnO + faint CuO |

Table 6.14 DSC results for $(Zn_{0.75}Cu_{0.25})_{2.5}(OH)_2TM \cdot 2H_2O$.

### *6.3e Decomposition of $(Zn_{0.18}Cu_{0.82})$ trimellitate*

*$(Zn_{0.18}Cu_{0.82})_{1.5}TM \cdot 2H_2O$, decomposition under inert atmosphere.*

Heating a sample up to 780°C under argon decomposed it to a black powder. XRD of the product produced both zinc oxide and copper patterns. Elemental analysis gave a copper, zinc, carbon ratio of 0.8:0.2:3.1 (≡ 1.2Cu + 0.3ZnO + 4.7C). At the end of the reactor tube a small amount of zinc had been deposited, but no benzoic acid.

| Product | Temperature (°C) | | | | | | |
|---|---|---|---|---|---|---|---|
| | 130-395 | 296, 307 | 424 | 615 | 712 | 721 | 780 |
| $CO_2$ | — | 632 | 141 | — | — | — | — |
| CO | — | 11.0 | 8.9 | 94.5 | — | — | 24.2 |
| $H_2O$ | 337 | — | — | — | — | 50.5 | — |
| $C_6H_6$ | — | — | 22.3 | — | — | — | — |
| $H_2$ | — | — | — | — | — | 141 | — |
| $CH_4$ | — | — | — | — | 6.7 | — | — |

Table 6.15 Peak areas for the TPDec under argon of $(Zn_{0.18}Cu_{0.82})_{1.5}TM \cdot 2H_2O$.

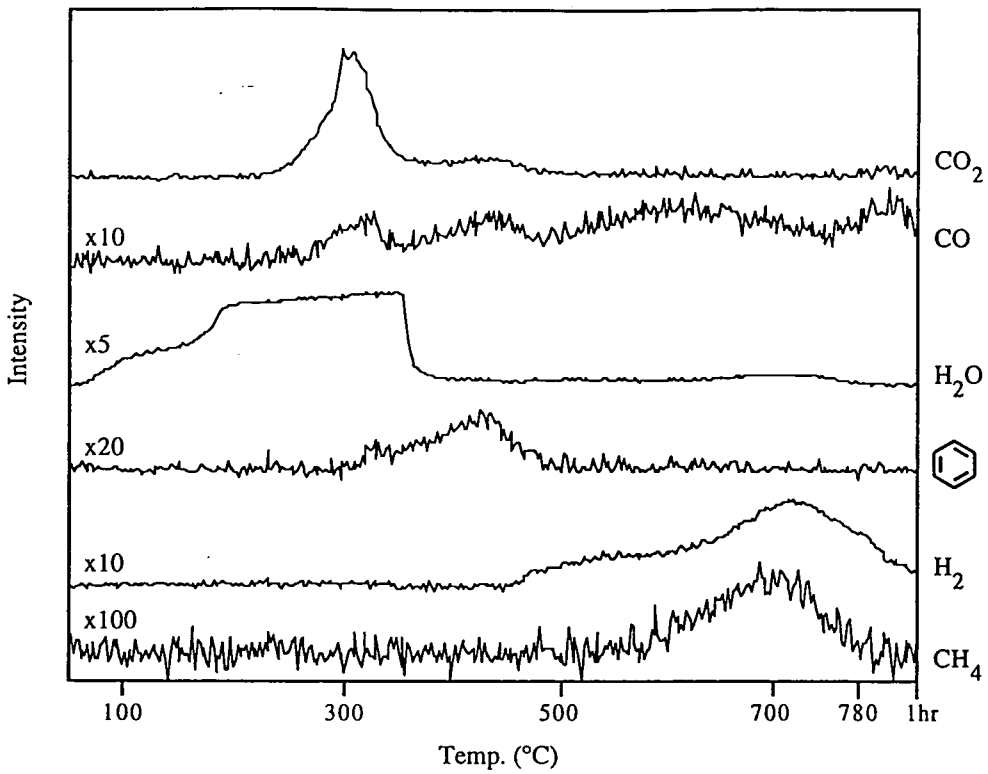


Figure 6.15 TPDec profile of $(Zn_{0.18}Cu_{0.82})_{1.5}TM \cdot 2H_2O$ under argon.

This salt was different to the previous mixed metal trimellitates because it was zinc substituted into copper trimellitate. The TPDec profile, figure 6.15, was similar to that for the copper salt, figure 6.6. The onset of decarboxylation (~260°C) was unchanged and the peak had two maxima, 296 and 307°C. In addition there was a further evolution of carbon dioxide and also some carbon monoxide at 424°C, which were not detected for the copper salt. A further difference was that benzene was evolved at higher temperature for the mixed salt, now coinciding with the carbon dioxide peak at 424°C.

The area of the carbon oxide peaks at 424°C was 19% of the total carbon oxide areas up to 500°C. This suggests that the zinc (18% of the metal content) and copper elements decarboxylated separately, the zinc at higher temperature. One explanation is that the sample consisted of two phases, a zinc-rich and copper-rich phase. Apart from the lack of evidence of a second phase from powder XRD of the sample, one would expect there to have been a benzene peak at 327°C if there was a copper trimellitate phase (cf. figure 6.6). Although benzene started to be evolved at 327°C, it actually reached a maximum at 427°C. It therefore appears that the decomposition of the mixed metal trimellitate first involved the loss of carboxylate groups coordinated to copper centres. Little benzene was produced because the aromatic groups were still carboxylates coordinated to zinc. The zinc aromatic carboxylates decomposed at 424°C, producing carbon dioxide, monoxide and benzene.

After the decomposition there was one extra feature in the mixed metal TPDec profile, i.e. a small amount of carbon monoxide at 780°C. This was probably due to the reduction of some zinc oxide by carbon, forming carbon monoxide and zinc. The metal produced would be evaporated to the end of the reactor tube, as was found after the experiment.

*$(Zn_{0.18}Cu_{0.82})_{1.5}TM$ . $2H_2O$, decomposition under oxidising atmosphere.*

Heating a sample to 780°C under oxygen calcined the salt to copper oxide and zinc oxide, as determined by XRD. Benzoic acid was found at the end of the reactor tube in contrast to the decomposition under argon, which produced no acid.

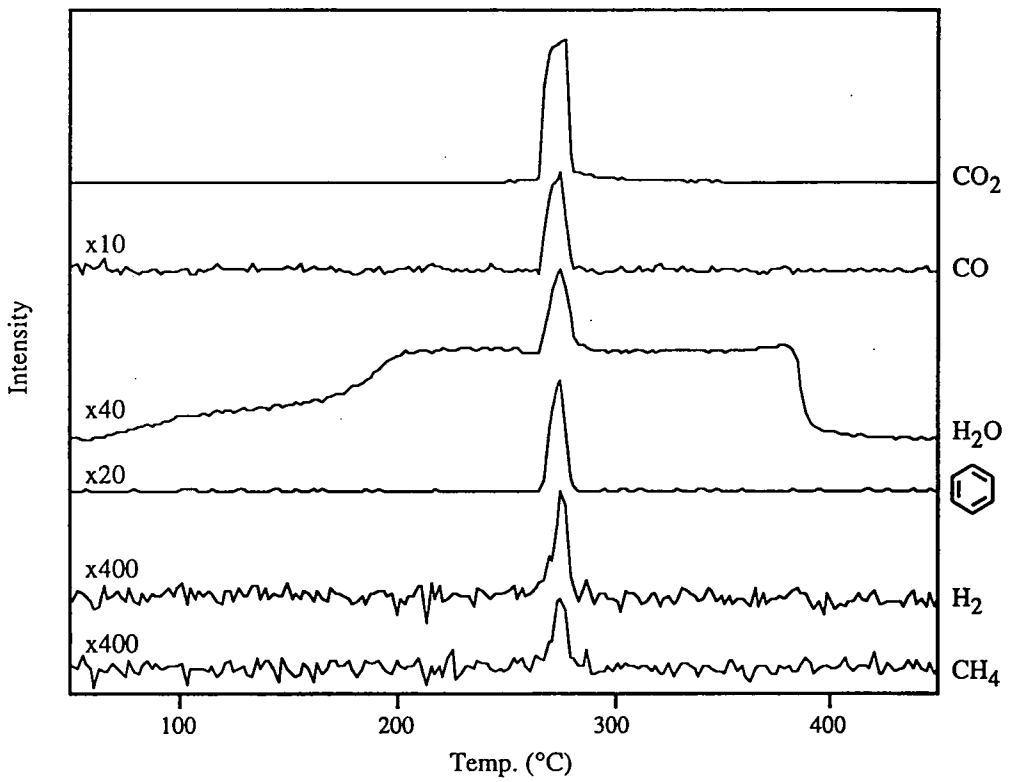


Figure 6.16 TPDec profile of $(Zn_{0.18}Cu_{0.82})_{1.5}TM$ . $2H_2O$ under oxygen.

The TPDec profile, figure 6.16, shows that the salt decomposed at 270°C, as did copper trimellitate, figure 6.8. The incorporation of zinc did not alter the decomposition temperature because oxidative decomposition occurred with the initial decarboxylation, which was unaffected by zinc. It was shown in the argon TPDec that the onset of decarboxylation was unchanged in the mixed metal salt, but extra features were detected at higher temperatures.

| Product | Temperature (°C) | | |
|---|---|---|---|
| | 145-390 | 265-279 | 275 |
| $CO_2$ | — | 2260 | — |
| CO | — | 27.0 | — |
| $H_2O$ | 577 | — | 24.3 |
| $C_6H_6$ | — | — | 47.1 |
| $H_2$ | — | — | 2.1 |
| $CH_4$ | — | — | 1.5 |

Table 6.16 Peak areas for the TPDec under oxygen of $(Zn_{0.18}Cu_{0.82})_{1.5}TM \cdot 2H_2O$.

Two thermodynamic events were detected by DSC, table 6.17, i.e. an endotherm at 228°C (loss of water) and an exotherm at 310°C (decomposition). The DSC results were similar to those found for copper trimellitate. The XRD of the product showed only zinc and copper(II) oxides, but the percentage weight loss was slightly lower than expected, at 64.7%.

| Temp. (°C) | ΔH (kJ $mol^{-1}$) | % weight loss | | XRD |
|---|---|---|---|---|
| | | found | calculated | |
| 228 | 80 | — | — | — |
| 310 (380sh) | -2885 | 63.7 | 64.7 | ZnO + CuO |

Table 6.17 DSC results for $(Zn_{0.18}Cu_{0.82})_{2.5}(OH)_2TM \cdot 2H_2O$.

The results and discussion of the thermal decompositions of zinc, copper and two mixed metal pyromellitates now follow.

### *6.3f Decomposition of zinc pyromellitate*

*$Zn_2PM \cdot 4H_2O$, decomposition under inert atmosphere.*

Decomposition under argon produced zinc oxide and carbon. A 1:2.5 ratio of the respective products was determined by elemental analysis (≡ 2ZnO + 5C). At the end of the reactor tube there was a small amount of zinc metal but no organic residue.

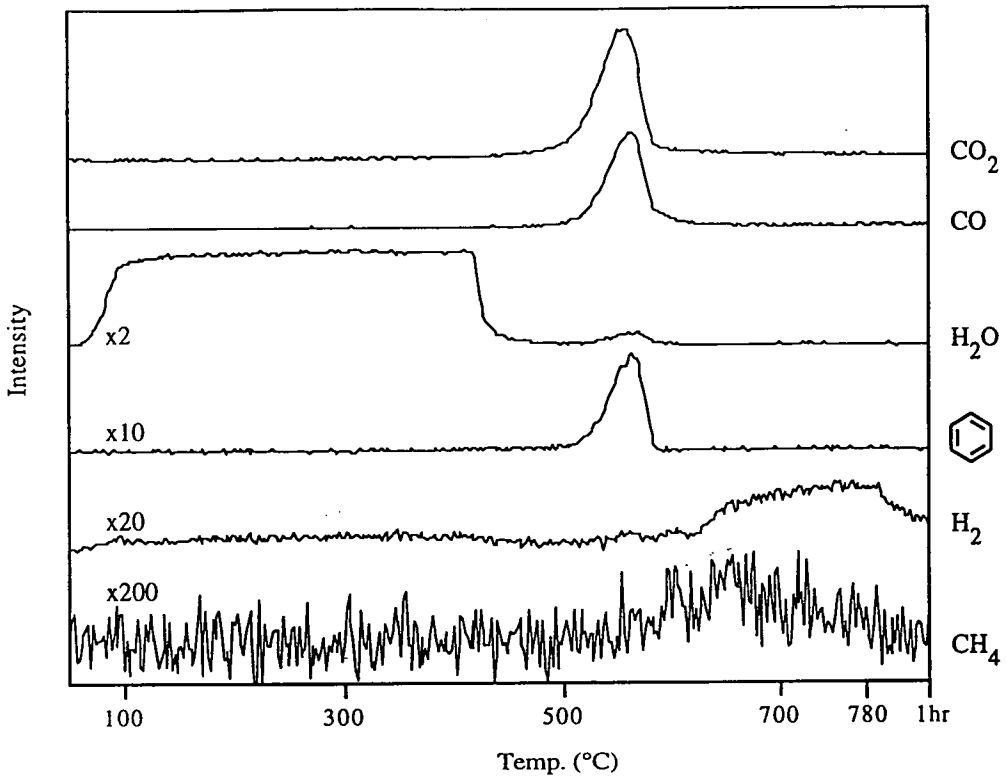


Figure 6.17 TPDec profile of $Zn_2PM$ . $4H_2O$ under argon.

The TPDec profile, figure 6.17, shows that water was evolved from 70°C and that decomposition occurred at ~560°C. Carbon dioxide was produced at 556°C and carbon monoxide, benzene and water were all evolved at 564°C. Hydrogen was desorbed at higher temperatures after the decomposition.

| Product | Temperature (°C) | | | | |
|---|---|---|---|---|---|
| | 70-435 | 556 | 564 | 665 | 624-812 |
| $CO_2$ | — | 531 | — | — | — |
| CO | — | — | 307 | — | — |
| $H_2O$ | 604 | — | 10.4 | — | — |
| $C_6H_6$ | — | — | 28.4 | — | — |
| $H_2$ | — | — | — | — | 46.5 |
| $CH_4$ | — | — | — | 3.2 | — |

Table 6.18 Peak areas for the TPDec under argon of $Zn_2PM$ . $4H_2O$.

The amount of carbon dioxide and monoxide produced can be deduced based on the following assumptions:

i) the only source of oxygen was from the carboxylate groups;

ii) oxygen was required for the formation of two moles of zinc oxide;

iii) the sample was anhydrous prior to decarboxylation; and

iv) the amount of water produced during decomposition was negligible.

The carbon dioxide to monoxide ratio was 1.7:1, which gives 2.33 and 1.35 moles of the respective products per mole of pyromellitate. The thermal decomposition becomes:

$$Zn_2PM \cdot 4H_2O \xrightarrow[-\,4H_2O]{\Delta} Zn_2PM \xrightarrow{\Delta} 2ZnO + 5C + 2.33CO_2 + 1.35CO + 0.22\,\text{C}_6\text{H}_6 + 0.34H_2$$

Unlike zinc trimellitate the decomposition occurred in one stage. The amount of benzene produced was approximately a quarter that for zinc trimellitate and no benzoic acid was produced, both signs of greater ring degradation. The loss of carboxylate groups from zinc pyromellitate involved more ring degradation because the salt contained no hydroxyl groups nor any other source of electrophile for a Henkel-type reaction.

*$Zn_2PM \cdot 4H_2O$, decomposition under oxidising atmosphere.*

Calcination of zinc pyromellitate produced a cream coloured powder of zinc oxide. No residues were deposited at the end of the reactor tube.

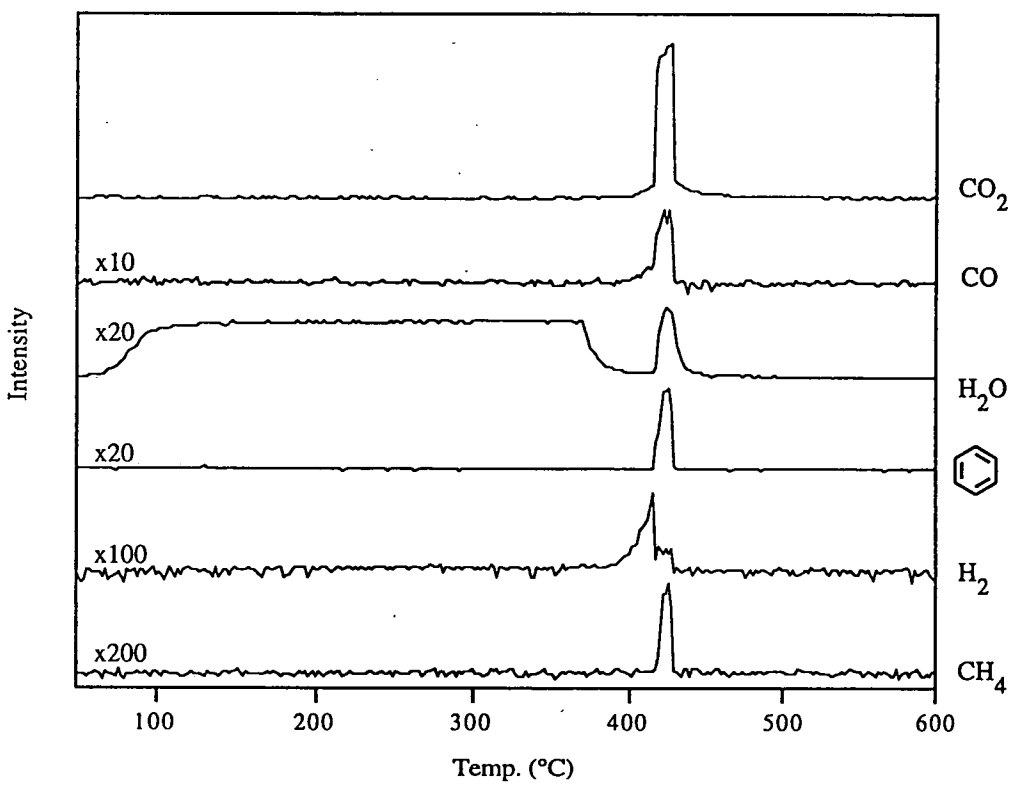


Figure 6.18 TPDec profile of $Zn_2PM \cdot 4H_2O$ under oxygen.

| Product | Temperature (°C) | | |
|---|---|---|---|
| | 65-385 | 416 | 416-430 |
| $CO_2$ | — | — | 2060 |
| CO | — | — | 91.7 (422, 426°C) |
| $H_2O$ | 783 | — | 37.5 |
| $C_6H_6$ | — | — | 33.4 |
| $H_2$ | — | 9.0 | 1.8 |
| $CH_4$ | — | — | 2.6 |

Table 6.19 Peak areas for the TPDec under oxygen of $Zn_2PM$ . $4H_2O$.

The TPDec profile, figure 6.18, shows that the sample decomposed between 416 and 430°C, coinciding with the onset of decarboxylation under argon, figure 6.17. A small amount of hydrogen, carbon dioxide and carbon monoxide was evolved prior to the main decomposition at 416°C, indicating some decarboxylation/decomposition before 416°C. During the oxidative decomposition (416-430°C) little hydrogen was detected because it was reacting, forming water, benzene and methane.

| Temp. (°C) | ΔH (kJ $mol^{-1}$) | % weight loss found | % weight loss calculated |
|---|---|---|---|
| 126 (143sh) | 253 | — | — |
| 493 | -1089 | 63.4 | 64.1 |

Table 6.20 DSC results for $Zn_2PM$ . $4H_2O$.

Two thermodynamic events were detected by DSC, table 6.20, i.e. an endotherm at 126°C (loss of water) and an exotherm from 460°C to 530°C (decomposition). The weight loss was close to that expected for decomposition to zinc oxide (64.1%).

### *6.3g Decomposition of copper pyromellitate*

*$Cu_2PM$ . $6H_2O$, decomposition under inert atmosphere.*

Copper pyromellitate decomposed under an inert atmosphere to copper and carbon. The TPDec product was a black powder and elemental analysis of the product gave a copper to carbon ratio of 2:5.4. No organic residues were deposited at the end of the reactor tube, but some copper was found on the quartz tubing underneath the substrate.

| Product | Temperature (°C) | | | | |
|---|---|---|---|---|---|
| | 80-522 | 283 | 597 | 694 | 726 |
| $CO_2$ | — | 532 (289°C sh) | — | — | — |
| CO | — | 5.9 | 135 | — | — |
| $H_2O$ | 724 | 2.5 | — | — | — |
| $H_2$ | — | — | — | — | 58.8 |
| $CH_4$ | — | — | — | 5.1 | — |

Table 6.21 Peak areas for the TPDec under argon of $Cu_2PM \cdot 6H_2O$.

It can be seen from the TPDec profile, figure 6.19, that only carbon dioxide was produced during the decomposition at 283°C. After the decomposition carbon monoxide (600°C), methane (695°C) and hydrogen (725°C) were desorbed. It appears that negligible non-destructive decarboxylation occurred, as benzene was not detected during the decomposition. Carbon monoxide was not produced during the decomposition because oxygen was not required to produce the metal oxide (the copper was reduced to Cu°). However, carbon monoxide was desorbed after the decomposition. There are several possible explanations: copper could have been partially oxidised after the decomposition and then reduced by carbon at higher temperatures; or adsorbed carbon dioxide (from a carboxylate group) could have been reduced by carbon forming the monoxide. There were insufficient data to deduce the cause of the carbon monoxide formation.

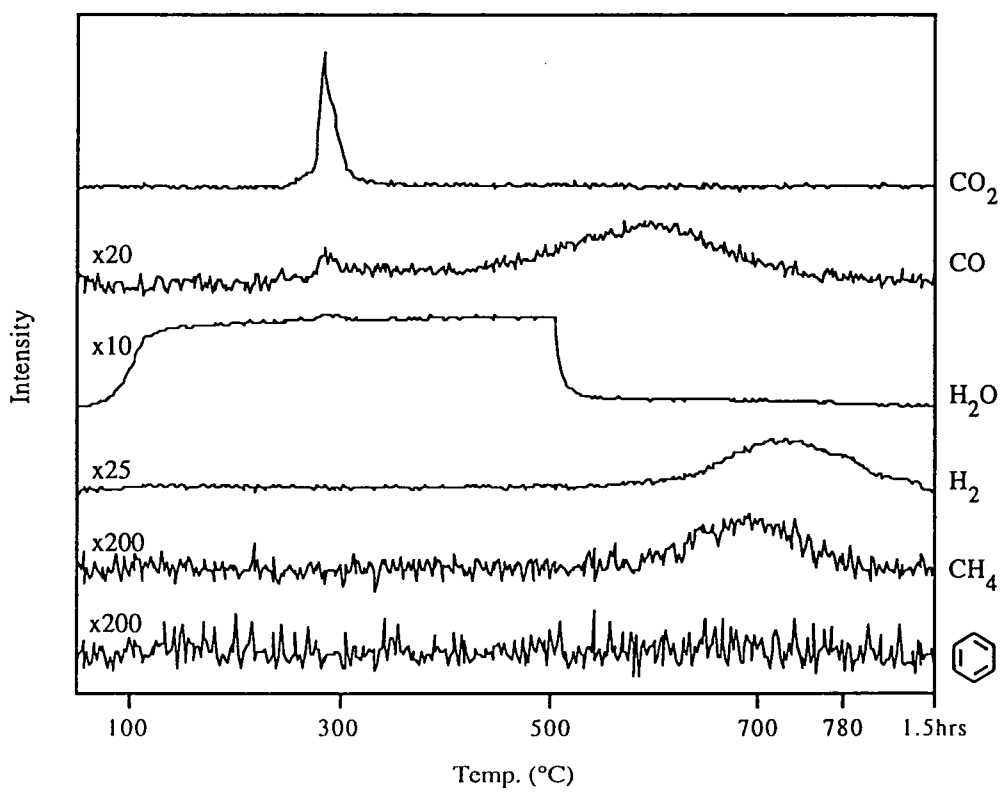


Figure 6.19 TPDec profile of $Cu_2PM \cdot 6H_2O$ under argon.

The ratio of carbon dioxide to monoxide was 7:2. Assuming that the carboxylate groups dissociated forming only carbon oxides, the following stoichiometries for the decomposition were deduced (in good agreement with the elemental analysis).

$$Cu_2PM \,.\, 6H_2O \xrightarrow[-\,6H_2O]{\Delta} Cu_2PM \xrightarrow{\Delta} 2Cu + 5.5C + 3.5CO_2 + CO + H_2$$

*$Cu_2PM \,.\, 6H_2O$, decomposition under oxidising atmosphere.*

The salt decomposed under an oxidising atmosphere to copper(II) oxide, the TPDec product was a black powder. A very small amount of benzoic acid was found at the end of the reactor tube. From the TPDec profile, figure 6.20, we see that decomposition started at 262°C and ended by 274°C, occurring with the initial decarboxylation (cf. argon TPDec). In contrast with the decomposition under argon, some benzene was evolved.

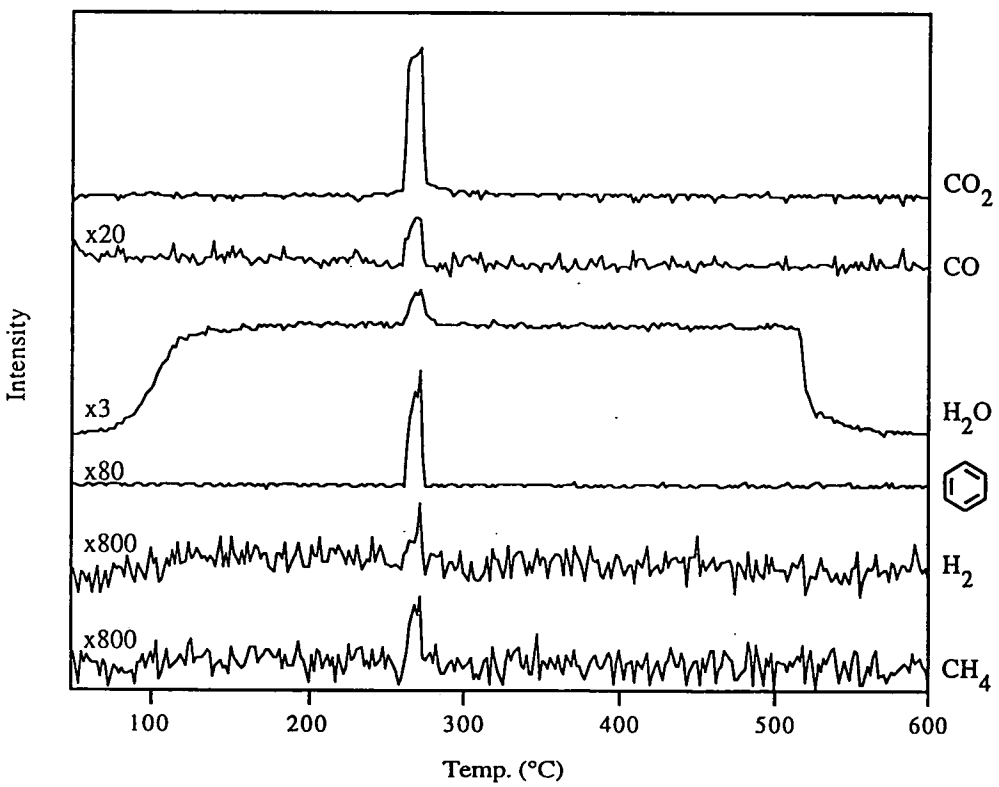


Figure 6.20 TPDec profile of $Cu_2PM \,.\, 6H_2O$ under oxygen.

| Product | Temperature (°C) | | |
|---|---|---|---|
| | 80-530 | 262-274 | 272 (268 sh) |
| $CO_2$ | — | 1880 | — |
| CO | — | 27.1 | — |
| $H_2O$ | 1010 | — | 8.3 |
| $C_6H_6$ | — | — | 11.0 |
| $H_2$ | — | — | 0.3 |
| $CH_4$ | — | — | 0.5 |

Table 6.22 Peak areas for the TPDec under oxygen of $Cu_2PM . 6H_2O$.

Two thermodynamic events were detected by DSC, table 6.23, i.e. an endotherm at 133°C (loss of water) and an exotherm at 340°C (decomposition). The exotherm was approximately twice that found for zinc pyromellitate. The weight loss was close to that expected (67.2%) for an end product of copper(II) oxide.

| Temp. (°C) | ΔH (kJ $mol^{-1}$) | % weight loss | |
|---|---|---|---|
| | | found | calculated |
| 133 | 240 | — | — |
| 340 | -2102 | 67.8 | 67.2 |

Table 6.23 DSC results for $Cu_2PM .6H_2O$.

Benzene and benzoic acid were both formed during the decomposition under oxygen, but were not observed under argon. This raises the question of why non-destructive decarboxylation only took place under oxygen. But water, methane and a tiny amount of hydrogen were also observed, none of which were detected during the decomposition under argon. Thus the question becomes, why did hydrogenation occur under oxygen? Two possibilities are that under oxygen the substrate had higher catalytic activity towards hydrogenation, or that the hydrogen was no longer efficiently adsorbed/absorbed, making it accessible for hydrogenation reactions. The products of decomposition under argon and oxygen were copper/carbon and copper(II) oxide, respectively. It may be that copper oxide has a higher catalytic activity than the copper/carbon substrate.

However, greater hydrogenation during decomposition under oxygen was also observed for zinc pyromellitate (and, to a greater or lesser extent, for all the trimellitates). Zinc pyromellitate decomposed to zinc oxide under both conditions, carbon was also produced under argon. This suggests that the enhanced hydrogenation was not due to the metal oxide, but to the absence of carbon from the substrate. It might be that carbon inhibits catalytic hydrogenation, but in view of the well-known

adsorption/absorption capabilities of carbon (e.g. activated charcoal) it is more likely that under argon the hydrogen was sorbed to the carbon. This would make the hydrogen less accessible to other reagents and active species. The heat of adsorption for hydrogen on graphite is 3.8kJmol$^{-1}$ for physisorption[133] and 240kJmol$^{-1}$ for chemisorption[131].

### *6.3h Decomposition of ($Zn_{0.5}Cu_{0.5}$) pyromellitate*

*$(Zn_{0.5}Cu_{0.5})_{2.5}OH(PM)\ .\ 7H_2O$, decomposition under inert atmosphere.*

The mixed metal salt decomposed under an inert atmosphere to copper, zinc oxide and carbon. A copper, zinc, carbon ratio of 0.5:0.4:2.2 was determined by elemental analysis (≡ 1.3 Cu + ZnO + 5.5 C). The amount of zinc oxide in the product was low because some zinc (~15mg) was deposited at the end of the reactor tube, no organic residues were found.

| Product | Temperature (°C) | | | | | |
|---|---|---|---|---|---|---|
| | 40-455 | 268, 285 | 473 | 493 | 605 | 665-780 |
| $CO_2$ | — | 506 | 232 (493°C sh) | — | — | — |
| CO | — | 1.25 | — | 47.1 | 38.3 | 22.7 (780°C) |
| $H_2O$ | 787 | — | — | — | — | — |
| $C_6H_6$ | — | — | — | 14.8 (473°C sh) | — | — |
| $H_2$ | — | — | — | — | — | 66.5 (545sh, 715°C) |
| $CH_4$ | — | — | — | — | — | 3.5 (670°C) |

Table 6.24 Peak area for the TPDec under argon of $(Zn_{0.5}Cu_{0.5})_{2.5}OH(PM)\ .\ 7H_2O$.

The TPDec profile, figure 6.21, was more complicated than those for the single metal pyromellitates. Water was detected from 40 to 455°C, carbon dioxide was evolved at 268°C and then smaller amounts at 285°C and 473°C. The first two peaks could not be satisfactorily resolved, but the sum of their areas is given in table 6.24. Carbon monoxide was evolved at higher temperatures (493, 605 and 780°C). Benzene was produced during the last carbon dioxide and first carbon monoxide peak. Hydrogen and a small amount of methane were desorbed at 715 and 670°C respectively.

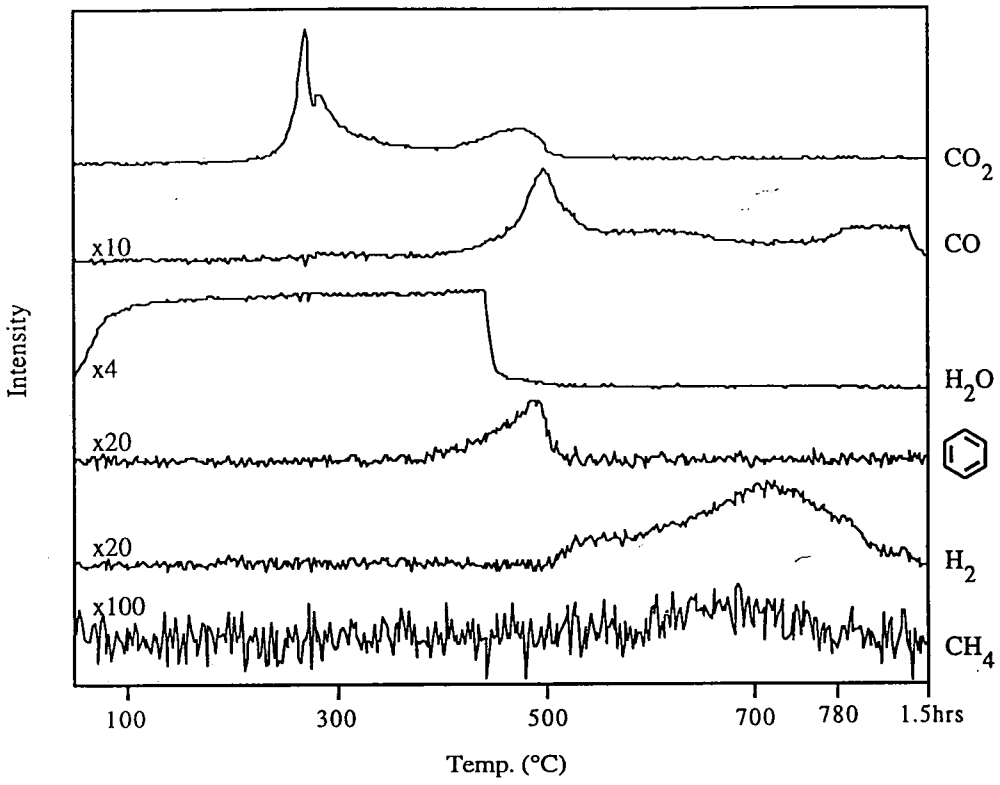


Figure 6.21 TPDec profile of $(Zn_{0.5}Cu_{0.5})_{2.5}OH(PM) \cdot 7H_2O$ under argon.

It was possible to deduce the events during the TPDec experiment from the results of the previous single and mixed metal trimellitates and pyromellitates. Starting at 780°C (and working backwards) it is believed that carbon monoxide was produced from the reduction of zinc oxide by carbon. The broad carbon monoxide peak at 605°C was desorption from the copper, as observed for other copper containing salts. The carbon dioxide and monoxide evolutions at 470-500°C were due to loss of carboxylate groups from a zinc aromatic carboxylate intermediate. The decomposition of the zinc-rich intermediate also produced benzene. This was similar to the argon TPDec of $(Zn_{0.18}Cu_{0.82})_{1.5}TM \cdot 2H_2O$) (figure 6.15), in which the same decomposition volatiles were detected at 425°C, and were attributed to the decomposition of a zinc-rich intermediate. The carbon dioxide peak at 285°C was decarboxylation associated with the copper cation (copper pyromellitate decarboxylated at 283°C).

The first carbon dioxide peak, 268°C, occurred at a lower temperature than copper pyromellitate, suggesting that it was owing to a property unique to the mixed metal salt. The two salts have different structures, and it may be that the decarboxylation at 268°C was owing to a difference in the coordination (the data are not available for the mixed salt). The mixed metal pyromellitate was a basic salt (copper and zinc pyromellitates had no hydroxyl groups), therefore a different decarboxylation route was possible (e.g. Henkel) and this may account for the lower temperature decarboxylation.

*$(Zn_{0.5}Cu_{0.5})_{2.5}OH(PM)$ . $7H_2O$, decomposition under oxidising atmosphere.*

Calcination of the mixed metal salt oxidised it to copper(II) oxide and zinc oxide. After the TPDec experiment, a very small amount of benzoic acid was found at the end of the reactor tube.

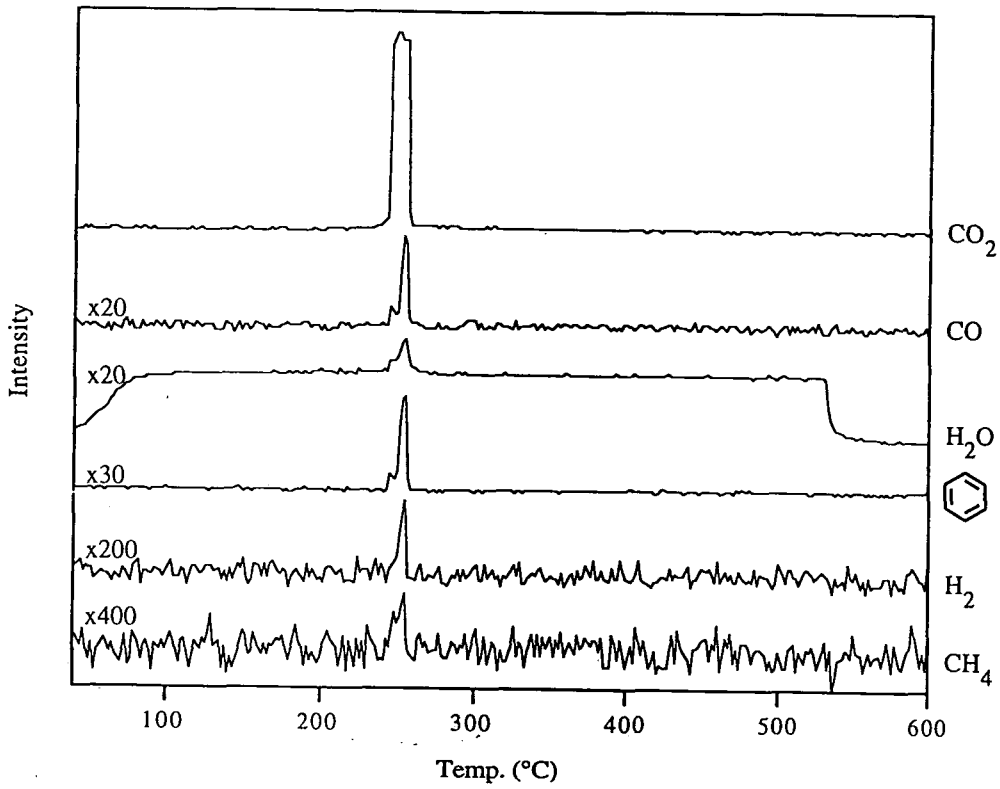


Figure 6.22 TPDec profile of $(Zn_{0.5}Cu_{0.5})_{2.5}OH(PM)$ . $7H_2O$ under oxygen.

It can be seen from the TPDec profile, figure 6.22, that the decomposition started at 244°C, coinciding with the onset of decarboxylation, and finished by 285°C. The decomposition temperature was approximately 20°C lower than copper pyromellitate because the mixed metal salt started decarboxylating at lower temperatures. The same volatile products as before were detected and, apart from carbon dioxide, all peaked at 256°C with a shoulder at 247°C.

| Product | Temperature (°C) | | |
|---|---|---|---|
| | 40-540 | 244-258 | 256 (247sh) |
| $CO_2$ | — | 1750 | — |
| CO | — | — | 18.4 |
| $H_2O$ | 1130 | — | — |
| $C_6H_6$ | — | — | 14.9 |
| $H_2$ | — | — | 1.3 |
| $CH_4$ | — | — | 0.4 |

Table 6.25 Peak areas for the TPDec under oxygen of $(Zn_{0.5}Cu_{0.5})_{2.5}OH(PM)$ . $7H_2O$.

| Temp. (°C) | ΔH (kJ mol$^{-1}$) | % weight loss found | % weight loss calculated |
|---|---|---|---|
| 127 (80sh) | 250 | — | — |
| 277 | -547 | — | — |
| 405 (320sh, 360sh) | -2570 | 63.0 | 63.7 |

Table 6.26 DSC results for $(Zn_{0.5}Cu_{0.5})_{2.5}OH(PM) \cdot 7H_2O$.

Three thermodynamic events were detected by DSC, table 6.26. These were an endotherm at 127°C (loss of water) and exotherms at 277°C and 405°C. The faster heating rate appears to have separated the shoulder seen in the TPDec profile (247°C), forming two distinct features. The weight loss was close to that expected (63.7%) for a final product of copper(II) oxide and zinc oxide.

### *6.3i Decomposition of $(Zn_{0.33}Cu_{0.67})$ pyromellitate*

*$(Zn_{0.33}Cu_{0.67})_{2.5}OH(PM) \cdot 7H_2O$, decomposition under inert atmosphere.*

The salt decomposed to copper, zinc oxide and carbon. Approximately 15mg of zinc was deposited at the end of the reactor tube during the TPDec experiment and some copper was observed on the quartz tubing around the sample.

| Product | Temperature (°C) | | | | | |
|---|---|---|---|---|---|---|
| | 45-457 | 271, 294 | 453 | 506 | 617 | 680-780 |
| $CO_2$ | — | 632 | 224 | — | — | — |
| CO | — | — | — | 34.7 | 58.8 | 12.7 (780°C) |
| $H_2O$ | 902 | — | — | — | — | — |
| $C_6H_6$ | — | — | 15.5 | 4.9 | — | — |
| $H_2$ | — | — | — | — | — | 61.7 (582sh, 727°C) |
| $CH_4$ | — | — | — | — | — | 4.7 (680°C) |

Table 6.27 Peak area for the TPDec under argon of $(Zn_{0.33}Cu_{0.67})_{2.5}OH(PM) \cdot 7H_2O$.

The profile, figure 6.24, had the same features as the previous mixed metal salt, but the relative intensities were different. As one would expect, the peak areas of events associated with copper were greater for the copper-rich salt than for the $(Zn_{0.5}Cu_{0.5})$ pyromellitate. These events were the second decarboxylation peak at 294°C and carbon monoxide desorption at 617°C. As was also expected, a decrease was observed for the peak areas associated with zinc, loss of carboxylate groups (carbon dioxide at 453°C and carbon monoxide at 506°C), and reduction of zinc oxide (carbon monoxide at 780°C).

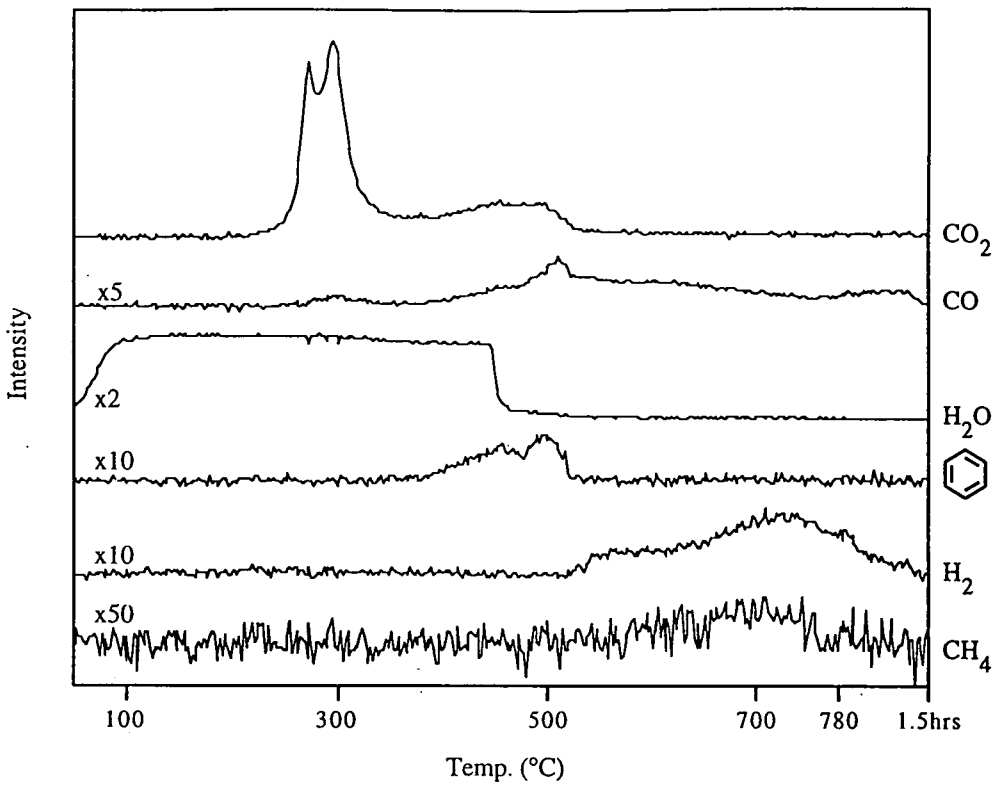


Figure 6.23 TPDec profile of $(Zn_{0.33}Cu_{0.67})_{2.5}OH(PM) \cdot 7H_2O$ under argon.

If the first decarboxylation was associated with the hydroxyl group, as speculated, then one would expect the peak area to remain the same as there was still one hydroxyl group per pyromellitate. Unfortunately, it has not been possible to verify this because the peak overlaps with the second decarboxylation. Qualitatively, the first decarboxylation peaks for the two salts appear to be of similar magnitude.

*$(Zn_{0.33}Cu_{0.67})_{2.5}OH(PM) \cdot 7H_2O$, decomposition under oxidising atmosphere.*

Under oxidising conditions the mixed metal salt decomposed to copper(II) oxide and zinc oxide. After the TPDec experiment, a very small amount of benzoic acid was found at the end of the reactor tube. It can be seen from the carbon dioxide profile, figure 6.24, that decomposition occurred from 245°C to 261°C, the same as the previous mixed metal salt.

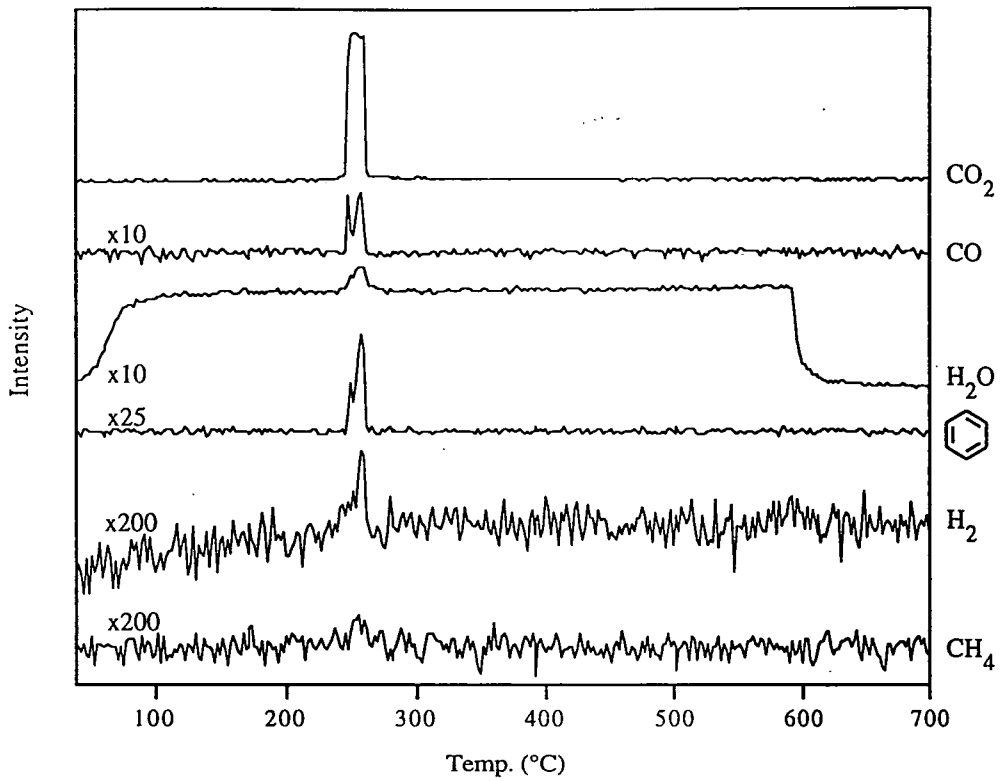


Figure 6.24 TPDec profile of $(Zn_{0.33}Cu_{0.67})_{2.5}OH(PM) \cdot 7H_2O$ under oxygen.

Comparing the oxygen TPDec profiles of the two mixed metal salts, it was evident that the lower temperature feature (~249°C) in the carbon monoxide and benzene profiles was more pronounced for the copper-rich pyromellitate. This suggests that the decomposition detected at 249°C was associated with the copper in the salt. The relative area of the peak was too small (with respect to the peak at 257°C) for it to account for all the decomposition associated with copper, and it is more likely to be related to the partial occupancy of a particular metal site in the crystal structure. Unfortunately the relevant crystallographic data are not available.

| Product | Temperature (°C) | | |
|---|---|---|---|
| | 45-600 | 245-261 | 257 |
| $CO_2$ | — | 1930 | — |
| CO | — | — | 17.3 (249°C) |
| $H_2O$ | 1150 | — | 7.5 (249°C sh) |
| $C_6H_6$ | — | — | 7.2 (249°C) |
| $H_2$ | — | — | 0.7 (249°C) |
| $CH_4$ | — | 0.3 | — |

Table 6.28 Peak areas for the TPDec of $(Zn_{0.33}Cu_{0.67})_{2.5}OH(PM) \cdot 7H_2O$ under oxygen.

| Temp. (°C) | ΔH (kJ mol$^{-1}$) | % weight loss found | % weight loss calculated |
|---|---|---|---|
| 59 | 8.7 | — | — |
| 120 | 345 | — | — |
| 220-480 (279, 318, 339, 409) | -3175 | 65.5 | 63.8 |

Table 6.29 DSC results for $(Zn_{0.33}Cu_{0.67})_{2.5}OH(PM) \cdot 7H_2O$.

Six thermodynamic events were detected by DSC, table 6.29. A small endotherm at 59 and another at 120°C were assumed to be loss of water. There was also an exothermic region consisting of four overlapping peaks (279, 318, 339, 409°C), the last peak being the greatest in intensity. Comparing the DSC results with the previous salts, table 6.26, the peaks at 59, 318, and 339°C for the copper-rich salt were only shoulders in the DSC of the $(Zn_{0.5}Cu_{0.5})$ salt, suggesting that these features were related to the amount of copper in the compound. The sum of the exotherms was comparable between the two salts but the loss of water for the copper-rich pyromellitate had a larger value of ΔH.

## 6.4 Summary and Conclusions

It was found that zinc/copper trimellitates and pyromellitates decomposed under an inert atmosphere to a copper/zinc oxide/carbon product, and under oxygen produced a copper oxide/zinc oxide product. Table 6.30 summarises the decomposition temperatures found for trimellitates and pyromellitates reported in this chapter.

| Compound | Decomposition temperature under $O_2$ (°C) | Decarboxylation temperature under Ar (°C) |
|---|---|---|
| $Zn_{2.5}(OH)_2TM \cdot 2H_2O$ | 410 [a] | 382, 462, 500(CO) |
| $(Zn_{0.9}Cu_{0.1})_{2.5}(OH)_2TM \cdot 2H_2O$ | 320 | 359, 460, 495(CO) |
| $(Zn_{0.75}Cu_{0.25})_{2.5}(OH)_2TM \cdot 2H_2O$ | 330 | 330, 464, 491(CO) |
| $(Zn_{0.2}Cu_{0.8})_{1.5}TM \cdot 2H_2O$ | 265 | 296, 307, 424 |
| $Cu_{1.5}TM \cdot 2H_2O$ | 265 | 278, 301, 309, 327 |
| $Zn_2PM \cdot 4H_2O$ | 420 | 556, 564(CO) |
| $(Zn_{0.5}Cu_{0.5})_{2.5}OH(PM) \cdot 7H_2O$ | 245 | 268, 285, 473, 493(CO) |
| $(Zn_{0.33}Cu_{0.67})_{2.5}OH(PM) \cdot 7H_2O$ | 245 | 271, 295, 453, 506(CO) |
| $Cu_2PM \cdot 6H_2O$ | 265 | 283 |

Table 6.30 Decomposition and decarboxylation temperatures found for trimellitate and pyromellitate salts. CO in parentheses signifies decarbonylation.
[a] Also decarboxylation at 387°C.

The single metal zinc salts had the highest temperatures for decomposition under oxygen. For the trimellitates, the copper-rich salts had the lowest decomposition temperature. It was found that the mixed metal pyromellitates decomposed under oxygen at lower temperatures than the single metal pyromellitates, and also all the trimellitates studied.

It has been shown that zinc trimellitate decomposed under argon by the loss of carboxylate groups in three stages. Henkel type decarboxylations occurred first producing terephthalate and benzoate. In the final stage, the benzoate intermediate could be protonated, forming benzoic acid, or benzene could be produced through loss of a carboxylate group as carbon dioxide or carbon monoxide. Some aromatic rings dissociated during the decomposition, forming carbon and hydrogen. Under oxygen the main decomposition occurred with the second decarboxylation stage.

Oxidative decomposition involved the oxidation of the products from aromatic ring degradation (carbon and hydrogen). This reaction was very exothermic, heating the surrounding substrate and causing the rest of the material to thermally decompose/decarboxylate. The decompositions under oxygen had very narrow peak widths, from 10 to 15°C. Narrow peak widths are often indicative of an autocatalytic decomposition[134,135], in which the thermolysis product catalyses the decomposition. But for zinc trimellitate, the thermolysis product was zinc oxide which was also produced under inert conditions where no autocatalytic decomposition was observed. It therefore seems unlikely that the decomposition under oxygen was catalysed by zinc oxide.

In general, more hydrogenation products (e.g. benzene, water and methane) were observed for the oxidative decompositions. This appears to be due to the hydrogen being more accessible during the decomposition under oxygen. It was speculated that under inert conditions the hydrogen was adsorbed/absorbed to the carbon formed, making it less available for further reaction.

Copper trimellitate decarboxylated under argon in one stage. Ring degradation was associated with the initial decarboxylation, which meant that under oxygen, oxidative decomposition occurred with the initial decarboxylation.

It was found that the substitution of copper into zinc trimellitate produced an initial decarboxylation at lower temperature than that for the zinc salt. Incorporation of more copper did not decrease the temperature for initial decarboxylation, but more decarboxylation was detected at the lower temperature. Under oxygen the decomposition temperature for the mixed metal salts was ~90°C, lower than that for zinc trimellitate. This was because the decomposition was now occurring with the initial decarboxylation. Both mixed metal salts decomposed at approximately the same temperature.

Substitution of zinc into copper trimellitate did not change the initial decarboxylation under argon, but decomposition at higher temperatures was detected.

This was assumed to be the decomposition of a zinc aromatic carboxylate. Under oxygen the decomposition temperature was the same as copper trimellitate. The incorporation of zinc did not affect the temperature of oxidative decomposition because it occurred with the initial decarboxylation, which had not been altered by the inclusion of zinc.

The pyromellitates were found to decompose in a similar way to the trimellitates. Zinc pyromellitate decomposed in one stage when under argon (cf. the three stages found for zinc trimellitate) because the salt possessed no hydroxyl groups for a Henkel decarboxylation. Under oxygen the decomposition coincided with the initial decarboxylation. The decomposition of copper pyromellitate was very similar to copper trimellitate. Copper pyromellitate was the only salt not to produce benzene during decomposition under argon. With these less complicated decompositions it was possible to determine the moles of the products formed.

$$Zn_2PM \cdot 4H_2O \xrightarrow[-\,4H_2O]{\Delta} Zn_2PM \xrightarrow{\Delta} 2ZnO + 5C + 2.33CO_2 + 1.35CO + 0.22\text{C}_6\text{H}_6 + 0.34H_2$$

$$Cu_2PM \cdot 6H_2O \xrightarrow[-\,6H_2O]{\Delta} Cu_2PM \xrightarrow{\Delta} 2Cu + 5.5C + 3.5CO_2 + CO + H_2$$

The mixed metal pyromellitates were basic salts, unlike the single metal pyromellitates which possessed no hydroxyl groups. It was deduced that when heated under argon, the mixed metal salts underwent decarboxylation associated with copper at ~290°C, and decomposition associated with zinc at 470-500°C. There was also decarboxylation at 268°C, a lower decarboxylation temperature than any previous salt. It was uncertain what caused the low temperature decarboxylation but it was speculated that it was owing to the hydroxyl groups, allowing a Henkel-type decarboxylation. Under oxygen the mixed metal salts decomposed at the same temperatures (244°C, lower than any other samples) and occurred with the initial decarboxylation.

Referring back to the DTA-TG experiments by Brzyska *et al*[90-92], it was proposed in section 6.1 that the decompositions under air of aromatic polycarboxylates reported by them actually involved two events. This was deduced from the large loss of weight occurring at the beginning of the broad decomposition exotherm, and a much smaller weight loss detected during the rest of the exotherm. From the findings of the present work, one can deduce that the large weight loss detected at the beginning of the decomposition was associated with the loss of the carboxylate groups, evolving carbon oxides, benzene and possibly benzoic acid. The very exothermic reaction detected would have been the oxidation of carbon produced from aromatic ring dissociation.

To conclude, it has been shown that similar processes occurred for the decomposition under inert atmosphere for the trimellitates and pyromellitates. These consisted of dehydration, loss of carboxylate groups, and aromatic ring dissociation.

Three types of carboxylate loss were deduced: i) non-destructive (Henkel), ii) ring degradation and iii) decarbonylation. The latter was when the carboxylate group dissociated to form carbon monoxide, e.g. zinc salts decomposed, forming zinc oxide, and required oxygen from some of the carboxylate groups to form the metal oxide. Copper decarboxylates at lower temperatures than zinc and greater ring degradation was detected for samples containing copper.

Under oxidising conditions decomposition occurred with the initial decarboxylation because of the associated ring degradation. The exception was zinc trimellitate because no ring degradation accompanied the first decarboxylation. The presence of oxygen did not hinder decarboxylation, but the oxidation of carbon from ring degradation caused localised heating of the substrate, which forced the surrounding material to rapidly decarboxylate/decompose.

Future work should include a more detailed study of the decomposition of mixed metal pyromellitates to determine the cause of the first decarboxylation. For example, IR and XRD could be used to identify the intermediate thermolysis products. The study should also be extended to cover zinc-rich pyromellitates.

From the results discussed, it appears that in the mixed metal salts, the copper part of the salt decomposed before the zinc part. It would be interesting to study the formation of copper and zinc oxide during decomposition (e.g. by XPS and TEM) to deduce whether the decomposition is as segregated as it appears.

The effect of a reducing atmosphere on decarboxylation would be another interesting area to explore. For example, would using hydrogen in the carrier gas aid decarboxylation, allowing more non-destructive decarboxylation at lower temperature? If so, one would expect this to produce more benzene and benzoic acid. It would also be interesting to see how much carbon remained in the end product. If all the carbon was hydrogenated to methane, then Cu/ZnO would be formed in one process.

# 7. CONCLUSIONS

The aim of this project was to prepare zinc/copper trimellitates and pyromellitates, and to study the thermal decomposition of these salts. The carboxylates were prepared by reacting zinc/copper hydroxycarbonates with an aqueous solution of the carboxylic acid. The research can be divided into four areas:

i) preparation of zinc/copper hydroxycarbonates;
ii) preparation and characterisation of zinc/copper trimellitates;
iii) preparation and characterisation of zinc/copper pyromellitates; and
iv) thermal decomposition of trimellitate and pyromellitate salts.

The preparation of single phase zinc/copper hydroxycarbonates was not as straightforward as previously assumed. Problems encountered not only included formation of mixed phases, but also hydrolysis of the hydroxycarbonate, forming copper(II) oxide. It was found that precipitation reactions (adding a carbonate solution to zinc/copper nitrate solution) yielded mixed phases, except for zinc-rich preparations undertaken at ~0°C. Copper-rich hydroxycarbonates were prepared by precipitations at constant pH (pH, 6-8 and 20-60°C).

Compounds of the solid solution series $(Zn_xCu_{1-x})_{1.5+y}(OH)_{2y}TM \cdot 2H_2O$ were prepared by the hydroxycarbonate route. It was found that the series had a limited solid solution (x=1-0.5). Crystals were grown with x=0.5 and 1.0 using the gel method, and the crystal structures were deduced. There were two metal sites, both square based pyramidal, and the salts had a polymeric layer structure.

It was deduced from the crystal structures that copper preferentially occupied one of the metal sites. It would appear that the other metal site was unsuitable for copper occupancy, because copper in this metal site would distort the structure, disrupting the polymeric layers. This is believed to be the reason why the solid solution series had limited copper substitution.

Zinc substitution into a copper salt was less successful. For the neutral salt $(Zn_xCu_{1-x})_{1.5} \cdot 2H_2O$ zinc was incorporated up to x=0.2.

The crystal structure of $CuHTM \cdot 2.5H_2O$ was also determined. This has a polymeric layer structure, and the copper is square based pyramidal. The layers pack very closely with the trimellitate groups (which protrude from either side of the layer) overlapping those from adjacent layers.

Two solid solution series for zinc/copper pyromellitates were prepared from the hydroxycarbonate.

$(Zn_xCu_{1-x})_{2.5}OH(PM) \cdot 7H_2O$

$(Zn_xCu_{1-x})_2PM \cdot nH_2O$

The series based on the neutral salt ($M_2PM$) had a limited solid solution (x=0.2-0.4), but the basic salt ($M_{2.5}OHPM$) could accommodate most cation ratios (x=0.1-0.8).

Attempts to prepare salts outside these limits yielded single metal salts, $Zn_2PM \cdot 4H_2O$ and $Cu_2PM \cdot 6H_2O$, with very little substitution of the other cation into these salts.

The crystal structure of $ZnH_2PM \cdot 6H_2O$ was determined. This salt has an ionic structure consisting of layers of $[Zn(H_2O)_6]^{2+}$ separated by pyromellitate dianions $[H_2PM]^{2-}$. The dianion has an interesting structure, in which the acidic protons bridge between adjacent carboxylate groups, forming a strong intramolecular H-bond. Similar bonding has also been reported[65] for $CoH_2PM \cdot 6H_2O$.

The use of $\Delta\nu_{(asym\text{-}sym)}$, the separation between $\nu(CO_2)_{(asym)}$ and $\nu(CO_2)_{(sym)}$, has been used to deduce the carboxylate coordination for some trimellitate and pyromellitate salts. Using the carboxylate coordinations found in trimellitate and pyromellitate crystals, it was shown that the separation between the two $\nu(CO_2)$ absorptions was dependant on the type of coordination of the carboxylate group. This trend was similar to that reported for acetate salts[70]. The $\Delta\nu_{(asym\text{-}sym)}$ assignments have been deduced from a limited number of crystal structures (three for the trimellitates and eight for the pyromellitates), and it is hoped that these assignments will be refined as more crystal structures are solved.

The thermal decomposition of zinc/copper trimellitates and pyromellitates under an inert atmosphere comprised three events.

i) dehydration;
ii) loss of carboxylate groups; and
iii) breakdown of the aromatic ring.

It was deduced that carboxylate groups were dissociated in three ways.

i) decarboxylation with no ring degradation (e.g. Henkel decarboxylation);
ii) decarboxylation with ring degradation; and
iii) decarbonylation (only for samples containing zinc).

Decomposition under oxygen occurred with initial decarboxylation, except in the case of zinc trimellitate. Under oxygen the products from ring degradation (carbon and hydrogen) were oxidised, which caused localised heating of the substrate (the oxidation was very exothermic). This forced the rest of the sample to rapidly decarboxylate/decompose. Some ring degradation occurred with initial decarboxylation for all the salts except zinc trimellitate. This was why oxidative decomposition did not occur with the initial decarboxylation of zinc trimellitate, but instead with the second decarboxylation step.

It was found for mixed metal trimellitates, that the substitution of copper into the basic zinc salt greatly reduced the temperature of decomposition under oxygen (by ~90°C). The dramatic decrease in the decomposition temperature was because the substitution of copper for zinc resulted in oxidative decomposition occurring with the initial decarboxylation. The mixed metal salts also started decarboxylating at lower temperatures than zinc basic trimellitate.

Substituting zinc for copper in the neutral salt had little effect on the oxidative decomposition temperature, because the mixed metal salt had the same initial decarboxylating temperature as copper trimellitate.

The mixed metal pyromellitate salts decomposed at lower temperatures than the single metal salts. It is believed that this was because the mixed metal pyromellitate salts were basic salts, and that the hydroxyl groups allowed lower temperature decarboxylations than either the zinc or copper salts, which had no hydroxyl groups.

Specific areas for further work have been outlined at the end of the conclusions for each chapter. A potential use for zinc/copper benzene polycarboxylates is as precursors for methanol synthesis catalysts (i.e. Cu/ZnO supported on alumina). The suitability of the compounds reported here as catalyst precursors should be assessed. This would include determining the dispersion of the Cu/ZnO products and study of the catalytic activity of the potential catalysts. It is hoped that future work will determine the effect of the precursor on the resultant catalyst. For example, the study should be extended to other zinc/copper salts in order to determine whether the size of ligand has any effect on the dispersion of the metals. It will also be of interest to deduce whether the mechanism or the thermodynamics of the decomposition affects the catalytic activity.

In summary, a new area of zinc/copper benzene polycarboxylates was investigated. Instrumental in the preparation of these salts was the use of hydroxycarbonate compounds as zinc/copper templates. The mechanism for the thermal decomposition of the carboxylates was deduced and the effect of substituting another cation into the salts was determined. It is hoped that the work reported here will be used as a basis for further studies of mixed metal carboxylates and of novel catalyst precursors.

# REFERENCES


1. Keeble A.D., Ph.D. Thesis, University of Durham, 1990.
2. MacBride J.A.H., Wade K., Unpublished Studies, University of Durham, 1990.
3. Hauptman Z.V., Wade K., Unpublished Studies, University of Durham, 1991.
4. Jaffe H.W., Introduction to Crystal Chemistry, Student ed., Cambridge Press, Cambridge, 1988.
5. Kitaigorodsky A.I., Mixed Crystals, Springer Verlag, New York, 1984.
6. Megaw H.D., Crystal Structures: A Working Approach, W.B. Saunders Co., London, 1973.
7. Purcell K.F., Kotz J.C., Inorganic Chemistry, W.B. Saunders Co.,London, 1977.
8. Chaudhuri P., Oder K., Wieghardt K., Gehring S., Haase W., Nuber B., Weiss J., *J. Am. Chem. Soc.*, 1988, **110**, 3657-58.
9. Gonzalez M., Cervateslee F., Terhaar L.W., *Abs. Papers Amer. Chem. Soc.*, 1992, **204**, 235.
10. Brauman S.K., *J. Fire Retard. Chem.*, 1980, **7**, 161-71.
11. Brauman S.K., *J. Fire Retard. Chem.*, 1980, **7**, 175-82.
12. Brauman S.K., *J. Fire Retard. Chem.*, 1980, **7**, 130-35.
13. Fields E.K., Zimmerschied W.J., Palmer D.A., Patent U.S. 4,065,442, 1977; Chem. Abstr. **88**:95479.
14. Bridger G.W., Spencer M.S., The Catalyst Handbook, 2nd Ed, Chap. 9, Ed. Twigg M.V., Wolfe Publishing Ltd., London, 1989.
15. Ogata T., Taga T., Osaki K., *Bull. Chem. Soc. Jpn.*, 1977, **50**, 1674-79.
16. Henisch H.K., Crystal Growth in Gels, Penn. State University Press, London, 1970.
17. Duprez D., Ferhat-Hamida Z., Bettahar M.M., *J. Catal.*, 1990, **124**, 1-11.
18. Herman R.G., Klier K., Simmons G.W., Finn B.P., Bulko J.B., Kobylinski T.P., *J. Catal.*, 1979, **56**, 407-29.
19. Himelfarb P.B., Simmons G.W., Klier K., Herman R.G., *J. Catal.*, 1985, **93**, 442-50.
20. Pollard A.M., Thomas R.G., Williams P.A., Just J., Bridge P.J., *Mineral. Mag.*, 1991, **55**, 163-66.
21. Porta P., De Rossi S., Ferraris G., Lo Jacono M., Minelli G., Moretti G., *J. Catal.*, 1988, **109**, 367-77.
22. Tohji K., Udagawa Y., Mizushima T., Ueno A., *J. Phys. Chem.*, 1985, **89**, 5671-76.
23. Mehrotra R.C., Bohra R., Metal Carboxylates, Academic press, London, 1983.
24. Luehrs D.C., Cornilsen B.C., Glover C.B., Neils T.L., *Inorg. Chim. Acta*, 1988, **145**, 81-84.
25. Poleti D., Karanovic L., *Acta Cryst.*, 1989, **C45**, 1716-18.

26. Brzyska W., Kowalcwicz J., *Zesz. Nauk Politech. Slask. Chem.*, 1981, **677**, 141-48.
27. Robl C., *Z. Anorg. Allg. Chem.*, 1988, **561**, 57-65.
28. Pech R., Pickardt J., *Acta Cryst.*, 1988, **C44**, 992-94.
29. Pech R., Pickardt J., *Acta Cryst.*, 1990, **C46**, 1928-30.
30. Banait J.S., Pahil P.I.C., *Polyhedron*, 1985, **4**, 1031-33.
31. Robl C., *Z. Anorg. Allg. Chem.*, 1987, **554**, 79-86.
32. Robl C., *Z. Naturforsch, B: Chem. Sci.*, 1988, **43**, 993-97.
33. Baillie M.J., Brown D.H., Moss K.C., Sharp D.W.A., *J. Chem. Soc., A*, 1968, 3110-14.
34. Vasenta E.N., Srivastava G., Mehrotra R.C., *Inorg. Chim. Acta*, 1978, **26**, 47-50.
35. Zenina G.V., Sheverdina N.I., Kocheshkov K.A., *Dokl. Akad. Nauk SSSR*, 1970, **195**, 96-97.
36. Zachariasen W.H., *J. Am. Chem. Soc.*, 1940, **62**, 1011-13.
37. Amirthalingam V., Padmanabhan V.M., *Acta Cryst.*, 1958, **11**, 896-97.
38. Van Niekerk J.N., Schoening F.R.L., Talbot J.H., *Acta Cryst.*, 1953, **6**, 720-23.
39. De Meester P., Fletcher S.R., Skapski A.C., *J. Chem. Soc. Dalton*, 1973, 2575-78.
40. Barclay G.A., Kennard C.H.L., *J. Chem. Soc.*,1961, 3289-94.
41. Kiriyama R., Ibamato H., Matsuo K., *Acta Cryst.*, 1954, **7**, 482-83.
42. Alyea E.C., Dias S.A., Ferguson G., Khan M.A., Roberts P.J., *Inorg. Chem.*, 1979, **18**, 2433-37.
43. Doedens R.J., *Prog. Inorg. Chem.*, 1976, **21**, 209-231.
44. Catterick J., Thornton P., *Adv. Inorg. Chem. Radiochem.*, 1977, **20**, 291-362.
45. Mounts R.D., Ogura T., Feranado Q., *Inorg. Chem.*, 1974, **13**, 802-05.
46. Cingi M.B., Lanfredi A.M.M., Tiripicchio A., Camellini M.T., *Acta Cryst.*, 1979, **B35**, 312-16.
47. Langs D.A., Hare C.R., *J. Chem. Soc., Chem. Commun.*, 1967, 890-91.
48. Uchtman V.A., Jandacek R.J., *Inorg. Chem.*, 1980, **19**, 350-55.
49. Cingi M.B., Guastini C., Musatti A., Nardelli M., *Acta Cryst.*, 1969, **B25**, 1833-40.
50. Cingi M.B., Lanfredi A.M.M., Tiripicchio A., Camellini M.T., *Acta Cryst.*, 1978, **B34**, 134-37.
51. Prout C.K., Carruthers J.R., Rossotti F.J.C., *J. Chem. Soc., A*, 1971, 3350-54.
52. Cingi M.B., Lanfredi A.M.M., Tiripicchio A., Camellini M.T., *Acta Cryst.*, 1977, **B33**, 659-64.
53. Cingi M.B., Lanfredi A.M.M., Tiripicchio A., Camellini M.T., *Acta Cryst.*, 1978, **B34**, 412-16.
54. Cingi M.B., Lanfredi A.M.M., Tiripicchio A., Camellini M.T., *Acta Cryst.*, 1978, **B34**, 406-11.

55. Cingi M.B., Lanfredi A.M.M., Tiripicchio A., Camellini M.T., *Acta Cryst.*, 1978, **B34**, 774-78.
56. Cingi M.B., Guastini C., Musatti A., Nardelli M., *Acta Cryst.*, 1970, **B26**, 1836-43.
57. Cingi M.B., Lanfredi A.M.M., Tiripicchio A., Camellini M.T., *Acta Cryst.*, 1981, **B37**, 2159-63.
58. Krstanovic I., Karanovic Lj., Stojakovic Dj., *Acta Cryst.*, 1985, **C41**, 43-45.
59. Prelesnik B., Herak R., Stojakovic D., Poleti D., *Monatsh. Chem.*, 1986, **117**, 47-49.
60. Bakalbassis E.G., Bozopoulos A.P., Mrozinski J., Rentzperis P.J., Tsipis C.A., *Inorg. Chem.*, 1988, **27**, 529-32.
61. Verdaguer M., Gouteron J., Jeannin S., Jeannin Y., Kahn O., *Inorg. Chem.*, 1984, **23**, 4291-96.
62. Robl C., Hentschel S., *Mater. Res. Bull.*, 1991, **26**, 1355-62.
63. Robl C., *Mater. Res. Bull.*, 1992, **27**, 99-107.
64. Usubaliev B.T., Shnulin A.N., Mamedov Kh. S., *Koord. Khim.*, 1982, **8**, 1532-38.
65. Ward D.L., Luehrs D.C., *Acta Cryst.*, 1983, **C39**, 1370-72.
66. Maxwell W.R., Dartington J.R., *Trans. Faraday Soc.*, 1937, **33**, 670-78.
67. Robl C., Hentshel S., *Z. Naturforsch., B: Chem. Sci.*, 1991, **46**, 1188-92.
68. Tamura H., Ogawa K., *J.Crystallogr. Spectrosc. Res.*, 1992, **22**, 237-47.
69. Tamura H., Ogawa K., Mori W., *J.Crystallogr. Spectrosc. Res.*, 1989, **19**, 203-13.
70. Deacon G.B., Phillips R.J., *Coord. Chem. Rev.*, 1980, **33**, 227-50.
71. Alcock N.W., Tracy V.M., Waddington T.C., *J.Chem. Soc., Dalton Trans.*, 1976, 2243-46.
72. Ito K., Bernstein H.J., *Can. J. Chem.*, 1956, **34**, 170-78.
73. Waller D., Stirling D., Stone F.S., Spencer M.S., *Faraday Discuss. Chem. Soc.*, 1989, **87**, 107-20.
74. Pollard A.M., Spencer M.S., Thomas R.G., Williams P.A., Holt J., Jennings J.R., *App. Catal., A: General*, 1992, **85**, 1-11.
75. Segal D.L., *J. Non-Cryst. Solids*, 1984, **63**, 183-91.
76. Trimm D.L., Stanislaus A., *App. Catal.*, 1986, **21**, 215-38.
77. Yoshimatsu H., Yabuki T., Kawasaki H., *J. Non-Cryst. Solids*, 1988, **100**, 413-17.
78. Fields E.K., Meyerson S., *J. Org. Chem.*, 1976, **41**, 916-20.
79. Boldyrev V.V., *React. Solids*, 1990, **8**, 231-46.
80. Galwey A.K., *React. Solids*, 1990, **8**, 211-230.
81. Galwey A.K., Brown M.E., *J. Chem. Soc., Faraday Trans. I*, 1982, **78**, 411-24.
82. Galwey A.K., Mohamed M.A., Brown M.E., *J. Chem. Soc., Faraday Trans. I*, 1988, **84**, 57-64.
83. Galwey A.K., Herley P.J., Mohamed M.A., *J. Chem. Soc., Faraday Trans. I*, 1988, **84**, 729-38.

84. Carr N.J., Galwey A.K., *Proc. R. Soc. Lond. A*, 1986, **404**, 101-26.
85. Carr N.J., Galwey A.K., *J. Chem. Soc., Faraday Trans. I*, 1988, **84**, 1357-73.
86. Mohamed M.A., Galwey A.K., *Thermo Chimica Acta*, 1993, **217**, 263-76.
87. Galwey A.K., Mohamed M.A., Rajam S., Brown M.E., *J. Chem. Soc., Faraday Trans. I*, 1988, **84**, 1349-56.
88. Galwey A.K., Jamieson D.M., Brown M.E., *J. Phys. Chem.*, 1974, **78**, 2664-70.
89. Taki K., Kim P.H., Namba S., *Bull. Chem. Soc. Japan*, 1970, **43**, 1450-54.
90. Brzyska W., Wolodkiewicz W., *J. Therm. Anal.*, 1988, **34**, 1207-15.
91. Brzyska W., Wanczowskafonfara D., *J. Therm. Anal.*, 1989, **35**, 727-33.
92. Brzyska W., Wolodkiewicz W., *J. Therm. Anal.*, 1986, **31**, 961-65.
93. Goeta A.E., Rigotti G., Sileo E.E., Blesa M.A., *Solid State Ionics*, 1993, **62**, 159-65.
94. Revankar V.V.S., Doraiswamy L.K., *Ind. Eng. Chem. Res.*, 1992, **31**, 781-86.
95. Grinblat M.P., Rozova N.I., Kats I.A., Shabalina L.I., Lukina N.A., Reikhafel'd V.O., Zvegintseva G.B., Spiridonova S.A., Galil-Ogly F.A., Patent U.S.S.R. 378,400, 1973; Chem. Abstr. **79**:67640.
96. Michell E.W.J., Shah D., *J. Vinyl Tech.*, 1989, **11**, 141-50.
97. Merkur'eva E.V., Galafeev V.A., Kharitonov V.M., Kiro Z.B., Rubinshtein B.I., Pakamonov V.I., Nagdaseva I.P., Gerbich A.Ya., Ambainis J., Farbtukh Z.E., Patent U.S.S.R. SU 1,525,175, 1989; Chem. Abstr. **113**:99294.
98. Kitao T.,Oda H., Patent Ger. Offen. DE 3,907,872, 1989; Chem. Abstr. **112**:108658.
99. Lianfang L., Faming Zhuanli Shenqing Gongkai Shuomingshu CN 86,107,180, 1988; Chem. Abstr. **112**:72282.
100. Ogawa H.,Patent Japan. 71 22,740, 1971; Chem. Abstr. **77**:91071.
101. Ota N., Imamura T., Patent Japan. 71 05,686, 1971; Chem. Abstr. **74**:124852.
102. Ruppert R., Patent Can. 966,750, 1975; Chem. Abstr. **83**:62440.
103. Ichikawa Y., Yanagi S., Hosoi E., Nishikawa K., Masudi K., Ito N., Patent Japan. 69 32,303, 1969; Chem. Abstr. **72**:122829.
104. Ghose S., *Acta Cryst.*, 1964, **17**, 1051-57.
105. Wells A.F., *Acta Cryst.*, 1951, **4**, 200-04.
106. Bridge P.J., Just J., Hey M.H., *Mineral. Mag.*, 1979, **43**, 97-98.
107. Nowacki W., Schiedegger R., *Helvetica Chim. Acta*, 1952, **46**, 375-90.
108. Haraldsen H.Z., Z. Anorg. Allg. Chem., 1939, 240, 337.
109. Brzyska W., Wolodkiewicz W., *Pol. J. Chem.*, 1986, **60**, 697-702.
110. Corbin K.M., Glerup J., Hodgson D.J., Lynn M.H., Michelsen K., Nielsen K.M., *Inorg. Chem.*, 1993, **32**, 18.
111. Lippert E.L., Truter M.R., *J. Chem. Soc.*, 1960, 4996.
112. Zviedre I.I., Bel'skii V.K., Fundamenskii V.S., Shvarts E.M., *Latv. PSR Zinat. Akad. Vestis, Khim.* Ser., 1987, 221.

113. Podlahova J., Kratochvil B., Podlaha J., Hasek J., *J. Chem. Soc., Chem. Comm.*, 1990, 576.
114. Looney A., Cornebise D., Miller D., Parkin G., *Inorg. Chem.*, 1992, **31**, 989.
115. Hurlburt P.K., Kellet P.J., Anderson O.P., Strauss S.H., *J. Chem Soc., Chem. Comm.*, 1990, 576.
116. Hambley T.W., Snow M.R., *Aust. J. Chem.*, 1983, **36**, 1249.
117. Grewe H., Udupa M.R., Krebs B., *Inorg. Chim. Acta*, 1982, **63**, 119.
118. Cousson A., *Acta Cryst.*, 1985, **C41**, 1758-61.
119. Cousson A., Stout B., Nectoux F., Pages M., Gasperin M., *J. Less-Common Met.*, 1986, **125**, 111-15.
120. Karasev V.E., Steblevskaya N.I., Petrochenkova N.V., *Koord. Khim.*, 1988, **14**, 1377-84.
121. Nectoux F., Abazli H., Jove J., Cousson A., Pages M., Gasperin M., Choppin G., *J. Less-Common Met.*, 1984, **97**, 1-10.
122. Yan X., Zongsheng J., Zhibang D., Jazuan N., *Kexue Tonglao*, 1987, **32**, 212; Chem. Abstr. **107**:125828.
123. Yan X., Zhongsheng J., Zhibang D., Jiazan N., *Hauxue Xuebao*, 1987, **45**, 1044-47; Chem. Abstr. **108**:105241.
124. Brzyska W., Kula A., *J. Therm. Anal.*, 1982, **25**, 531-37.
125. Brzyska W., Kurpiel-Gorgol R., Dabkowska M., *J. Therm. Anal.*, 1983, **28**, 333-39.
126. Brzyska W., Sadowski P., *Pol. J. Chem.*, 1984, **58**, 669-74.
127. Shimanochi N., *Kochi Kogyo Koto Semmon Gakko Gakujutsu Kiyo*, 1981, **17**, 83-89; Chem Abrs., 96:96558.
128. Ellison A., Overton T.L., Bencze L., *J. Chem. Soc. Faraday Trans.*, 1993, **89**, 843-49.
129. Cornu A., Massot R., Compilation of Mass Spectral Data, 2nd ed., vol. 1, Heyden and Son, London, 1975.
130. Sykes P., A Guidebook to Mechanism in Organic Chemistry, 6th ed., Longman, London, 1986, pp 285-87.
131. Weast R.C., Handbook of Chemistry and Physics, 64th ed.,CRC press, Boca Raton (Florida), 1983.
132. Bowker M., Houghton H., Waugh K.C., *J. Chem. Soc., Faraday Trans. 1*, 1981, 77, 3023-36.
133. Flood A.E., The Solid-Gas Interface, Vol. 1, Edward Arnold (Pub.) Ltd., London, 1967.
134. McCarty J., Falconer J., Madix R., *J. Catal.*, 1973, **30**, 325-49.
135. Falconer J.L., Madix R.J., *Surf. Sci*, 1974, **46**, 473-504.

# APPENDIX 1. EXPERIMENTAL TECHNIQUES

## 1. Gases

BOC "white spot" nitrogen, BOC reforming gas ($N_2/H_2$, 75/25), oxygen and argon (both BOC, 99.9% purity) were piped into the laboratory from an outside cylinder store. The gases were dried at the bench by passage through columns packed with A4 molecular sieve and phosphorous pentoxide. Compressed air was piped to the laboratory from a mechanical pump.

## 2. Glove Box

Air sensitive compounds were handled in a Faircrest glove box purged with BOC "white spot" nitrogen. The atmosphere in the box was continually passed through columns of A4 molecular sieve to remove water (regenerated periodically by heating under vacuum), copper catalyst to remove oxygen and activated charcoal to remove other impurities. A copper/zeolite catalyst was used (although its action was stoichiometric rather than catalytic) and was regenerated periodically by heating in a stream of reforming gas: $N_2/H_2$, 75/25.

## 3. Measurement of pH

The pH was measured using a Jenway 3020 pH meter fitted with a Jenway PCP 505 combination electrode and an automatic temperature compensation probe.

## 4. Elemental Analysis

Carbon, hydrogen and nitrogen were determined on a Carlo Erba Strumentazione Elemental Analyser (model 1106). Metals were determined on a Perkin Elmer 5000 Atomic Absorption Spectrophotometer. Air sensitive samples were sealed in pre-weighted tin or gelatine capsules in a glove box.

## 5. Infra Red

Infra red spectra, in the range 4000-400$cm^{-1}$, were recorded on a 1600 series Perkin Elmer FT-IR spectrometer. Samples were pressed into KBr discs.

## 6. X-ray Powder Diffraction

X-ray powder photographs were recorded using a Philips X-ray generator (PW1009/80) fitted with a CuK$\alpha$ ($\lambda$=1.5443Å) tube, with the beams being controlled by a Hiltonbrooks DG2-2 window shutter controller. An Enraf-Nonius Guinier de Wolff camera number 2 was used. The Guinier method involves focusing arrangements between the source, monochromator, sample and film, producing higher resolved diffraction lines than Debye-Scherrer cameras. A silicon grease mull of the sample was

spread onto the frame, four such samples could be prepared simultaneously, and the flat samples reciprocate during the exposure. The resultant diffraction lines were at 4θ and a correction factor, c, was applied to compensate for the camera, altering the effective wave length ($c\lambda$=1.5499Å). Owing to the camera being repositioned, the effective wavelength for the XRD's of the pyromellitate salts was $c\lambda$=1.5472Å.

**7. Differential Scanning Calorimetry**

All measurements were carried out using a Mettler differential scanning calorimeter, which comprised a TC11 central processor unit and a DSC25 calorimetric cell. The cell was heated from 20-600°C, at a heating rate of 10°Cmin$^{-1}$. Samples, ~5mg, were encapsulated in aluminium crucibles using a cold seal technique. The lids were pierced twice, forming holes ~0.5mm in diameter. During the experiment, atmospheric air was passed over the sample. If an inert atmosphere was required, then argon (BOC wielding grade) was passed through the calorimeter (~50cm$^3$min$^{-1}$).

**8. Thermal Decomposition**

Thermal decompositions were carried out in a furnace consisting of resistance wire wound on silica tubing (diameter 30mm, length 220mm) encased in a further piece of silica tubing (diameter 50mm, length 220mm). Power was supplied to the furnace via a Eurotherm 815P programmable temperature controller with a chromel/alumel thermocouple as the sensor.

**9. Temperature Programmed Decomposition**

The sample (1.0g) was loaded into a quartz reactor tube. A carrier gas (oxygen or argon) was passed over the sample at a flow rate of 25cm$^3$min$^{-1}$. The furnace (controlled by a Eurotherm 815P programmable temperature controller) was heated from room temperature up to 780°C at a rate of 1°Cmin$^{-1}$. A VG SX200 quadrupole mass spectrometer was connected via a heated capillary tube to the outlet of the microreactor. The mass specrometer was multiplexed to a PC computer, allowing the simultaneous acquisition of up to 50 m/e profiles.

It is known that the sensitivity of quadrupole mass spectrometers decreases with increasing mass[A1]. Correction factors were calculated for some gases, using the appropriate ion gauge sensitivity factor[A2] (this calculation did not take into account differing pumping speeds for the various gases[A1]). Correction factors for water and benzene were not calculated because the experiment required the supply of the pure sample gas to the mass spectrometer. It was decided that allowing so much water and benzene into the high vacuum chamber would be detrimental to the equipment and may present a severe contamination problem.

A1. Ko E.I., Benziger J.B., Madix R.J., *J. Catal.*, 1980, **62**, 264-74.
A2. Barteau M.A., Bowker M., Madix R.J., *Surf. Sci.*, 1980, **94**, 303-22.

## APPENDIX 2. COLLOQUIA, LECTURES AND SEMINARS FROM INVITED SPEAKERS

### UNIVERSITY OF DURHAM 1991 - 1994

1991

| | |
|---|---|
| October 17 | Dr. J. A. Salthouse, University of Manchester<br>*Son et Lumiere - a demonstration lecture.* |
| October 31 | Dr. R. Keely, Metropolitan Police Forensic Science<br>*Modern Forensic Science.* |
| November 6 | Prof. B. F. G. Johnson†, University of Edinburgh<br>*Cluster-Surface Analogies.* |
| November 7 | Dr. A. R. Butler, St. Andrews University<br>*Traditional Chinese Herbal Drugs.* |
| November 13 | Prof. D. Gani†, St. Andrews University<br>*The Chemistry of PLP Dependent Enzymes.* |
| November 20 | Dr. R. More O'Ferrall†, Dublin<br>*Some Acid-Catalysed Rearrangements in Organic Chemistry.* |
| November 28 | Prof. I. M. Ward, Leeds University<br>*The Science & Technology of Orientated Polymers.* |
| **December 4** | **Prof. R. Grigg†, Leeds University**<br>***Palladium Catalysed Cyclisation and Ion Capture Processes.*** |
| **December 5** | **Prof. A. L. Smith, ex Unilever**<br>***Soap Detergents and Black Puddings.*** |
| **December 11** | **Dr. W. A. Cooper†, Shell Research**<br>***Colloid Science, Theory, and Practice.*** |

1992

| | |
|---|---|
| January 16 | Dr. N. J. Long, University of Exeter<br>*Metallocenophanes-Chemical sugar-tongs.* |
| **January 22** | **Dr. K. D. M. Harris†, University of St. Andrews**<br>***Understanding the Properties of Solid Inclusion Compounds.*** |
| January 29 | Dr. A. Holmes†, University of Cambridge<br>*Cycloaddition Reactions in the Service of the Synthesis of Piperidine and Endolizidine Natural Products.* |
| **January 30** | **Dr. M. Anderson, Sittingbourne Research Centre, Shell Research**<br>***Recent Advances in the Safe and Selective Chemical Control of Insect Pests.*** |
| **February 12** | **Dr. D. E. Fenton†, University of Sheffield**<br>***Polynuclear Complexes of Molecular Clefts as Models for Copper Biosites.*** |
| February 13 | Dr. J. Saunders, Glaxo Group Research Limited<br>*Molecular Modelling in Drug Discovery.* |
| **February 19** | **Prof. E. J. Thomas†, University of Manchester**<br>***Application of Organo-Stannanes to Organic Synthesis.*** |

**February 20** **Prof. E. Vogel, University of Cologne**
***The Musgrave Lecture: Porphyrins, Molecules of Interdisciplinary Interest.***

February 25 Prof. J. F. Nixon, University of Sussex
*Phospha-alkynes, New Building Blocks in Inorganic and Organometallic Chemistry.*

**February 26** **Prof. M. L. Hitchman†, University of Strathclyde**
***Chemical Vapour Deposition.***

**March 5** **Dr. N. C. Billingham, University of Sussex**
***Degradable Plastics - Myth or Magic ?***

**March 11** **Dr. S. E. Thomas†, Imperial College London**
***Recent Advances in Organo-iron Chemistry.***

**March 12** **Dr. R. A. Hann, ICI Image Data**
***Electronic Photography - An Image of the Future***

March 18 Dr H. Maskill†, University of Newcastle
*Concerted or stepwise fragmentation in a deamination-type reaction.*

April 7 Prof. D. M. Knight, Philosophy Department, University of Durham
*Interpreting experiments: the begining of electrochemistry.*

May 13 Dr. J-C. Gehret, Ciba Geigy, Basel
*Some aspects of Industrial Agrochemical Research.*

**October 14** **Dr. S. C. Rawle, University of Warwick**
***Flourescent Sensors for Metal Ions.***

October 15 Dr M. Glazer & Dr. S. Tarling, Oxford University & Birkbeck College, London
*It Pays to be British! - The Chemist's Role as an Expert Witness in Patent Litigation.*

October 20 Dr. H. E. Bryndza, Du Pont Central Research
*Synthesis, Reactions and Thermochemistry of Metal (Alkyl) Cyanide Complexes and Their Impact on Olefin Hydrocyanation Catalysis.*

**October 22** **Prof. A. Davies, University College London**
***The Ingold-Albert Lecture: The Behaviour of Hydrogen as a Pseudometal.***

**October 28** **Dr. J. K. Cockcroft, University of Durham**
***Recent Developments in Powder Diffraction.***

October 29 Dr. J. Emsley, Imperial College, London
*The Shocking History of Phosphorus.*

**November 4** **Dr. T. P. Kee, University of Leeds**
***Synthesis and Co-ordination Chemistry of Silylated Phosphites.***

November 5 Dr. C. J. Ludman, University of Durham
*Explosions, A Demonstration Lecture.*

November 11 Prof. D. Robins†, Glasgow University
*Pyrrolizidine Alkaloids : Biological Activity, Biosynthesis and Benefits.*

November 12 Prof. M. R. Truter, University College, London
*Luck and Logic in Host - Guest Chemistry.*

**November 18** **Dr. R. Nix†, Queen Mary College, London**
***Characterisation of Heterogeneous Catalysts.***

November 25 Prof. Y. Vallee. University of Caen
*Reactive Thiocarbonyl Compounds.*

November 25 Prof. L. D. Quin†, University of Massachusetts, Amherst
*Fragmentation of Phosphorous Heterocycles as a Route to Phosphoryl Species with Uncommon Bonding.*

November 26 Dr. D. Humber, Glaxo, Greenford
*AIDS - The Development of a Novel Series of Inhibitors of HIV.*

December 2 Prof. A. F. Hegarty, University College, Dublin
*Highly Reactive Enols Stabilised by Steric Protection.*

December 2 Dr. R. A. Aitken†, University of St. Andrews
*The Versatile Cycloaddition Chemistry of $Bu_3P.CS_2$.*

December 3 Prof. P. Edwards, Birmingham University
*The SCI Lecture - What is Metal?*

**December 9** **Dr. A. N. Burgess†, ICI Runcorn**
***The Structure of Perfluorinated Ionomer Membranes.***

1993

**January 20** **Dr. D. C. Clary†, University of Cambridge**
***Energy Flow in Chemical Reactions.***

January 21 Prof. L. Hall, Cambridge
*NMR - Window to the Human Body.*

January 27 Dr. W. Kerr, University of Strathclyde
*Development of the Pauson-Khand Annulation Reaction : Organocobalt Mediated Synthesis of Natural and Unnatural Products.*

January 28 Prof. J. Mann, University of Reading
*Murder, Magic and Medicine.*

February 3 Prof. S. M. Roberts, University of Exeter
*Enzymes in Organic Synthesis.*

**February 10** **Dr. D. Gillies†, University of Surrey**
***NMR and Molecular Motion in Solution.***

February 11 Prof. S. Knox, Bristol University
*The Tilden Lecture: Organic Chemistry at Polynuclear Metal Centres.*

February 17 Dr. R. W. Kemmitt†, University of Leicester
*Oxatrimethylenemethane Metal Complexes.*

February 18 Dr. I. Fraser, ICI Wilton
*Reactive Processing of Composite Materials.*

February 22 Prof. D. M. Grant, University of Utah
*Single Crystals, Molecular Structure, and Chemical-Shift Anisotropy.*

February 24 Prof. C. J. M. Stirling†, University of Sheffield
*Chemistry on the Flat-Reactivity of Ordered Systems.*

| | |
|---|---|
| **March 3** | **Dr. P. Fagan, DuPont**<br>***Advances in Chemistry of $C_{60}$*** |
| March 10 | Dr. P. K. Baker, University College of North Wales, Bangor<br>*'Chemistry of Highly Versatile 7-Coordinate Complexes'.* |
| March 11 | Dr. R. A. Y. Jones, University of East Anglia<br>*The Chemistry of Wine Making.* |
| March 17 | Dr. R. J. K. Taylor†, University of East Anglia<br>*Adventures in Natural Product Synthesis.* |
| **March 24** | **Prof. I. O. Sutherland†, University of Liverpool**<br>***Chromogenic Reagents for Cations.*** |
| **May 13** | **Prof. J. A. Pople, Carnegie-Mellon University, Pittsburgh, USA**<br>***The Boys-Rahman Lecture: Applications of Molecular Orbital Theory*** |
| May 21 | Prof. L. Weber, University of Bielefeld<br>*Metallo-phospha Alkenes as Synthons in Organometallic Chemistry* |
| June 1 | Prof. J. P. Konopelski, University of California, Santa Cruz<br>*Synthetic Adventures with Enantiomerically Pure Acetals* |
| June 2 | Prof. F. Ciardelli, University of Pisa<br>*Chiral Discrimination in the Stereospecific Polymerisation of Alpha Olefins* |
| June 7 | Prof. R. S. Stein, University of Massachusetts<br>*Scattering Studies of Crystalline and Liquid Crystalline Polymers* |
| June 16 | Prof. A. K. Covington, University of Newcastle<br>*Use of Ion Selective Electrodes as Detectors in Ion Chromatography.* |
| June 17 | Prof. O. F. Nielsen, H. C. Arsted Institute, University of Copenhagen<br>*Low-Frequency IR - and Raman Studies of Hydrogen Bonded Liquids.* |
| **June 24** | **Dr.L. S. Field, University of Sydney**<br>***Activation of C-H Bonds at Metal Centre.*** |
| **July 23** | **Dr. F Wudl, University of California, Santa Barbara**<br>***Recent Advances in the Chemistry of Buckminsterfullerene, $C_{60}$*** |
| September 13 | Prof. Dr. A. D. Schlüter, Freie Universität Berlin, Germany<br>*Synthesis and Characterisation of Molecular Rods and Ribbons.* |
| September 13 | Prof. K. J. Wynne, Office of Naval Research, Washington, U.S.A.<br>*Polymer Surface Design for Minimal Adhesion* |
| September 14 | Prof. J. M. DeSimone, University of North Carolina, Chapel Hill, U.S.A.<br>*Homogeneous and Heterogeneous Polymerisations in Enviromentally Responsible Carbon Dioxide.* |
| September 28 | Prof. H. Ila., North Eastern University, India<br>*Synthetic Strategies for Cyclopentanoids via OxoKetene Dithiacetals.* |
| **October 4** | **Prof. F. J. Feher†, University of California at Irvine**<br>***Bridging the Gap between Surfaces and Solution with Sessilquioxanes.*** |
| October 14 | Dr. P. Hubberstey, University of Nottingham |

*Alkali Metals: Alchemist's Nightmare, Biochemist's Puzzle and Technologist's Dream.*

October 20 — Dr. P. Quayle†, Unversity of Manchester
*Aspects of Aqueous Romp Chemistry.*

**October 21** — **Prof. R. Adams†, University of S. Carolina**
***The Chemistry of Metal Carbonyl Cluster Complexes Containing Platinum and Iron, Ruthenium or Osmium and the Development of a Cluster Based Alkyne Hydrogenating Catalyst.***

October 27 — Dr. R. A. L. Jones†, Cavendish Laboratory
*'Perambulating Polymers'.*

November 10 — Prof. M. N. R. Ashfold†, University of Bristol
*High-Resolution Photofragment Translational Spectroscopy: A New Way to Watch Photodissociation.*

**November 17** — **Dr. A. Parker†, Laser Support Facility**
***Applications of Time Resolved Resonance Raman Spectroscopy to Chemical and Biochemical Problems.***

**November 24** — **Dr. P. G. Bruce†, University of St. Andrews**
***Synthesis and Applications of Inorganic Materials.***

**November 25** — **Dr. R.P. Wayne, University of Oxford**
***The Origin and Evolution of the Atmosphere***

December 1 — Prof. M. A. McKervey†, Queens University, Belfast
*Functionlised Calixerenes.*

December 8 — Prof. O. Meth-Cohen, Sunderland University
*Friedel's Folly Revisited.*

December 16 — Prof. R. F. Hudson, University of Kent
*Close Encounters of the Second Kind.*

1994

**January 26** — **Prof. J. Evans†, University of Southhampton**
***Shining Light on Catalysts.***

February 2 — Dr. A. Masters†, University of Manchester
*Modelling Water Without Using Pair Potentials.*

February 9 — Prof. D. Young†, University of Sussex
*Chemical and Biological Studies on the Coenzyme Tetrahydrofolic Acid.*

February 16 — Prof. K. H. Theopold, University of Delaware, U.S.A
Paramagnetic Chromium Alkyls: Synthesis and Reactivity.

**February 23** — **Prof. P. M. Maitlis†, University of Sheffield**
***Why Rhodium in Homogenous Catalysis.***

**March 2** — **Dr. C. Hunter†, University of Sheffield**
***Non Covalent Interactions between Aromatic Molecules.***

March 9 — Prof. F. Wilkinson, Loughborough University of Technology
*Nanosecond and Picosecond Laser Flash Photolysis.*

March 10 — Prof. S.V. Ley, University of Cambridge
*New Methods for Organic Synthesis.*

March 25 — Prof. J. Dilworth, University of Essex
*Technetium and Rhenium Compounds with Applications as Imaging Agents.*

April 28 — Prof. R. J. Gillespie, McMaster University, Canada
*The Molecular Structure of some Metal Fluorides and OxoFluorides: Apparent Exceptions to the VSEPR Model.*

**May 12** — **Prof. D. A. Humphreys, McMaster University, Canada**
***Bringing Knowledge to Life***

† Invited specially for the graduate training programme.

Colloquia attended in **bold**.